GROUP II METABOTROPIC GLUTAMATE RECEPTOR MODULATION OF SENSORY RESPONSES IN THE VENTROBASAL THALAMUS

Thesis presented to University College London for the degree of
Doctor of Philosophy (Ph.D)
2013

CAROLINE COPELAND

DEPARTMENT OF VISUAL NEUROSCIENCE
INSTITUTE OF OPHTHALMOLOGY
UNIVERSITY COLLEGE LONDON

ABSTRACT

The functional integrity of the thalamic reticular nucleus (TRN) is thought to be key in the control of selective attention (Crick, 1984; Pinault, 2004). This GABAergic structure (Houser et al., 1980) is responsible for ensuring synchronous activity within the appropriate thalamocortical circuits required for either sensory perception or for the preparation and execution of distinct motor and/or cognitive tasks. It is therefore imperative to ascertain the exact nature of how inhibitory innervation from the TRN to thalamic nuclei is controlled in order to understand how neurophysiological disease states associated with TRN malfunction (Huguenard, 1999; Rub et al., 2003; Barbas and Zikopoulos, 2007; Pinault, 2011) precipitate.

It has been previously demonstrated that the Group II metabotropic glutamate receptors (mGlu2/3) can modulate physiologically-evoked responses in the VB (Salt and Turner, 1998) by reducing inhibition from the TRN (Turner and Salt, 2003). However, it is not yet known what the relative contributions are of the two subtypes to this modulation, nor to what extent these receptors may be activated under physiological conditions during this process. Using single-neurone recording in the rat ventrobasal thalamus (VB) *in vivo* with local iontophoretic application of selective Group II mGlu receptor compounds, my findings were threefold. Firstly, I found that both mGlu2 and mGlu3 receptors contribute a component to the overall Group II mGlu receptor effect on sensory responses in the VB. Secondly, I was able to demonstrate that both Group II mGlu receptor subtypes are likely activated by endogenous 'glutamate spillover' from the synapses formed between excitatory sensory afferents and VB neurones following physiological sensory stimulation, and that this can lead to a reduction in sensory-evoked inhibition arising from the TRN. I propose that this potential Group II mGlu receptor modulation of inhibition could play an important role in discerning relevant information from background activity upon physiological sensory stimulation: a novel mechanism that could be of importance in attention and cognitive processes, whose malfunction could result in maladaption of sensory perception, such as that which can occur in psychiatric disease. Thirdly, I was able to provide evidence that mGlu2 receptors are likely located on astrocytic processes surrounding the VB-TRN synapse, and are able to mediate an astrocytic mechanism of action that reduces inhibitory synaptic transmission from the TRN to the VB. To the best of my knowledge this provides the first evidence that mGlu2 receptors are able to activate astrocytes, and of the involvement of astrocytes in the modulation of heterosynaptic transmission. As VB astrocytes are able to respond to synaptic stimulation (Parri et al., 2010), maladaption of mGlu2 receptor-mediated endogenous astrocytic activation may therefore have functional implications for the processing of somatosensory information and for the preparation and execution of distinct motor and/or cognitive tasks.

Finally, I also investigated the action of the putative endogenous selective Group II mGlu receptor agonist Xanthurenic Acid (XA), which is a metabolite of the kynurenine pathway. Changes in both of these systems have been implicated in the pathophysiology of schizophrenia and other psychiatric disorders, however little is known regarding the mechanism of action of XA. I therefore investigated the effects of XA in modulating inhibition in the VB from the TRN using the same *in vivo* electrophysiology preparation as described above, and also evaluated the ability of XA to bind to and activate mGlu2 receptors using *in vitro* molecular pharmacological methods.

Selective Group II mGlu receptor compounds that exploit this novel mechanism of endogenous activation may therefore be of importance in the modulation of sensory, attentional and cognitive processes for therapeutic strategies.

DECLARATION

I declare that this thesis submitted for the degree of Doctor of Philosophy is my own composition and the data presented herein is my own original work. Where information has been derived from other sources, I confirm that this has been indicated as appropriate.

……..

Caroline Copeland

ACKNOWLEDGEMENTS

First and foremost I'd like to thank Tom Salt for all his hard work and infinite patience. His approach to my supervision throughout my PhD has let me feel as if I was in charge of my own project, which has helped me to become more independent as a researcher, and has given me the courage to develop my own ideas. His fluidity with the Salt Laboratory budget has enabled me to go to several international conferences, experience of which was invaluable (and now I know how to attain a passport if you lose yours in New Orleans).

A big thank you also goes to the Stuart Neale, who together with Tom helped to secure the funding for this project from the Biotechnology and Biological Sciences Research Council and Merck Research Laboratories. His help and advice throughout my time in the Salt Laboratory has been very much appreciated. It was through his involvement that I was able to experience working in pharmaceutical industry and live in Philadelphia in Summer 2012, although I did miss out on sampling the delights of Motherwell. At this point I'd like to make a special mention to my friends and colleagues who made my time in Philadelphia so enjoyable - thank you to everyone in the Cell Pharmacology team, especially to Joe Bruno, Cheryl Gretzula, Rob Robinson and Cindy Nuss, whose supervision enabled me to execute the molecular pharmacology protocols described in this thesis; deserved thanks also go to Scott Mosser, Tom Harkins and Julie O'Brien for providing me with their help and support (less so for their continual mocking of my accent); finally, to all my 2121 mansionmates, thanks for making me feel at home.

I would also like to thank the Sillito Laboratory for their help and advice, although not for my newfound addiction to fresh coffee. Also deserved thanks are for the BRU staff, the porters and the Institute administration team for all their behind the scenes work. Thanks also to Seetal Chavda for being my PhD partner in crime. I'm sure Tom will miss the spontaneous cackles bursting out of our office.

Finally, I would like to thank my family and friends. Special thanks go to my parents and brother for their optimism, and for their concerted efforts in trying to understand exactly what I do; Bryony Graham and Charlie Arber for showing me how it can be done; and of course Bryn, whose eternal beliefs in my abilities, tolerance of arriving home from work at 1am, and endlessly blurting out science in mid-conversation has been the true foundation supporting me throughout this PhD.


me and mGluR

ABBREVIATIONS

3-HK	3-hydroxykynurenine
5-HT	5-hydroxytryptamine
5-HT_{2A} receptor	5-hydroxytryptamine sub-type 2A receptor
7-TM domain	Seven transmembrane domain
AMPA	α-amino-3-hydroxyl-5-methyl-4-isoxazole-propionate
bpm	Beats per minute
BINA	Biphenylindanone-A
cAMP	Adenylyl cyclase
CI	Confidence interval
CNS	Central nervous system
CRD	Cysteine-rich domain
CPM	Counts per minute
DG	Dentate gyrus
DMSO	Dimethyl sulfoxide
ECG	Electrocardiogram
EEG	Electroencephalogram
EPSC	Excitatory postsynaptic current
fEPSPs	Field excitatory postsynaptic potentials
FLIPR	Fluorometric imaging plate reader
FSK	Forskolin
GABA	Gamma-amino butyric acid
GDP	Guanosine 5’-diphosphate
GPCR	G-protein coupled receptor
GTP	Guanosine 5’-triphosphate

i.p.	Intraperiotoneal
i.v.	Intravenous
IPSP	Inhibitory postsynaptic potential
LGN	Lateral geniculate nucleus
mGlu receptor	Metabotropic glutamate receptor
mGlu1 receptor	Metabotropic glutamate receptor sub-type 1
mGlu2 receptor	Metabotropic glutamate receptor sub-type 2
mGlu3 receptor	Metabotropic glutamate receptor sub-type 3
mGlu4 receptor	Metabotropic glutamate receptor sub-type 4
mGlu5 receptor	Metabotropic glutamate receptor sub-type 5
mGlu6 receptor	Metabotropic glutamate receptor sub-type 6
mGlu7 receptor	Metabotropic glutamate receptor sub-type 7
mGlu8 receptor	Metabotropic glutamate receptor sub-type 8
mRNA	Messenger ribonucleic acid
ms	Milliseconds
MVE	Multiple vibrissa excitation
NAAG	N-acetylaspartateglutamate
NaCl	Sodium chloride
NAMs	Negative allosteric modulators
NMDA	*N*-methyl-D-aspartate
PA	Pennsylvania
PAMs	Positive allosteric modulators
PI hydrolysis	Phosphatidylinositol hydrolysis
POm	Posteromedial nucleus
PrV	Principal sensory trigeminal nucleus

PSTHs	Post-stimulus time histograms
RLUs	Relative light units
sec	Seconds
SpVi	Spinal interpolaris trigeminal nucleus
S1 cortex	Primary somatosensory cortex
S2 cortex	Secondary somatosensory cortex
s.c.	Subcutaneous
SVE	Single vibrissa excitation
TRN	Thalamic reticular nucleus
VB	Ventrobasal thalamus
VFD	Venus flytrap domain
VGLUTs	Vesicular glutamate transporters
UK	United Kingdom
USA	United States of America
XA	Xanthurenic acid

CONTENTS IN BRIEF

	PAGE NUMBER
ABSTRACT	i
DECLARATION	ii
ACKNOWLEDGEMENTS	iii
LIST OF ABBREVIATIONS	v
CONTENTS IN BRIEF	viii
CONTENTS IN FULL	ix
CHAPTER 1 INTRODUCTION	1
CHAPTER 2 THE SOMATOSENSORY THALAMUS	9
CHAPTER 3 THE GROUP II METABOTROPIC GLUTAMATE (MGLU) RECEPTORS	24
CHAPTER 4 THE GROUP II MGLU RECEPTORS IN THALAMOCORTICAL CIRCUITRY	49
CHAPTER 5 PROJECT HYPOTHESIS	58
CHAPTER 6 MATERIALS AND METHODS	60
CHAPTER 7 RESULTS	91
CHAPTER 8 DISCUSSION	152
REFERENCES	176
APPENDIX	208

CHAPTER CONTENTS IN FULL

	PAGE NUMBER
CHAPTER 1 INTRODUCTION	**1**
1.1 SOMATOTOPY	1
1.2 OVERVIEW OF THE RODENT VIBRISSAL SYSTEM	2
CHAPTER 1 FIGURES	6
CHAPTER 2 THE SOMATOSENSORY THALAMUS	**9**
2.1 THE VENTROBASAL THALAMUS	9
2.1.1 BASIC CIRCUITRY AND NOMENCLATURE	9
2.1.2 NEURONES OF THE VENTROBASAL THALAMUS	10
2.2 THE THALAMIC RETICULAR NUCLEUS	12
2.2.1 MULTIMODAL FUNCTION	12
2.2.2 BASIC CIRCUITRY	13
2.2.3 NEURONES OF THE THALAMIC RETICULAR NUCLEUS	15
2.3 RECURRENT AND LATERAL INHIBITION	16
2.4 LAYER VI MODULATORY CORTICOTHALAMIC PROJECTION	19
CHAPTER 2 FIGURES	20
CHAPTER 3 THE GROUP II METABOTROPIC GLUTAMATE (MGLU) RECEPTORS	**24**
3.1 THE GLUTAMATERGIC SYSTEM	24
3.2 MGLU RECEPTOR CLASSIFICATION	25
3.3 GROUP II MGLU RECEPTOR STRUCTURE	28
3.3.1 THE VENUS FLYTRAP DOMAIN	28
3.3.2 CYSTEINE-RICH DOMAIN	29
3.3.3 SEVEN TRANSMEMBRANE DOMAIN AND INTRACELLULAR LOOPS	30
3.3.4 C-TERMINUS	30
3.3.5 DIMERISATION	31
3.4 GROUP II MGLU RECEPTOR PHARMACOLOGY	32
3.4.1 SELECTIVE GROUP II MGLU RECEPTOR ORTHOSTERIC AGONISTS	33
3.4.2 GROUP II MGLU RECEPTOR ORTHOSTERIC ANTAGONISTS	34
3.4.3 GROUP II MGLU RECEPTOR ALLOSTERIC MODULATORS	35
3.4.4 XANTHURENIC ACID	37

3.4.4.1 The Kynurenine Pathway 38
3.4.4.2 Synthesis 38
3.4.4.3 Purported Mechanisms of Action 39
3.5 Group II mGlu Receptor Functional Anatomy 40
Chapter 3 Figures and Tables 42
Chapter 4 The Group II mGlu Receptors in Thalamocortical Circuitry 49
4.1 Localisation 49
4.2 Function 50
4.3 Clinical Implications 53
Chapter 4 Figures 56
Chapter 5 Project Hypothesis 58
Chapter 6 Materials and Methods 60
6.1 *In vivo* Electrophysiology 60
6.1.1 Animal Preparation 61
6.1.1.1 Subjects 61
6.1.1.2 Anaesthesia 62
6.1.1.3 Surgery 63
6.1.2 Recording and Iontophoresis 66
6.1.2.1 Glass Electrode Manufacture 66
6.1.2.2 Glass Electrode Filling 67
6.1.2.3 Recording 68
6.1.2.4 Compound Preparation for Iontophoresis 70
6.1.2.5 Iontophoresis 71
6.1.3 Compound Preparation for Intravenous Administration 74
6.1.4 Experimental Protocols 75
6.1.4.1 Sensory Stimulation 75
6.1.4.1.1 Protocol 1: Assessment of the effects of Group II mGlu receptor compounds on sensory responses to short- and long-duration vibrissal stimulation 76
6.1.4.1.2 Protocol 2: Assessment of the effects of Group II mGlu receptor compounds on inhibitory sensory responses using the condition-test paradigm 77

6.1.4.1.3 Protocol 3: Assessment of the effects of Group II mGlu receptor compounds on inhibitory sensory responses upon continuous NMDA application 78

6.1.4.2 Ionotropic Agonist Application 79

6.1.5 Data Analysis 80

6.2 Molecular Pharmacology 81

6.2.1 cAMP Assay 82

6.2.1.1 Cell Line 82

6.2.1.2 Materials 82

6.2.1.3 Instruments 83

6.2.1.4 Assay 83

6.2.1.5 Data Analysis 83

6.2.2 Radioligand Binding 84

6.2.2.1 Materials 84

6.2.2.2 [^{3}H]LY341495 Binding to Human mGlu2 Membranes 84

6.2.2.3 Data Analysis 85

Chapter 6 Figures and Tables 86

Chapter 7 Results **91**

7.1 The effects of the Group II mGlu receptor agonist LY354740 and the mGlu2 PAM LY487379 on sensory responses to short-duration vibrissal stimulation 92

7.2 The effects of the Group II mGlu receptor agonist LY354740 and the mGlu2 PAM LY487379 on inhibitory sensory responses 94

7.3 The effects of the Group II mGlu receptor agonist LY354740 and the mGlu2 PAM LY487379 on recurrent and lateral inhibition 96

7.4 The effects of the Group II mGlu receptor agonist LY354740 and the mGlu2 PAM LY487379 on sensory responses to long-duration vibrissal stimulation 97

7.5 The effects of the Group II mGlu receptor antagonist LY341495 on sensory responses to short- and long-duration vibrissal stimulation 98

7.6 The effects of the dual mGlu2 agonist/mGlu3 antagonist LY395756 on sensory responses to long-duration vibrissal stimulation 99

7.7 The effects of the Group II mGlu receptor agonist LY354740, the mGlu2 PAM LY487379, and the dual mGlu2 agonist/mGlu3 antagonist on ionotropic glutamate receptor agonist responses 100

7.8 The mGlu2 PAM LY487379 effect on sensory responses is mediated via astrocytes 101

7.9 Xanthurenic Acid 105

7.9.1 *IN VIVO* ELECTROPHYSIOLOGY AND IONTOPHORESIS 105

7.9.1.1 THE EFFECT OF XA ON LATERAL INHIBITION IN THE VB 105

7.9.1.2 THE EFFECT OF XA ON LATERAL INHIBITION IN THE VB WHEN APPLIED SYSTEMICALLY 106

7.9.1.3 THE EFFECTS OF XA ON IONOTROPIC GLUTAMATE RECEPTOR AGONIST RESPONSES 107

7.9.2 MOLECULAR PHARMACOLOGY 108

7.9.2.1 XA MODULATION OF CAMP FORMATION 108

7.9.2.2 XA BINDING TO THE MGLU2 RECEPTOR 109

CHAPTER 7 FIGURES AND TABLES 110

CHAPTER 8 DISCUSSION **152**

8.1 GROUP II MGLU RECEPTOR ACTIVATION FACILITATES RESPONSES TO SENSORY STIMULATION OF THE PRINCIPAL VIBRISSA 153

8.2 GROUP II MGLU RECEPTOR ACTIVATION REDUCES LATERAL INHIBITION IN THE VB EVOKED BY SENSORY STIMULATION OF THE SECONDARY VIBRISSA 155

8.3 THE GROUP II MGLU RECEPTORS MAY BE ACTIVATED BY 'GLUTAMATE SPILLOVER' FROM THE SENSORY AFFERENT SYNAPSE 156

8.4 ASTROCYTIC MGLU2 RECEPTORS MODULATE SYNAPTIC TRANSMISSION AT THE TRN-VB SYNAPSE VIA A PRESYNAPTIC MECHANISM 159

8.5 GROUP II MGLU RECEPTOR PHYSIOLOGY IN THE RAT VB REFLECTS THE DISTINCT CELLULAR LOCALISATIONS OF THE TWO SUBTYPES 162

8.6 XANTHURENIC ACID 164

8.6.1 *IN VIVO* ELECTROPHYSIOLOGICAL INVESTIGATIONS OF XA 164

8.6.2 MOLECULAR PHARMACOLOGICAL INVESTIGATIONS OF XA 166

8.6.3 POTENTIAL MECHANISMS OF ACTION OF XA 167

8.6.4 MODULATION OF HIPPOCAMPAL SYNAPTIC TRANSMISSION BY XA 169

8.7 CONCLUSIONS 170

8.8 FUTURE DIRECTIONS 173

CHAPTER 8 FIGURES 174

REFERENCES **176**

APPENDIX **208**

CHAPTER 1 INTRODUCTION

The thalamus functions as a processing station and filter of information in conjunction with the neocortex. With over thirty distinct nuclear groups, each relaying a characteristic signal to a functionally distinct area of the cortex, the thalamus can be considered as concerned with almost, if not all, functional modalities (Sherman and Guillery, 2001). Thalamic nuclei can be classed as either *first-order* or *higher-order* nuclei based upon the source of their *driver* inputs of information. First-order nuclei transmit driver inputs from the periphery to the cortex (e.g. auditory, visual, somatosensory), with higher-order nuclei serving to transmit information between cortical areas, receiving driver inputs from cortical layer V (Guillery, 1995; Sherman, 2007) (**FIGURE 1.1**). First-order nuclei therefore provide us with the opportunity to investigate thalamic function under physiological conditions, as it is possible to physiologically activate driver inputs upon sensory stimulation (Salt, 1989; Weinberger and Bakin 1998; Wang et al., 2011). By understanding basic principles of thalamic function in a first-order nucleus, it is then possible to extend this basic knowledge to understand the function of more complex thalamic circuitries, such as those of the higher-order thalamic nuclei and thalamic nuclei of more complex species (see Jones [2007] for a review).

1.1 SOMATOTOPY

Sensory pathways possess a characteristic high degree of order. The relay of somatosensory stimulation from the periphery to the cortex involves the generation of point-to-point

connectivity maps that tell the brain not only what kind of somatosensory information it is receiving, but also from where this information is being sensed. At all levels of the pathways, the spatial distribution of neurones and their afferent fibres results in a somatotopic representation – that is, the physical distribution of peripheral sensory receptors are faithfully reiterated in central pathways.

A renowned example of such somatotopy is the rodent vibrissal system, which has become one of the most valuable models for neuroscience research due to the homologous arrangement of each of its major component parts. Vibrissal somatosensory inputs are relayed from the periphery to the brainstem, thalamus and neocortex, where morphologically and functionally distinct somatotopic maps termed *barrellettes* (brainstem), *barreloids* (thalamus) and *barrels* (cortex) can be detected that replicate the patterned organisation of the vibrissa on the snout (Erzurumlu and Jhaveri, 1992; Waite et al., 2000; Deschênes et al., 2005; Diamond et al., 2008) (**FIGURE 1.2**). The highly segregated organisation of the rodent vibrissal system therefore represents a unique opportunity to address key questions regarding somatosensory transmission.

1.2 OVERVIEW OF THE RODENT VIBRISSAL SYSTEM

On each side of a rodent's snout there are vibrissa arranged into five rows, designated A-E and numbered in arcs in a posterior-anterior fashion, thus enabling individual vibrissae to be identified using coordinates, (e.g. D2; **FIGURE 1.2**). Each vibrissa is anchored to the skin by a follicle and innervated by peripheral branches of the infraorbital nerve of the trigeminal

ganglion, whose nerve endings convert mechanical energy into action potentials via low-threshold mechanoreceptors (Dorfl, 1985). These afferents carry vibrissa-specific information past the cell bodies of the trigeminal ganglion to form somatotopic focalized terminal arbors, termed *barrelettes*, in the principal sensory (PrV) and spinal interpolaris (SpVi) trigeminal nuclei in the brainstem (Torvik, 1956; Clarke and Bowsher, 1962; Belford and Killackey, 1979a; b; Ma and Woolsey, 1984; Waite and Tracey, 1985; Ma, 1991; 1993) (**FIGURE 1.2)**. From the trigeminal ganglion, second-order PrV and SpVi neurons project to the downstream thalamic and cortical somatosensory centres via two main parallel pathways (**FIGURE 1.2)**:

1. A LEMNISCAL PATHWAY, which arises from PrV neurons, transits through the ventrobasal thalamus (VB) before terminating in the granular zone of the primary somatosensory (S1) cortex (Woolsey and Van der Loos, 1970; Killackey, 1973; Pierret et al., 2000; Veinante et al., 2000a).

2. A PARALEMNISCAL PATHWAY, which arises from the SpVi, transits through the posteromedial nucleus (POm) (Pierret et al., 2000; Veinante et al., 2000a; Furuta et al., 2006) and projects to the dysgranular zone of the S1 cortex (Koralek et al., 1988; Lu and Lin, 1993; Bureau et al., 2006), the secondary somatosensory (S2) cortex (Carvell and Simons, 1987; Alloway et al., 2000; Pierret et al., 2000), the primary motor cortex (Castro-Alamancos and Connors, 1997) and other subcortical brain regions (Diamond et al., 2008).

An extralemniscal pathway, has also been identified, which arises from the caudal part of the SpVi, projects in parallel to the lemniscal and paralemniscal pathways to the ventrolateral domain of the VB (Pierret et al., 2000; Furuta et al., 2006) and terminates in the septa between the S1 and S2 cortical areas (Pierret et al., 2000). In addition, a fourth pathway has also been recently reported (Urbain and Deschênes, 2007), which ascends from the PrV through the VB, although the cortical targets of the pathway have not yet been determined.

PrV neurones that give rise to the lemniscal pathway possess dendrites spatially confined within the limits of their respective barrelettes, and thus their receptive fields are dominated by a single vibrissa (Ma and Woolsey, 1984; Henderson and Jacquin, 1995; Veinante and Deschênes, 1999). In contrast, SpVi neurons possess dendritic trees that extend across several barrelettes, and thus respond vigourously to the deflection of several vibrissae (Jacquin et al., 1989; Veinante et al., 2000a). Consequentially, PrV targets in the VB and S1 cortex faithfully maintain the patterned organisation of terminal arbors in two further somatotopic maps, termed *barreloids* in the VB (Barbaresi et al., 1986; Harris, 1986; Ohara and Havton, 1994; Veinante et al., 2000a; Varga et al., 2002) and *barrels* in the S1 cortex (Woolsey and Van der Loos, 1970; Welker, 1971; 1976; Killackey, 1973; Simons, 1978; Killackey and Belford, 1979), whereas this high degree of somatotopy is not maintained to the same extent in SpVi targets, such as the POm (Jacquin et al., 1989; Veinante et al., 2000a).

As a pivotal component of this project relies upon the patterned organisation of the vibrissa on the snout to be faithfully maintained in the thalamus, all experiments were carried out in the VB. For this and other reasons (see the last paragraph in section 2.2.1 below), the POm shall not be further discussed, but for a comprehensive review of POm structure and function, see Deschênes et al., (2005).

It is important to note however that information processing in the PrV and SpVi are not completely isolated from each other, in that the PrV receives projections from the SpVi (Jacquin et al., 1990). As the SpVi relays multivibrissa responses to the PrV via internuclear axons, this renders PrV neurones, and the downstream targets of their afferent projections, responsive to adjacent vibrissa (Minnery and Simons, 2003; Timofeeva et al., 2004). However, even though neurones in each of the somatotopic maps (PrV barellettes, VB barreloids, S1 barrels) possess receptive fields that extend to several vibrissae, it is usually clear – both in anaesthetized and in awake animals – that a single, topographically appropriate vibrissa exercises the strongest influence on a neurone's firing (Ma and Woolsey, 1984; Bourassa et al., 1995; Henderson and Jacquin, 1995; Veinante and Deschênes, 1999; Desîlets-Roy et al., 2002; Petersen, 2007; Alloway, 2008). In this way, the somatotopic maps of the vibrissal system are able to tell the brain not only what kind of sensory information it is receiving, but also where on the snout this information is being sensed.

CHAPTER 1 FIGURES

		Page Number
FIGURE 1.1	Basic circuitry formed between first-order and higher-order thalamic nuclei, cortex and TRN.	7
FIGURE 1.2	Schematic organisation of the rodent vibrissal system.	8

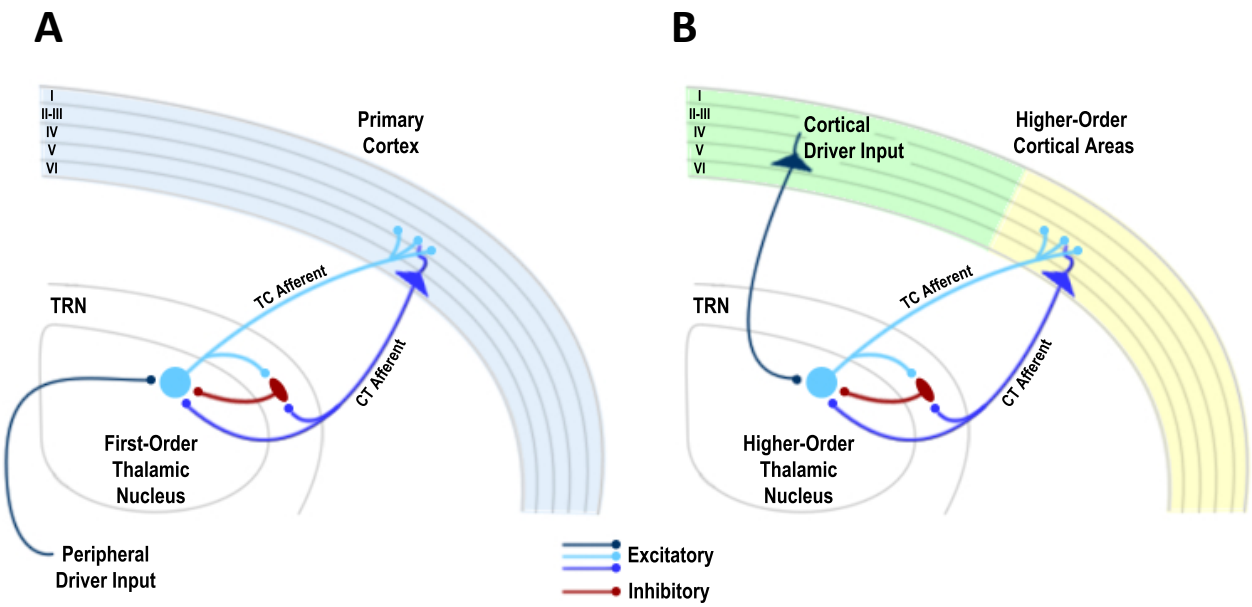

FIGURE 1.1 Basic circuitry formed between first-order and higher-order thalamic nuclei, cortex and TRN. First-order nuclei receive driver inputs from peripheral sources (**A**), with higher-order nuclei receiving driver inputs from cortical layer V (**B**). All thalamic nuclei project thalamocortical (TC) afferents to layer IV of the cortex, and also receive reciprocal *modulatory* corticothalamic (CT) inputs from layer VI, which modulate how driver inputs are transmitted (Sherman and Guillery, 2001). Both TC and CT afferents also innervate the associated TRN, which serves to provide feedback inhibition to thalamic nuclei.

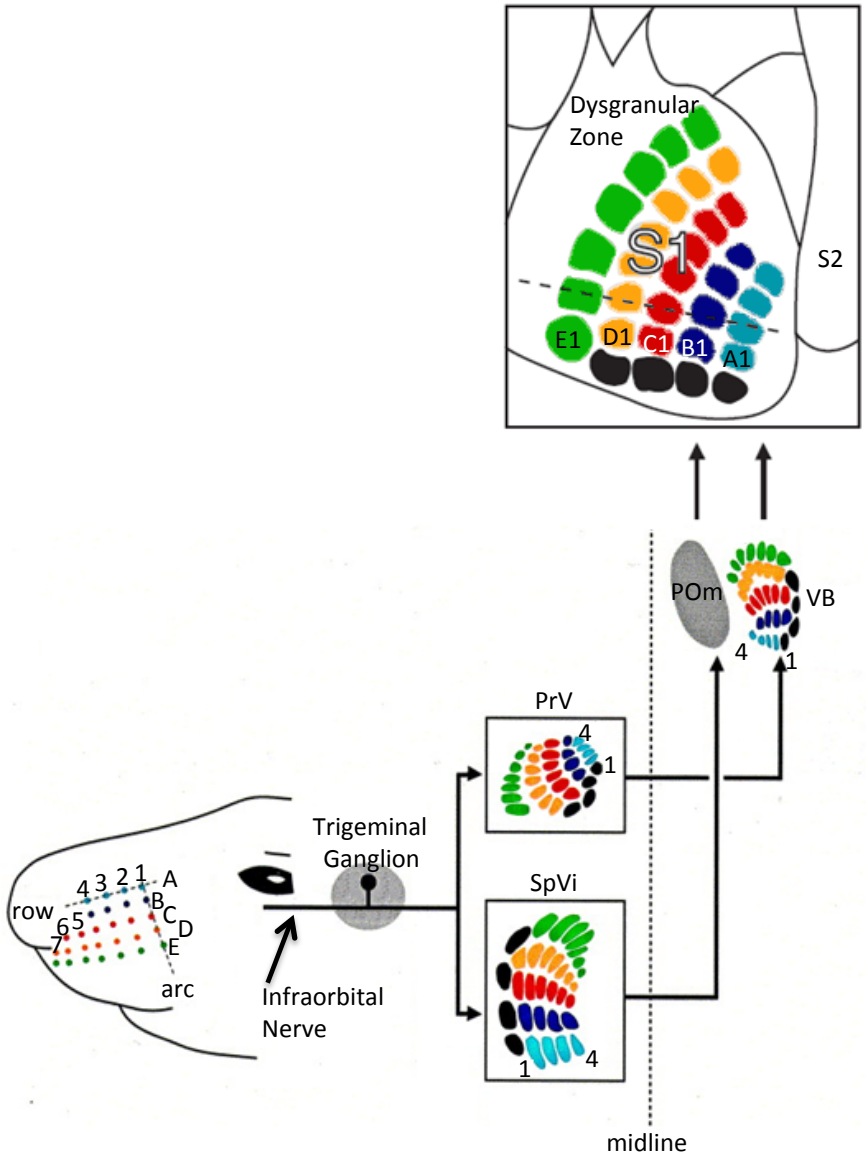

FIGURE 1.2 Schematic organisation of the rodent vibrissal system. The patterned organisation of the vibrissa on the rodent snout (rows A-E, arcs 1-7) is faithfully maintained centrally by arrays of cellular aggregates in the brainstem PrV and SpVi nuclei, the VB, and S1 cortex. PrV – principal sensory trigeminal nucleus; Pom – posteromedial nucleus; S1 – primary somatosensory cortex; S2 – secondary somatosensory cortex; SpVi – spinal interpolaris trigeminal nucleus; VB – ventrobasal thalamic nucleus. Adapted from Deschênes et al., (2005).

CHAPTER 2 THE SOMATOSENSORY THALAMUS

2.1 THE VENTROBASAL THALAMUS

2.1.1 BASIC CIRCUITRY AND NOMENCLATURE

The rodent VB is a somatosensory thalamic nucleus complex comprising the ventroposteromedial nucleus, the ventroposterolateral nucleus and the ventroposteroinferior nucleus (Sherman and Guillery, 2001). It is classed as a first-order thalamic nucleus as it receives driver inputs exclusively from the PrV via the lemniscal pathway (Woolsey and Van der Loos, 1970; Killackey, 1973; Pierret et al., 2000; Veinante et al., 2000a). Common to all thalamic nuclei, thalamocortical afferents project to layer IV of the cortex, and also receive reciprocal *modulatory* corticothalamic inputs from layer VI, which modulate how driver inputs are transmitted (Guillery, 1995; Sherman, 2007). Both thalamocortical and corticothalamic afferents also innervate the associated thalamic reticular nucleus (TRN), which serves to provide both feedback and feedforward inhibition to thalamic nuclei upon thalamocortical and corticothalamic innervation, respectively (Jones, 1985; Salt, 1989; Shosaku et al., 1989; Pinault and Deschênes, 1998a; b; Crabtree, 1999) (**FIGURE 2.1**). In the rodent VB, this circuitry specifically comprises of reciprocal thalamocortical and corticothalamic afferents, which project from/to the VB, to/from layer IV/VI of the S1 cortex and to the internal tier of the somatosensory sector of the TRN (Harris and Hendrickson, 1987; Pinault, 1994; Pinault and Deschênes, 1998a). The rodent VB possesses this basic thalamo-cortico-thalamic circuitry without any additional components (e.g. inhibitory interneurones, additional afferent projections) (Ralston, 1983; Jones, 1985;

Barbaresi et al., 1986; Harris and Hendrickson, 1987; Ohara and Lieberman, 1993; Sherman and Guillery, 2001) thus making it an ideal candidate with which to understand the basic principles of thalamic function.

It is important to note however that some first-order and higher-order nuclei also contain higher-order and first-order circuits. For example, the POm receives principal driver inputs from both the periphery via the paralemniscal pathway and from layer V of the S1, S2, motor, perirhinal and insular cortices (Hoogland et al., 1987; Deschênes et al., 1998; Veinante et al., 2000b), and thus possesses a complex circuitry in comparison to that of the first-order VB. Such nuclei may be considered *mixed* nuclei (Sherman and Guillery, 2001).

2.1.2 Neurones of the Ventrobasal Thalamus

Clustered into their respective barreloids, VB neurones respond strongly to stimulation of a single somatotopically-related vibrissa (Bourassa et al., 1995; Veinante and Deschênes, 1999; Desîlets-Roy et al., 2002), and more weakly to that of one to four adjacent vibrissae (Simons and Carvell 1989; Armstrong-James and Callahan, 1991; Chiaia et al., 1991; Diamond et al., 1992; Friedberg et al., 1999; Minnery et al., 2003), which can be attributed to the SpVi-PrV internuclear projection (Jacquin et al., 1990). The VB comprises a single class of neurone (Ralston, 1983; Barbaresi et al., 1986; Harris and Hendrickson, 1987; Ohara and Lieberman, 1993), which receive only three main types of input to morphologically distinct areas of the dendritic tree:

1. An ascending excitatory input from PrV axons that makes synaptic contacts onto thick proximal dendrites (Spacek and Lieberman, 1974; Williams et al., 1994).

2. An excitatory corticothalamic input from the S1 cortex that principally distributes over the distal dendrites (Hoogland et al., 1987; Mineff and Weinberg, 2000).

3. An inhibitory input from TRN neurones that distributes throughout the dendritic tree (Ohara and Lieberman, 1993; Varga et al., 2002)

The dendritic field of VB neurones comprises of thick proximal dendrites that remain within the confines of their home barreloid, and bushy radiating distal dendrites that extend beyond the perimeter of their home barreloid into neighbouring barreloids (Barbaresi et al., 1986; Harris, 1986; Ohara and Havton, 1994; Land et al., 1995; Haidarliu and Ahissar, 2001; Varga et al., 2002) (**FIGURE 2.2**). This extension of the dendritic field is thought to be key in the mediation of sensory discriminative processes by the TRN, via the induction of differential modes of inhibitory innervation (Salt, 1989; Lavallee and Deschênes, 2004), which can be manipulated to provide a framework with which to study TRN function.

2.2 The Thalamic Reticular Nucleus

2.2.1 Multimodal Function

The rodent TRN has been demonstrated to comprise at least seven major sectors, five sensory (somatosensory, auditory, visual, visceral and gustatory) (Price and Slotnick, 1983; Shosaku and Sumitomo, 1983; Shosaku et al., 1984; Cornwall et al., 1990; Villa, 1990; Hayama et al., 1994; Coleman and Mitrofanis, 1996; Stehberg et al., 2001), one motor and one limbic (Gonzalo-Ruiz and Lieberman, 1995a; b; Pinault and Deschênes, 1998a). Although there are olfactory inputs to the mediodorsal nucleus of the thalamus of the rat (Price and Slotnick, 1983), which has been demonstrated to be reciprocally connected with the rostral part of the TRN (Groenewegen, 1988; Cornwall et al., 1990; Pinault and Deschênes, 1998a), it has yet to be determined whether there is an olfactory TRN sector. Each sector has its own anatomical organisation, which is determined by the efferent and afferent connections each sector has with its corresponding first-order or higher-order nucleus and related cortical areas (Pinault, 1994; Cox et al., 1995; Pinault and Deschênes, 1998a). In the somatosensory sector of the rodent TRN there are three reticular tiers (internal, intermediate and external), with those projecting to first-order nuclei, such as the VB, displaying a well-defined topography (Guillery and Harting, 2003), which is not observed in tiers that project to higher-order nuclei, such as the POm (Lozsadi, 1994; Pinault, 1994; Pinault and Deschênes, 1998a).

2.2.2 BASIC CIRCUITRY

Composed exclusively of gamma amino butyric acid (GABA) neurones (Houser et al., 1980), the TRN surrounds the entire anteroposterior extent of the dorsal thalamus; therefore dictating that all thalamocortical and corticothalamic projections must pass through its mesh of inhibitory interneurons (Jones, 1985). As indicated in Chapter 1, branching collaterals from excitatory thalamocortical and corticothalamic axons innervate the TRN, and the TRN sends a reciprocal inhibitory projection back to the thalamic area from which it receives its thalamocortical innervation (Jones, 1985; Salt, 1989; Shosaku et al., 1989; Pinault and Deschênes, 1998a; b; Crabtree, 1999) (**FIGURE 1.1**).

Various anatomical and functional studies have attempted to demonstrate the mechanism by which interneuronal communication within the rodent TRN is mediated (Scheibel and Scheibel, 1966; Ahlsen and Lindstrom, 1982; Ohara and Lieberman, 1985; Pinault et al., 1997; Sanchez-Vives et al., 1997; Liu and Jones, 1999; Landisman et al., 2002; Pinault, 2004; Zhang and Jones, 2004). Ahlsen and Lindstrom (1982) were the first to record mutual inhibitory syntaptic interactions between TRN neurones in anaesthetised cats, and it was later shown in ferrets that local application of glutamate *in vitro* in the visual sector of the TRN was able to induce $GABA_A$-dependent inhibitory postsynaptic potentials (IPSPs) in neurones closely located to the site of the application (Sanchez-Vives et al., 1997). In addition, disynpatic or polysynaptic $GABA_A$-mediated inhibitions have also been recorded in mouse TRN *in vitro* slice preparations following focal electrical stimulation of layer VI in the related cortical area (Zhang and Jones, 2004). Taken together, these findings strongly suggest that excitation of a subset of TRN neurones can trigger widespread inhibitions in the

TRN (Ulrich and Huguenard, 1996; Sanchez-Vives et al., 1997; Debarbieux et al., 1998; Zhang and Jones, 2004). However, a separate *in vitro* study comprising dual single-cell recordings in rodent thalamic slices was unable to reveal the presence of inhibitory chemical synaptic connections between adjacent TRN neurones (Landisman et al., 2002). In this study, paired-cell recordings in rodent thalamic slices demonstrated the presence of functional electrical neuronal couplings in the TRN, whereby the morphological substratum was thought to be gap junctions. However, despite such electrical synapses having not yet been observed during ultrastructural analyses of the TRN in various species (Deschênes et al., 1985; Yen et al., 1985; Ohara and Lieberman, 1985; Ohara, 1988; Pinault et al., 1997; Liu and Jones, 2003), it is important to highlight that such close membrane junctional complexes are difficult to see in the brain, even in the cerebral cortex (Tamas et al., 2000). Therefore, neither the anatomical substrate of potential synaptic neurone-neurone communications in the TRN has been established (see Figure 2.1C for purported intra-TRN connections), nor has the exact function of this widespread inhibition been determined. However, it has been postulated that the purpose of this mechanism is to limit the number and synchrony of TRN neuronal bursts (Sohal and Huguenard, 2003).

In addition to the thalamocortical and corticothalamic glutamatergic afferents, the TRN also receives GABAergic (Pare et al., 1987; Cucchiaro et al., 1993; Gandia et al., 1993; Asanuma, 1994), cholinergic and monoaminerigic (Cropper et al., 1984; Woolf and Butcher, 1986; Hallanger et al., 1987; Levey et al., 1987; Asanuma, 1992; Huang et al., 1992) inputs, most of which are thought to be involved in the control of vigilance (Pinault, 2004).

2.2.3 Neurones of the Thalamic Reticular Nucleus

TRN axons, which can emerge from either the soma or dendrite of a neurone, penetrate the thalamus perpendicular to the thalamus-TRN interface (Minderhoud, 1971; Pinault, 1994; 1996) and terminate in arbours complementary to the somatodendritic architecture of the corresponding postsynaptic VB neurone (Pinault and Deschênes, 1998a). Although the rodent VB does not contain any inhibitory interneurones (Ralston, 1983; Barbaresi et al., 1986; Harris and Hendrickson, 1987; Ohara and Lieberman, 1993), in those thalamic nuclei that do possess them (Sherman and Guillery, 2001; Jones, 2007), they do not appear to be a major synaptic target of TRN axon terminals (Liu et al., 1995; Wang et al., 2001).

TRN axons innervate almost all thalamic nuclei according to a loose parallel pattern (Scheibel and Scheibel, 1966; Jones, 1975; Hale et al., 1982; Steriade et al., 1984; Velayos et al., 1989; Gonzalo-Ruiz and Lieberman, 1995a; Kultas-Ilinsky et al., 1995; Tai et al., 1995). Specifically, adjacent TRN neurones whose somatodendritic domains do not overlap project to adjacent but distinct areas in the corresponding thalamic nucleus; whereas those with overlapping somatodendritic domains also have overlapping terminal arbours. However, divergent TRN projections have also been demonstrated to exist (Scheibel and Scheibel, 1966; Steriade et al., 1984; Kolmac and Mitrofanis, 1997; Pinault and Deschênes, 1998b). For example, a minority of TRN neurones in the rodent somatosensory sector (<5%) possess axons that bifurcate, innervating both the first-order VB and the functionally related higher-order POm (Pinault and Deschênes, 1998a). From a functional viewpoint, the TRN may therefore be acting as a *hub* (Llinas and Pare, 1997), modulating ongoing thalamocortical activity not only in separate parallel processes, but also interactions between pathways

involving distinct but functionally related thalamic nuclei. Such circuitry would provide the TRN with the power to select appropriate intrathalamic pathways for the perception and/or execution of sensory, motor and cognitive tasks.

2.3 Recurrent and Lateral Inhibition

By taking advantage of the highly segregated organisation of the rodent vibrissal system, it has been possible to demonstrate, both anatomically and physiologically, the presence of both closed- and open-loop circuits formed between the thalamus and the TRN, which lead to the generation of recurrent and lateral inhibitions, respectively (**Figure 2.3**).

Using a double-labelling protocol, it was revealed that TRN neurones exclusively project within the limits of the VB barreloid representing the principal vibrissa of their receptive field (Desîlets-Roy et al., 2002). Therefore, when considering the anatomy of VB neurones described above - that is that the dendritic field of VB neurones can extend beyond the perimeter of their home barreloid into neighbouring barreloids (Barbaresi et al., 1986; Harris, 1986; Ohara and Havton, 1994; Land et al., 1995; Haidarliu and Ahissar, 2001; Varga et al., 2002) – a single TRN neurone should be able to exert both recurrent inhibition on VB neurones located within the barreloid from which it receives its innervation, whilst also exerting a simultaneous lateral inhibition onto VB neurones whose dendrites extend into the activated barreloid.

Indeed, both *in vitro* (Pinault and Deschênes, 1998a; Gentet and Ulrich, 2003) and *in* vivo (Shosaku, 1986; Shosaku et al., 1989) studies have revealed VB-TRN neuronal pairs with closed disynaptic loops. Using a double-labelling protocol, Pinault and Deschênes (1998b), were able to provide evidence that VB-TRN cells do form closed disynaptic loops, and Shosaku (1986) was able to demonstrate that VB and TRN neurones with receptive fields on the same vibrissa could interact with each other via induction of excitations and/or inhibitions. This reciprocal interaction is thought to be the basis upon which the TRN is able to exert recurrent inhibition in thalamic nuclei.

In addition, Pinault and Deschênes (1998a) were also able to demonstrate histologically the presence of open dysynaptic loops formed between the VB and TRN, which are thought to mediate lateral inhibition. A recent study combining *in vitro* and *in vivo* techniques also provided a comprehensive demonstration of lateral inhibition: using a preparation whereby VB neurones were rendered monovibrissa-responsive by lesion of the SpVi, Varga et al., (2002) were able to demonstrate that lateral inhibition strongly correlates with the degree to which dendrites extend into an adjacent barreloid.

Lateral inhibition is asymmetrically distributed with respect to adjacent vibrissae due to anatomical restrictions: barreloids are centre-to-centre spaced ~100µm apart within rows and ~200µm between rows (Land et al., 1995; Haidarliu and Ahissar, 2001), and as the dendritic fields of VB neurones do not exceed 250µm (Ohara and Havton, 1994; Varga et al., 2002), these factors physically limit the spread of dendrites into a barreloid of a different

row. In accordance with this constraint, most VB neurones fail to demonstrate lateral inhibition following stimulation of vibrissae in an adjacent row (Deschênes et al., 2005). Despite this large amount anatomical and physiological data, neither the functional significance nor the relative importance of these two types of inhibition have been determined in any thalamocortical circuit or species (Pinault, 2004). However, this circuitry within the rodent VB-TRN has been postulated to be of importance in sensory discriminative processes (Salt, 1989; Lavallee and Deschênes, 2004).

It is important to note that TRN afferent inhibition likely plays a more complex role in thalamic nuclei that possess GABAergic interneurones (Sherman and Guillery, 2001; Jones, 2007), even though these interneurones are themselves not direct targets of TRN afferent projections (Liu et al., 1995; Wang et al., 2001). Indeed, whilst the VB is void of inhibitory interneurones (Ralston, 1983; Barbaresi et al., 1986; Harris and Hendrickson, 1987; Ohara and Lieberman, 1993), it is well documented that these interneurones are present in other rodent thalamic nuclei, such as the visual lateral geniculate nucleus (LGN), and in thalamic nuclei of higher-order species such as the cat and non-human primate (Sherman and Guillery 2001; Jones, 2008). This further highlights the importance of first understanding thalamic operations in a simplified circuit model, such as that provided by the VB, before beginning to consider the functions of additional circuitry. Indeed, whilst the rodent thalamic nuclei are largely devoid of interneurones, there are more complex rodent thalamic nuclei, such as the mediodorsal thalamus, which receives excitatory driver inputs from both subthalamic and cortical areas, and also inhibitory innervations from not only the TRN, but also from the ventral pallidum (Ray et al., 1992; Ray and Price, 1992).

2.4 Layer VI Modulatory Corticothalamic Projection

The pathway from cortical layer VI to the thalamus is a property of all thalamic relay nuclei (for review see Sherman and Guillery [2001] and Jones [2007]). Its size in terms of the number of constituent neurones far exceeds that of the thalamocortical pathway by around 40 to 1 (Sherman and Koch, 1986), and it appears that most if not all corticothalamic axons branch to innervate TRN neurones en route to their innervation of thalamocortical neurones. Corticothalamic axon terminals in the TRN are much more numerous (~10 fold) than those of thalamocortical axons (Guillery, 1967; Jones, 1985), and thus this pathway is able to directly excite thalamocortical neurones and indirectly inhibit them via the TRN. This cortical input therefore likely plays an important role in the modulation of thalamocortical processing.

The rodent vibrissal system has also proved a useful model in understanding the anatomy as well as the physiological behaviour of the local circuitry due to its highly segregated organisation (Hoogland et al., 1987; Chiaia et al., 1991; Diamond et al., 1992; Lu and Lin, 1993; Golshani et al., 2001; Landisman and Connors, 2007; Cruikshank et al., 2010). However, despite these extensive anatomical findings, the functional significance of corticothalamic connections is poorly understood. Speculations about the function of corticothalamic connections include sharpening and/or amplifying receptive field responses, focusing attention and modulating receptive field properties based on contextual information (Steriade, 1993; Sherman and Guillery, 2002; Sillito and Jones, 2002).

CHAPTER 2 FIGURES

Page Number

FIGURE 2.1 Circuitry underlying the generation of feedback and feedforward inhibition in thalamic circuitry. 21

FIGURE 2.2 The relationship between barreloid structure and VB neurone dendroarchitecture. 22

FIGURE 2.3 VB circuitry underlying the generation of recurrent and lateral inhibition. 23

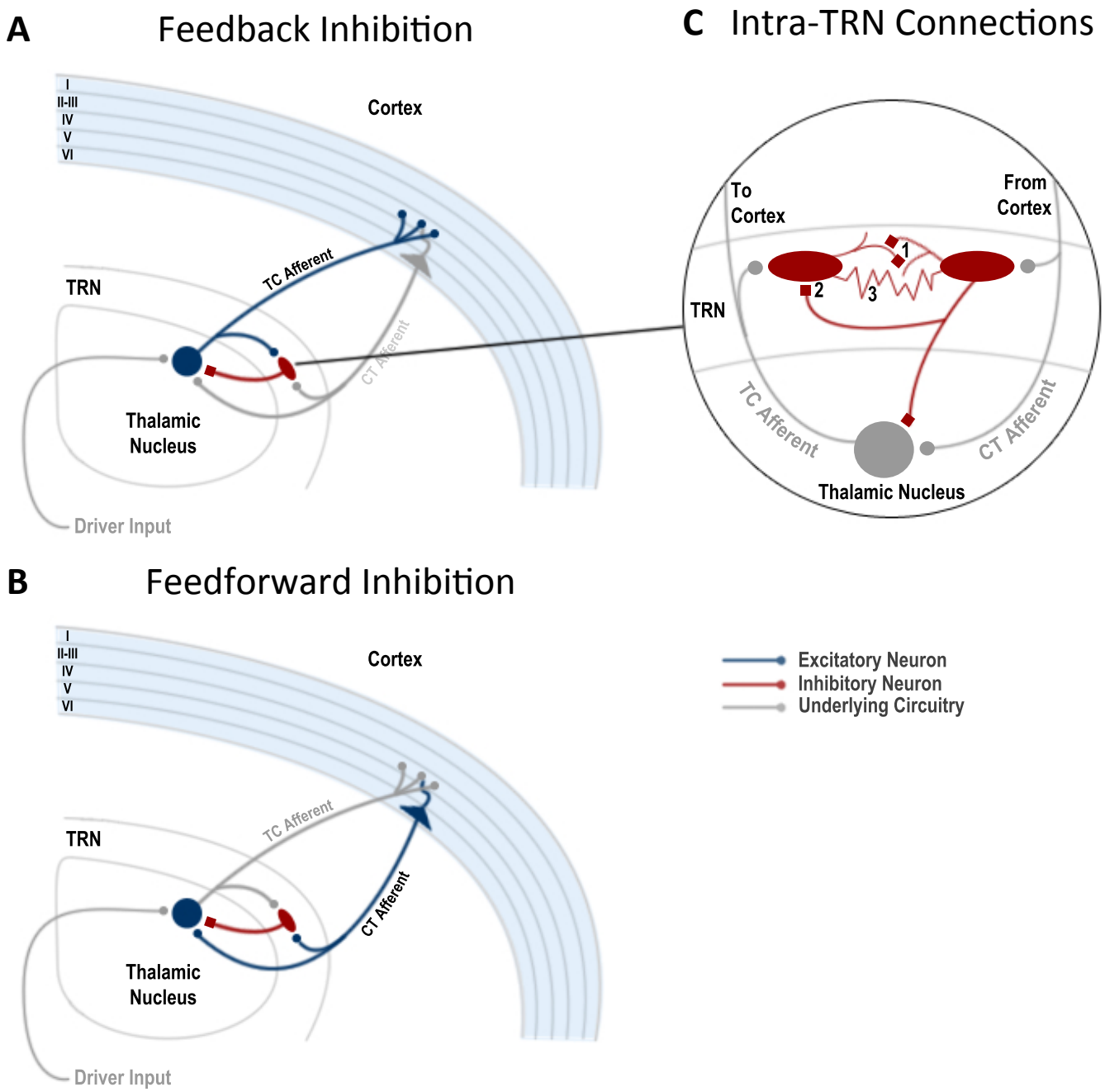

FIGURE 2.1 Circuitry underlying the generation of feedback and feedforward inhibition in thalamic circuitry. A. Thalamocortical afferents send an axon collateral to the TRN upon traversing this structure during its ascent to the cortex, with the TRN sending a reciprocal inhibitory projection back to the thalamocortical neurone from which it receives its innervation. Therefore, upon activation of the thalamocortical afferent, the TRN provides feedback inhibition. **B.** Layer VI corticothalamic afferents projecting to thalamic nuclei also send axon collaterals to the TRN. Therefore, upon activation of the corticothalamic afferent, the thalamocortical neurone receives a direct monosynaptic excitatory input and an indirect disynaptic feedforward inhibitory input from the TRN. **C.** Widespread inhibitions in the TRN, generated by intraneuronal TRN communcation, is thought to limit the number and synchrony of TRN neuronal bursts. However, the anatomical substrate of intraneuronal communication within the rodent TRN has not been definitively established, with three potential mechanisms that may facilitate mutual inhibitory interactions between TRN neurones identified: **1.** Dendrodentritic synapses; **2.**Axodendritic synapses; **3.** Gap junctions. Abbreviations: TC – thalamocortical; CT – corticothalamic; TRN – thalamic reticular nucleus.

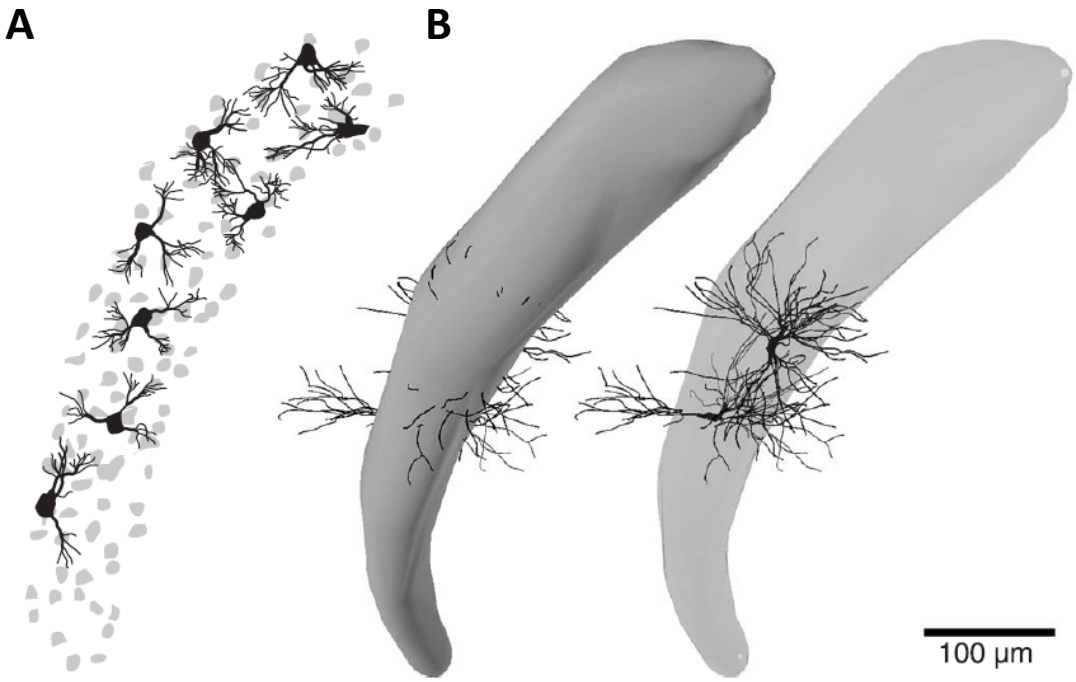

FIGURE 2.2 The relationship between barreloid structure and VB neurone dendroarchitecture. Adapted from Varga et al., (2002), the proximal dendrites of 8 VB neurones responsive to C1, C2 or D2 vibrissal stimulation were reconstructed following juxtacellular staining with Neurobiotin. VB neurones were placed in a reference barreloid (barreloid C2, outlined), in accordance with their actual location and orientation in their respective barreloid (**A**)**.** Note that thin distal dendrites do cross barreloid boundaries, whereas the thick proximal dedrites to not, as indicated in the renderings in **B** with and without transparency.

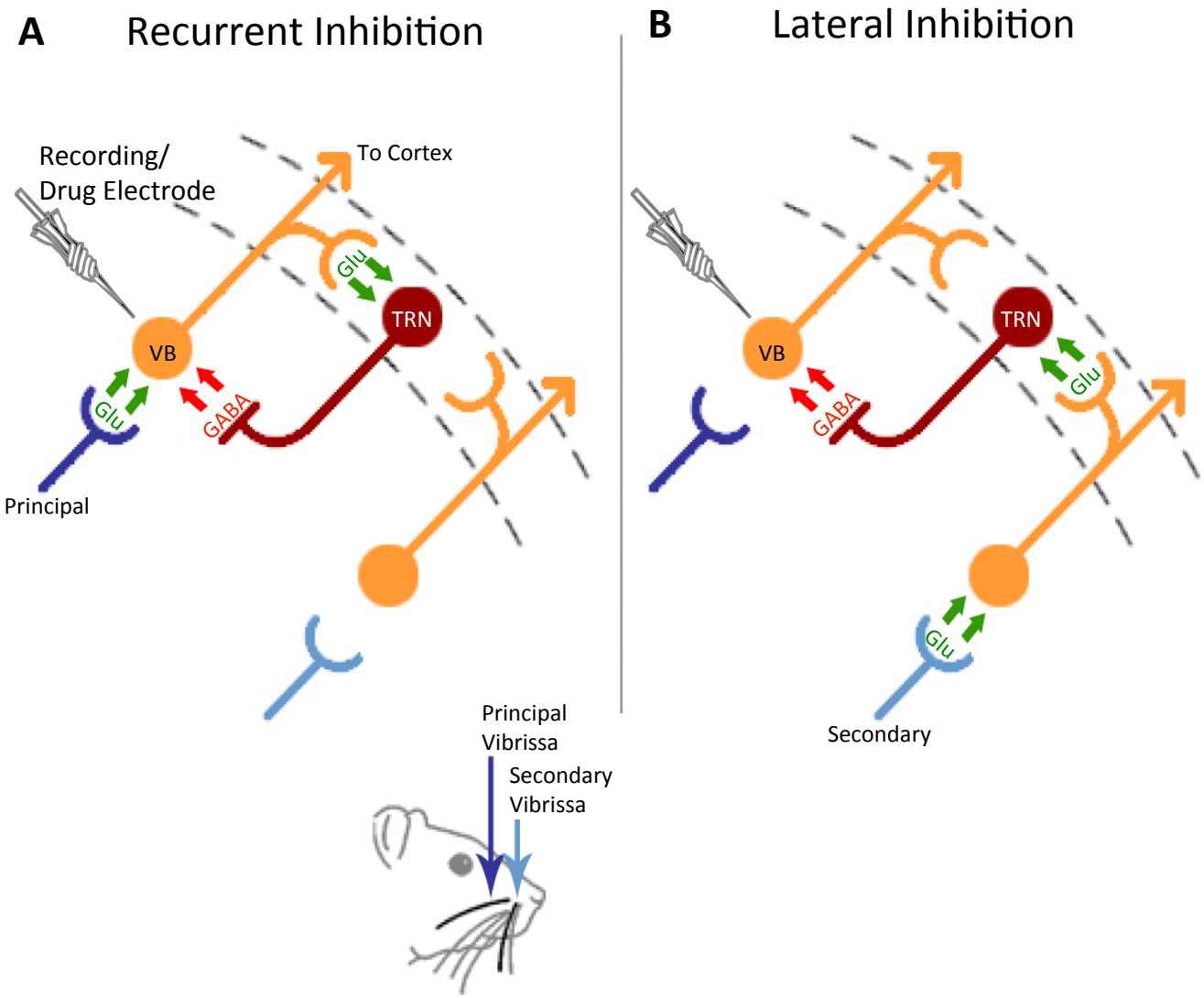

FIGURE 2.3 VB circuitry underlying the generation of recurrent and lateral inhibition. A. Stimulation of the principal vibrissa drives excitation in the VB neurone from which we are recording from (VB), which is followed by recurrent inhibition from the TRN. **B.** Stimulation of an adjacent secondary vibrissa drives a lateral inhibition in the VB neurones from which we are recording from, via the TRN. Abbreviations: Glu – Glutamate; VB – VB neurone; TRN – TRN neurone.

CHAPTER 3 THE GROUP II METABOTROPIC GLUTAMATE (MGLU) RECEPTORS

3.1 THE GLUTAMATERGIC SYSTEM

The amino acid L-glutamate is the major excitatory neurotransmitter in the central nervous system (Watkins and Evans, 1981; Fonnum, 1984) and likely mediates the majority of excitatory synaptic transmission between the excitatory pathways to and from the thalamus. Glutamate is known to act at two major receptor categories that have been extensively characterised: the ionotropic glutamate receptors and the metabotropic glutamate receptors (mGlu) (Nakanishi, 1992; Hollmann and Heinemann, 1994; Conn and Pin, 1997). There are three major types of ionotropic glutamate receptors: *N*-Methyl-D-aspartic acid (NMDA) receptors, α-amino-3-hydroxyl-5-methyl-4-isoxazole-propionate (AMPA) receptors and kainate receptors. Each of these receptor types is directly coupled to ion channels and facilitates fast synaptic transmission upon activation, whilst the mGlu receptors modulate slow synaptic transmission via intracellular messenger cascades (Hollmann and Heinemann, 1994; Nakanishi et al., 1998). The mGlu receptor type provides a mechanism for glutamate to fine-tune activity at the same synapses at which it evokes fast synaptic responses.

The Group II mGlu receptors (mGlu2/3) (see section 2.2 for mGlu receptor classification) represent a subclass of the mGlu receptor family, and the heterogeneous expression of these receptors throughout the central nervous system (CNS) suggests that they participate

in a wide variety of neuronal mechanisms, and therefore represent ideal targets for selective therapeutic compounds for the treatment of a number of associated CNS disorders.

3.2 mGlu Receptor Classification

All mGlu receptors are members of the G-protein-coupled receptor (GPCR) family, which transduce intracellular signals upon activation by bound agonist (Pin et al., 1994; Gomeza et al., 1996). Binding of agonist induces a conformational change in mGlu receptors, resulting in the activation of G-protein, which comprise a heteromeric complex of α, β, and γ subunits. When inactive, G-proteins are bound to guanosine 5'-diphosphate (GDP) and upon activation, G-proteins promote the exchange of guanosine5'-triphosphate (GTP) for GDP within the α subunit. Activated G-protein subunits then modulate the function of various effector molecules such as enzymes, ion channels and transcription factors via an intracellular signalling cascade. Inactivation of G-proteins occurs when bound GTP is hydrolysed to GDP, resulting in reassembly of the heterodimer (Conn and Pin, 1997).

The GPCR family comprises several subgroups, with the majority of classical neurotransmitter GPCRs belonging to family A. These receptors are often termed rhodopsin-like GPCRs and are structurally similar in that they consist of an extracellular N-terminal domain, seven transmembrane-spanning domains, and an intracellular C-terminus (Conn and Pin, 1997). In contrast to family A receptors, mGlu receptors belong to family C GPCRs. These receptors are distinguished from their family A relatives by the presence of a large

extracellular N-terminal domain that contains the orthosteric ligand-binding site (O'Hara et al., 1993; Okamoto et al., 1998; Jingami et al., 2003).

Thus far eight members of the mGlu receptor family have been identified in the rat using molecular cloning, and are termed the mGlu sub-type 1 (mGlu1) receptor to the mGlu sub-type 8 (mGlu8) receptor (Houamed et al., 1991; Masu et al., 1991; Abe et al., 1992; Pin et al., 1992; Tanabe et al., 1992; Nakajima et al., 1993; Iversen et al., 1994; Minakami et al., 1994; Okamoto et al., 1994; Saugstad et al., 1994; Duvoisin et al., 1995; Joly et al., 1995; Laurie et al., 1996). The mGlu receptors were named/numbered in their order of discovery, with the mGlu1 receptor (now known as the mGlu1a receptor) cloned first in 1991 (Houamed et al., 1991; Masu et al., 1991). Some human mGlu receptors have also been cloned and these share approximately 94% sequence homology with the rat mGlu receptors (Wu et al., 1998). Examination of the receptors' sequence homology, preferred signal transduction mechanism and relative pharmacology has enabled their classification into three distinct groups (Nakanishi, 1992; Conn and Pin, 1997):

1. GROUP I comprises the mGlu1 and mGlu5 receptors, which couple to G_q/G_{11} and activate phospholipase C_β, resulting in the hydrolysis of phosphotinositides and generation of inositol 1,4,5-triphosphate and diacyl-glycerol. This classical pathway leads to calcium mobilisation and activation of protein kinase C. However, it is now recognised that these receptors can modulate additional signalling pathways including other cascades downstream of G_q, pathways stemming from $G_{i/o}$, G_s, and

other molecules independent of G-proteins (Hermans and Challiss, 2001; Hou and Klann, 2004; Page et al., 2006; Li et al., 2007).

2. GROUP II consists of the mGlu2 and mGlu3 receptors, which couple predominantly to $G_{i/o}$ proteins (Gilman, 1989; Prezeau et al., 1992; Baba et al., 1993). $G_{i/o}$ linked receptors are classically coupled to inhibition of adenylyl cyclase (cAMP) and directly regulate ion channels and other downstream signalling partners via liberation of $G_{\beta\gamma}$ subunits (Tanabe et al., 1992; 1993; Baba et al., 1993; Prezeau et al., 1994a; Parmentier et al., 1996). As with Group I mGlu receptors, it is becoming increasingly evident that Group II (and Group III) mGlu receptors can also couple to other signalling pathways (Iacovelli et al., 2002), providing further complexity regarding the mechanisms by which these receptors can regulate synaptic transmission.

3. GROUP III includes the mGlu4, mGlu6, mGlu7 and mGlu8 receptors, and also couple predominantly to $G_{i/o}$ (see above for signal transduction pathway).

As a number of expression systems have been used to delineate these effects, it is important to note that mGlu receptors may couple to other second messenger pathways in normal physiological systems. In addition, as some experiments examining the transduction mechanisms have been elucidated by the expression of these receptors in non-neuronal cells, the exact transduction mechanisms in neuronal and glial cells may differ to those in

the non-neuronal cell types used in the expression systems (Prezeau et al., 1994b; Saugstad et al., 1994; Casabona et al., 1997; Conn and Pin, 1997; Tempia et al., 1998).

mGlu receptors of the same group show about 70% sequence homology, whereas between groups this percentage decreases to about 45% (Pin and Bockaert, 1995). mGlu receptor multiplicity can also be further generated through alternative splicing patterns, which often results in the generation of different C-terminal domains (Pin and Duvoisin, 1995; Laurie et al., 1996; Flor et al., 1997; Corti et al., 1998; Malherbe et al., 1999; Zhu et al., 1999; Valerio et al., 2001; Schulz et al., 2002; Sartorius et al., 2006). This is of importance as multiple proteins interact directly with the C-terminal domains of each of the mGlu receptor subtypes to regulate their trafficking and function (see review by Niswender and Conn [2010] for further details).

3.3 Group II mGlu Receptor Structure

As for all the mGlu receptor subtypes, the Group II mGlu receptors comprise a large extracellular N-terminus, a cysteine-rich domain (CRD), a seven transmembrane (7-TM) domain and an intracellular C-terminus tail (**Figure 3.1**).

3.3.1 The Venus Flytrap Domain

As mentioned above, mGlu receptors contain a large extracellular N-terminal domain, termed the venus flytrap domain (VFD), which contains the orthosteric binding site (O'Hara

et al., 1993; Okamoto et al., 1998; Jingami et al., 2003). Crystal structures of mGlu receptor N-terminal domains have revealed that each VFD consists of two lobes, with the orthosteric binding site located in the cleft formed between the two lobes (Kunishima et al., 2000; Tsuchiya et al., 2002; Muto et al., 2007). Evidence suggests that two VFDs dimerise together (see section 2.6.2.5 below), and large conformational changes are induced when agonists bind to one or both VFDs (Jingami et al., 2003). Three main states of the VFD dimer exist: open-open, open-closed, and closed-closed. The open-open (inactive) conformation is stabilised by antagonists; the open-closed and closed-closed conformations are induced by the binding of orthosteric agonists to one or both VFDs. The mutation of residues that prevent closure of the VFD can switch the pharmacology of antagonists to agonists (Bessis et al., 2002), indicating that the relative orientation of these domains is important for receptor activation.

3.3.2 Cysteine-Rich Domain

Conformational changes induced by orthosteric agonist binding are propagated from the VFD via the CRD to the 7-TM domain and C-terminal tail (Rondard et al., 2006; Muto et al., 2007). The CRD contains nine critical cysteine residues, eight of which are linked by disulfide bridges (Muto et al., 2007).

3.3.3 Seven Transmembrane Domain and Intracellular Loops

The 7-TM domain of mGlu receptors shows very low sequence homology with the 7-TM domain of other GPCRs (Pin et al., 2003). However, the 7-TM domains of mGlu receptors and other GPCRs share a similar general fold, with a relatively central helix 3, and a possible amphipathic helix 8 (Pin et al., 2003). The majority of characterised allosteric compounds that modulate mGlu receptor activity bind within the 7-TM domain (Schaffhauser et al., 2003; Hemstapat et al., 2007; Hampson et al., 2008; Rowe et al., 2008) (See section 3.4.3 for further details regarding Group II mGlu receptor allosteric modulators).

The intracellular components of the 7-TM domain are important in the functioning of the receptor, with an ionic interaction between intracellular residues of helices 3 and 6 key in maintaining the receptor in the inactive conformation (Binet et al., 2007); with the intracellular loops 2 and 3, as well as helix 8, important in G-protein coupling selectivity (Pin et al., 2003).

3.3.4 C-Terminus

The C-termini of mGlu receptors are important regions for modulating G-protein coupling. Additionally, this region of several of the mGlu receptors is subject to alternative splicing, regulation by phosphorylation, and modulatory protein-protein interactions (see review Niswender and Conn [2010] for further details).

3.3.5 DIMERISATION

For many years, the mGlu receptors were thought to exist as monomeric, non-interacting polypeptides. However, recent studies have revealed that these receptors do indeed form functional homodimers and heterodimers, stabilised by an intersubunit disulphide bond (Romano et al., 1996), and may even exist within higher-order structures (Gama et al., 2001; Tsuchiya et al., 2002; Bonde et al., 2006; Muto et al., 2007). It has been postulated that dimerisation of these receptors may play key roles in protein maturation, cell surface delivery and in providing a suitable framework to enable protein interactions for signal generation (Milligan, 2008). As a group of receptors that are the subject of intensive research for the development of therapeutic strategies for a number of diseases and disorders, the discovery that these receptors can form homomeric and heteromeric structures provides a new therapeutic target. Indeed, recent reports have suggested that mGlu2 receptors can form functional complexes with 5-hydroxytryptamine sub-type 2A (5-HT_{2A}) receptors via interactions through specific transmembrane helix domains (Gonzalez-Maeso et al., 2008); a structural relationship that may represent a promising new therapeutic targets in the treatment of psychosis.

There is some controversy as to whether binding of orthosteric agonist to only one VFD within the dimer is sufficient to activate the entire complex. In the case of the $GABA_B$ receptor, another family C GPCR which is a heterodimer consisting of $GABA_{B1}$ and $GABA_{B2}$ subunits, ligand binding to $GABA_{B1}$ is sufficient to activate the receptor (Galvez et al., 2000). However, this may not be the case for mGlu receptors: glutamate was unable to activate dimers formed by one wild-type and one mutant form of mGlu1, suggesting that glutamate

binding to one VFD is not sufficient for activation (Kammermeier and Yun, 2005); whereas Kniazeff at al., (2004) showed that one glutamate molecule can activate mGlu5 receptor homodimers. Furthermore, Suzuki et al., (2004) showed that glutamate binding to one VFD exerts negative cooperativity for binding to the second VFD, suggesting that glutamate binds to both dimers but that this binding can induce complexities in receptor pharmacology. Further work is therefore necessary to understand how agonist binding leads to activation of the 7-TM domain.

3.4 Group II mGlu Receptor Pharmacology

The conformationally restricted glutamate analog 1*S*3*R*-ACPD was the first compound to be identified as a selective mGlu receptor agonist, displaying no agonist or antagonist activity at ionotropic glutamates receptors at concentrations up to 100µM (Irving et al., 1990; Schoepp et al., 1991; Schoepp et al., 1992a). For this reason, 1*S*3*R*-ACPD was widely used in the study of mGlu receptors both *in vitro* and *in vivo*. However, this molecule has limited use, as it is a promiscuous mGlu receptor agonist with similar potency observed across all the mGlu receptor subtypes (Schoepp et al., 1992b; Cartmell et al., 1993; Kristensen et al., 1993; Tanabe et al., 1993; Wu et al., 1998), with the exception of mGlu7 (Flor et al., 1997; Wu et al., 1998). Intensive research into the synthesis of group and subtype selective compounds for the mGlu receptors has since ensued, with a dramatic increase in the number of selective compounds taking place in recent years. A summary of compounds active at the Group II mGlu receptors can be found in **Table 3.1**.

3.4.1 Selective Group II mGlu Receptor Orthosteric Agonists

The advent of modern Group II mGlu receptor pharmacology can be attributed to the synthesis of orthosteric agonists bearing a cyclopropyl moiety in their structure. DCG-IV and L-CCG-I, were the first such ligands with submicromolar potencies at both Group II mGlu receptor subtypes (Hayashi et al., 1992; Lombardi et al., 1993; Brabet et al., 1998; Mutel et al., 1998; Cartmell et al., 1999), but these compounds have been shown to activate other mGlu receptor subtypes at low micromolar concentrations. Synthesis of 2*R,*4*R*-APDC by replacing the C4-methylene group of 1*S*,3*R*-ACPD with an amino functionality, represented an improvement in selectivity and potency of available orthosteric Group II mGlu receptor agonists at the time of its discovery (Schoepp et al., 1995; Monn et al., 1996; Schoepp et al., 1996), but is now perceived to display a relatively low potency in comparison to currently available agonists: the glutamate analogue LY354740 was the first compound in a subsequent series to be synthesised displaying marked selectivity and potency for the Group II mGlu receptors (Monn et al., 1997; Schaffhauser et al., 1997; Schoepp et al., 1997; Schoepp et al., 1998; Wu et al., 1998) with EC_{50} values of 5.1nM and 24nM at the mGlu2 and mGlu3 receptors respectively (Schoepp et al., 1997). First characterised in non-neuronal cells expressing recombinant human mGlu receptor subtypes, it has since been used extensively to define the roles that the Group II mGlu receptors play in behavioural (Schoepp et al., 2003; Nordquist et al., 2008) and physiological (Flor et al., 2002; Moldrich et al., 2003) responses in both the human and rodent CNS *in vivo* and *in vitro*. LY354740 was followed by the synthesis of two further compounds, LY379268 and LY389795 (Monn et al., 1999), which display a further increase in potency.

There are no commercially available orthosteric agonists or antagonists that can differentiate between mGlu2 and mGlu3 receptors, with the exception of N-acetylaspartateglutamate (NAAG), which has been reported to selectively activate mGlu3 receptors (Wroblewska et al., 1997). However, see Chopra et al., (2009) for a report questioning the purity of commercially available preparations of NAAG.

Recently, there was an interesting addition to the Group II mGlu receptor toolbox upon the synthesis and characterisation of LY395756, a novel compound that possesses dual selectivity as an mGlu2 agonist and an mGlu3 antagonist (Dominguez et al., 2005).

3.4.2 Group II mGlu Receptor Orthosteric Antagonists

After the discovery of the non-selective mGlu receptor antagonist action of MCPG (Eaton et al., 1993; Jane et al., 1993; Kemp et al., 1994), several other phenylglycine derivatives were developed with the aim of finding Group II mGlu receptor-selective competitive antagonists. This resulted in the discovery of MTPG and MCCG, which display Group II mGlu receptor antagonist activity (Jane et al., 1995; Salt and Eaton, 1995a; Vignes et al., 1995; Bushell et al., 1996); however, these compounds also have activity at other mGlu receptor subtypes (Kemp et al., 1996; Thomsen et al., 1996). Since the development of these compounds, more potent and specific antagonists have been synthesised and include LY341495 and RS-APICA. LY341495 is a nanomolar potent antagonist at the Group II mGlu receptors with IC_{50} values of 2.3 and 1.3 at mGlu2 and mGlu3 respectively (Fitzjohn et al., 1998; Kingston et al., 1998; Ornstein et al., 1998; Johnson et al., 1999), but does possess submicromolar to

micromolar potencies at all other mGlu receptor subtypes (Schoepp et al., 1999). RS-APICA, which is selective for the Group II mGlu receptors with no significant effect at either of the other two sub-groups, possesses an unusual inverse agonist-like action and has been shown to increase extracellular glutamate concentrations (Krenz et al., 2000; Xi et al., 2002).

3.4.3 Group II mGlu Receptor Allosteric Modulators

The allosteric site on a given receptor is one that is topographically distinct from the orthosteric site for endogenous and exogenous agonists and competitive antagonists. Allosteric modulators act primarily by changing the three-dimensional receptor conformation, and thereby the affinities and/or efficacies of bound orthosteric ligand. As these compounds bind to a site distinct from the orthosteric sites, they are generally structurally diverse; unrelated to orthosteric ligands, particularly to the endogenous orthosteric agonists for the receptor type in question. Allosteric agonists are able to directly activate the receptor, whereas positive allosteric modulators (PAMs) act to potentiate the response of the receptor to orthosteric agonist without possessing any intrinsic agonist activity (**Figure 3.2A**). Negative allosteric modulators (NAMs) antagonise the activity of agonists in a non-competitive fashion by binding to a site other than the agonist (**Figure 3.2B**). Interestingly, truncation of the N-terminal domain of the mGlu5 receptor subtype results in a receptor that can be directly activated by PAMs (Goudet et al., 2004). This suggests that there is a conformational restraint induced by the VFD-CRD region that prevents PAMs from acting as agonists until orthosteric agonist is bound.

The concept of allosteric modulation has received considerable attention in recent years; in part due to the clinical success of the anxiolytic benzodiazepines, which enhance the function of the ionotropic $GABA_A$ receptor (Sigel and Buhr, 1997), but also due to numerous advantages that this compound class has over exogenous orthosteric compounds. Firstly, orthosteric agonists activate given receptors independently of their physiological state, whereas PAMs act to enhance the action of receptors activated by endogenous agonist. As a result, PAMs act to enhance physiological receptor activation with temporal and spatial relevance, and are therefore likely to possess a lower side effect profile than orthosteric agonists. For example, the $GABA_B$ receptor PAMs CGP7930 and GS39783 (Urwyler et al., 2001; 2003) do not elicit the hypothermic, sedative and muscle relaxant effects associated with the orthosteric agonist baclofen (Carai et al., 2004; Cryan et al., 2004). Secondly, PAMs are thought to induce either no or only low levels of receptor desensitisation, negating the consequence of receptor down-regulation that can occur upon persistent agonist treatment, as has been demonstrated for the $GABA_B$ receptor (Gjoni and Urwyler, 2008). Finally, many PAMs are highly selective for a specific receptor, given the lack of necessity for allosteric binding sites to be conserved during evolution. This is in contrast to the requirement for the orthosteric site to be conserved for binding of endogenous agonist. However, it is important to consider that this also represents a potential disadvantage for the use of allosteric modulators in experimental design and interpretation. Indeed, although the low evolutionary conservation of allosteric sites facilitates subtype selectivity, it is important to consider that this may result in significant differences across species.

The synthesis of pyridine-sulfonamide derivatives in the early 2000s represented the first such class of compound displaying PAM selectivity for the mGlu2 receptor. Biphenyl-indanone-A (BINA) and LY487379 are two of such compounds (Johnson et al., 2003; Schaffhauser et al., 2003; Poisik et al., 2005; Galici et al., 2006), with LY487379 being the most widely studied. LY487379 is a highly selective PAM at the mGlu2 receptor with no intrinsic agonist or antagonist activity, but does enhance responses to sub-maximal glutamate doses (EC_{50} value decreased 2-fold upon LY487379 application 0.72 vs. 1.7μM) (Johnson et al., 2003). First characterised in Syrian hamster AV-12 cells expressing human mGlu receptor subtypes using an intracellular Ca^{2+} assay, it has since been used for a number of behavioural and *in vitro* electrophysiology studies in the rodent CNS (Schaffhauser et al., 2003; Galici et al., 2005; Poisik et al., 2005; Harich et al., 2007; Nikiforuk et al., 2010). In addition, Group II mGlu receptor NAMs have been reported that block both mGlu2 and mGlu3 receptors (Hemstapat et al., 2007; Woltering et al., 2008a; Woltering et al., 2008b), however, they are not commercially available.

So far, there have been no reports of selective mGlu3 receptor allosteric modulators. Furthermore, no endogenous allosteric ligands, termed *endocoids* (Nicoletti et al., 2011), have been identified

3.4.4 XANTHURENIC ACID

Xanthurenic Acid is an endogenous metabolite of the kynurenine pathway that has recently been purported to be a selective Group II mGlu receptor agonist.

3.4.4.1 THE KYNURENINE PATHWAY

The kynurenine pathway is the principal metabolic route for the catabolism of tryptophan (Leklem, 1971) (**FIGURE 3.3**). Numerous studies since the 1970s have identified several intermediate kynurenines that can influence brain function, including quinolinic acid, which acts as a selective NMDA receptor agonist (Stone and Perkins, 1981), and kynurenic acid, which acts as a competitive antagonist at the ionotropic glutamate receptors (Perkins and Stone, 1982; Parsons et al., 1997) and the α7 nicotinic acetylcholine receptor (Wu et al. 2010; Hilmas et al., 2001; Grilli et al., 2006; Stone, 2007). The physiological function of kynurenic acid is thought to be neuroprotective, as it is released by astrocytes into the immediate vicinity of glutamatergic synapses, possibly acting to reduce the neurotoxic effects of excitatory amino acid (Guidetti et al., 1995; 2007; Ceresoli et al., 1997). These findings have raised the possibility that the kynurenine pathway and the metabolites of tryptophan could be involved in various neuroregulatory and neuropathological phenomenon in the CNS.

3.4.4.2 SYNTHESIS

Indoleamine 2,3 dioxygenase, which is present in the brain, transforms tryptophan into kynurenine that is either transaminated into kynurenic acid by kynurenine aminotransferase or hydroxylated into 3-hydroxykynurenine (3-HK) by kynurenine 3-hydroxylase; with transamination of 3-HK leading to XA synthesis (Gobaille et al., 2008). The XA pathway is thought to provide a detoxification process that reduces the concentration of 3-HK, as spontaneous oxidation of 3-HK induces free radical generation and apoptosis, both *in vitro*

and *in vivo* (Okuda et al., 1996; Wei et al., 2000). However, a transaminase specific for 3-HK has not been identified in man. In mammals, it is generally thought that 3-HK is transformed to XA by the same kynurenine transaminase isoenzymes that catalyse the transamination of kynurenine to kynurenic acid (Urenjak and Obrenovitch, 2000).

3.4.4.3 PURPORTED MECHANISMS OF ACTION

The activity of XA has been extensively studied in mosquitoes transmitting yellow fever (*Aedes aegypti*) and in anopheline mosquitos transmitting malaria (Gobaille et al., 2008). In comparison, the role of XA in mammals is not well defined, although a number of studies have indicated that XA may possess properties consistent neuromodulatory functions: wide-spread, heterogeneous CNS levels; accumulation in synaptic terminals; release of XA upon electrical stimulation (Gobaille et al., 2008); intracerebrocentricular XA administration inducing seizures (Lapin, 1978a; b); intraperitoneal administration in inducing sedation and anaesthesia (Heyliger et al., 1998; Fazio et al., 2012a); inhibition of vesicular glutamate transporters (VGLUTs) (Bartlett et al., 1998; Carrigan et al., 2002); selective activation of Group II mGlu receptors (Fazio et al., 2012a).

It was recently shown by Fazio et al., (2012a) that XA was able to inhibit forskolin (FSK)-induced cAMP formation in primary cultures of cerebellar granule cells, indicative of activation of $G_{i/o}$ coupled G-proteins such as that observed upon Group II/III mGlu receptor activation (Conn and Pin, 1997). Furthermore, XA was not able to activate phosphatidylinositol (PI) hydrolysis in mouse cortical slices, which is associated with G_q

coupled G-protein activation as that observed upon Group I mGlu receptor activation (Conn and Pin, 1997) (**FIGURE 3.4**). Upon this observation, HEK293 cells were transfected with either mGlu2, mGlu3, mGlu4 or mGlu7 receptors, and XA was found to significantly reduce FSK-induced cAMP formation in HEK293 cells expressing mGlu2 or mGlu3 receptors (**FIGURE 3.5**).

3.5 GROUP II MGLU RECEPTOR FUNCTIONAL ANATOMY

mGlu3 receptor expression is extensive throughout the brain, whereas that of the mGlu2 receptor is more restricted to specific brain regions (Ohishi et al., 1993a; b; Tanabe et al., 1993; Testa et al., 1994; Petralia et al., 1996a; Tamaru et al., 2001). mGlu2 receptors are uniquely localised in neurones (however see Taylor et al., [2005] and Mineff and Valtschanoff [1999] for evidence of glial mGlu2), particularly in the preterminal region of axons far removed from the active zone of neurotransmitter release (Yokoi et al., 1996; Lujan et al., 1997; Shigemoto et al., 1997; Tamaru et al., 2001), whereas mGlu3 receptors are found at both presynaptic and postsynaptic sites as well as in glial cells (Ohishi et al., 1993a; b; Tanabe et al., 1993; Testa et al., 1994; Makoff et al., 1996; Petralia et al., 1996a; Ciccarelli et al., 1997; Mineff and Valtschanoff, 1999; Aronica et al., 2000; Tamaru et al., 2001). Presynaptic Group II mGlu receptors are thought to be activated by an excess of synaptic glutamate, termed *glutamate spillover* (Ohishi et al., 1994; Wada et al., 1998; Vogt and Nicoll, 1999; Mitchell and Silver, 2000; Semyanov and Kullmann, 2000; Arnth-Jensen et al., 2002; Piet et al., 2003; 2004), or, alternatively, by glutamate released from astrocytes either via the cysteine-glutamate membrane antiporter (see Kalivas [2009]) or potentially via gliotransmission (see Santelio et al., [2012]). A major function of presynaptic Group II mGlu receptors is to inhibit neurotransmitter release (Ohishi et al., 1994; Anwyl, 1999;

Mitchell and Silver, 2000; Marti et al., 2001; Tamaru et al., 2001; Pisani et al., 2002) via mechanisms including the suppression of presynaptic voltage-dependent calcium channels, the activation of presynaptic potassium channels and the direct inhibition of regulated exocytosis (for a review, see Anwyl [1999]). It is important to note that the Group II mGlu receptors have also been shown to co-localise at synapses to modulate the release of not only glutamate, but also of GABA (Desai and Conn, 1991; Stefani et al., 1994; Poncer et al., 1995) and other neurotransmitters such as dopamine (Hu et al., 1999), 5-hydroxytryptatmine (5-HT) (Maione et al., 1998; Cartmell and Schoepp 2000; Lee and Croucher, 2003) and acetylcholine (Marti et al., 2001; Pisani et al., 2002). Whilst the Group II mGlu receptors do predominantly mediate presynaptic actions, these receptors are also expressed and able modulate neuronal function at post- and extra-synaptic localisations throughout the CNS (Conn and Pin, 1997; Niswender and Conn, 2010).

CHAPTER 3 FIGURES AND TABLES

		Page Number
FIGURE 3.1	Schematic representation of an mGlu receptor.	43
FIGURE 3.2	Schematic of typical PAM and NAM activity using an in vitro functional assay.	44
FIGURE 3.3	The kynurenine pathway.	45
FIGURE 3.4	XA effects on FSK-induced cAMP formation and PI hydrolysis in cerebellar granule cells and cortical slices, respectively.	46
FIGURE 3.5	XA effects on FSK-induced cAMP formation in HEK293 cells transiently transfected with mGlu2, mGlu3, mGlu4 or mGlu7 receptors	47
TABLE 3.1	Summary of Group II mGlu receptor ligands.	48

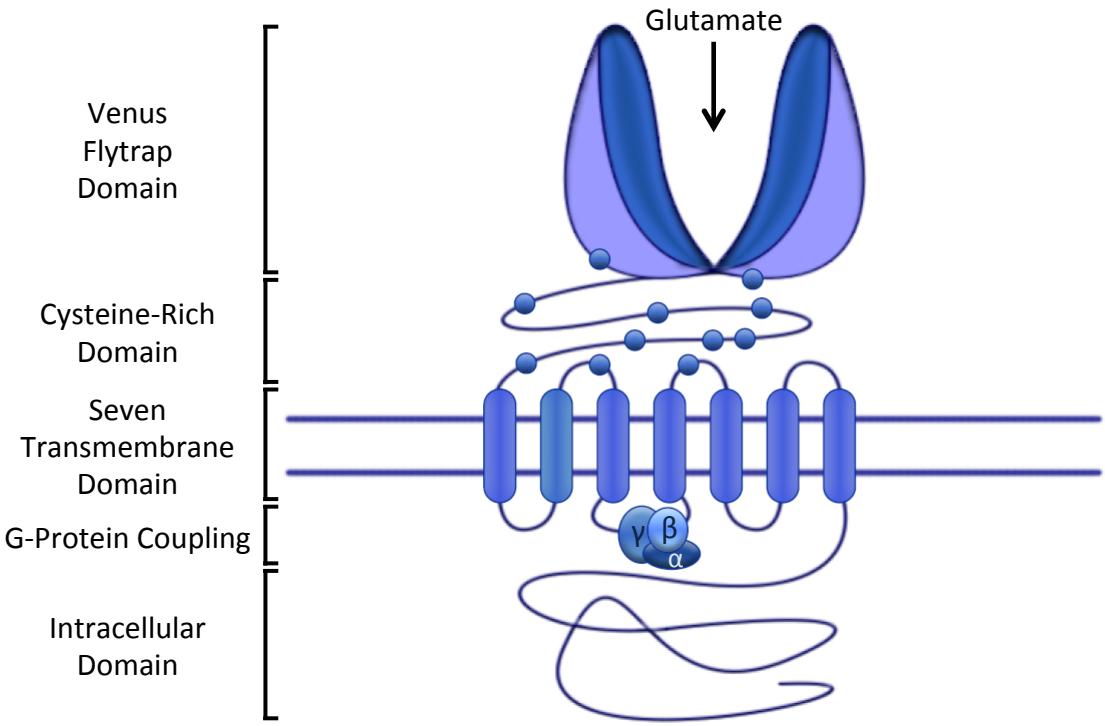

FIGURE 3.1 Schematic representation of an mGlu receptor. Common to all subtypes, mGlu receptors comprise a large extracellular N-terminus, which forms the orthosteric compound binding pocket, a cysteine-rish domain, a seven transmembrane domain, including intracellular loops, the later of which are important in G-protein coupling selectivity, and an intracellular C-terminus tail.

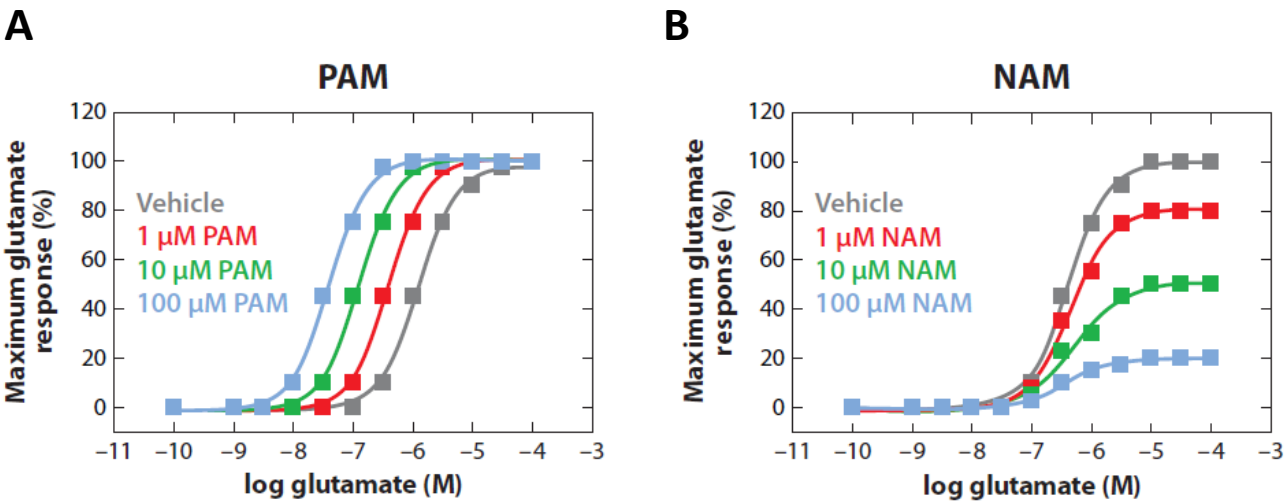

FIGURE 3.2 Schematic of typical PAM and NAM activity using an *in vitro* functional assay. In a given functional assay such as calcium mobilisation, increasing PAM concentrations (**A**) progressively shift the glutamate dose-response curve for mGlu receptor activation to the left, whereas increasing NAM concentrations progressively shift the magnitude of the glutamate dose-response curve whilst having little effect on potency (**B**), which is indicative of a type of non-competitive antagonism. Adapted from Niswender and Conn (2010).

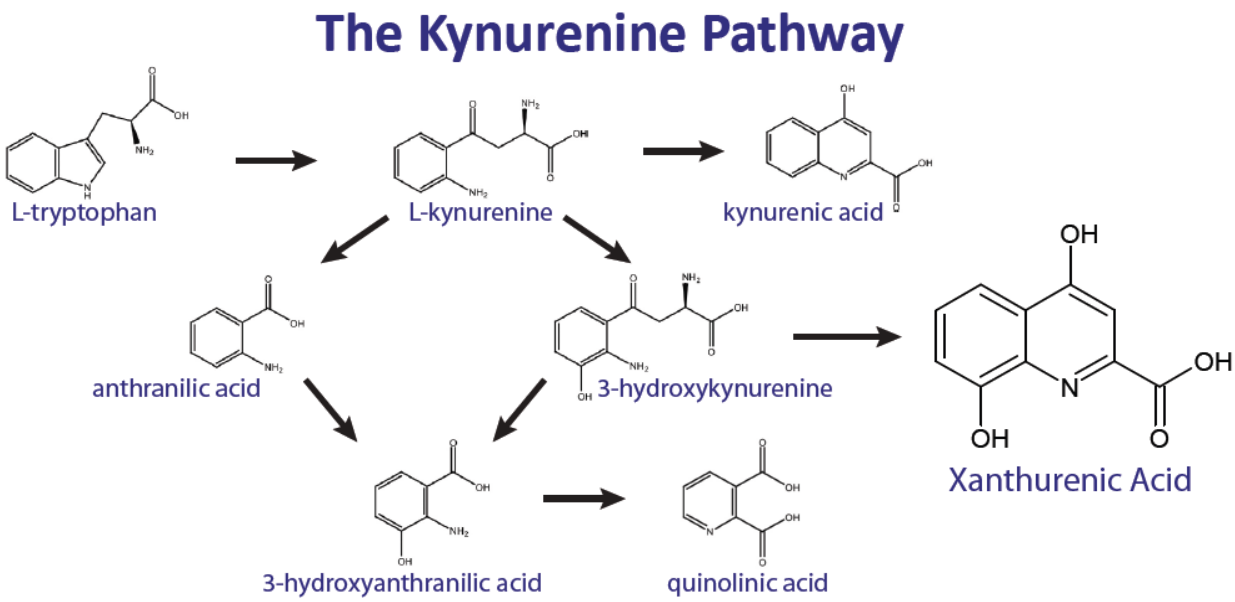

FIGURE 3.3 The kynurenine pathway.

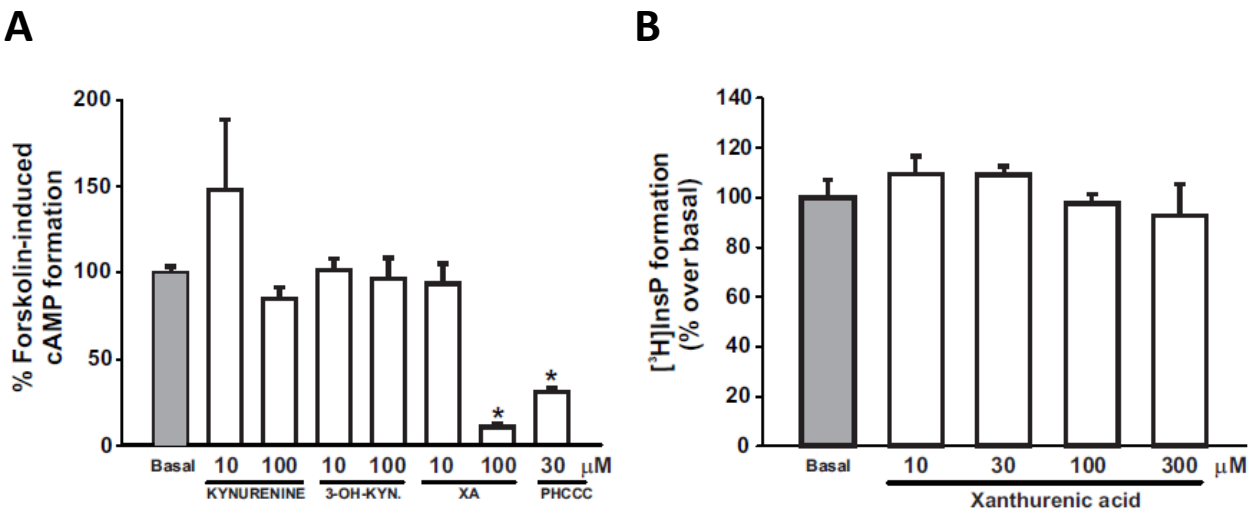

FIGURE 3.4 XA effects on FSK-induced cAMP formation and PI hydrolysis in cerebellar granule cells and cortical slices, respectively. A. Inhibition of FSK-induced cAMP formation by XA and PHCCC, an mGlu4 PAM, in cerebellar granule cells. Values were calculated from 6-8 determinations from two independent experiments. No effect was elicited by kynurenine or 3-OH-kynurenine, which are two XA parent compounds in the kynurenine pathway. **B.** Lack of effect of XA in stimulating PI hydrolysis in slices prepared from cortical slices of CD1 mice PN8-9 (n=9-15). Data are expressed as a percentage of the respective control values (mean ±SEM.). Adapted from Fazio et al., (2012a).

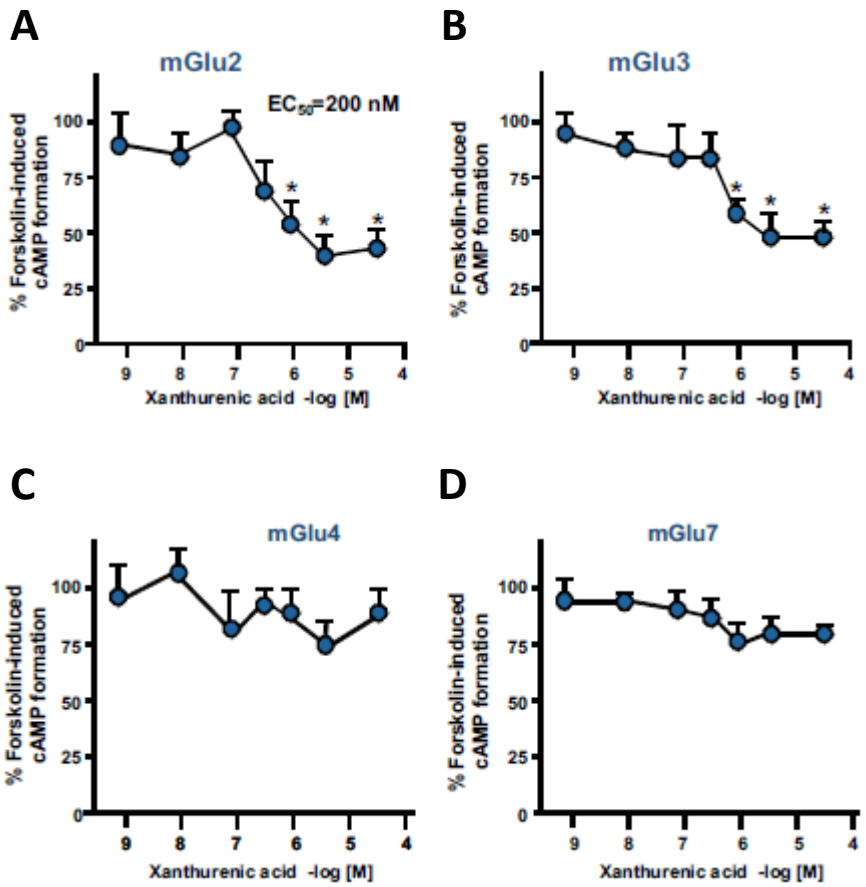

FIGURE 3.5 XA effects on FSK-induced cAMP formation in HEK293 cells transiently transfected with mGlu2, mGlu3, mGlu4 or mGlu7 receptors. XA was able to significantly reduce FSK-induced cAMP formation in HEK293 cells transiently transfected with mGlu2 or mGlu3 receptors (**A** and **B**), but not in HEK293 cells transiently transfected with mGlu4 or mGlu7 receptors (**C** and **D**). Values were calculated from 6-9 determinations from 3 independent experiments. Data are expressed as a percentage of the respective control values (mean ±SEM). Adapted from Fazio et al., (2012a).

Compound	Chemical Name	Target	Activity
Nonselective mGlu Receptor Agonists			
L-glutamate	(S)-1-Aminopropane-1,3-dicaboxylic acid	Group I/Group II>Group III	Orthosteric agonist
(1S,3R)-ACPD	(1S,3R)-1-Aminocyclopentane-1,3-dicarboxylic acid	Group I/II>Group III	Orthosteric agonist
Selective Group II mGlu Receptor Agonists			
DCG IV	(2S,2'R,3'R)-2-(2',3'-Dicarboxycyclopro-pyl)glycine	Group II (but also NMDA)	Orthosteric agonist
L-CCG-I	(2S,1'S,2'S)-2-(Carboxycyclopropyl)gl-ycine	Group II	Orthosteric agonist
(2R,4R)-APDC	(2R,4R)-4-Aminopyrrolidine-2,4-dica-rboxylate	Group II	Orthosteric agonist
LY354740	(1S,2S,5R,6S)-2-Aminobucyclo[3.1.0] hexane-4,6-dicarboxylic acid	Group II	Orthosteric agonist
LY379268	(1R,4R,5S,6R)-4-Amino-2-ocabicyclo[3.1.0]hexane-4,6-dicarboxylic acid	Group II	Orthosteric agonist
LY389795	(-)-2-thia-4-aminobicylco[3.1.0]hexane-4,6-dicarboxylic acid	Group II	Orthosteric agonist
Selective Group II mGlu Receptor Antagonists			
LY341495	(2S)-2-Amino-2-[(1S,2S)-2-carboxycycloprop-1-yl]-3-(xanth-9-yl) propanoic acid	Group II≥Group III>Group I	Orthosteric antagonist
RS-APICA	(RS)-1-Amino-5-phosphonoindan-1-car-boxylic acid	Group II	Inverse agonist
MNI	4-(8-Bromo-2,3-dihydro-2-oxo-1H-1,5--benzodiazepin-4-yl)-2-pyridinecarbonitrile	Group II	NAM
mGlu2 Selective Ligands			
LY487379	2,2,2-Trifluoro-N-[4-(2-methoxyphenoxy)phenyl]-N-(3-pyridinylmethyl)ethanesulfonamide	mGlu2	PAM
BINA	Biphenyl-indanone A	mGlu2	PAM
mGlu3 Selective Ligands			
NAAG	N-acetylaspartateglutamate	mGlu3	Orthosteric agonist (but see Chopra et al., (2009)
Mixed Group II mGlu Receptor Ligands			
LY395756	(1S,2S,4R,5R,6S)-rel-2-Amino-4-meth-ylbicyclo[3.1.0]hexane-2,6-dicarboxylic acid	Group II	mGlu2 agonist/mGlu3 antagonist

Table 3.1 Summary of Group II mGlu receptor ligands. For further information regarding the relative potencies of the agonists and antagonists at the specific mGlu receptor subtypes see Schoepp et al., (1999).

CHAPTER 4 THE GROUP II MGLU RECEPTORS IN THALAMOCORTICAL CIRCUITRY

Molecular, physiological and pharmacological studies have provided substantial evidence that synaptically activated Group II mGlu receptors are present and functional within thalamocortical circuitry. Physiological evidence has been collated from the rodent VB and another rodent sensory thalamic nucleus, the LGN, which comprises the same basic thalamic circuitry present in the VB.

4.1 LOCALISATION

Protein staining has revealed a dense population of Group II mGlu receptors in the TRN, and a moderate population in the VB of rodents (Petralia et al., 1996b; Mineff and Valtschanoff, 1999; Tamaru et al., 2001). Within the VB, Group II mGlu receptors were found to be present in cortical terminals, GABAergic terminals and glial processes (Petralia et al., 1996a; Liu et al., 1998; Mineff and Valtschanoff, 1999; Tamaru et al., 2001).

Messenger ribonucleic acid (mRNA) analysis in the rat (Ohishi et al., 1993a; Lourenco Neto et al., 2000) and protein staining in mGlu2 deficient mice (Tamaru et al., 2001) has revealed that mGlu3 receptors are heavily localised within the TRN, but little signal was found in the VB. Double-labelling in the VB of mGlu2 deficient mice found Group II mGlu receptor protein to overlap with the GABAergic marker glutamic acid decarboxylase (Tamaru et al., 2001). As the VB lacks inhibitory interneurones (Ralston, 1983; Barbaresi et al., 1986; Harris and

Hendrickson, 1987; Ohara and Lieberman, 1993), this indicates that the mGlu3 receptor is likely to be present at GABAergic TRN terminals in the VB. In contrast to the highly localised nature of mGlu3 in the VB, the mGlu2 receptor has a diffuse staining pattern (Neki et al., 1996). mGlu2 receptor mRNA analysis showed no significant signal in the VB or the TRN; however mGlu2 mRNA was detected in layer VI of S1 cortex (Ohishi et al., 1993a). In addition, immunogold particle labelling has also revealed that both mGlu2 and mGlu3 receptors can be found extrasynaptically (Shigemoto et al., 1997; Mineff and Valtschanoff, 1999; Tamaru et al., 2001). Taken together, these results suggest that mGlu3 receptors are localised primarily on TRN GABAergic terminals in the VB, that mGlu2 receptors are primarily on glutamatergic cortical terminals, and that both subtypes may be present on glial processes in the VB. Furthermore, the absence of mGlu2 and mGlu3 receptor mRNA in the VB indicates an absence of Group II mGlu receptors on VB neuronal terminals in the TRN (Ohishi et al., 1993a; b).

4.2 FUNCTION

The Group II metabotropic glutamate receptors can modulate physiologically-evoked responses in the VB by reducing inhibition from the TRN. Several *in vivo* studies have demonstrated that iontophoretic application of several Group II mGlu receptor agonists (e.g. 1*S*,3*R*-ACPD, L-CCG-I, 2*R*,*4*R-APDC) can result in the disinhibition of sensory evoked responses in the VB (Salt and Eaton, 1995a; b, 1996; Salt and Turner, 1998); with a later complementary *in vitro* study demonstrating that the Group II mGlu receptor agonist LY354740 can reduce IPSP amplitude without affecting the postsynaptic cell membrane properties (Turner and Salt, 2003), thus indicating a pre- or extrasynaptic localisation of

these receptors. This inhibitory role has also been shown in the visual thalamic nucleus, the LGN (Alexander and Godwin, 2005).

In accordance with protein staining and mRNA indications that mGlu3 is expressed by TRN neurones, application of the Group II mGlu receptor agonists (2*R*,4*R*)-APDC and L-CCG-I were able to elicit a hyperpolarization and increase membrane conductance through K_{leak} potassium channels in TRN neurones. As these effects persisted in the presence of tetrodotoxin, this likely involves postsynaptic Group II mGlu receptors (Cox and Sherman, 1999); with the mGlu3 receptor the prime candidate to mediate these effects as the TRN is devoid of mGlu2 receptor mRNA (Ohishi et al., 1993a) and selective mGlu3 receptor activation replicates increased membrane conductance (Cox and Sherman, 1999; Alexander and Godwin, 2006).

Pharmacological and electrophysiological experiments have indicated that the Group II mGlu receptors can inhibit glutamate transmission at corticothalamic synapses in the TRN and the LGN (Alexander and Godwin, 2005; 2006). A reduction in the amplitude of the corticothalamic excitatory postsynaptic current (EPSC) was observed upon application of the Group II mGlu receptor agonists LY379268 or DCG-IV, as was an enhanced paired pulse facilitation ratio: effects which are consistent with evidence suggesting a presynaptic site of action of these receptors (Granseth et al., 2002; Zucker and Regehr, 2002; Shigemoto et al., 1997). The Group II mGlu receptors have also been shown to be synaptically activated in these areas by corticothalamic stimulation, as an increase in the EPSC amplitude during train

stimulation was observed upon application of the Group II mGlu receptor antagonist LY341495 (Alexander and Godwin, 2005; 2006). It appears that train stimulation therefore results in the activation of Group II mGlu receptors, which then leads to a reduction in glutamate release. This response to the train stimulation suggests that glutamate spillover from high-frequency stimulation may be required for the Group II mGlu receptors to become activated. Furthermore, the Group II mGlu receptor agonist LY379268 was unable to perturb responses at the sensory afferent-thalamic neurone synapse in the LGN, in accordance with the lack of immunocytochemical evidence for Group II mGlu receptors at that synapse (Alexander and Godwin, 2005). Finally, within the LGN, the Group II mGlu receptors have been shown to activate the dendritic terminals of inhibitory interneurones in the absence of action potentials, thereby inhibiting postsynaptic LGN neurones (Cox et al., 1998).

Finally, whilst there is anatomical evidence for both mGlu2 and mGlu3 receptors present in astrocytic processes surrounding the TRN-VB synapse (Mineff and Valtschanoff, 1999; Tamaru et al., 2001), their presence has not been definitively determined, nor has the role that these receptors may play in the functioning of thalamic circuitry.

A summary diagram indicating the known localisations of the Group II mGlu receptors within the VB and associated TRN can be found on page 57 (**FIGURE 4.1**).

4.3 Clinical Implications

The TRN is thought to be responsible for ensuring synchronous activity between the thalamus and cortex required for either sensory perception or for the preparation and execution of distinct motor and/or cognitive tasks, and it is therefore purported to be key in the control of selective attention (Crick 1986, Pinault 2011). It is therefore imperative to ascertain the exact nature of how inhibitory innervation from the TRN to thalamic nuclei is controlled in order to understand how neurophysiological disease states associated with TRN malfunction precipitate (Huguenard, 1999; Rub et al., 2003; Barbas and Zikopoulos, 2007; Pinault, 2011). Indeed, TRN malfunction has been postulated to underlie cortical alterations that precipitate characteristic cognitive abnormalities observed in schizophrenia (Javitt, 2009; Pinault, 2011).

Identification of the Group II mGlu receptors as novel targets in the treatment of schizophrenia began upon the discovery that the Group II mGlu receptor selective orthosteric agonist LY354740 can inhibit glutamatergic transmission (Battaglia et al., 1997). This observation enabled the hyperglutamatergic theory of schizophrenia (Aghajanian and Marek, 1999) to be probed, and LY354740 was found to ameliorate psychotic symptoms induced by phencyclidine (Moghaddam and Adams, 1998). Since then, several preclinical studies using Group II mGlu receptor agonists (Cartmell et al., 1999; 2000a; b; Marek et al., 2000; Schoepp and Marek, 2002; Lorrain et al., 2003a; b; Rorick-Kehn et al., 2007) and mGlu2 selective PAMs (Galici et al., 2005; 2006; Benneyworth et al., 2007; Harich et al., 2007; Ahnaou et al., 2009; Brnardic et al., 2010; Hackler et al., 2010; Nikiforuk et al., 2010), along with a pioneer clinical trial (Patil et al., 2007), have established these compounds as a

potential new class of antipsychotic drug. Furthermore, Group II mGlu receptors are moderately/highly expressed in limbic brain regions in healthy controls, (Petralia et al., 1996b; Wright et al., 2001; Gu et al., 2008), with expression in one of these regions, the prefrontal cortex, significantly reduced in schizophrenia (Corti et al., 2007; Gonzalez-Maeso et al., 2008; Ghose et al., 2009). Additionally, multiple polymorphisms in the mGlu3 receptor gene have been associated with the disorder (Cherlyn et al., 2010).

As both inhibition in the thalamus from the TRN and the Group II mGlu receptors have been implicated in the pathophysiology of schizophrenia, in this thesis I sought to investigate in detail how the Group II mGlu receptors are able to modulate inhibition originating from the TRN in a sensory thalamic nucleus.

In light of this, it is therefore also appropriate that I sought to investigate the properties of XA, which has been reported to possess selective Group II mGlu receptor agonist activity; especially as human postmortem studies have indicated that kynurenine metabolites are increased in the cerebrospinal fluid of patients with schizophrenia (Erhardt et al., 2001; Schwarcz et al., 2001; Nilsson et al., 2005; Miller et al., 2008), and that impairments in gene expression and activity of kynurenine pathway enzymes are present in cortical areas (Miller et al., 2004; Aoyama et al., 2006; Miller et al., 2006; Sathyasaikumar et al., 2009; Schwarcz et al., 2009). Indeed, as the Group II mGlu receptors and the kynurenine metabolism pathway have both been heavily implicated in the pathophysiology of schizophrenia, it is

possible that XA could play a pivotal role in antipsychotic research as its potential as an endogenous agonist represents a convergence within these two biological parameters.

CHAPTER 4 FIGURES AND TABLES

Page Number

FIGURE 4.1 Known distributions of the Group II mGlu receptors in the VB and TRN. 57

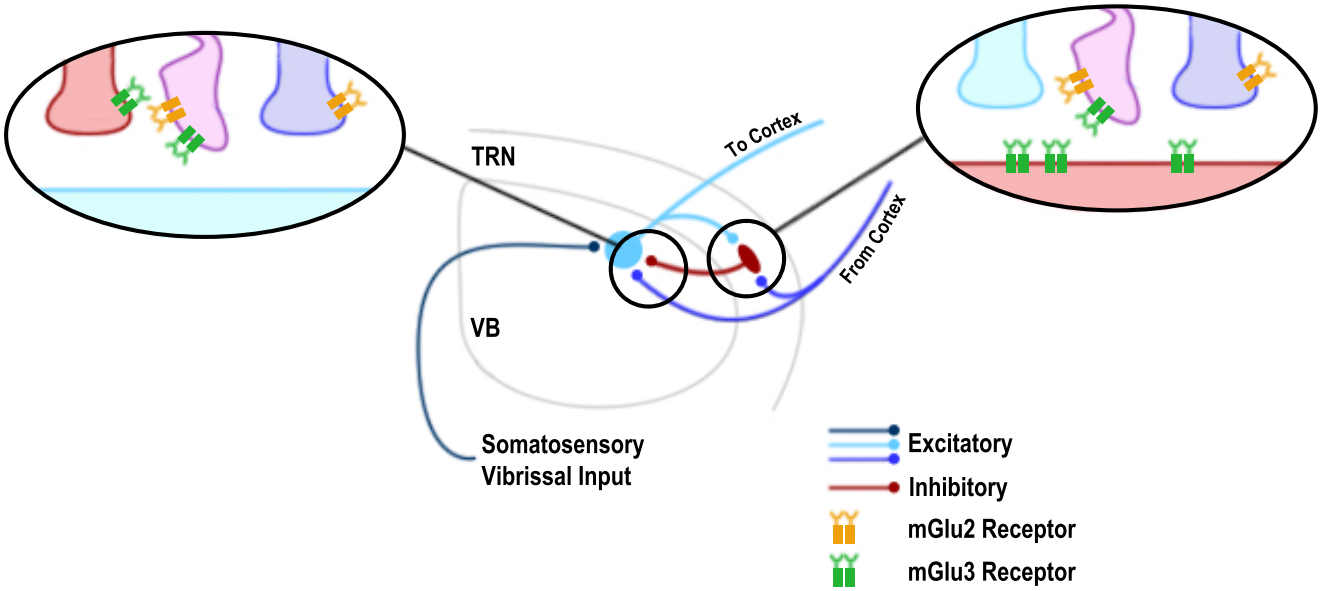

FIGURE 4.1 Known distributions of the Group II mGlu receptors in the VB and TRN. Within the VB, mRNA analysis and protein staining techniques suggest that mGlu3 receptors are localised primarily on TRN GABAergic terminals, that mGlu2 receptors are primarily on glutamatergic cortical terminals, and that both subtypes may be present on glial processes (represented by purple process) (Ohishi et al., 1993a; Shigemoto et al., 1998; Mineff and Valtschanoff 1999; Lourenco Neto et al., 2000; Tamaru et al., 2001). Within the TRN, mRNA analysis and protein staining suggest that mGlu3 receptors are localised on the postsnaptic TRN neurones, that mGlu2 receptors are localised on presynaptic corticothalamic terminals, and that both subtypes may be present on glial processes (Ohishi et al., 1993a; Cox and Sherman, 1999; Alexander and Godwin, 2006). Furthermore the absence of mGlu2 and mGlu3 receptor mRNA in the VB indicates an absence of Group II mGlu receptors on VB neuronal terminals in the TRN (Ohishi et al., 1993a; b). TRN – thalamic reticular nucleus; VB – ventrobasal thalamus.

CHAPTER 5 PROJECT HYPOTHESIS

It has been demonstrated using both *in vitro* and *in vivo* electrophysiology protocols that the Group II mGlu receptors can modulate sensory transmission at several points throughout thalamocortical circuitry (Salt and Eaton, 1995a; b; Salt et al., 1996; Cox et al., 1998; Salt and Turner, 1998; Cox and Sherman, 1999; Turner and Salt, 2003; Alexander and Godwin, 2005; 2006). However, despite this intensive research, the relative contributions of the two Group II mGlu receptor subtypes to the modulation of sensory transmission in thalamocortical circuits remains to be elucidated, as do their distinct cellular localisations, which can be attributed to the complete lack of selective mGlu2 or mGlu3 compounds at the time that these studies were conducted. At this point it is important to note that the putative selective mGlu3 agonist NAAG has been used as a tool to begin to address these questions (Turner and Salt, 2003; Alexander and Godwin, 2005; 2006); however, as doubt has now been cast over the purity, and therefore the selectivity of this compound (Chopra et al., 2009), researchers in the field have become reluctant to draw conclusions based purely upon the pharmacology of this compound.

However, thanks to intensive research into the development of mGlu2 subtype selective PAMs, the addition of this compound type to the Group II mGlu receptor toolbox has created a new avenue with which to investigate Group II mGlu receptor function in thalamocortical circuitry. In light of this, I specifically have sought to investigate how the Group II mGlu receptors can modulate TRN afferent GABAergic inhibition in the rat VB (Salt

and Eaton, 1995a; b; Salt and Turner, 1998; Turner and Salt, 2003) using *in vivo* electrophysiological techniques in conjunction with iontophoresis of selective Group II mGlu receptor compounds to address the following questions:

- Do both the Group II mGlu receptors contribute to the modulation of VB neurone responses?

- Are these receptors able to modulate both recurrent and lateral inhibition originating from the TRN?

- Are these receptors activated under normal physiological conditions, and if so, what is the likely mechanism of activation?

- Do these receptors have distinct cellular localisations, and if so, where?

In addition, as there was sufficient evidence to suggest that XA may be able to selectively activate the Group II mGlu receptors, I wanted to test the effects of XA in the same *in vivo* preparation to probe whether XA is physiologically active, and also to probe the mechanism of action of XA using *in vitro* cAMP and radioligand binding assays.

CHAPTER 6 MATERIALS AND METHODS

6.1 *IN VIVO* ELECTROPHYSIOLOGY

In vivo extracellular recordings were taken from single VB neurones responsive to vibrissal stimulation in anaesthetised rats. Agonist, antagonist and control ions were applied as required using iontophoresis during the concurrent execution of different stimulation protocols. Together, these protocols were designed to address the questions stated in the project hypothesis (Chapter 5) concerning how Group II mGlu receptors modulate inhibition from the TRN to the VB.

The use of an intact *in vivo* preparation and employment of iontophoresis will enable different types of sensory stimuli to be used during the concurrent application of the required Group II mGlu receptor compounds. Indeed, the key advantage in using an *in vivo* preparation is that it enables the examination of neuronal responses to physiologically relevant stimuli in an intact system. For the preparation described here, the qualitative and quantitative nature of afferent inputs to the VB are preserved, as are the involvement of any temporal events, therefore facilitating a better understanding of the processes that may be occurring in alert, behaving animals. Furthermore, this *in vivo* preparation has been demonstrated to efficiently reveal the action of other Group II mGlu receptor ligands *in vivo* (Salt and Eaton, 1995a; Turner and Salt, 1998), and maximises the likelihood of physiologically relevant mechanisms that may be required for Group II mGlu receptor activation, such as accessory proteins or co-factors, to function normally under our

experimental conditions. These experimental features will enable me to appropriately investigate the questions stated in the project hypothesis (Chapter 5). However, although *in vivo* electrophysiological techniques enable us to examine how activation of afferent connections can evoke an observed effect, it is important to note that the appropriate employment of *in vitro* electrophysiological techniques can facilitate the selective activation of individual afferent pathways. This can allow delineation of the relative contributions of individual afferent pathways to an overall observed effect. *In vitro* preparations do however also have their limitations. For example, they require electrical stimulation of afferent pathways, which is unlikely to exactly mimic physiological inputs, and that the overall circuitry of the system of interest is unlikely to be intact. The employment of both *in vivo* and *in vitro* electrophysiological techniques can therefore provide complementary information regarding the overall circuitry as well as the contributions of the individual afferent pathways to the overall observed effect.

6.1.1 Animal Preparation

6.1.1.1 Subjects

97 Adult male Wistar rats (Harlan Laboratories, UK) weighing 205-540g were used for all experiments. The animals were kept in cages in a conventional animal facility at a temperature range of 22-24^{o}C with a 12 hour light/dark cycle (Biological Research Unit, Institute of Ophthalmology, University College London, United Kingdom [UK]). Bedding was provided and food and water was given *ad libitum*. All procedures were approved by the

Home Office (UK) and were in accordance with the UK Animals (Scientific Procedures) Act 1986.

6.1.1.2 ANAESTHESIA

Animals were placed in a sealed chamber and anaesthetised with gaseous halothane until the righting reflex was lost. Animals were then removed from the chamber and urethane (1.2g/kg) was administered via intraperitoneal (i.p.) injection. Additional urethane anaesthetic was administered i.p. as required throughout the course of the experiment. 1% lignocaine with adrenaline was administered via subcutaneous (s.c.) injection at wound margins: thorax (tracheal cannulation), skull (surgical entry site for electroencephalogram [EEG] monitoring and craniotomy), and either the right and left front paws or the right front and hind paws depending upon the experimental protocol (electrocardiogram [ECG] monitoring, pin entry).

Upon cessation of the experiment, the animal received an overdose of urethane administered to the heart.

General anaesthesia is required to perform this type of *in vivo* electrophysiology. It is therefore important to consider that the use of general anaesthetics may alter the electrophysiological responses of neurones, and that any responses observed in anaesthetised animals may therefore not be representative of neuronal responses in

unanaesthetised animals. Urethane anaesthetic was used in the *in vivo* experiments in this project, and several studies have indicated that urethane is an appropriate anaesthetic for use in *in vivo* electrophysiological studies in the rat (Holmes and Houchin, 1966; Cross and Dyer, 1971; Bradley and Dray, 1973; Simon et al., 2006; Devonshire et al., 2010). It has been demonstrated that urethane administration has little effect on observed neuronal responses when compared to recordings taken from neurones in unanaesthetised rats (Holmes and Houchin, 1966; Simon et al., 2006). It is important to note however that urethane can antagonise the effects of glutamate acting at ionotropic receptors in the spinal cord (Evans and Smith, 1982).

6.1.1.3 SURGERY

An incision (1.5-2cm) was made along the midline in the skin overlying the trachea. The trachea was exposed, a small incision made along its width, and an appropriately sized glass cannula was inserted 0.5cm and secured in place with sutures. For experiments that also required intravenous (i.v.) drug administration, the jugular vein was also exposed and a saline-filled cannula was inserted approximately 1cm and secured in place with sutures. The overlying skin was sutured closed and a small piece of surgical tape was attached to the fur behind the cannula in order to prevent occlusion of the cannula by fur or skin folds. Cannulation was performed in order to ensure reflexive breathing could take place and be maintained as required throughout the experiment.

Animals were then transferred to a stereotaxic frame with a thermostatically controlled electric blanket (37^{o}C) where they were held in place with lignocaine gel-coated blunt ear bars and a nosebar. Anaesthetics can interfere with thermoregulatory mechanisms so it is important to ensure that anaesthetised animals are kept warm throughout an experiment in order to preserve optimal physiological conditions. Two surgical 25G needles were implanted s.c. into either the two front paws or the left front and hind paws in order for the ECG to be recorded. The ECG signal was amplified by the Neurolog A.C. Preamp Module (x2000), visualised on a Tektronik 211 Digital Storage Oscilloscope and relayed to the Spike2 software for recording and post-analysis via a 1401 interface (Cambridge Electronic Design) throughout the experiment; thus enabling the heart rate to be monitored, which was used as an indication of the physiological state of the animal.

A long (3-4cm) incision was then made along the midline in the skin overlying the dorsal surface of the skull whereupon it was pulled laterally away to reveal the dorsal skull and clamped in place. Any overlying muscle was then scraped away. Two holes were then drilled either side of the bregma fissure (coordinate range ML: 3mm from the midline; AP: +1mm/-1mm from Bregma) in which two small screws (10BA x 1/8 TND, cheese head) were implanted to enable monitoring of the EEG. These screws were then covered in dental cement to ensure electrical isolation. The EEG was amplified by the Neurolog A.C. Preamp Module (x50), visualised on a Tektronik 211 Digital Storage Oscilloscope and relayed and timed to the Spike2 software for recording and post-analysis via a 1401 interface (Cambridge Electronic Design) in order to enable the EEG to be monitored throughout the experiment as an indication of the level of anaesthesia. Throughout all drilling procedures

the bone was cooled with saline in order to prevent the heating and any subsequent potential damage of the underlying cortical tissue and also to prevent the formation of dust.

A small (5mm square diameter) craniotomy was then drilled over the right VB (Lambda +5.0mm anterior-posterior axis and +2.9mm medio-lateral axis) in order to reveal the cerebral cortex. Any overlying membranes and dura still present after drilling were then carefully removed with a pair of sharp forceps, along with any bone fragments that may have become caught within the craniotomy site. The site of the craniotomy, and the subsequent entry site for the electrode, was made at these co-ordinates according to the stereotaxic co-ordinates of the location of the VB as stated by Paxinos and Watson (1986). Upon completion of the craniotomy, a small piece of cotton wool that had been soaked in saline was placed over the craniotomy until the electrode was ready to be advanced into the brain in order to prevent dehydration of the brain tissue. The animal was then electrically earthed by the s.c. insertion of a silver wire through the skin in the back of the neck.

In order to perform *in vivo* electrophysiology, the method used in this thesis required the use of invasive surgical procedures. It is therefore important to consider that physiological changes may occur throughout the course of the experiment due to any trauma that may have been evoked by the surgery, which may alter the physiological condition of the preparation. Furthermore, the level of anaesthesia can drastically alter the responsivity of VB neurones to sensory stimulation, and was thus closely monitored through observation and interpretation of the EEG and ECG waveforms. Deep general anaesthesia, as indicated

by a synchronised/spindle EEG waveform (**Figure 6.1A**) and lower heart rate (~<300 beats per minute [bpm]), tended to result in a decrease in the responsivity of neurones to sensory stimulation. In such instances, execution of experimental protocols was delayed until a synchronous EEG waveform was observed (**Figure 6.1B**) along with a normal heart rate (~300-400bpm), which is indicative of a lighter level of general anaesthesia. A lighter level of general anaesthesia, but under which reflexive sensory responses to foot pinch were still absent, provided the optimal conditions under which to conduct the various sensory protocols as the propensity for neurones to respond to sensory stimulation was more consistent.

6.1.2 Recording and Iontophoresis

6.1.2.1 Glass Electrode Manufacture

Seven-barrel recording and iontophoretic glass electrodes were assembled from four borosilicate glass capillary tubes (Clark Electromedical GC150TF, internal diameter 1.17mm, length 10cm). Three of the capillaries were cut in half using a diamond tipped cutter and were arranged so that they surrounded the remaining full-length capillary tube. The capillary tubes were then held in this formation using drill chucks before being gently heated over a Bunsen flame, twisted and pulled apart; forming a *blank* (Stone, 1984). The blank was then removed from the drill chucks and the un-fused end of each of the shorter capillary tubes was pulled away from the central long capillary tube over a small Bunsen flame in order to aid the filling processes and to minimise cross-contamination between the barrels. The long capillary tube of the blank was then placed in another drill chuck and

suspended over a heating coil. A small weight was then fused to the tip of the blank to enable elongation and tip formation (~1μm in diameter) of the electrode using the heating coil. See **FIGURE 6.2** for examples of the different stages of electrode manufacture.

Throughout each stage of glass electrode manufacture it is essential that exposure to dust and other foreign objects be kept to a minimum in order to prevent the electrode becoming contaminated. Contamination of the electrode can lead to blocking of the barrels during iontophoresis, to the formation of micro-fractures and subsequent cross-contamination between barrels or to contamination of the drug solutions themselves. For these reasons, the electrodes manufacturing areas were thoroughly cleaned before and after the process took place and once the electrodes were complete they were stored in clean glass jars.

6.1.2.2 GLASS ELECTRODE FILLING

Immediately prior to filling the electrode the tip was broken back against a clean glass bead using a microscope and a manipulator to form an open tip between 6-8μm. This tip size represents a satisfactory compromise between sufficient passages of iontophoretic current, which requires a larger tip size, and optimal recording of extracellular activity, which requires a smaller tip size. Electrodes were filled with the required drug and control solutions (See section 6.1.2.4 for further details) before being placed in a glass jar with water in the bottom to prevent evaporation of the drug solutions. The jar was then put in a fridge (3-5^{o}C) 15-60 minutes prior to use to allow for the drug solutions to fill the electrode tip and for any bubbles to come out of solution.

As with glass electrode manufacture, it is imperative that exposure to dust and other foreign objects is kept to a minimum during filling in order to prevent the electrode becoming contaminated.

6.1.2.3 RECORDING

Seven-barrel recording and iontophoretic glass electrodes were advanced vertically into the VB through the cortex at the appropriate stereotaxic co-ordinates (Lambda +5.0mm anterior-posterior axis and +2.9mm medio-lateral axis) using a stepping micro-drive. Once the electrode was on course to the VB, a warmed agar solution was applied to the craniotomy site to reduce any brain movements that may affect the quality of the recording and to prevent dehydration of the brain tissue. VB neurones that were responsive to sensory stimulation of the vibrissae were found approximately 4.7-5mm from the surface of the brain.

Upon reaching the superficial VB, the electrode was not moved for 30-45 minutes to stabilise any brain movements evoked by advancement of the electrode. After this time, the electrode was moved using small steps until a single neurone suitable for recording was identified.

Extracellular recordings were made from single VB neurones through the central barrel (filled with 4M sodium chloride [NaCl]) of the electrode. Extracellular action potentials, which were amplified by the Axoprobe 1A (Axon Instruments) (x100), and the Neurolog AC DC Amp module (x100), were selected for recording based upon spike height using a waveform discriminator (built in-house). Spikes were timed and counted using a 1401 interface and Spike2 Software (Cambridge Electronic Design). This software also recorded the output from the iontophoresis unit and triggered some of the sensory stimuli sequences. Inspection of the extracellular waveform can provide an indication of the proximity of the recording electrode to the neurone (Sefton, 1969). As spike size is dependent upon the extent of current flow in the extracellular space, the spikes will become larger as the recording tip approaches the neurones membrane. The shape of the waveform is also an indication of the distance between the electrode and the neurone as the waveform may appear as a wholly negative potential at distances of around 50µm from the neurone, which usually changes to a waveform with a small positive and larger negative component nearer the unit (Bishop et al., 1962a; b). Recording sites were made through a single electrode track with data in a typical experiment obtained from a portion of the VB spanning 150-500um in depth. VB neurones were identified based upon their responsiveness to vibrissal stimulation.

Due to the large diameter of the electrodes used in these experiments, it is important that they were advanced through the brain slowly in order to minimise damage and to increase the stability of the recording.

6.1.2.4 COMPOUND PREPARATION FOR IONTOPHORESIS

All drugs were dissolved in a saline and water solution to achieve the desired concentration, apart from LY487379 that required to first be dissolved in the solvent dimethyl sulfoxide (DMSO) (see **TABLE 6.1** for details). Each drug was ionised in solution by adjusting the pH either with 1M HCl or 1M NaOH, as appropriate: a requirement essential for their use in iontophoresis in order to control their retention and ejection from the electrode tip. All drugs used in these experiments were obtained from Tocris and/or Sigma.

The use of solvents such as alcohol or dimethyl sulfoxide (DMSO) to dissolve a drug into solution for iontophoresis (see section 3.3.5 below), such as in the case of LY487379, must be controlled for as it is possible that these solvents may be biologically active. In these experiments, a 1% DMSO solution was iontophoretically applied where appropriate in order to determine whether its inclusion in the LY487379 drug solution caused a perturbation of the neuronal responses.

When selecting an appropriate pH for each drug solution, it is important to consider how far away from neutrality the drug solution is. Highly basic or acidic solutions will result in a greater proportion of OH^- and H^+ being ejected along with the drug ions, and these ions may alter the membrane properties of the cell and therefore the neuronal responses observed. In these experiments the drug solutions used were at pH values close to neutrality (see Table 2). However, if the use of a drug solution that is either highly basic or acidic was

required, it would be advisable to control for the effects of such a pH on the neuronal responses by ejection of a saline solution with the same pH as the drug solution.

6.1.2.5 IONTOPHORESIS

The movement of drug ions within a solvent results from the passage of current, with movement of drug ions out of the electrode tip occurring as they carry the current passed. This technique was first used in the 1950s to apply very small quantities of acetylcholine for very short periods of time at the neuromuscular junction, thus attempting to mimic synaptic transmission (Del Castillo and Katz, 1955). This technique was then adapted by Curtis and Eccles (1958) for use within the CNS: they used multibarreled micropipettes to demonstrate that acetylcholine was the transmitter between motor axon collaterals and the inhibitory Renshaw cells in the spinal cord.

Iontophoretic drug applications were performed using the outer barrels of the electrode. Each barrel contained one of the drug or control solutions stated in **TABLE 6.1** as required, and a silver wire was placed in each solution in order to facilitate the passing of current. Petroleum jelly was then placed at the open end of each of the barrels in order to minimise evaporation of the solutions. All drugs were iontophoretically ejected as anions at an appropriate current, except LY487379 and 1% DMSO which were ejected as cations, and were prevented from diffusing out of the pipette by using a retaining current (10-20nA) of opposite polarity to that of the ejection current. Appropriate ejection currents for

compounds were determined for individual neurones in order to ensure submaximal effects on neuronal responses to sensory stimulation were produced.

In order to ensure that each barrel can pass current, the resistance of each barrel was measured using the iontophoretic apparatus (NeuroPhore BH-2 system, Medical Systems Corp.). This was done when the electrode first touched the surface of the cortex before being advanced to the VB and is performed by passing a test current of 50nA through each barrel. If the resistance of the barrel to passing this current is too high (>100MΩ) it is unlikely that the drug ions will be ejected sufficiently, and if the resistance of the barrel is too low (<10MΩ) it is likely that the drug ions will leak out of the electrode tip. Barrel resistances can vary throughout the course of an experiment and can occur due to a number of reasons, such as a barrel becoming occluded by a piece of cell membrane or tissue, or by precipitation of the drug solution or the gathering of glass particles in the electrode tip. If a barrel does become blocked during the course of the experiment, the iontophoretic apparatus will signal that the required current level cannot be passed through the barrel by flashing the appropriate light-emitting diode display.

In each of the experiments performed, a continuous current was passed through one of the iontophoretic electrode barrels containing 1M sodium chloride in order to minimise the effect of current passage on the neurone. The current passed through this barrel was equal to the total current being passed through the other iontophoretic barrels but was of an

opposite polarity, therefore nullifying the current at the tip of the electrode. This practice, known as current balancing, was automatically performed by the iontophoretic equipment.

Iontophoresis is the only method of drug administration that enables the direct application of very small quantities of multiple drugs onto neurones during an *in vivo* experiment, and thus minimises any perturbations of the neuron and extracellular space, along with any systemic effects (see Stone, [1984], for a comprehensive overview of practical aspects of this technique). However, it is not possible to quantify the amount of drug being applied or the concentration of drug present in the extracellular environment of the neurone. It is therefore dangerous to assume that you can construct concentration-response curves using iontophoresis, nor is it possible to directly compare the potencies of different compounds. These issues can be resolved by the conduction of a complementary *in vitro* experiment as this type of experiment allows us to apply known concentrations of drugs: a critical feature if using a drug with selectivity for certain receptors at different concentrations.

It is required that an appropriate retaining current is applied to each iontophoretic barrel in order to prevent spontaneous efflux of drug from the electrode tip. A very high retaining current is likely required to completely abolish the spontaneous efflux of drug. However, this means that over time there will be a movement of drug ions away from the tip of the electrode. Small retaining currents (10-25nA) were therefore used in these experiments in order to ensure that there was a reasonable availability of drug at the electrode tip as it has

been demonstrated that use of large retaining currents can significantly reduce the amount of drug available for ejection (Bradshaw and Szabadi, 1974).

There is some debate as to the use of current balancing during iontophoresis. The argument for using it during drug ejection is that it compensates for current flow, therefore minimising the electrical perturbation of the neuronal membrane properties. However, the argument against using current balancing is that as the balance barrel is passing a current of opposite polarity to that of the drug eject barrel, it is possible that the balance barrel is accumulating drug particles. Therefore, it is possible that throughout the course of the experiment, drug ions may be undesirably ejected through the balance barrel. However, as the concentration of NaCl in the balance barrel is very high (1M) in comparison to the concentrations of ejected compounds ($\leq$50mM), the majority of the current passed through the balance barrel will be by Na+/Cl- ions. Furthermore, any compound accumulated in the balance barrel during compound ejection would be immediately ejected upon its cessation due to the current reversal, which would therefore minimally perturb the temporal accuracy of iontophoretic compound application.

6.1.3 Compound Preparation for Intravenous Administration

Xanthurenic Acid (50mg/kg) was systemically applied via i.v. injection. Solution was administered using a three-way tap using a 5ml syringe pumped by hand. The EEG and ECG were monitored throughout.

Administration of i.v. drugs in the rat needs care and consideration as the total blood volume of an adult rat weighing 300g is approximately 20ml (Lee and Blaufox, 1985), meaning even a small increase in actual volume can cause a large increase in overall percentage volume. To address this issue, compound was dissolved in the minimum volume of solute possible.

6.1.4 Experimental Protocols

6.1.4.1 Sensory Stimulation

Vibrissa deflection was performed using fine air-jets directed through 23G needles mounted on micro-manipulators positioned and orientated close to the vibrissa to ensure deflection of a single vibrissa was achieved. Air-jets were electronically gated with solenoid valves that produced a rising air pulse at the vibrissa 8ms after switching. Response latencies were calculated from the start of the gating pulse. Using such an approach it is possible to use air-jets to evoke an excitatory response from stimulation of a single vibrissa, as described previously (Salt, 1989).

It is important that single vibrissae receive stimulation by the air-jet due to the possibility of evoking unwanted inhibition/excitation, which can occur upon stimulation of secondary vibrissae adjacent to the primary vibrissa. If required, vibrissae that were not the focus of

the sensory stimulation protocol were trimmed in order to prevent their unwanted stimulation.

6.1.4.1.1 Protocol 1: Assessment of effects of Group II mGlu receptor compounds on sensory responses to short- and long-duration vibrissal stimulation.

Cycles of sensory stimulation (10s long) were established and repeated continuously whilst recording from neurones. Cycles contained two types of sensory stimuli, which consisted of electronically gated short (10-30ms) and long (500-1000ms) duration air-jets directed at the principal vibrissa, with 4-5s interstimulus intervals. Dependent upon the response profile of the neurone undergoing investigation, the long air-jet was applied as either a continual stimulation or as a train of stimuli at a frequency of 5-10Hz. After several control cycles displaying consistent neuronal responses had been recorded, compounds were iontophoretically ejected either alone or in conjunction with each other for 2-20 minutes as required. After cessation of compound ejection, sensory stimulation cycles were continued until neuronal responses had returned to control levels. An inter-stimulus interval of 4-5s is sufficient to ensure that any post-stimulus effects from either stimulus type are no longer apparent upon subsequent stimulation (Salt, 1989; Turner and Salt, 2003). This experimental protocol was also followed when current was passed through the DMSO vehicle barrel either alone or in conjunction with compound as appropriate.

6.1.4.1.2 Protocol 2: Assessment of effects of Group II mGlu receptor compounds on inhibitory sensory responses using the condition-test paradigm

As stated in the introduction, upon stimulation of the principal vibrissa the responses of a VB neurone are the the result of excitatory glutamatergic input from the lemniscal pathway and recurrent GABAergic inhibition from the TRN (Salt, 1989; Shosaku et al., 1989; Lee et al., 1994; Hartings and Simons, 2000; Binns et al., 2003), whereas upon stimulation of surrounding secondary vibrissae a lateral GABAergic inhibition from the TRN is evoked (Salt, 1989; Pinault and Deschênes, 1998; Crabtree, 1999) (**Figure 2.3**). In order to reveal these GABAergic inhibitory processes arising from the TRN, we used a condition-test paradigm with two air-jets each directed at an adjacent receptive field area (Salt, 1989). A conditioning stimulus presented to a secondary vibrissa preceding a test stimulus to a principal vibrissa by 20-60ms can inhibit the response of a VB neurone to stimulation of the principal vibrissa (Salt, 1989; Turner and Salt, 2003) (**Figure 6.3**). The precise interval between presentation of the conditioning stimulus and the test stimulus was altered within the 20-60ms time-window to produce the maximum inhibition achievable for each individual cell. The secondary vibrissa was normally in the same row as the principal vibrissa, but removed from the principal vibrissa by one or two positions (Lavallee and Deschênes, 2004). Several control cycles, which each contained two sensory stimulations (presentation of the test stimulus alone and then the condition-test stimuli, separated by an inter-stimulus interval of 4-5s) that demonstrated the establishment of sensory inhibition were recorded, and these were then repeated during the concurrent application of compound for 2-10 minutes as required. After cessation of compound ejection, cycles were continued until neuronal responses had returned to control levels. This experimental

protocol was also followed when the DMSO vehicle was iontophoretically ejected either alone or in conjunction with compound as required. The degree of inhibition was quantified as a percentage as follows:

Percentage inhibition = $(1 - T_C / T) \times 100\%$

where T is the total number of action potentials evoked to the test stimulus and T_C is the total number of action potentials evoked to the test stimulus when preceded by the condition stimulus. Using this calculation, the maximum inhibitory response that can be achieved is 100%. Action potentials evoked 10-50ms following test stimuli were counted in analysis, as all responses occurred within 100ms of stimulus presentation: the approximate time scale during which inhibition evoked by principal or secondary vibrissa stimulation is likely to reach its peak (Salt, 1989; Turner and Salt, 2003). It is important to note that the condition stimulus used to evoke an inhibition of a test response may in itself produce an excitatory response in some neurones.

6.1.4.1.3 Protocol 3: Assessment of effects of Group II mGlu receptor compounds on inhibitory sensory responses upon continuous NMDA application

As an alternative means of revealing functional recurrent or lateral inhibition onto VB neurones, NMDA was continuously applied to neurones whilst alternate presentations of short duration stimuli to either the principal or secondary vibrissa took place (separated by

5s). NMDA ejections were adjusted to produce stable sub-maximal increases in action potential firing of neurones, typically into the range of 12-16Hz. The degree of inhibition produced when either the principal or secondary vibrissa was stimulated was quantified from cumulative post-stimulus time histograms (PSTHs) of action potential spikes before, during and after the stimulus was applied. The first 100ms of evoked inhibition was used in the quantification analysis as this is the approximate time scale during which inhibition evoked by principal or secondary vibrissa stimulation is likely to reach its peak (Salt, 1989; Turner and Salt, 2003). Spikes counted during this period of inhibition are expressed as a percentage of the background firing rate. After several control cycles displaying consistent neuronal responses had been recorded, compounds were iontophoretically ejected for 10-15 minutes as required. After cessation of compound ejection, cycles were continued until neuronal responses had returned to control levels.

6.1.4.2 IONOTROPIC AGONIST APPLICATION

In order to directly assess the effects of compounds on postsynaptic responses to NMDA and/or AMPA receptor activation, cycles consisting of brief ejections (10-15s) of NMDA or AMPA with intervals of 50-60s, were established and repeated continuously. NMDA and/or AMPA ejection parameters were adjusted to ensure that excitatory neuronal responses evoked by these ejections were sub-maximal. After several cycles of NMDA and/or AMPA responses had been recorded under control conditions, compounds were iontophoretically ejected during one to three cycles of NMDA/AMPA ejection as required. After cessation of compound ejection, NMDA/AMPA ejection cycles were continued until neuronal responses had returned to control levels.

6.1.5 Data Analysis

Comparisons between the control and drug responses for each type of experimental protocol were made using non-parametric statistics (Wilcoxon Matched-Pairs Test), whereby a significant result was determined when $p < 0.05$. This statistical test, which controls for experimental variability, was chosen as it is appropriate for comparing two paired groups with non-Gaussian data populations. All results are expressed as a percentage of control ±SEM. Data were analysed by plotting PSTHs from these recordings and counting the spikes evoked by either ionotropic glutamate receptor agonist ejection or sensory stimulation using Spike2 software (Cambridge Electronic Design). Responses to sensory stimulation during control, drug and recovery periods were averaged over 6-30 trials as appropriate for the different sensory and ionotropic agonist stimulation protocols, with bin size (2ms-1s) for graphical demonstration selected in order to best illustrate the response profile under examination.

Comparisons between control and drug conditions when looking at EEG power spectra were made using non-parametric statistics (Wilcoxon Matched-Pairs Test to compare power spectra peak amplitudes, and Two-Sample Kolmogorov-Smirnov tests to compare power spectra distributions), whereby a significant result was determined when $p < 0.05$. These statistical tests, which control for experimental variability, were chosen as they are appropriate for comparing two paired groups with non-Gaussian data populations.

6.2 Molecular Pharmacology

By performing radioligand binding studies I will be able to determine whether XA binds to mGlu2 receptors as an orthosteric ligand, and repetition of the cAMP assays performed by Fazio et al., (2012a), but with co-application of the Group II mGlu receptor antagonist LY341495 and mGlu2 PAM LY487379, will enable me to ascertain whether the XA effect on FSK-induced cAMP formation is dependent upon Group II mGlu receptor activation.

These molecular pharmacology assays were the ones made available to me during my CASE industrial internship, which was completed April-July 2012, at Merck Research Laboratories, West Point, PA, USA. Protocols that had been optimised by the Cell Culture and Compound Evaluation Molecular Pharmacology teams were provided, as were materials for their execution.

The cAMP assay is a prototypical cell physiology assay used to detect $G_{i/o}$ G-protein induction upon mGlu receptor activation. As the signal transduction mechanism of the Group II mGlu receptors ultimately results in a reduction in cAMP formation, FSK is used to raise the levels of intracellular cAMP, achieving this by activating the enzyme adenylul cyclase. This assay was therefore an appropriate choice to investigate whether XA is able to act as a Group II mGlu receptor agonist by measuring levels of cAMP formation. The radioligand binding assay was chosen in order to determine whether XA is able to act as a Group II mGlu receptor orthosteric agonist. Initially, I had also planned to use a fluorometric imaging plate reader (FLIPR) to measure calcium mobilsation upon Group II mGlu receptor

activation. However, XA was found to produce a fluorescent artefact upon exposure to the light wavelength used by the FLIPR to detect activation of the calcium dye FURA-2 (Results section 7.9.2.1; **FIGURE 7.32**), therefore making use of this assay void.

6.2.1 cAMP ASSAY

6.2.1.1 CELL LINE

The cAMP Hunter™ CHO-K1 GRM2 cell line, was obtained from DiscoveRx Corporation (Fremont, California). Cells were cultured in F12 nutrition media (Invitrogen, Germany), 10% heat inactivated fetal bovine serum (FBS; Invitrogen), 1X Pen/Strep/Glu (Invitrogen), 0.4mg/ml G418 (Invitrogen) and then frozen at 1 x 10^6 cells/ml in Dulbecco's Modified Eagle Media (Invitrogen) containing 20% dialysed FBS and 10% DMSO at -80^{o}C.

6.2.1.2 MATERIALS

The HitHunter™ cAMP XS+ Assay kit was purchased from DiscoveRx. LY341495, LY354740 and LY487379 were synthesised at Merck Research Laboratories (PA, USA). XA was purchased from Sigma-Aldrich (Germany).

6.2.1.3 INSTRUMENTS

A Countess™ automated cell counter (Invitrogen, Germany) was used for cell and viability counts. Chemiluminescence in 384-well plates was read at 1s per well in an EnVision™ multilabel plate reader (PerkinElmer, Massachusetts).

6.2.1.4 ASSAY

Cells were thawed, resuspended in Hanks' balanced salt solution buffer, pH7.4, containing (HEPES 10mM), bovine serum albumin (0.06%) and pluronic acid F-68 (0.1%), plated at 10,000 cells per well in 384-well microplates (Costar, Corning) and incubated for 1h at 37^{o}C. Determination of intracellular cAMP through enzyme fragment complementation chemiluminesence detection was resolved using the HitHunter™ cAMP XS+ Assay kit according to the manufacturer's instructions and an EnVision™ multilabel plate reader. Cells were stimulated with FSK (1µM) and compounds for 30 minutes.

6.2.1.5 DATA ANALYSIS

Functional data were analysed using Microsoft Excel, GraphPad Prism and Matlab. Experiments were performed in quads. Nonlinear regressions and EC_{50} determinations were determined using the four parameter model. A 95% confidence interval (CI) using bootstrap resampling was employed to ascertain data significance, as it was not appropriate to use a statistical test for data analysis. Data are expressed as the mean % FSK-induced cAMP formation along with the CI.

6.2.2 Radioligand Binding

6.2.2.1 Materials

[^{3}H]LY341495 (40 Ci/mmol) was radiolabeled by American Radiolabeled Chemicals, Inc. (Missouri). XA was purchased from Sigma-Aldrich. ChemiSCREEN^{TM} recombinant human mGlu2 receptor membrane preparation was purchased from Millipore (Massachusetts) and stored at -20^{o}C.

6.2.2.2 [^{3}H]LY341495 Binding to Human mGlu2 Membranes

Membrane was diluted in assay buffer (20mM HEPES, 100mM NaCl, 3mM $MgCl_2$, pH 7.4) to give a final concentration of 6.6µg/ml. To start the reaction, membrane (0.75µg/well) was added to deep-well polypropylene microtiter plates containing [^{3}H]LY341495 (1nM) and appropriate concentrations of XA in assay buffer. Final assay volume was 0.2ml. Nonspecific binding was defined with 100µM LY354740. Assay plates were incubated at room temperature (21-23^{o}C) for 2h, and bound and free radioligands were separated by rapid filtration with 3X 1ml of cold assay buffer using Whatman GF-B uniplates (Brandel Inc., Maryland) presoaked in 0.3% polyethylenimine (Sigma-Aldrich). The uniplates were dried at 37^{o}C for 30 minutes, 50µl Microscint 20 (PerkinElmer) added to each well, and radioactivity determined using a Packard Topcount 2 (PerkinElmer).

6.2.2.3 DATA ANALYSIS

Functional data were analysed using Microsoft Excel, GraphPad Prism and Matlab. Experiments were performed in duplicates performed 4 times. Comparisons between the control and drug responses were made using non-parametric statistics (Wilcoxon Matched-Pairs Test) whereby a significant result was deemed when when $p < 0.05$. This statistical test, which controls for experimental variability, was chosen as it is appropriate for comparing two paired groups with non-Gaussian data populations. Data are expressed as counts per minute (CPM) (±SEM).

CHAPTER 6 FIGURES AND TABLES

		Page Number
FIGURE 6.1	Different depths of anaesthesia as indicated upon inspection of the EEG.	87
FIGURE 6.2	Different stages of electrode manufacture.	88
FIGURE 6.3	Example condition-test protocol responses.	89
TABLE 6.1	Compounds used for iontophoresis.	90

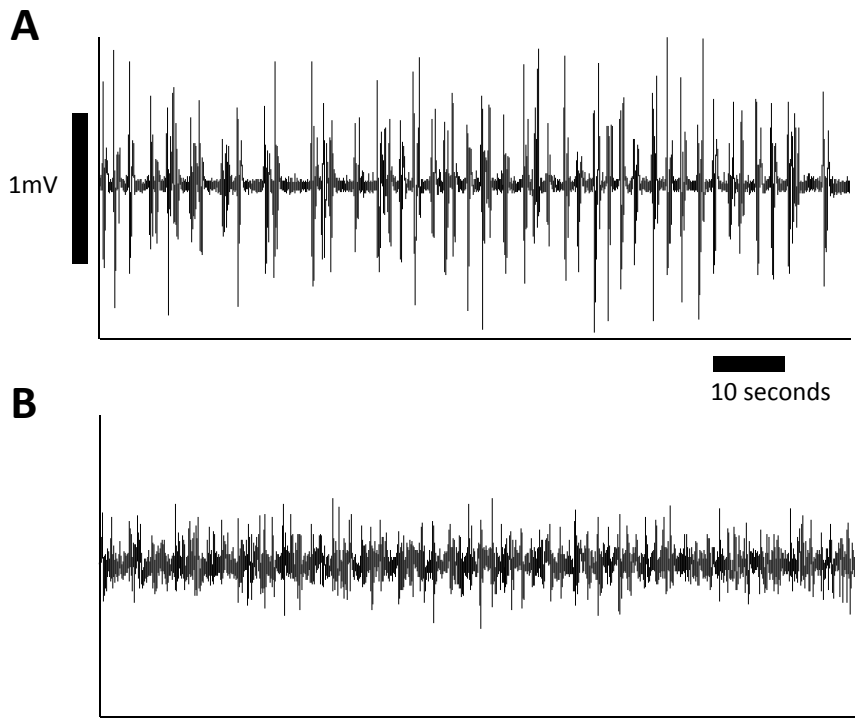

FIGURE 6.1. EEG waveforms at different depths of anaesthesia. A. A synchronised/spindle EEG waveform indicative of deep anaesthesia. **B.** An unsynchronised EEG waveform indicative of a lighter level of general anaesthesia. Waveforms are constructed from experiment CVB047.

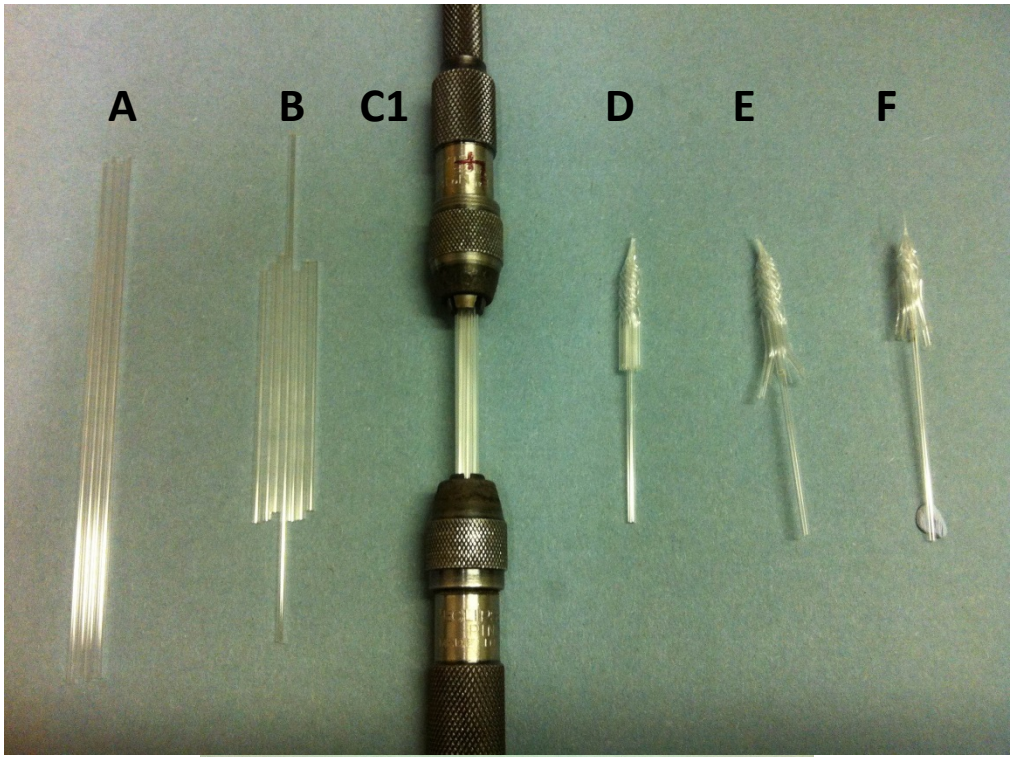

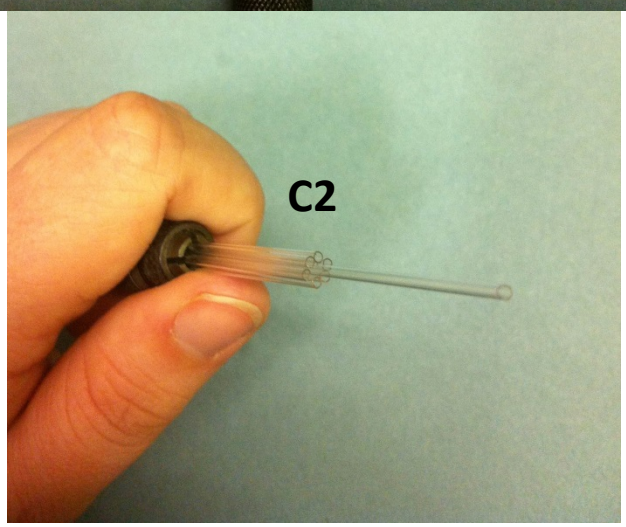

FIGURE 6.2 Different stages of electrode manufacture. A. Four borosilicate glass capillary tubes. **B.** Three of the glass capillary tubes cut in half, with the remaining whole capillary tube. **C1.** The six half and one full-length capillary tubes held in drill chucks, in a formation whereby the half capillary tubes surround the full length capillary tube (**C2**). **D.** A *blank*. **E.** A blank with the end of each shorter capillary tube pulled away. **F.** A finished electrode, ready for use.

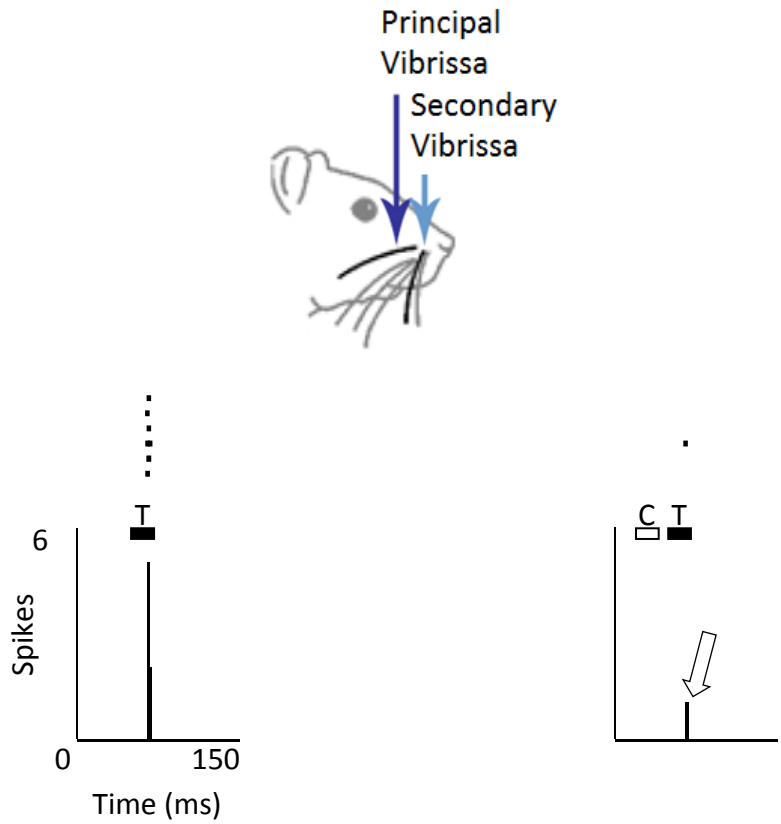

FIGURE 6.3 Example raster displays and PSTHs of condition-test protocol responses. Upon test stimulation of the principal vibrissa, for example C2, a robust response from the VB neurone from which I am recording from can be observed. When stimulation of this vibrissa is preceded by a conditioning stimulus to an adjacent secondary vibrissa, for example C3, in this instance by 30ms, an attenuation of the VB neurone response to the test stimulation occurs. T – 20ms short-duration test stimulation to the principal vibrissa; C – 20ms conditioning stimulation to a secondary vibrissa; Spikes - the total number of action potentials recorded per 2ms bin over 6 trials. PSTHs are constructed using responses from the same cell (CVB050b).

Compound	Concentration	Retaining Current	Ejecting Current	Comments
NMDA	50mM, pH8.5	+10 to + 25nA	-12nA to -163nA	Ionotropic glutamate receptor agonist
AMPA	50mM pH8.5	+10 to + 25nA	-17nA to -138nA	Ionotropic glutamate receptor agonist
LY354740	5mM in 75mM NaCl, pH8.0	+10 to + 25nA	-6nA to -75nA	Group II mGlu receptor agonist
LY341495	5mM in 75mM NaCl, pH8.5	+10 to + 25nA	-10nA to -50nA	Group II mGlu receptor antagonist
LY487379	1mM in 1% DMSO, 75mM NaCl, pH6.0	-5nA to -10nA	+12nA to +100nA	mGlu2 PAM
LY395756	5mM in 75mM NaCl, pH8.0	+10 to + 25nA	-15nA to -25nA	Dual mGlu2 agonist/mGlu3 antagonist
Xanthurenic Acid	5mM in 75mM NaCl, pH8.0	+10 to + 25nA	-12nA to -50nA	Putative Group II mGlu receptor agonist
1% DMSO	In 75mM NaCl, pH6.0	-5nA to -10nA	+12nA to +100nA	Solvent
Fluorocitrate	10Mm, pH8.5	+10 to + 25nA	-10nA to -40nA	Selective glial inhibitor
NaCl	1M & 4M			1M used for current balancing, + or – ejecting dependent upon the experimental protocol; 4M used for recording.

Table 6.1 Compounds used for iontophoresis. This table includes details of the concentrations used and the iontophoretic ejection parameters.

CHAPTER 7 RESULTS

It has been previously demonstrated that the selective activation of Group II mGlu receptors can modulate GABAergic afferent inhibition in VB (Salt and Eaton, 1995a; Salt and Turner, 1998; Turner and Salt, 2003). The results presented in this thesis are in accordance with these previous data whilst also providing information regarding the relative contribution of the two Group II mGlu receptor subtypes to this modulation, their distinct cellular localisations, and likely mechanism of endogenous activation.

The rat VB is well known to contain only VB neurones of a relatively homogeneous morphology (Peschanski et al., 1984; Harris, 1986; Ohara and Havton, 1994), but it is possible to categorise neurones functionally into single vibrissa excitation (SVE) or multiple vibrissa excitation (MVE) neurones (Ito, 1988; Brecht and Sakmann, 2002). In this study we recorded from both SVE (74% of cells) and MVE (26% of cells) neurones and did not find any differences in our results between these cell types. This suggests that our findings and interpretation are pertinent across different functional categories of VB neurones.

LY354740, was the chosen Group II mGlu receptor orthosteric agonist for these experiments as it is the best-studied selective Group II mGlu receptor orthosteric agonist (Schoepp et al., 2003) and has been extensively used to probe Group II mGlu receptor function in

behavioural (Schoepp et al., 2003; Nordquist et al., 2008) and physiological (Flor et al., 2002; Moldrich et al., 2003) responses in both the human and rodent CNS *in vivo* and *in vitro*.

LY487379, was the chosen mGlu2 PAM for this experiments as it is a highly selective mGlu2 PAM, which possesses no intrinsic agonist activity but does enhance responses to sub-maximal glutamate (Johnson et al., 2003), and has been used in behavioural and *in vitro* electrophysiological studies in the rodent CNS (Schaffhauser et al., 2003; Galici et al., 2005; Poisik et al., 2005; Harich et al., 2007; Hermes and Renaud, 2010; Nikiforuk et al., 2010).

Finally, the Group II mGlu receptor orthosteric antagonist LY341495 was chosen for these experiments as it has a relatively high selectivity with a nanomolar potency for the Group II mGlu receptors, with submicromolar potencies at all other mGlu receptor subtypes (Kingston et al., 1998; Schoepp et al., 1999). However, the iontophoretic parameters used for LY341495 in this thesis have been previously demonstrated to produce selective antagonism for the Group II mGlu receptors (Cirone et al., 2002).

7.1 The effects of the Group II mGlu receptor agonist LY354740 and the mGlu2 PAM LY487379 on sensory responses to short-duration vibrissal stimulation

Initial investigation began by testing the effects of the Group II mGlu receptor agonist and the mGlu2 PAM on VB neurones with vibrissal receptive fields that were responsive to a short-duration stimulus directed at the principal vibrissa. Neuronal responses to short-

duration stimuli were at a latency of 4–22ms (mean = 10.9±0.7ms), values which correspond closely to those described by others (Ito, 1988; Brecht and Sakmann, 2002). Iontophoretic ejections of the Group II mGlu receptor agonist alone significantly increased the number of responses of neurones to short-duration stimuli (128±4% of control, number of neurones [n]=42 from 32 rats ; **FIGURE 7.01Ai**), as did application of the mGlu2 PAM alone (128±6% of control, n=38 from 24 rats; **FIGURE 7.02A**). In order to confirm the specificity of the agonist and PAM applications, the Group II mGlu receptor antagonist LY341495 was subsequently co-applied with these agents in a subset of the same neurones. LY341495 reversed the effects of both the Group II mGlu receptor agonist (LY354740 alone: 137±2% of control; LY354740 plus LY341495 100±9% of control, n=5 from 4 rats; **FIGURE 7.03Ai**), and the mGlu2 PAM (LY487379 alone: 127±7% of control; LY487379 plus LY341495 104±4% of control, n=7 from 4 rats; **FIGURE 7.04**) on neuronal responses to short-duration stimuli, and the effect of the Group II mGlu receptor agonist on neuronal responses to the condition test paradigm (LY354740 alone: 24±4% reduction in sensory inhibition compared to control; LY354740 plus LY341495: 1±3% reduction in sensory inhibition compared to control; n=6 from 5 rats; **FIGURE 7.03B**). On a subset of the neurones upon which the effects of the Group II mGlu receptor agonist alone were tested, co-ejection of the mGlu2 PAM was found to significantly potentiate the agonist effect on neurone responses to the short-duration stimuli when compared to responses from the same neurones when the Group II mGlu receptor agonist was applied alone (LY354740 alone: 131±6% of control; LY354740 plus LY487379: 166±12% of control, n=22 from 18 rats; **FIGURE 7.01Bi**). These results provide the first indication that there is an mGlu2 component to the overall Group II mGlu receptor effect on sensory inhibition.

As a control for the use of DMSO vehicle in the mGlu2 PAM solvent, on some neurones an iontophoretic current was passed through the 1% DMSO solution that the mGlu2 PAM was dissolved in at the same current as the mGlu2 PAM ejection on the same neurones, either alone or in conjunction with the Group II mGlu receptor agonist as appropriate. Passing iontophoretic current through the DMSO vehicle barrel did not significantly alter responses of neurones to short-duration stimuli when applied alone (99±2% of control, n=6 from 6 rats; **FIGURE 7.05**), nor did it significantly potentiate the responses of neurones when co-applied with the Group II mGlu receptor agonist (LY354740 alone: 124±11% of control; LY354740 plus 1% DMSO: 135±13% of control, n=10 from 8 rats; **FIGURE 7.06A**).

7.2 THE EFFECTS OF THE GROUP II MGLU RECEPTOR AGONIST LY354740 AND THE MGLU2 PAM LY487379 ON INHIBITORY SENSORY RESPONSES

On a subset of the VB neurones upon which the responses to a single short-duration vibrissa stimulus during Group II mGlu receptor agonist and/or mGlu2 PAM application had been examined, an additional sensory stimulation protocol was performed. Condition–test protocols, which reveal GABAergic inputs from the TRN (Salt, 1989) (see Methods section 6.1.4.1.2), were carried out under control conditions and in the presence of the Group II mGlu receptor agonist and/or the mGlu2 PAM. For this population of VB neurones (n=35 from 24 rats) the degree of sensory inhibition observed under control conditions was 82±2%. The properties of the afferent-evoked inhibition in these data are similar to those that have been previously presented (Salt, 1989; Salt and Eaton, 1995a; Salt and Turner, 1998). Iontophoretic ejections of the Group II mGlu receptor agonist alone significantly reduced sensory inhibition (21±3% reduction in sensory inhibition compared to control,

n=29 from 21 rats; **FIGURE 7.01Aii**). The effect on sensory inhibition was reversed upon co-application of the Group II mGlu receptor antagonist LY341495 (LY354740: 22±4% reduction in sensory inhibition compared to control; LY354740 plus LY341495: 0.5±3% reduction in sensory inhibition compared to control, n=6 from 5 rats) in a subpopulation of the same neurons (**FIGURE 7.03Bii**). By contrast, iontophoretic ejections of the mGlu2 PAM alone had no significant effect on the degree of sensory inhibition compared to control (1±5% reduction in sensory inhibition, n=7 from 5 rats; **FIGURE 7.02B**). This result is of particular interest, as although the mGlu2 PAM when applied alone had no effect on sensory inhibition, responses to short-duration sensory stimulation of the principal vibrissa were significantly potentiated in the same population of neurones (134±14% of control, n=7 from 5 rats); a response profile to the short-duration stimulus which is reflected in the overall population of neurones upon which the mGlu2 PAM was applied alone (**FIGURE 7.02A**). On a subset of the neurones upon which the effects of the Group II mGlu receptor agonist alone were tested, the mGlu2 PAM was co-ejected with the Group II mGlu receptor agonist and was found to significantly potentiate the agonist effect on sensory inhibition when compared to the reduction in sensory inhibition in the same neurones when the Group II mGlu receptor agonist was applied alone (LY354740 alone: 20±4% reduction in sensory inhibition; LY354740 plus LY487379: 30±7% reduction in sensory inhibition, n=14 from 11 rats; **FIGURE 7.01Bii**).

Similarly to before, vehicle control experiments in which iontophoretic current was passed through the 1% DMSO vehicle barrel at the same current as the mGlu2 PAM application while ejecting the Group II mGlu receptor agonist on the same neurones indicated that

there was no significant effect of vehicle (LY354740 alone: 23±6% reduction in sensory inhibition; LY354740 plus 1% DMSO: 20±5% reduction in sensory inhibition, n=7 from 5 rats; **FIGURE 7.06Bii**).

7.3 THE EFFECTS OF THE GROUP II MGLU RECEPTOR AGONIST LY354740 AND THE MGLU2 PAM LY487379 ON RECURRENT AND LATERAL INHIBITION

This experimental protocol was performed in order to further investigate why application of the mGlu2 PAM potentiated the VB neurone response to short-duration test stimulation at the principal vibrissa, but had no effect on the degree of sensory inhibition evoked by preceding test stimulation of the principal vibrissa with a conditioning stimulation of a secondary vibrissa. In this protocol, action potential firing rate of the neurone was elevated with a continuous iontophoretic ejection of NMDA while principal and secondary vibrissa stimuli were alternately delivered, and the degree of recurrent and lateral inhibition respectively was revealed by the reduction in NMDA-evoked neuronal firing (see Methods section 6.1.4.1.3).

Iontophoretic application of the Group II mGlu receptor agonist significantly reduced both the lateral and recurrent sensory inhibition to a similar degree in the same group of neurones (Lateral: 45±9% reduction in inhibition compared to control; Recurrent 45±7% reduction in inhibition compared to control, n=6 from 3 rats; **FIGURE 7.07**). In contrast, application of the mGlu2 PAM significantly reduced recurrent inhibition (29±5% reduction in inhibition compared to control, n=9 from 6 rats), but did not alter the level of lateral

inhibition (–3±5% reduction in inhibition compared to control, n=9 from 6 rats) in the same group of neurones (**FIGURE 7.08**). No significant effects of the Group II mGlu receptor agonist or the mGlu2 PAM on the neural firing evoked by NMDA were seen (see section 7.7 below for further details).

7.4 THE EFFECTS OF THE GROUP II MGLU RECEPTOR AGONIST LY354740 AND THE MGLU2 PAM LY487379 ON SENSORY RESPONSES TO LONG-DURATION VIBRISSAL STIMULATION

As synaptic activation of mGlu receptors has been often shown to be dependent upon repetitive stimulation of pathways *in vitro* in a number of brain regions (Ohishi et al., 1994; Fitzsimonds and Dichter, 1996; Wada et al., 1998; Vogt and Nicoll, 1999; Mitchell and Silver, 2000; Semyanov and Kullmann, 2000; Turner and Salt, 2000; Arnth-Jensen et al., 2002; Piet et al., 2003; Piet et al., 2004; Neale and Salt, 2006), I thought it important to investigate whether such activity-dependent activation occurs *in vivo* in response to physiological stimuli. This was done by examining the effects of Group II mGlu receptor activation on neuronal responses to repetitive vibrissal stimulation using a long-duration stimulus directed at the principal vibrissa. Iontophoretic ejections of the Group II mGlu receptor agonist alone significantly increased the responses of neurones to long-duration stimuli (154±10% of control, n=21 from 15 rats; **FIGURE 7.09A**), as did application of the mGlu2 PAM alone (135±5%of control, n=29 from 20 rats; **Figure 7.10**). Co-ejection of the mGlu2 PAM along with the Group II mGlu receptor agonist significantly potentiated the agonist effect on neurone responses to long-duration stimuli when compared to responses from the same neurones when the Group II mGlu receptor agonist was applied alone (LY354740 alone: 170±20% of control; LY354740 plus LY487379: 246±30% of control, n=8 from 8 rats; **Figure**

7.09B).

As in previous protocols, passing iontophoretic current through the 1% DMSO vehicle barrel did not significantly alter responses of neurones to long-duration stimulation when applied alone (100±2% of control, n=10 from 10 rats; **FIGURE 7.11**), nor did it further potentiate the responses of neurones when co-applied with the Group II mGlu receptor agonist (LY354740 alone: 159±20% of control; LY354740 plus 1% DMSO: 159±21% of control, n=6 from 6 rats; **FIGURE 7.12**).

7.5 THE EFFECTS OF THE GROUP II MGLU RECEPTOR ANTAGONIST LY341495 ON SENSORY RESPONSES TO SHORT- AND LONG-DURATION VIBRISSAL STIMULATION

As the mGlu2 PAM was able to potentiate neuronal responses to both the short- and long-duration stimulation of the principal vibrissa, which is indicative of endogenous agonist release, the Group II mGlu receptor antagonist was applied as an additional means to reveal this potential mechanism of endogenous activation of the Group II mGlu receptors during these sensory stimulation protocols. Iontophoretic ejections of the Group II mGlu receptor antagonist alone significantly reduced the responses of neurones to both short- (91±4% compared to control, n=12 from 5 rats) and long- (86±4% compared to control, n=7 from 4 rats) duration stimuli of the principal vibrissa (**FIGURE 7.13**).

7.6 The effects of the dual mGlu2 agonist/mGlu3 antagonist LY395756 on sensory responses to long-duration vibrissa stimulation

During the course of this thesis, the dual mGlu2 agonist/mGlu3 antagonist LY395756, which has been characterized in several *in vitro* pharmacological assays (Dominguez et al., 2005), became commercially available. As use of the mGlu2 PAM was able to reveal an mGlu2 component to the overall Group II mGlu receptor effect on sensory inhibition, I thought it may be possible to use the dual mGlu2 agonist/mGlu3 antagonist to reveal whether there is also an mGlu3 component. Iontophoretic ejections of the dual mGlu2 agonist/mGlu3 antagonist significantly reduced the responses of neurones to long-duration stimulation of the principal vibrissa (83±3% compared to control, n=6 from 5 rats; **Figure 7.14**), indicating antagonism of endogenously activated mGlu3 receptors as this effect is similar to that observed when the Group II mGlu receptor antagonist LY341495 is applied alone (see above Results section 7.5). Furthermore, upon co-application of the mGlu2 PAM on the neurones upon which the dual mGlu2 agonist/mGlu3 antagonist was applied alone, a reversal of the dual mGlu2 agonist/mGlu3 antagonist effect was changed to that of potentiation (LY395756 alone: 82%±2% compared to control; LY395756 plus LY487379: 146±10%; n=6 from 5 rats; **Figure 7.14**), therefore providing further support that there is indeed an mGlu2 component to the overall Group II mGlu receptor effect on sensory inhibition.

7.7 The effects of the Group II mGlu agonist LY354740, the mGlu2 PAM LY487379, and the dual mGlu2 agonist/mGlu3 antagonist LY395756 on ionotropic glutamate receptor agonist responses

As it is known that VB neurone responses to vibrissal stimulation are mediated via AMPA and NMDA receptors (Salt, 1986; 1987), an experimental protocol was performed in order to investigate whether the Group II mGlu receptor agonist, the mGlu2 PAM and the dual mGlu2 agonist/mGlu3 antagonist could exert their effects on VB neurone responses via a postsynaptic interaction with NMDA and/or AMPA receptors. AMPA and NMDA were applied iontophoretically to produce sub-maximal excitation of VB neurones in a manner concordant with that of previous work (Salt and Eaton, 1996; Binns et al., 2003). Iontophoretic ejections of the Group II mGlu receptor agonist did not significantly alter the responses of neurones to agonist ejections (AMPA: 108±7% of control; NMDA: 105±7% of control, n=23 from 18 rats; **Figure 7.15**); nor did iontophoretic ejections of the mGlu2 PAM (AMPA: 102±8%of control; NMDA: 102±6% of control, n=13 from 7 rats; **Figure 7.16**) or the dual mGlu2 agonist/mGlu3 antagonist (AMPA: 99±6%of control; NMDA: 103±5% of control, n=7 from 5 rats; **Figure 7.17**).

During the course of this set of experiments, it was considered that the Group II mGlu receptor agonist might be exerting a dose-dependent dual effect on the responses of the VB neurones to AMPA and NMDA stimulation. Therefore, all VB neurone responses to AMPA and NMDA application during Group II mGlu receptor agonist co-application were correlated with the number of times that magnitude of response was observed. By looking at the distribution of the data points in this way, it is possible to determine whether the data are

normally distributed around the 100% control response mark, thus indicating a single population response profile, or whether the data are distributed in two distinct groups either side of the 100% control mark, thus indicating a dual population of response profiles. If the latter of these scenarios were true, the dual population would be concealed upon performing a mean of the Group II mGlu receptor agonist effect on VB neurone responses to AMPA and NMDA application, so it was therefore important to visualise the data in a distribution plot. The data were found to be normally distributed around the 100% of control response mark, and although a mild potentiation is apparent (<110% of the control response for VB neurone responses to both AMPA and NMDA application), this was statistically insignificant (**FIGURE 7.18**). The distribution of this data therefore indicates that there is a single population to the Group II mGlu receptor agonist effect on VB neurone responses to AMPA and NMDA application.

7.8 THE MGLU2 PAM LY487379 EFFECT ON SENSORY RESPONSES IS MEDIATED VIA ASTROCYTES

As described above, under normal conditions the Group II mGlu receptors are able to modulate physiologically-evoked responses in the VB by reducing inhibition from the TRN (Salt and Eaton, 1995a; Salt and Turner, 1998; Turner and Salt, 2003) (**FIGURE 7.01A**). As ultrastructural studies indicate that TRN terminals exclusively express the mGlu3 subtype (Tamaru et al., 2001), we sought to ascertain the cellular localisation from where the mGlu2 component is able to exert its effects on sensory-evoked inhibition in the VB.

Fluorocitrate is the toxic metabolite of the naturally-occurring non-toxic compound

fluoroacetate (Peters, 1963), and would be considered as an irreversible inhibitor of glial function in the *in vivo* electrophysiology experiments conducted in this thesis. Fluorocitrate loses a fluoride ion upon binding tightly, although not covalently, with the enzyme aconitase (Villafranca and Platus 1973; Tecle and Casida, 1989; Clarke, 1991; Lauble et al., 1996), whose function is integral to the generation of energy via the Krebs (citric acid) cycle (Beinert et al., 1993; Flint et al., 1996; Beinert et al., 1996). Although it has been demonstrated that aconitase inhibition is reversible (Villafranca and Platus, 1973), the time scale within which this recovery of function occurs (12-24 hours post-fluorocitrate treatment) (Paulsen et al., 1987) far exceeds that of the time-scale of experiments conducted here (<30 minutes).

It is generally accepted that there is a compartmentation of cerebral metabolism involving two metabolically distinct Krebs cycles. One Krebs cycle metabolises acetate, which is the precursor for glutamate, and is termed the 'small' compartment in reference to the size of the associated glutamate pool. The other Krebs cycle is relatively inaccessible to acetate and is not associated with glutamine synthesis; rather this cycle avidly metabolises glucose. This latter compartment was termed the 'large' compartment (Berl and Clarke, 1969). The small compartment was later identified as glial cells and the large compartment as neurones (Balázs et al., 1973; Martinez-Hernandez et al., 1977; Minchin and Beart, 1974; Sonnewald et al., 1993; Hassel et al., 1992). Several lines of evidence indicate that fluorocitrate is able to selectively inhibit the function of the glial cell small compartment (Lahri and Quastel 1963; Clarke et al., 1970; Cheng et al., 1972; Paulsen et al., 1987; Virgili et al., 1991; Hassel et al., 1992; Hassel et al., 1995), and it is therefore, when used appropriately, a useful tool

to examine specific properties of glial function. Indeed, whilst fluorocitrate is a purported specific glio-toxic agent, this specificity applies only to a narrow concentration range and therefore must be used with care to ensure only glial, and not neuronal, toxicity or is effected (Fonnum et al., 1997).

Several calibration experiments were first performed with fluorocitrate in order to determine the current ejection parameters within which fluorocitrate was able to produce a sustained effect on VB neurone responses to sensory stimulation. Fluorocitrate current ejects $\leq$10nA were found to have no effect on VB neurone responses to sensory stimulation (**FIGURE 7.19A**), whilst ejection currents $\geq$40nA usually resulted in VB neuronal responses to become erratic and unstable (**FIGURE 7.19B**). Therefore, for each of the experiments described here, fluorocitrate was first applied at a current eject of 10nA, which was then increased until an apparent fluorocitrate effect was observed (**FIGURE 7.19C**).

Fluorocitrate elicited a reduction in neuronal responses to long-duration (500-1000ms) 10Hz train stimulation of principal vibrissae. Specifically, the maintained component of the neuronal response profile was significantly reduced (68±4% of control, n=16 from 9 rats), whereas the initial component remained unaffected (101±3% of control, n=16 from 9 rats; **FIGURE 7.20**). The maintained component of neuronal responses to vibrissa stimulation comprises an NMDA-mediated contribution under normal physiological conditions (Salt, 1986). However, as neuronal responses to iontophoretic NMDA application were unaffected in the presence of fluorocitrate (102±4% of control, n=11 from 5 rats; **FIGURE 7.20**), this

indicates that inhibition of astrocyte function does not directly impact upon post-synaptic neuronal excitability. Indeed, if the fluorocitrate ejection current was increased beyond the ejection current that produced a selective effect on VB neurone responses to sensory stimulation, neuronal responses to long-duration stimulation of the principal vibrissa began to increase, which was then followed by a deterioration of stable responses to the ionotropic agonist (**FIGURE 7.21**), which is indicative of fluorocitrate eliciting non-specific effects.

As described above, both the Group II mGlu receptor agonist LY354740 and the mGlu2 PAM LY487379 were able to significantly increase neuronal responses to long-duration stimulation of principal vibrissae under normal conditions (**FIGURES 7.09 & 7.10**). However, when looking within the same population of neurones, the mGlu2 PAM effect was abolished (LY487379 alone: 144±10% of control; LY487379 plus fluorocitrate 91±5% of fluorocitrate control; n=6 from 6 rats; **FIGURE 7.22**), whereas the Group II mGlu receptor agonist effect remained (LY354740 alone: 156±12% of control; LY354740 plus fluorocitrate 156±9% of fluorocitrate control; n=6 from 6 rats; **FIGURE 7.22**) in the presence of fluorocitrate. Therefore, the mGlu2 PAM effect requires normal astrocytic function in order to exert its effects on sensory inhibition in the VB. Furthermore, this indicates that the Group II mGlu receptor agonist effect does not solely rely upon the activation of mGlu2 receptors, indicating that there is also a neuronal mGlu3 receptor component to the overall Group II mGlu receptor effect on sensory inhibition at the TRN-VB synapse.

7.9 Xanthurenic Acid

7.9.1 *In vivo* electrophysiology and iontophoresis

Stimulation of this group of VB neurones (n=22 from 15 rats) with the alternating test, condition-test protocol revealed a 71±3% degree of lateral inhibition under control conditions, which is similar to the mean level of afferent-evoked lateral inhibitions that have been previously reported (Salt, 1989; Salt and Eaton, 1995b; Salt and Turner, 1998).

7.9.1.1 The effect of XA on lateral inhibition in the VB

Iontophoretic ejections of either XA or the Group II mGlu receptor agonist LY354740 were found to significantly reduce lateral inhibition compared to control (XA: 22±2% reduction in lateral inhibition compared to control, n=13 from 8 rats; LY354740: 20±2% reduction in lateral inhibition compared to control, n=14 from 11 rats; **Figure 7.23 & Figure 7.26a**). On the same neurones upon which the effects of either XA or the Group II mGlu receptor agonist were tested, the mGlu2 PAM LY487379 was iontophoretically co-applied with these compounds. The Group II mGlu receptor agonist effect on lateral inhibition was significantly potentiated upon co-application of the mGlu2 PAM (LY354740 plus LY487379: 30±3% reduction in lateral inhibition compared to control, n=14 from 11 rats), whereas the XA effect on lateral inhibition remained unchanged (XA plus LY487379: 21±2% reduction in lateral inhibition compared to control, n=13 from 8 rats; **Figure 7.23 & Figure 7.26a**). The effect of the Group II mGlu receptor agonist on lateral inhibition when iontophoretically applied either alone or in conjunction with the mGlu2 PAM concords with the data collected for the experiments described above in this thesis.

In order to determine whether the XA effect was indeed mediated by the Group II mGlu receptors, XA and the Group II mGlu receptor agonist were iontophoretically applied either alone or in conjunction with the selective Group II mGlu receptor antagonist LY341495. The Group II mGlu receptor antagonist was able to significantly reverse the effects of both XA and the Group II mGlu receptor agonist on lateral inhibition on the same neurones (XA alone: 20±1% reduction in lateral inhibition compared to control; XA plus LY341495: 1±1% reduction in lateral inhibition compared to control, n=5 from 4 rats; LY354740 alone: 24±4% reduction in lateral inhibition compared to control; LY354740 plus LY341495: 1±3% reduction in lateral inhibition compared to control, n=6 from 5 rats) (**FIGURE 7.24 AND FIGURE 7.26B**).

7.9.1.2 THE EFFECT OF XA ON LATERAL INHIBITION IN THE VB WHEN APPLIED SYSTEMICALLY

On a subset of the same neurones upon which XA had been iontophoretically applied alone and then in conjunction with the Group II mGlu receptor antagonist, systemic administration of XA (50 mg/kg) was also performed. Systemic administration of XA was able to significantly reduce lateral inhibition compared to control (34±7% reduction in lateral inhibition compared to control, n=6 from 6 rats); an effect that could be reversed upon iontophoretic co-application of the Group II mGlu receptor antagonist (XA plus LY341495: 12±5% reduction in lateral inhibition compared to control n=6 from 6 rats). Once Group II mGlu receptor antagonist co-application ceased, the effect of systemic XA on lateral inhibition became evident again (27±8% reduction in lateral inhibition compared to control, n=6 from 6 rats) (**FIGURE 7.25 AND FIGURE 7.26C**). The XA effect on lateral inhibition manifested itself 4-9 minutes following systemic administration for this population of

neurones, lasting for 11-16 minutes. XA had no statistically significant (p<0.05) effect on EEG waveforms (n=6 from 6 rats), determined upon examination of the power spectrum, when administered systemically (**FIGURE 7.27**). Vehicle control (saline; 150mM) systemic administration had no statistically significant (p<0.05) effect upon lateral inhibition (Saline: 1% reduction in lateral inhibition ±1% compared to control, n=5 from 5 rats; **FIGURE 7.28**) or EEG waveforms (n=5 from 5 rats) (**FIGURE 7.29**). Systemic administration of neither XA nor vehicle significantly altered heart rate.

7.9.1.3 THE EFFECTS OF XA ON IONOTROPIC GLUTAMATE RECEPTOR AGONIST RESPONSES

As VB neurone responses to vibrissa stimulation are mediated via ionotropic glutamate receptors (Salt, 1986; 1987; Salt and Eaton, 1989), XA was co-applied with NMDA to ascertain whether XA was exerting its effect on VB neurone responses via a postsynaptic interaction with NMDA receptors. NMDA application excited VB neurones in a manner concordant with that of previous work from this laboratory (Salt and Eaton, 1996; Binns et al., 2003) and co-application of XA did not significantly perturb neuronal responses to this NMDA application (99±3% of control, n=8 from 4 rats; **FIGURE 7.30**).

A summary table of all the *in vivo* electrophysiological data obtained can be found on page 150 (**TABLE 7.1**).

7.9.2 Molecular pharmacology

7.9.2.1 XA modulation of cAMP formation

As XA appeared to modulate lateral inhibition in the VB via a Group II mGlu receptor dependent mechanism, we proceeded to investigate the action of XA in inhibiting FSK-induced cAMP formation. cAMP Hunter CHO-K1 cells expressing the human mGlu2 receptor were challenged with the Group II mGlu receptor agonist LY354740 or XA, and inhibition of FSK-induced cAMP formation was assessed. XA significantly reduced FSK-induced cAMP formation in a concentration-dependent manner (**Figure 7.31A & Table 7.1**). This effect could not be prevented by co-application of the Group II mGlu receptor antagonist LY341495 (**Figure 7.31A and Table 7.1A**). The Group II mGlu receptor agonist also significantly reduced cAMP formation in a concentration-dependent manner (**Figure 7.31B and Table 7.1**), and this effect could indeed be reversed upon co-application of the Group II mGlu receptor antagonist (**Figure 7.31B and Table 7.1B**). In addition, co-application of the mGlu2 PAM LY487379 significantly increased the potency of the Group II mGlu receptor agonist in reducing cAMP formation, but had no effect on the potency of XA (**Figure 7.32**). Taken together, these results indicate that XA is able to reduce FSK-induced cAMP formation via a signalling transduction mechanism independent of mGlu2 receptor activation. Further functional assays using the FLIPR platform could not be performed due to fluorescence artefacts produced by XA (**Figure 7.33**).

7.9.2.2 XA BINDING TO THE MGLU2 RECEPTOR

In membranes stably expressing the human mGlu2 receptor, XA (1µM-1mM) had no effect on specific binding of 1nM [^{3}H]LY341495 (**FIGURE 7.34**). In contrast, 100µM of the Group II mGlu receptor agonist LY354740 was able to significantly displace [^{3}H]LY341495 binding (2.6±1.0% of control specific binding; n=8; **FIGURE 7.34**).

CHAPTER 7 FIGURES AND TABLES

Page Number

FIGURE 7.01 VB neurone responses before, during, and after iontophoretic application of the Group II agonist LY354740 either alone or co-applied with the mGlu2 PAM LY487379 upon short-duration stimulation of the principal vibrissa and execution of the condition-test protocol. 116

FIGURE 7.02 VB neurone responses before, during, and after iontophoretic application of the mGlu2 PAM LY487379 upon short-duration stimulation of the principal vibrissa and execution of the condition-test protocol. 117

FIGURE 7.03 VB neurone responses before, during, and after iontophoretic application of the Group II agonist LY354740 either alone or co-applied with the Group II mGlu receptor antagonist LY341495 upon short-duration stimulation of the principal vibrissa and execution of the condition-test protocol. 118

FIGURE 7.04 VB neurone responses before, during, and after iontophoretic application of the mGlu2 PAM LY487379 either alone or co-applied with the Group II mGlu receptor antagonist LY341495 upon short-duration stimulation of the principal vibrissa. 119

FIGURE 7.05 VB neurone responses before, during, and after iontophoretic application of either the mGlu2 PAM LY487379 or 1% DMSO vehicle upon short-duration stimulation of the principal vibrissa. 120

FIGURE 7.06 VB neurone responses before, during, and after iontophoretic application of the Group II mGlu receptor agonist LY354740 either alone or co-applied with the 1% DMSO vehicle upon short-duration stimulation of the principal vibrissa and execution of the condition-test protocol. 121

FIGURE 7.07 VB neurone responses before, during, and after iontophoretic application of the Group II mGlu receptor agonist LY354740 upon stimulation of either the principal or secondary vibrissa to evoke recurrent and lateral inhibition respectively. 122

FIGURE 7.08 VB neurone responses before, during, and after iontophoretic application of the mGlu2 PAM LY487379 upon stimulation of either the principal or secondary vibrissa to evoke recurrent and lateral inhibition respectively. 123

FIGURE 7.09 VB neurone responses before, during, and after iontophoretic application of the Group II mGlu receptor agonist LY354740 either alone or co-applied with the mGlu2 PAM LY487379 upon long-duration stimulation of the principal vibrissa. 124

FIGURE 7.10 VB neurone responses before, during and after iontophoretic application of the mGlu2 PAM LY487379 upon long-duration stimulation of the principal vibrissa. 125

FIGURE 7.11 VB neurone responses before, during, and after iontophoretic application of either the mGlu2 PAM LY487379 or 1% DMSO vehicle upon long-duration stimulation of the principal vibrissa. 126

FIGURE 7.12 VB neurone responses before, during, and after iontophoretic application of the Group II mGlu receptor agonist LY354740 either alone or co-applied with 1% DMSO vehicle upon long-duration stimulation of the principal vibrissa. 127

FIGURE 7.13 VB neurone responses before, during and after iontophoretic application of the Group II mGlu receptor antagonist LY341495 upon short- and long-duration stimulation of the principal vibrissa. 128

FIGURE 7.14 VB neurone responses before, during, and after iontophoretic application of the dual mGlu2 agonist/mGlu3 antagonist LY395756 either alone or co-applied with the mGlu2 PAM LY487379 upon long-duration stimulation of the principal vibrissa. 129

FIGURE 7.15 VB neurone responses to NMDA and AMPA iontophoretic application before, during and after co-application of the Group II mGlu receptor agonist LY354740. 130

FIGURE 7.16 VB neurone responses to NMDA and AMPA iontophoretic application before, during and after co-application of the mGlu2 PAM LY487379. 131

FIGURE 7.17 VB neurone responses to NMDA and AMPA iontophoretic application before, during and after co-application of the dual mGlu2 agonist/mGlu3 antagonist LY341495. 132

FIGURE 7.18 Distribution plots of the Group II mGlu receptor agonist effect on VB neurone responses to ionotropic agonist application. 133

FIGURE 7.19 Line graphs demonstrating the dose-dependency of FCT 134

application on VB neuronal responses to long-duration stimulation of the principal vibrissa.

FIGURE 7.20 VB neurone responses to long-duration 10Hz train stimulation of the principal vibrissa and NMDA iontophoretic application before and during application of the selective glial inhibitor fluorocitrate. 135

FIGURE 7.21 VB neurone responses to long-duration 10Hz train stimulation of the principal vibrissa and NMDA iontophoretic application before and during application of the selective glial inhibitor fluorocitrate. 136

FIGURE 7.22 VB neurone responses before, during, and after iontophoretic application of the mGlu2 PAM LY487379 or Group II mGlu receptor agonist LY354740 either alone or co-applied with selective glial inhibitor fluorocitrate upon long-duration 10Hz stimulation of the principal vibrissa. 137

FIGURE 7.23 VB neurone responses before, during, and after iontophoretic application of either XA or the Group II mGlu receptor agonist LY354740 alone or co-applied with the mGlu2 PAM LY487379 upon execution of the condition-test paradigm. 138

FIGURE 7.24 VB neurone responses before, during, and after iontophoretic application of either XA or the Group II mGlu receptor agonist LY354740 alone or co-applied with the Group II mGlu receptor antagonist LY341495 upon execution of the condition-test paradigm. 139

FIGURE 7.25 VB neurone responses before, during and following systemic XA administration upon execution of the condition-test paradigm. The Group II mGlu receptor 140

antagonist LY341395 was iontophoretically co-applied for a short period when XA was affecting sensory inhibition.

FIGURE 7.26 Summary of XA and Group II mGlu receptor agonist effects on sensory inhibition in the VB. 141

FIGURE 7.27 Effects of systemic XA on electro-cortical activity. 142

FIGURE 7.28 VB neurone responses before and during systemic saline (150mM NaCl) administration upon execution of the condition-test paradigm. 143

FIGURE 7.29 Effects of systemic saline on electro-cortical activity. 144

FIGURE 7.30 VB neurone responses to NMDA before, during, and after iontophoretic application of XA. 145

FIGURE 7.31 Effects of XA and the Group II mGlu receptor agonist LY354740 on FSK-induced cAMP formation. 146

FIGURE 7.32 Dose-response curves and computed EC_{50} values for the Group II mGu receptor agonist LY354740 and XA in the cAMP assay under control conditions and in the presence of increasing concentrations of the mGlu2 PAM LY487379. 147

FIGURE 7.33 XA auto-fluoroscence upon exposure to light. 148

FIGURE 7.34 Effects of XA and the Group II mGlu receptor agonist LY354740 in the mGlu2 receptor radioligand binding assay. 149

TABLE 7.1 Summary table of all the *in vivo* electrophysiological data obtained. 150

TABLE 7.2 The effects of XA and the Group II mGlu receptor agonist LY354740 on FSK-induced cAMP formation alone and in the presence of the Group II mGlu receptor antagonist 151

LY341495.

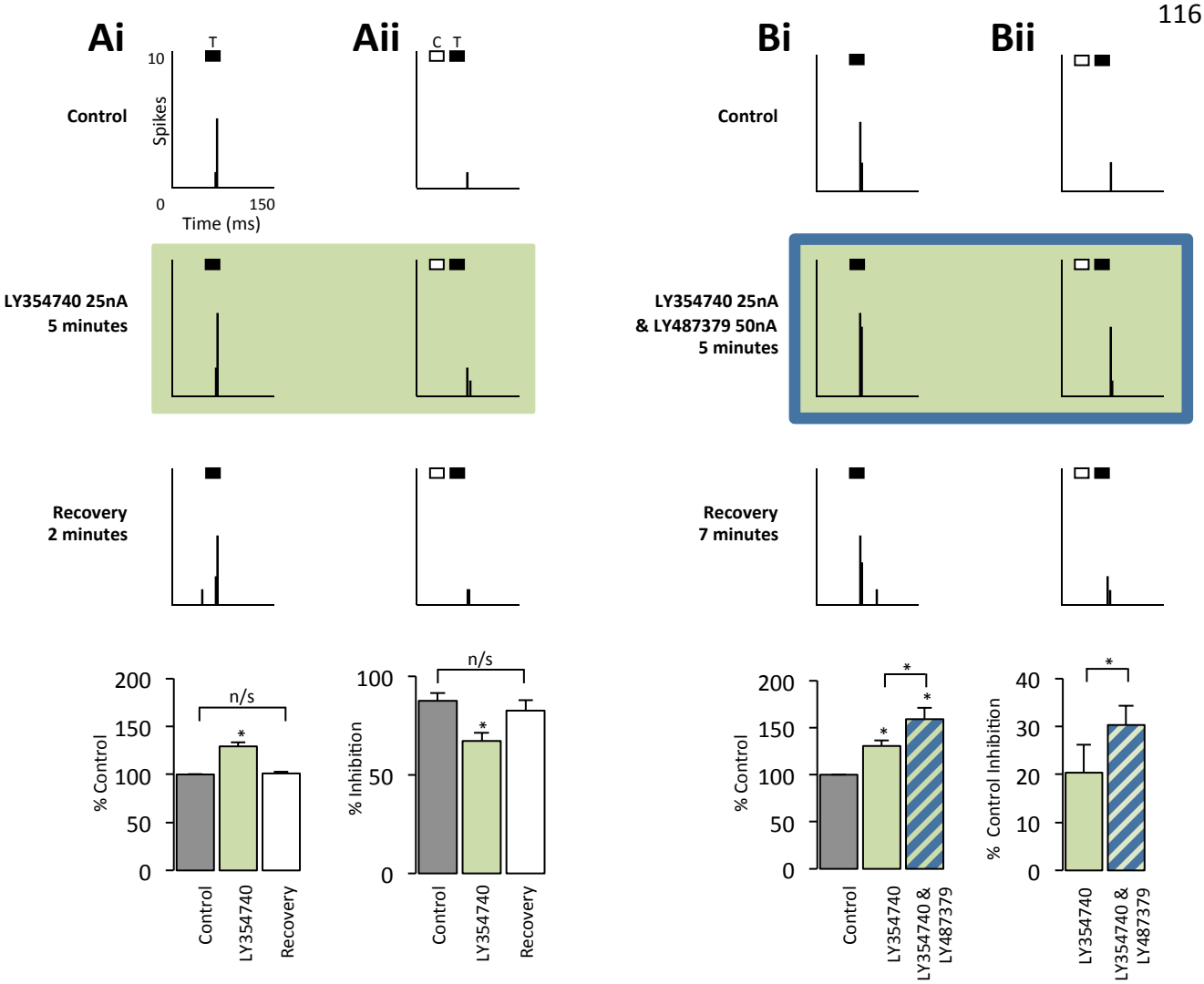

FIGURE 7.01 VB neurone responses before, during, and after iontophoretic application of the Group II agonist LY354740 either alone or co-applied with the mGlu2 PAM LY487379 upon short-duration stimulation of the principal vibrissa and execution of the condition-test protocol. Ai. The top three PSTHs represent responses from a single neurone to short-duration stimulation of the principal vibrissa under control conditions, during application of the Group II mGlu receptor agonist, and during recovery. The bottom histogram represents the mean responses of a group of neurones (n=44) to short-duration stimulation of the principal vibrissa under the same conditions. **Aii.** The top three PSTHs represent responses from a single neurone upon execution of the condition-test paradigm under control conditions, during application of the Group II mGlu receptor agonist, and during recovery. The bottom histogram represents the mean inhibitions of a group of neurones (n=25) to the condition-test paradigm under the same conditions. **Bi.** The top three PSTHs represent responses from a single neurone to short-duration stimulation of the principal vibrissa under control conditions, upon co-application of the Group II mGlu receptor agonist and the mGlu2 PAM and during recovery. The bottom histogram represents the mean responses of a group of neurones (n=22) to short-duration stimulation of the principal vibrissa under control conditions, upon application of the Group II mGlu receptor agonist alone and upon co-application of the Group II mGlu receptor agonist and the mGlu2 PAM. **Bii.** The top three PSTHs represent responses from a single neurone to the condition-test paradigm under control conditions, during co-application of the Group II mGlu receptor agonist and the mGlu2 PAM, and during recovery. The bottom histogram represents the mean reduction in sensory inhibition of a group of neurones (n=14) compared to control to application of the Group II agonist alone, or co-applied with the mGlu2 PAM upon execution of the condition-test paradigm. T – 20ms short-duration test stimulation to the principal vibrissa; C – 20ms conditioning stimulation to a secondary vibrissa; Spikes - the total number of action potentials recorded per 2ms bin over 6 trials; n/s – not significant. All PSTHs are constructed using responses from the same cell (CVB050b). Histogram data are expressed as mean ± SEM. * indicates $p<0.05$ when compared to control, unless otherwise indicated.

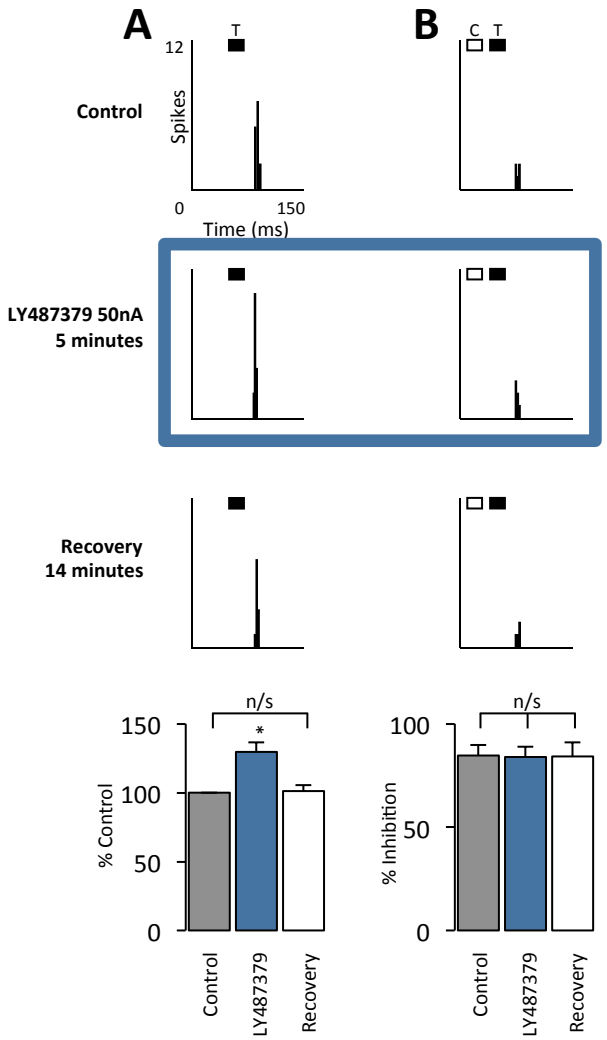

FIGURE 7.02. VB neurone responses before, during, and after iontophoretic application of the mGlu2 PAM LY487379 upon short-duration stimulation of the principal vibrissa and execution of the condition-test protocol. A. The top three PSTHs represent responses from a single neurone to short-duration stimulation of the principal vibrissa under control conditions, during application of the mGlu2 PAM, and during recovery. The bottom histogram represents the mean responses of a group of neurones (n=39) to short-duration stimulation of the principal vibrissa under the same conditions. **B.** The top three PSTHs represent responses from a single neurone upon execution of the condition-test paradigm under control conditions, during application of the mGlu2 PAM, and during recovery. The bottom histogram represents the mean inhibitions of a group of neurones (n=7) to the condition-test paradigm under the same conditions. T – 20ms short-duration test stimulation to the principal vibrissa; C – 20ms conditioning stimulation to a secondary vibrissa; Spikes - the total number of action potentials recorded per 2ms bin over 6 trials; n/s – not significant. All PSTHs are constructed using responses from the same cell (CVB049c). Histogram data are expressed as mean ± SEM. * indicates $p<0.05$ when compared to control, unless otherwise indicated.

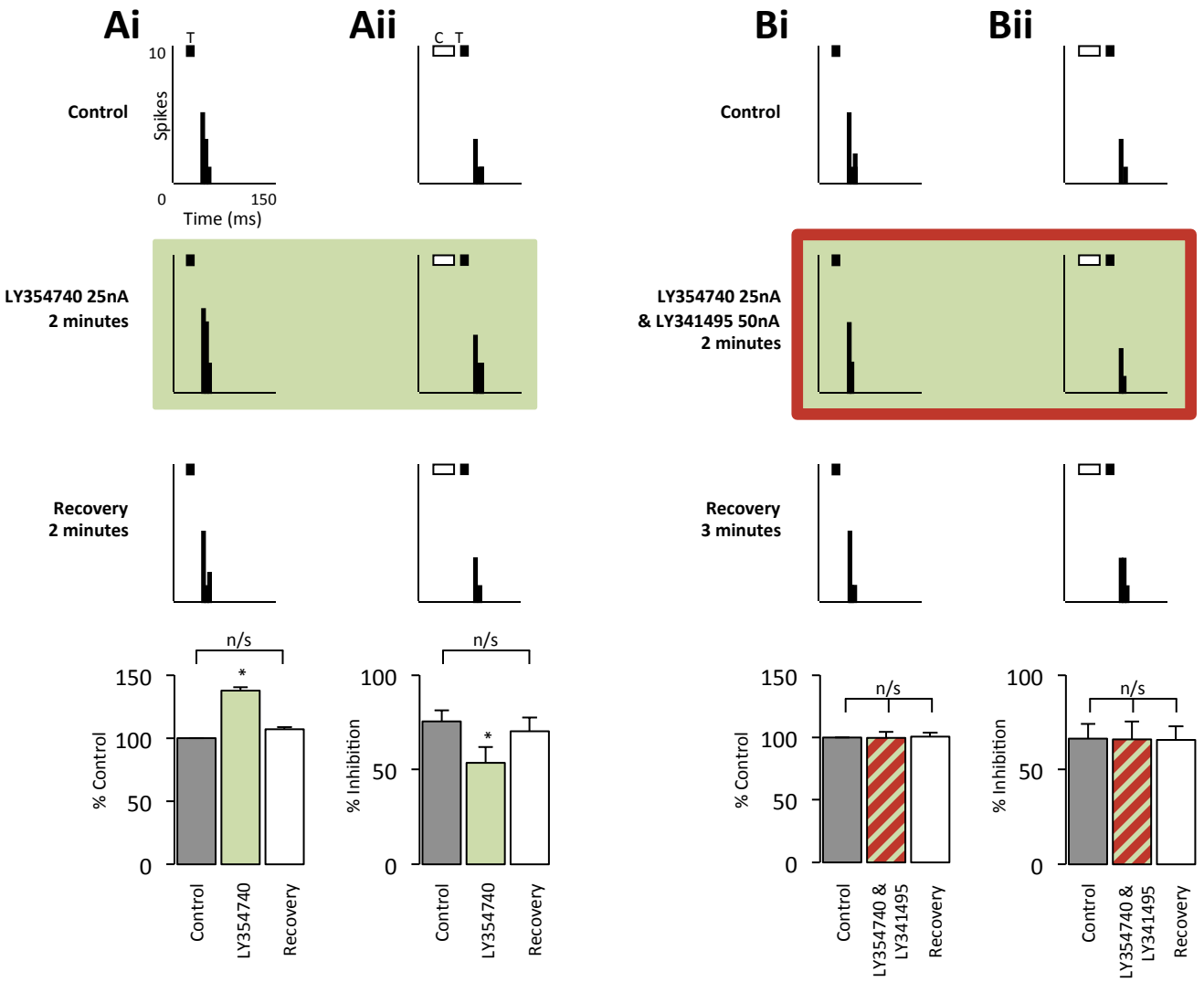

FIGURE 7.03 VB neurone responses before, during, and after iontophoretic application of the Group II agonist LY354740 either alone or co-applied with the Group II mGlu receptor antagonist LY341495 upon short-duration stimulation of the principal vibrissa and execution of the condition-test protocol. Ai. The top three PSTHs represent responses from a single neurone to short-duration stimulation of the principal vibrissa under control conditions, during application of the Group II mGlu receptor agonist, and during recovery. The bottom histogram represents the mean responses of a group of neurones (n=6) to short-duration stimulation of the principal vibrissa under the same conditions. **Aii.** The top three PSTHs represent responses from a single neurone upon execution of the condition-test paradigm under control conditions, during application of the Group II mGlu receptor agonist, and during recovery. The bottom histogram represents the mean inhibitions of a group of neurones (n=6) to the condition-test paradigm under the same conditions. **Bi.** The top three PSTHs represent responses from a single neurone to short-duration stimulation of the principal vibrissa under control conditions, upon co-application of the Group II mGlu receptor agonist and the Group II mGlu receptor antagonist, and during recovery. The bottom histogram represents the mean responses of a group of neurones (n=22) to short-duration stimulation of the principal vibrissa under the same conditions. **Bii.** The top three PSTHs represent responses from a single neurone to the condition-test paradigm under control conditions, during co-application of the Group II mGlu receptor agonist and the Group II mGlu receptor antagonist, and during recovery. The bottom histogram represents the mean responses of a group of neurones (n=6) upon execution of the condition-test paradigm under the same conditions. T – 10ms short-duration test stimulation to the principal vibrissa; C – 30ms conditioning stimulation to a secondary vibrissa; Spikes - the total number of action potentials recorded per 2ms bin over 6 trials; n/s – not significant. All PSTHs are constructed using responses from the same cell (CVB052b). Histogram data are expressed as mean ± SEM. * indicates $p<0.05$ when compared to control, unless otherwise indicated.

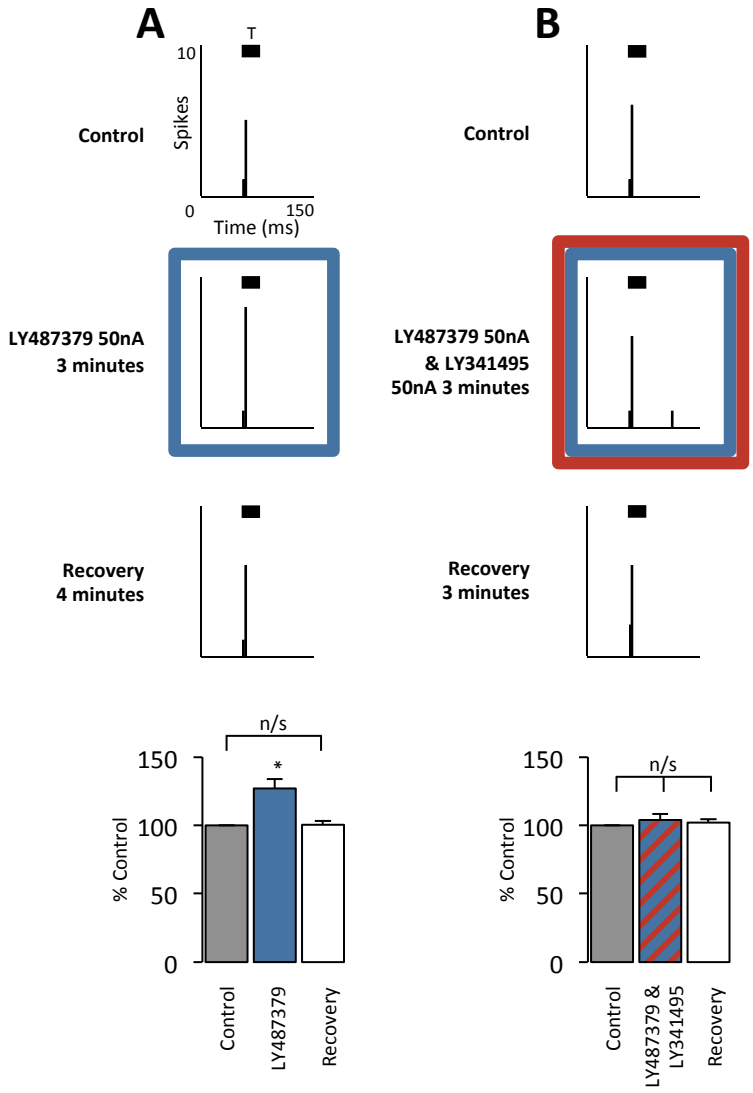

FIGURE 7.04 VB neurone responses before, during, and after iontophoretic application of the mGlu2 PAM LY487379 either alone or co-applied with the Group II mGlu receptor antagonist LY341495 upon short-duration stimulation of the principal vibrissa. A. The top three PSTHs represent responses from a single neurone to short-duration stimulation of the principal vibrissa under control conditions, during application of the mGlu2 PAM, and during recovery. The bottom histogram represents the mean responses of a group of neurones (n=7) to short-duration stimulation of the principal vibrissa under the same conditions. **B.** The top three PSTHs represent responses from a single neurone to short-duration stimulation of the principal vibrissa under control conditions, during co-application of the mGlu2 PAM and the Group II mGlu receptor antagonist, and during recovery. The bottom histogram represents the mean inhibitions of a group of neurones (n=7) to short-duration stimulation of the principal vibrissa under the same conditions. T – 20ms short-duration test stimulation to the principal vibrissa; Spikes - the total number of action potentials recorded per 2ms bin over 6 trials; n/s – not significant. All PSTHs are constructed using responses from the same cell (CVB083b). Histogram data are expressed as mean ± SEM. * indicates $p<0.05$ when compared to control, unless otherwise indicated.

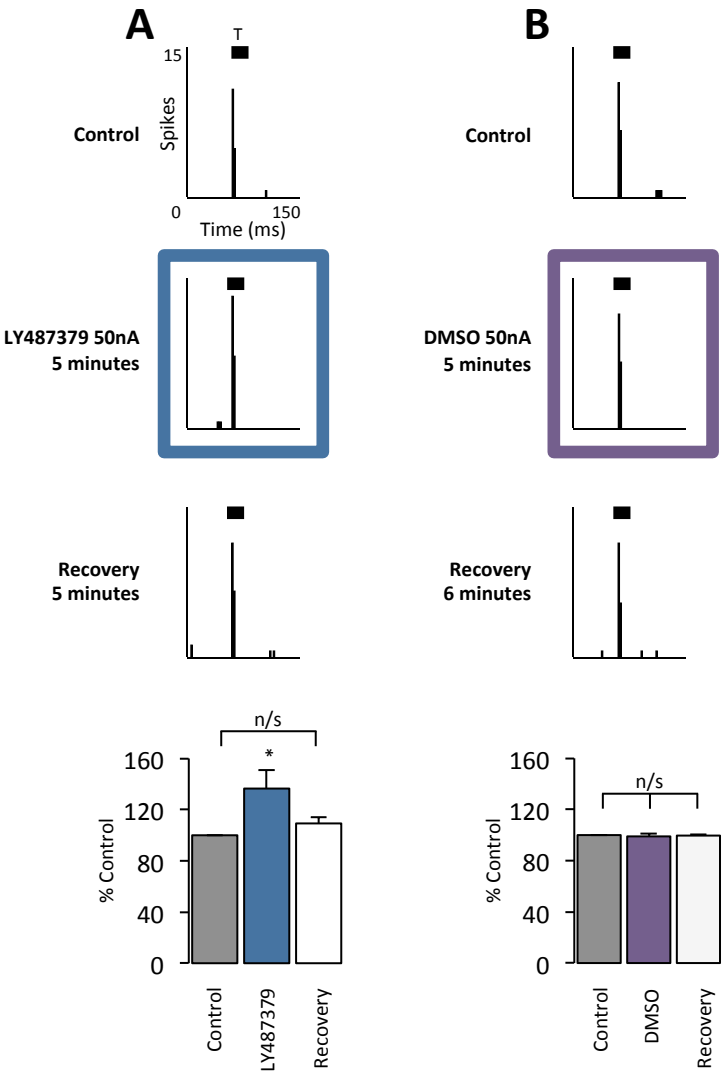

FIGURE 7.05 VB neurone responses before, during, and after iontophoretic application of either the mGlu2 PAM LY487379 or 1% DMSO vehicle upon short-duration stimulation of the principal vibrissa. A. The top three PSTHs represent responses from a single neurone to short-duration stimulation of the principal vibrissa under control conditions, during application of the mGlu2 PAM, and during recovery. The bottom histogram represents the mean responses of a group of neurones (n=6) to short-duration stimulation of the principal vibrissa under the same conditions. **B.** The top three PSTHs represent responses from a single neurone to short-duration stimulation of the principal vibrissa under control conditions, during application of the 1% DMSO vehicle, and during recovery. The bottom histogram represents the mean inhibitions of a group of neurones (n=6) to short-duration stimulation of the principal vibrissa under the same conditions. T – 20ms short-duration test stimulation to the principal vibrissa; Spikes - the total number of action potentials recorded per 2ms bin over 6 trials; n/s – not significant. All PSTHs are constructed using responses from the same cell (CVB034c). Histogram data are expressed as mean ± SEM. * indicates $p<0.05$ when compared to control, unless otherwise indicated.

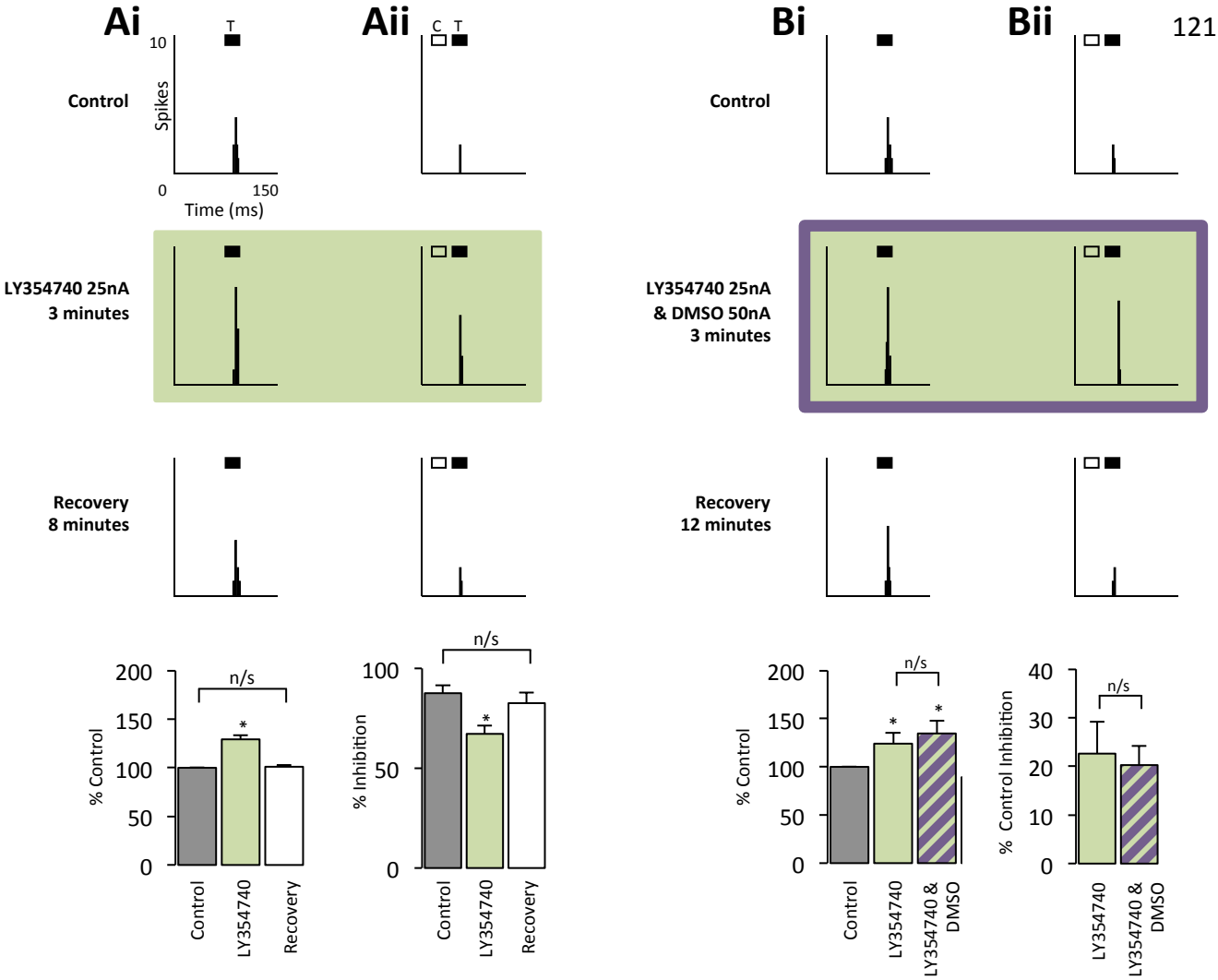

FIGURE 7.06 VB neurone responses before, during, and after iontophoretic application of the Group II mGlu receptor agonist LY354740 either alone or co-applied with the 1% DMSO vehicle upon short-duration stimulation of the principal vibrissa and execution of the condition-test protocol. Ai. The top three PSTHs represent responses from a single neurone to short-duration stimulation of the principal vibrissa under control conditions, during application of the Group II mGlu receptor agonist, and during recovery. The bottom histogram represents the mean responses of a group of neurones (n=10) to short-duration stimulation of the principal vibrissa under the same conditions. **Aii.** The top three PSTHs represent responses from a single neurone upon execution of the condition-test paradigm under control conditions, during application of the Group II mGlu receptor agonist, and during recovery. The bottom histogram represents the mean inhibitions of a group of neurones (n=10) to the condition-test paradigm under the same conditions. **Bi.** The top three PSTHs represent responses from a single neurone to short-duration stimulation of the principal vibrissa under control conditions, upon co-application of the Group II mGlu receptor agonist and the 1% DMSO vehicle and during recovery. The bottom histogram represents the mean responses of a group of neurones (n=10) to short-duration stimulation of the principal vibrissa under control conditions, upon application of the Group II mGlu receptor agonist alone and upon co-application of the Group II mGlu receptor agonist and the 1% DMSO vehicle. **Bii.** The top three PSTHs represent responses from a single neurone to the condition-test paradigm under control conditions, during co-application of the Group II mGlu receptor agonist and the 1% DMSO vehicle, and during recovery. The bottom histogram represents the mean reduction in sensory inhibition of a group of neurones (n=10) compared to control to application of the Group II mGlu receptor agonist alone, or co-applied with the 1% DMSO vehicle upon execution of the condition-test paradigm. T – 20ms short-duration test stimulation to the principal vibrissa; C – 20ms conditioning stimulation to a secondary vibrissa; Spikes - the total number of action potentials recorded per 2ms bin over 6 trials; n/s – not significant. All PSTHs are constructed using responses from the same cell (CVB052b). Histogram data are expressed as mean ± SEM. * indicates $p<0.05$ when compared to control, unless otherwise indicated.

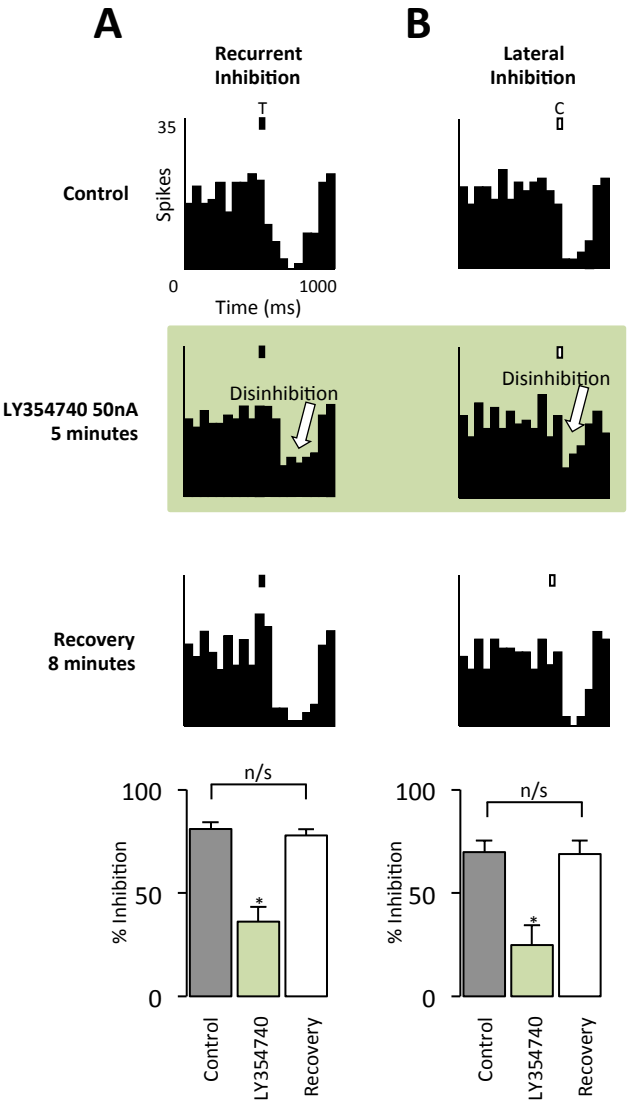

FIGURE 7.07. VB neurone responses before, during, and after iontophoretic application of the Group II mGlu receptor agonist LY354740 upon stimulation of either the principal or secondary vibrissa to evoke recurrent and lateral inhibition respectively. A. The top three PSTHs represent responses from a single neurone during continuous NMDA application (see Methods section 6.1.4.3) to short-duration stimulation of the principal vibrissa under control conditions, during application of the Group II mGlu receptor agonist, and during recovery. The bottom histogram represents the mean inhibitions of a group of neurones (n=6) to short-duration stimulation of the principal vibrissa under the same conditions. **B.** The top three PSTHs represent responses from a single neurone during continuous NMDA application to short-duration stimulation of a secondary vibrissa under control conditions, during application of the Group II mGlu receptor agonist, and during recovery. The bottom histogram represents the mean inhibitions of a group of neurones (n=6) to short-duration stimulation of a secondary vibrissa under the same conditions. T – 30ms short-duration test stimulation to the principal vibrissa; C – 30ms conditioning stimulation to a secondary vibrissa; Spikes - the total number of action potentials recorded per 50ms bin over 30 trials; n/s – not significant. All PSTHs are constructed using responses from the same cell (CVB060b). Histogram data are expressed as mean ± SEM. * indicates $p<0.05$ when compared to control, unless otherwise indicated.

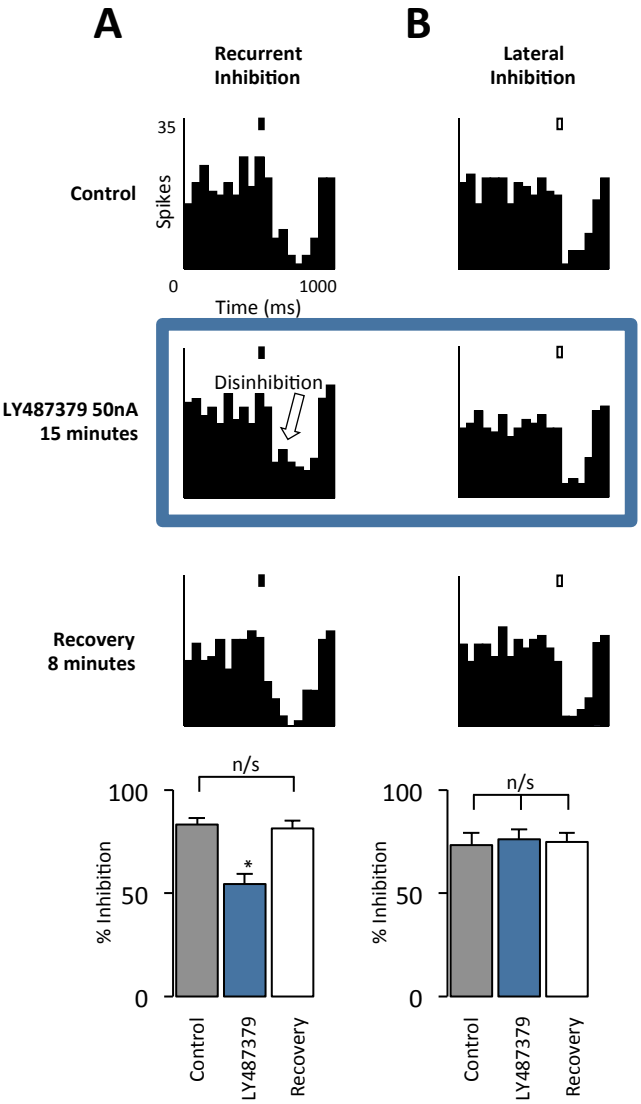

FIGURE 7.08. VB neurone responses before, during, and after iontophoretic application of the mGlu2 PAM LY487379 upon stimulation of either the principal or secondary vibrissa to evoke recurrent and lateral inhibition respectively. A. The top three PSTHs represent responses from a single neurone during continuous NMDA application (see Methods section 6.1.4.3) to short-duration stimulation of the principal vibrissa under control conditions, during application of the mGlu2 PAM, and during recovery. The bottom histogram represents the mean inhibitions of a group of neurones (n=6) to short-duration stimulation of the principal vibrissa under the same conditions. **B.** The top three PSTHs represent responses from a single neurone during continuous NMDA application to short-duration stimulation of a secondary vibrissa under control conditions, during application of the mGlu2 PAM, and during recovery. The bottom histogram represents the mean inhibitions of a group of neurones (n=6) to short-duration stimulation of a secondary vibrissa under the same conditions. T – 30ms short-duration test stimulation to the principal vibrissa; C – 30ms conditioning stimulation to a secondary vibrissa; Spikes - the total number of action potentials recorded per 50ms bin over 30 trials; n/s – not significant. All PSTHs are constructed using responses from the same cell (CVB060b). Histogram data are expressed as mean ± SEM. * indicates $p<0.05$ when compared to control, unless otherwise indicated.

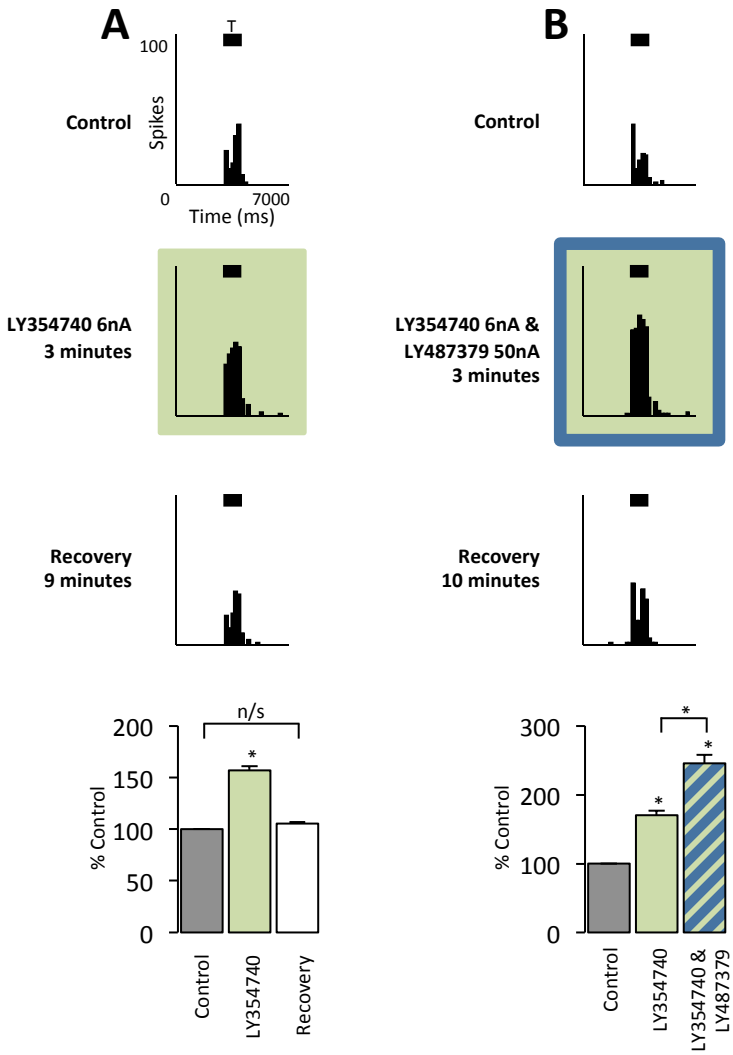

FIGURE 7.09. VB neurone responses before, during, and after iontophoretic application of the Group II mGlu receptor agonist LY354740 either alone or co-applied with the mGlu2 PAM LY487379 upon long-duration stimulation of the principal vibrissa. A. The top three PSTHs represent responses from a single neurone to long-duration stimulation of the principal vibrissa under control conditions, during application of the Group II mGlu receptor agonist, and during recovery. The bottom histogram represents the mean responses of a group of neurones (n=21) to long-duration stimulation of the principal vibrissa under the same conditions. **B.** The top three PSTHs represent responses from a single neurone to long-duration stimulation of the principal vibrissa under control conditions, upon co-application of the Group II mGlu receptor agonist and the mGlu2 PAM, and during recovery. The bottom histogram represents the mean responses of a group of neurones (n=8) to long-duration stimulation of the principal vibrissa under control conditions, upon application of the Group II mGlu receptor agonist alone and upon co-application of the Group II mGlu receptor agonist and the mGlu2 PAM. T – 1000ms long-duration test stimulation to the principal vibrissa; Spikes - the total number of action potentials recorded per 200ms bin over 18 trials; n/s – not significant. All PSTHs are constructed using responses from the same cell (CVB038d). Histogram data are expressed as mean ± SEM. * indicates $p<0.05$ when compared to control, unless otherwise indicated.

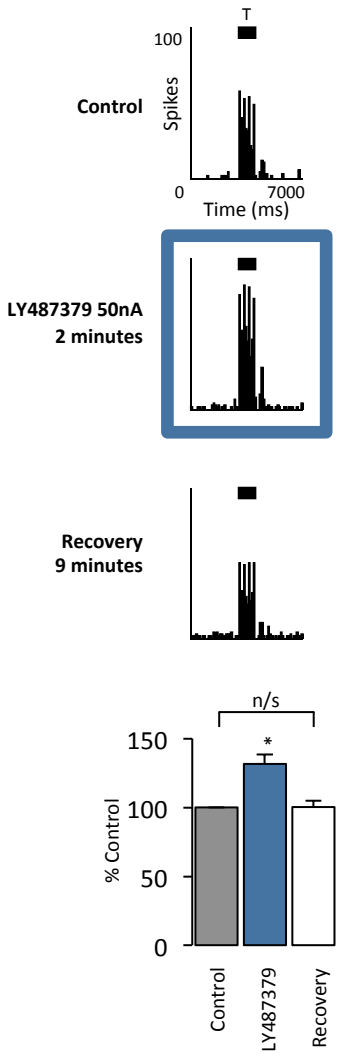

FIGURE 7.10. VB neurone responses before, during and after iontophoretic application of the mGlu2 PAM LY487379 upon long-duration stimulation of the principal vibrissa. The top three PSTHs represent responses from a single neurone to long-duration stimulation of the principal vibrissa under control conditions, during application of the mGlu2 PAM, and during recovery. The bottom histogram represents the mean responses of a group of neurones (n=29) to long-duration stimulation of the principal vibrissa under the same conditions. T – 1000ms long-duration test stimulation to the principal vibrissa; Spikes - the total number of action potentials recorded per 100ms bin over 18 trials; n/s – not significant. All PSTHs are constructed using responses from the same cell (CVB043a). Histogram data are expressed as mean ± SEM. * indicates $p<0.05$ when compared to control, unless otherwise indicated.

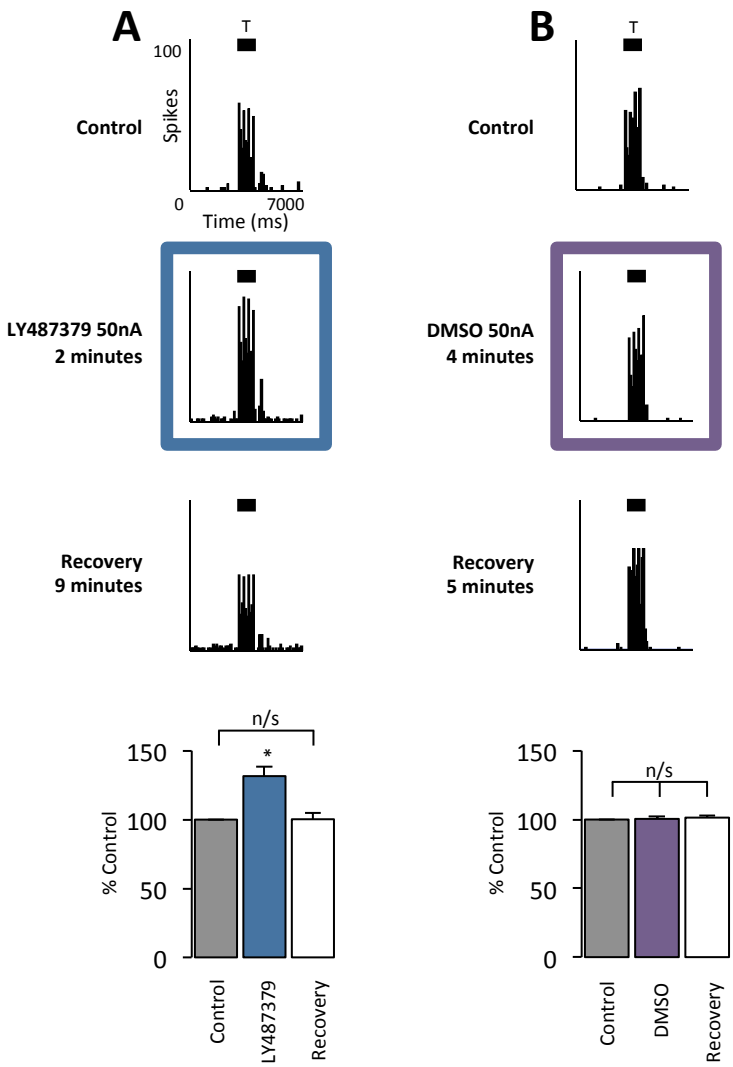

FIGURE 7.11 VB neurone responses before, during, and after iontophoretic application of either the mGlu2 PAM LY487379 or 1% DMSO vehicle upon long-duration stimulation of the principal vibrissa. A. The top three PSTHs represent responses from a single neurone to long-duration stimulation of the principal vibrissa under control conditions, during application of the mGlu2 PAM, and during recovery. The bottom histogram represents the mean responses of a group of neurones (n=10) to long-duration stimulation of the principal vibrissa under the same conditions. **B.** The top three PSTHs represent responses from a single neurone to long-duration stimulation of the principal vibrissa under control conditions, during application of the 1% DMSO vehicle, and during recovery. The bottom histogram represents the mean inhibitions of a group of neurones (n=10) to long-duration stimulation of the principal vibrissa under the same conditions. T – 1000ms long-duration stimulation of the principal vibrissa; Spikes - the total number of action potentials recorded per 100ms bin over 18 trials; n/s – not significant. All PSTHs are constructed using responses from the same cell (CVB043a). Histogram data are expressed as mean ± SEM. * indicates $p<0.05$ when compared to control, unless otherwise indicated.

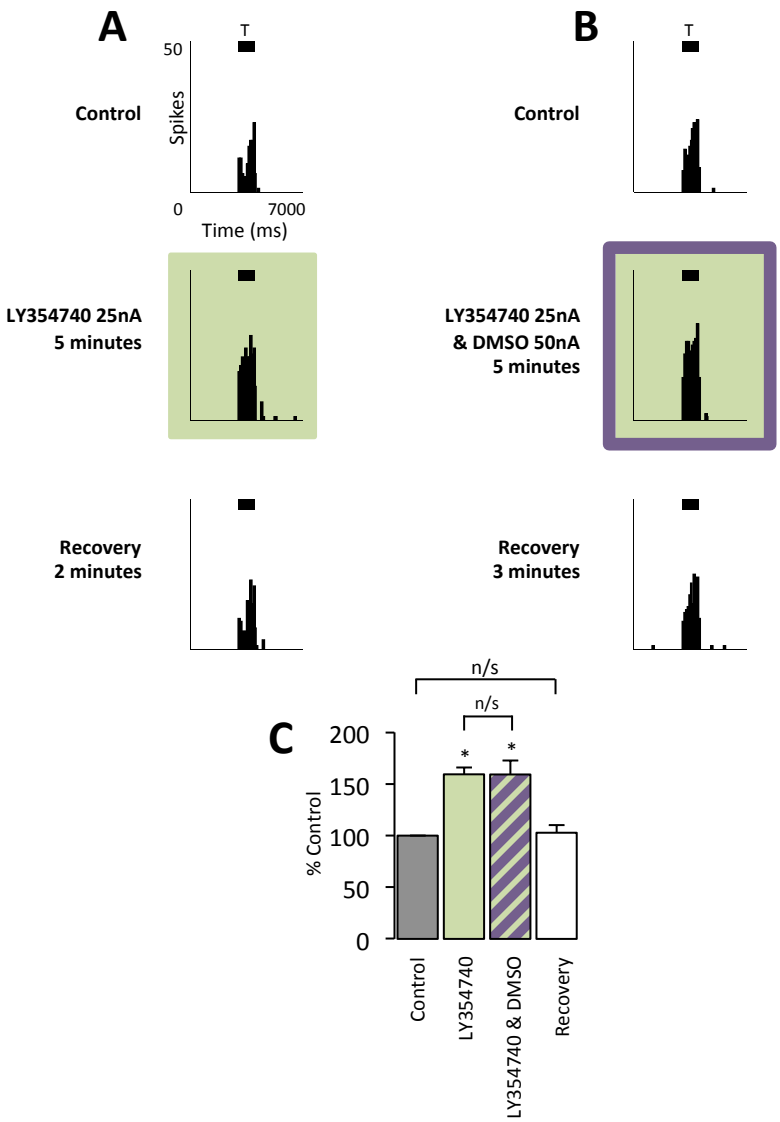

FIGURE 7.12 VB neurone responses before, during, and after iontophoretic application of the Group II mGlu receptor agonist LY354740 either alone or co-applied with 1% DMSO vehicle upon long-duration stimulation of the principal vibrissa. A. The top three PSTHs represent responses from a single neurone to long-duration stimulation of the principal vibrissa under control conditions, during application of the Group II mGlu receptor agonist, and during recovery. **B.** The top three PSTHs represent responses from a single neurone to long-duration stimulation of the principal vibrissa under control conditions, during co-application of the Group II mGlu receptor agonist and the 1% DMSO vehicle, and during recovery. **C.** The bottom histogram represents the mean responses of a group of neurones (n=6) to long-duration stimulation of the principal vibrissa under the same conditions. T – 1000ms long-duration stimulation of the principal vibrissa; Spikes - the total number of action potentials recorded per 100ms bin over 18 trials; n/s – not significant. All PSTHs are constructed using responses from the same cell (CVB038d). Histogram data are expressed as mean ± SEM. * indicates $p<0.05$ when compared to control, unless otherwise indicated.

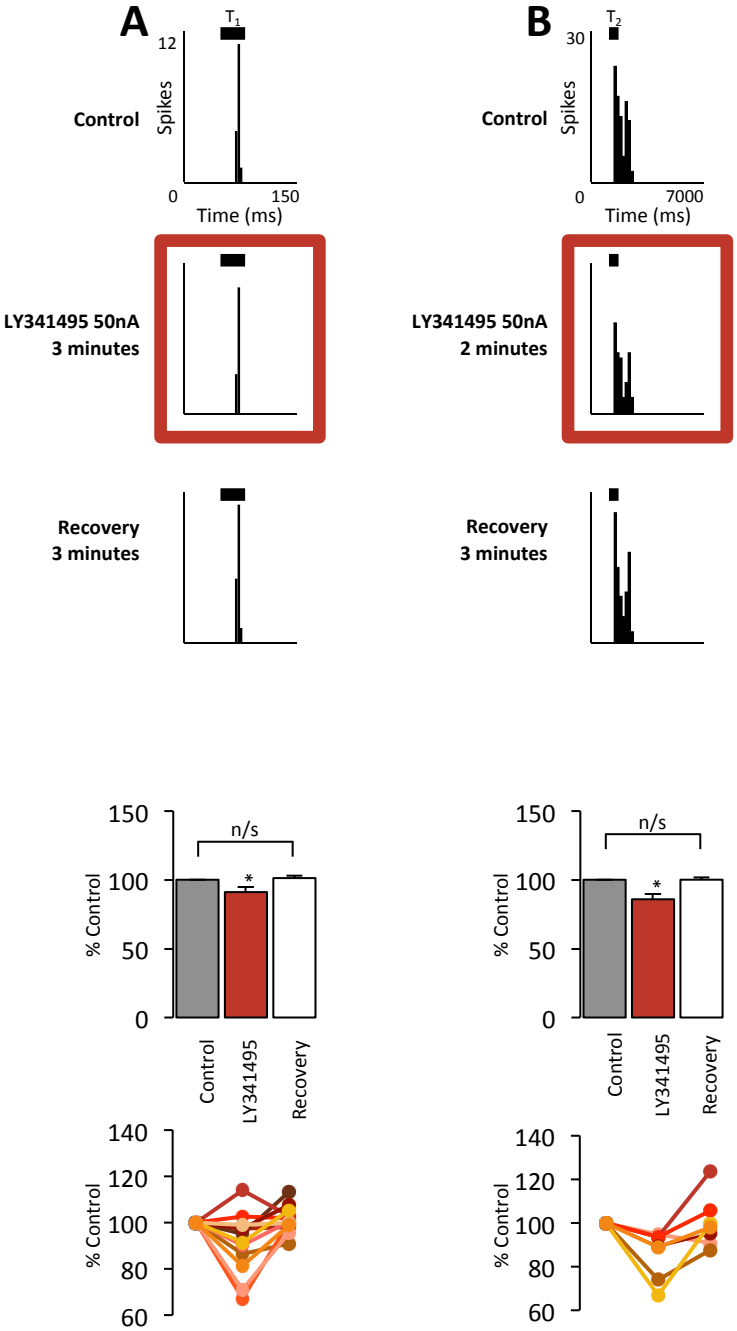

FIGURE 7.13. VB neurone responses before, during and after iontophoretic application of the Group II mGlu receptor antagonist LY341495 upon short- and long-duration stimulation of the principal vibrissa. A. The top three PSTHs represent responses from a single neurone to short-duration stimulation of the principal vibrissa under control conditions, during application of the Group II mGlu receptor antagonist, and during recovery. The bottom histogram represents the mean responses of a group of neurones (n=12), displayed individually in the below scatter plot, to short-duration stimulation of the principal vibrissa under the same conditions. **B.** The top three PSTHs represent responses from a single neurone upon to long-duration stimulation of the principal vibrissa under control conditions, during application of the Group II mGlu receptor antagonist, and during recovery. The bottom histogram represents the mean inhibitions of a group of neurones (n=7), displayed individually in the below scatter plot, to the condition-test paradigm under the same conditions. T_1 – 30ms short-duration test stimulation to the principal vibrissa; T_2 – 500ms long-duration test stimulation to the principal vibrissa; Spikes - the total number of action potentials recorded per bin (2ms bins in A, 100ms bins in B) over 6 trials; n/s – not significant. All PSTHs are constructed using responses from the same cell (CVB085c). Histogram data are expressed as mean ± SEM. * indicates $p<0.05$ when compared to control, unless otherwise indicated.

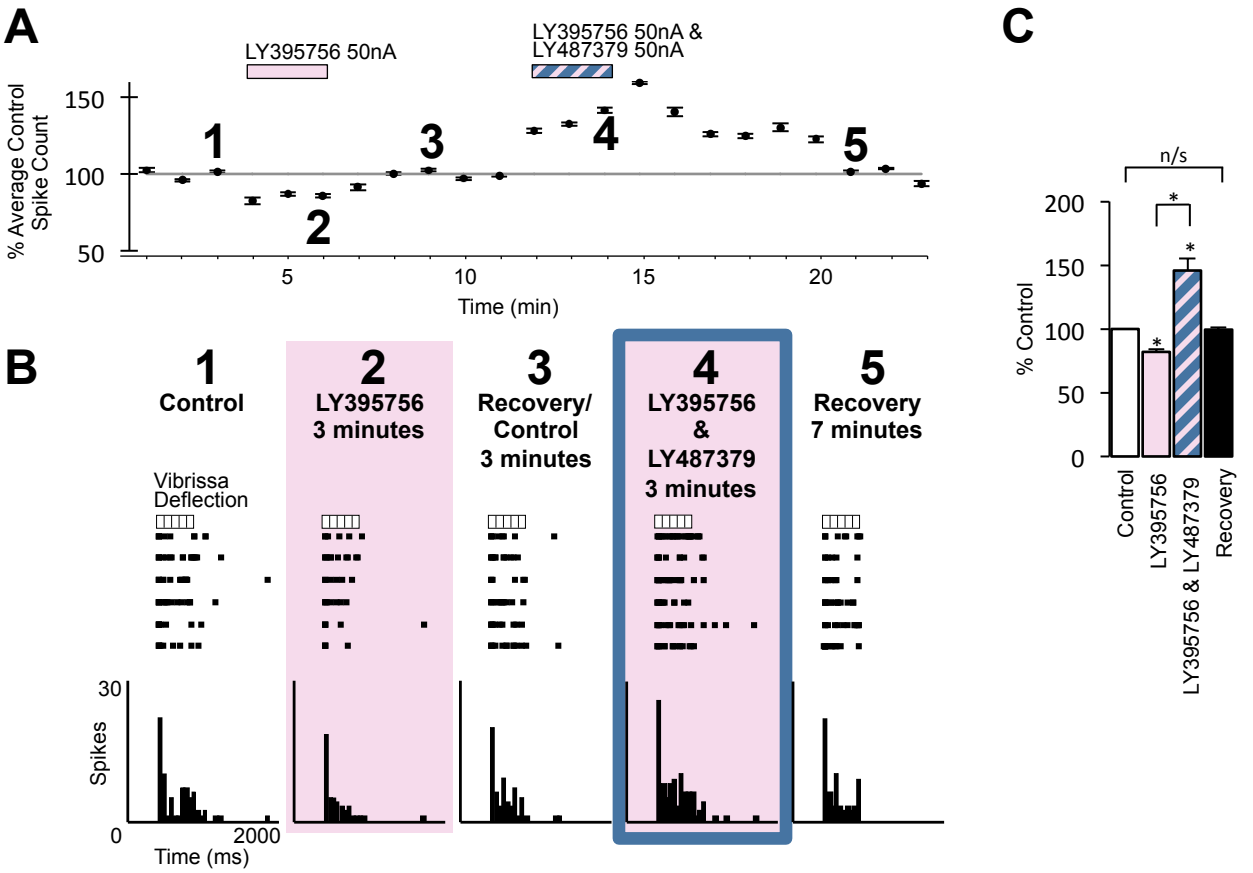

FIGURE 7.14 VB neurone responses before, during, and after iontophoretic application of the dual mGlu2 agonist/mGlu3 antagonist LY395756 either alone or co-applied with the mGlu2 PAM LY487379 upon long-duration stimulation of the principal vibrissa. A. Time line indicating VB neuronal responses (averaged over 60s) to 10Hz long-duration (500ms) stimulation under control conditions and in the presence of the dual mGlu2 agonist/mGlu3 antagonist either alone or co-applied with the mGlu2 PAM. **B.** Raster displays and PSTHs representing responses from a single neurone to long-duration stimulation of the principal vibrissa under control conditions, during application of the dual mGlu2 agonist/mGlu3 antagonist, during a recovery/control period, during co-application of the dual mGlu2 agonist/mGlu3 antagonist with the mGlu2 PAM, and during recovery. **C.** Histogram representing the mean responses of a group of neurones (n=6) to long-duration stimulation of the principal vibrissa under the same conditions. Spikes - the total number of action potentials recorded per 50ms bin over 6 trials; n/s – not significant. All PSTHs are constructed using responses from the same cell (CVB122c). Histogram data are expressed as mean ± SEM. * indicates $p<0.05$ when compared to control, unless otherwise indicated.

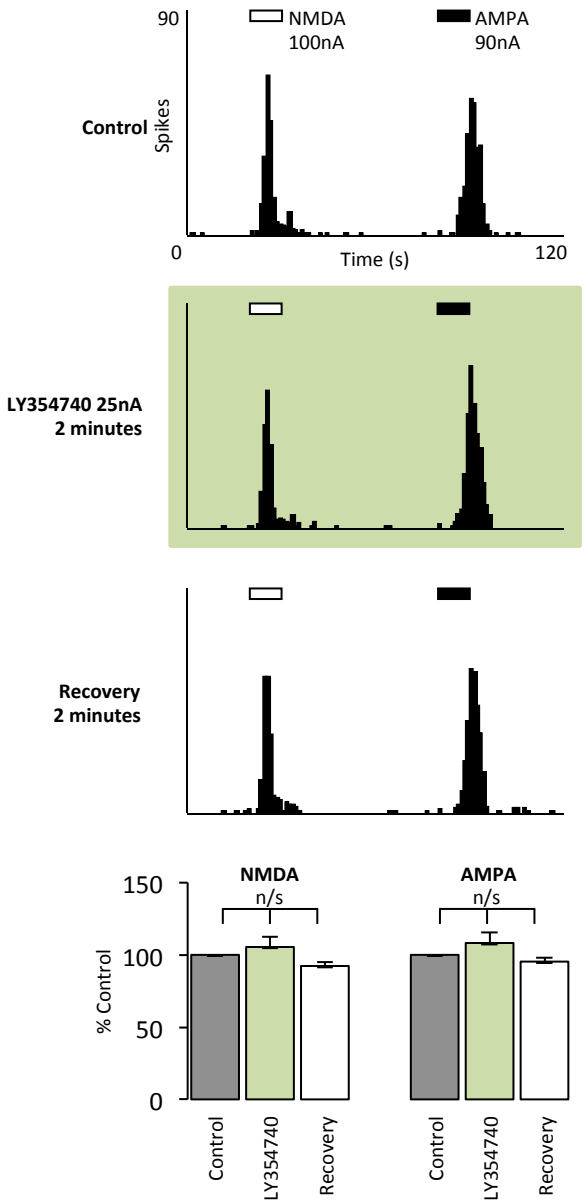

FIGURE 7.15. VB neurone responses to NMDA and AMPA iontophoretic application before, during and after co-application of the Group II mGlu receptor agonist LY354740. The top three PSTHs represent responses from a single neurone to NMDA and AMPA iontophoretic application under control conditions, during co-application of the Group II mGlu receptor agonist, and during recovery. The bottom histogram represents the mean responses of a group of neurones (n=24) upon NMDA and AMPA iontophoretic application under the same conditions. Spikes - the total number of action potentials recorded per 1s bin over 2 trials; n/s – not significant. All PSTHs are constructed using responses from the same cell (CVB030b). Histogram data are expressed as mean ± SEM.

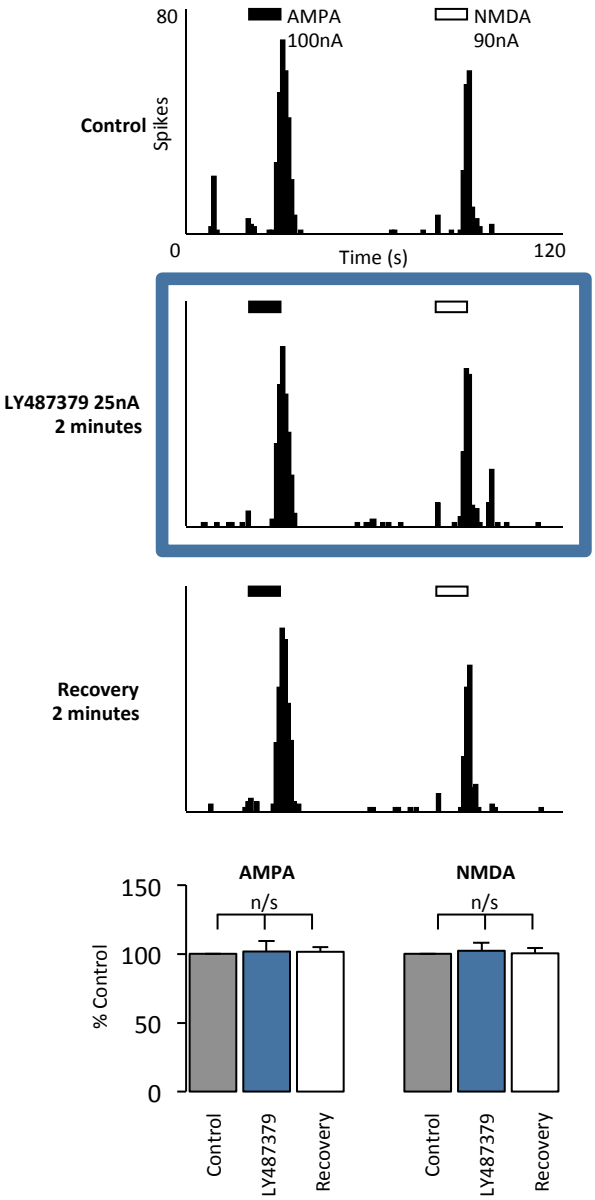

FIGURE 7.16. VB neurone responses to NMDA and AMPA iontophoretic application before, during and after co-application of the mGlu2 PAM LY487379. The top three PSTHs represent responses from a single neurone to NMDA and AMPA iontophoretic application under control conditions, during co-application of the mGlu2 PAM, and during recovery. The bottom histogram represents the mean responses of a group of neurones (n=13) upon NMDA and AMPA iontophoretic application under the same conditions. Spikes - the total number of action potentials recorded per 1s bin over 2 trials; n/s – not significant. All PSTHs are constructed using responses from the same cell (CVB046c). Histogram data are expressed as mean ± SEM.

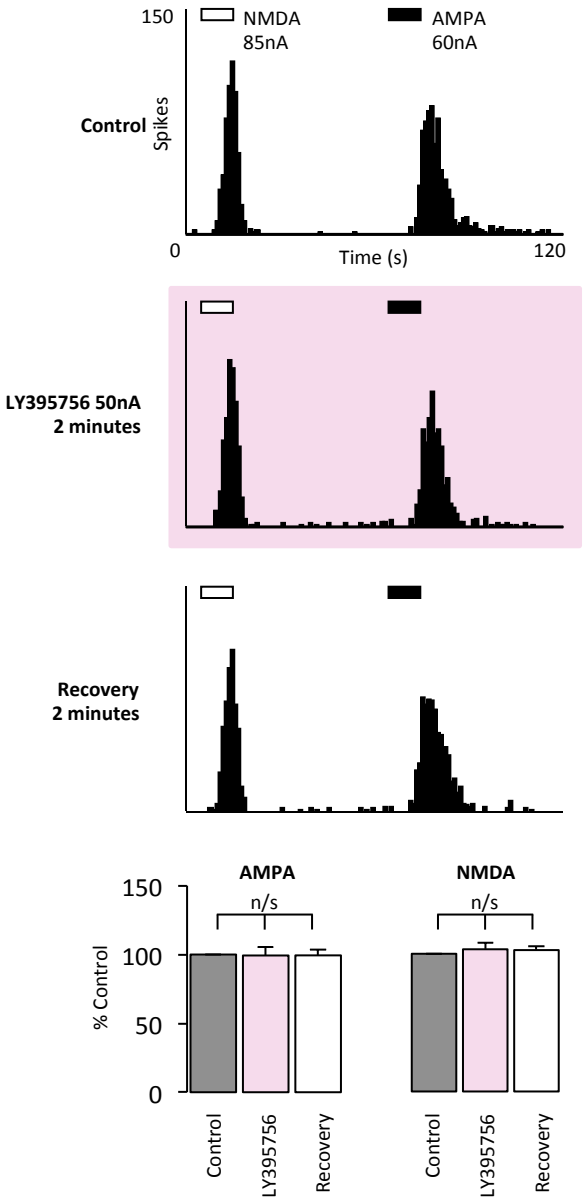

FIGURE 7.17. VB neurone responses to NMDA and AMPA iontophoretic application before, during and after co-application of the dual mGlu2 agonist/mGlu3 antagonist LY341495. The top three PSTHs represent responses from a single neurone to NMDA and AMPA iontophoretic application under control conditions, during co-application of the dual mGlu2 agonist/mGlu3 antagonist, and during recovery. The bottom histogram represents the mean responses of a group of neurones (n=7) upon NMDA and AMPA iontophoretic application under the same conditions. Spikes - the total number of action potentials recorded per 1s bin over 2 trials; n/s – not significant. All PSTHs are constructed using responses from the same cell (CVB046c). Histogram data are expressed as mean ± SEM.

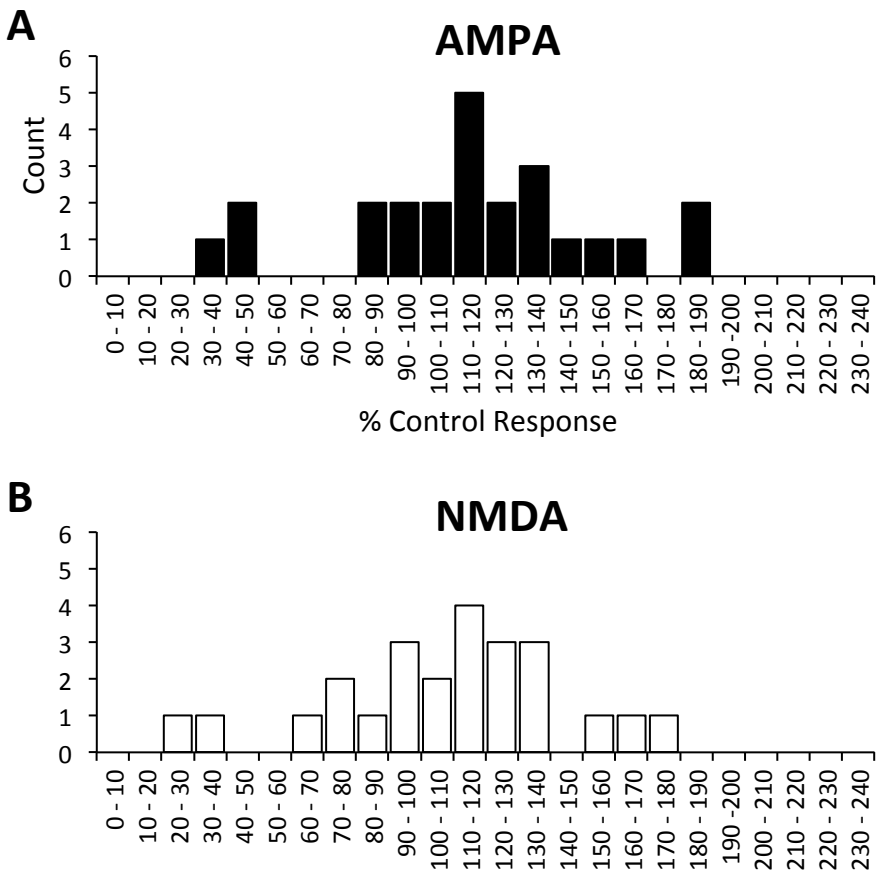

FIGURE 7.18. Distribution plots of the Group II mGlu receptor agonist effect on VB neurone responses to ionotropic agonist application. A. Group II mGlu receptor agonist effect on VB neurone responses to AMPA application. **B.** Group II mGlu receptor agonist effect on VB neurone responses to NMDA application. Count – the number of instances a particular response magnitude was recorded.

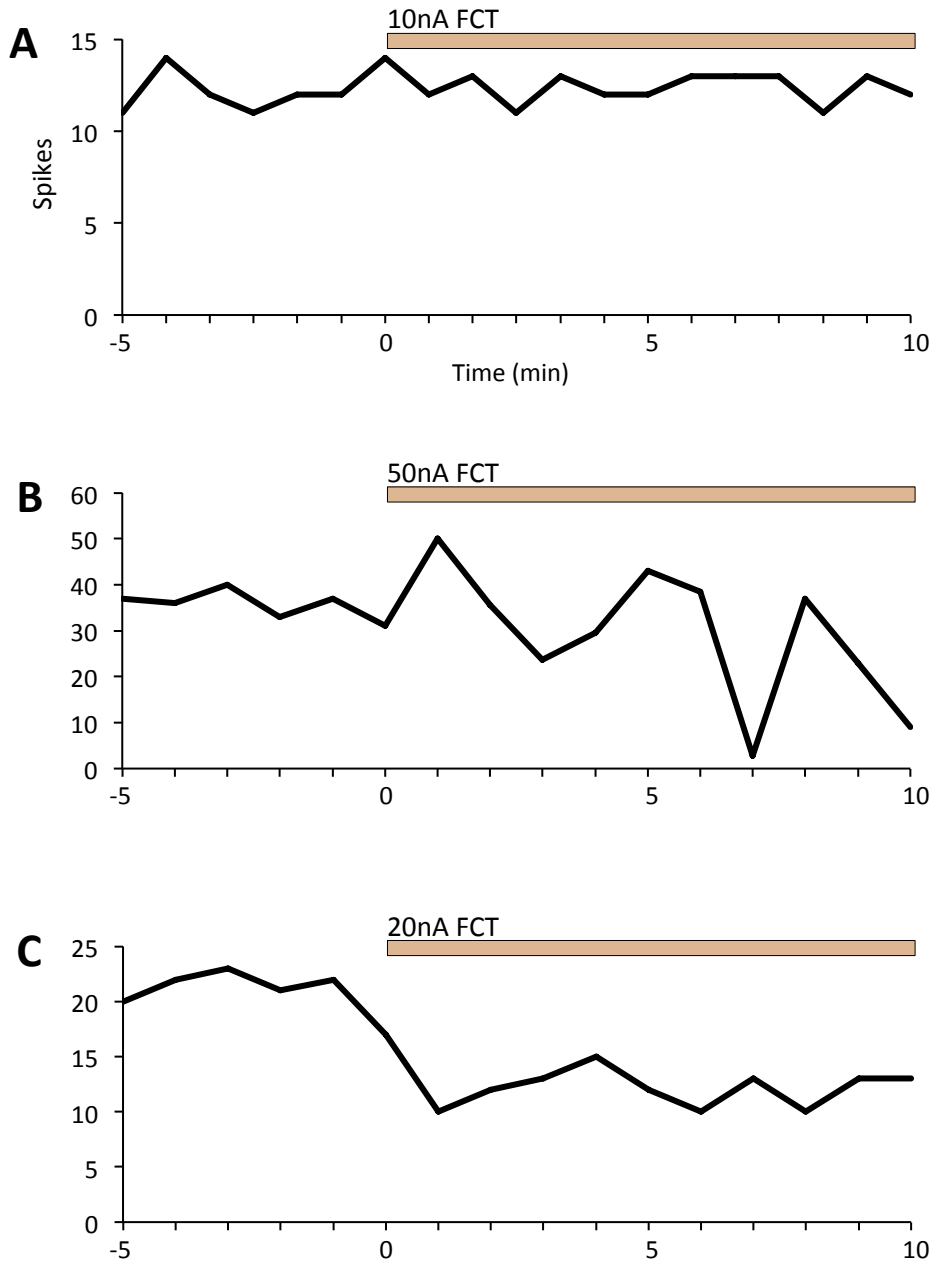

FIGURE 7.19 Line graphs demonstrating the dose-dependency of FCT application on VB neuronal responses to long-duration stimulation of the principal vibrissa. A. Line graph demonstrating that application of 10nA FCT has little effect on VB neuronal responses to long-duration stimulation (1000ms) when applied for 10min (Cell CVB131a). **B.** Line graph demonstrating that application of 50nA FCT results in VB neuronal responses to long-duration stimulation (1000ms) to become erratic and unstable when applied for 10min (Cell CVB130c). **C.** Line graph demonstrating that application of 20nA FCT causes a stable decrease in VB neuronal responses to long-duration stimulation (1000ms) when applied for 10min (Cell CVB130d). Spikes - the total number of action potentials recorded per minute upon long-duration stimulation.

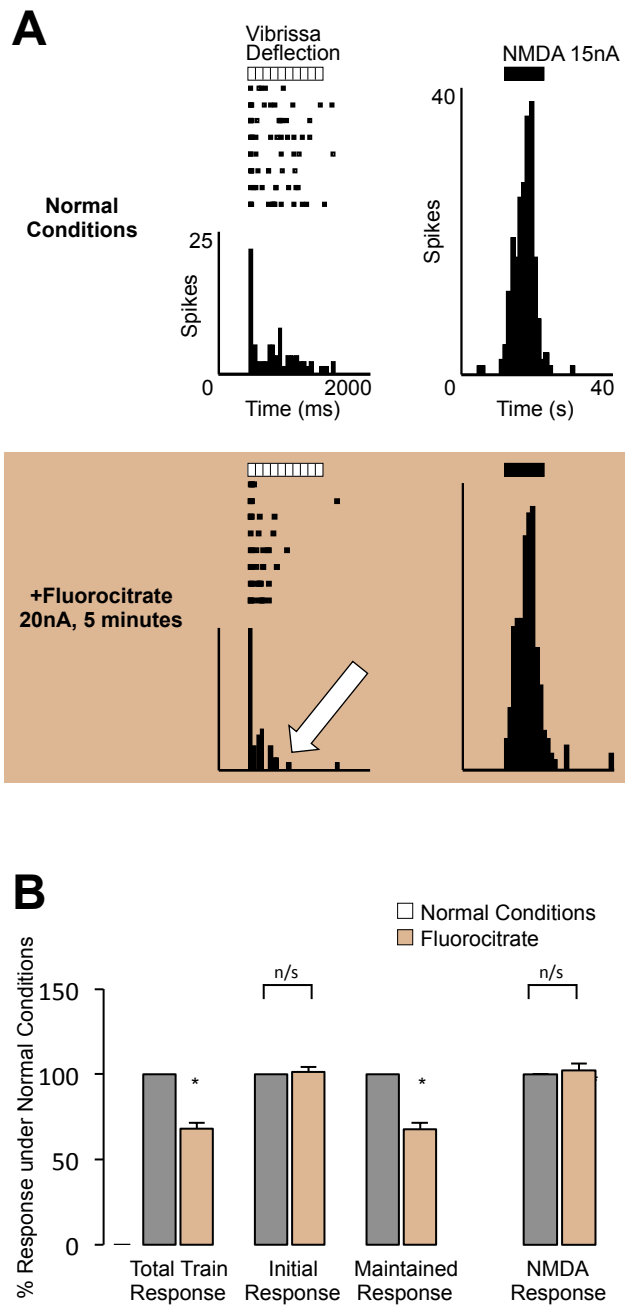

FIGURE 7.20 VB neurone responses to long-duration 10Hz train stimulation of the principal vibrissa and NMDA iontophoretic application before and during application of the selective glial inhibitor fluorocitrate. A. Raster displays and PSTHs of responses of a VB neurone to either long-duration (1000ms) 10Hz train stimulation of a single vibrissa or iontophoretic NMDA application under normal conditions and in the presence of fluorocitrate. **B**. Bars represent the mean % response (±SEM) under normal conditions (100%) and in the presence of fluorocitrate to train stimulation (total, initial and maintained) of single vibrissae (n=16) and NMDA application (n=11). Spikes - the total number of action potentials recorded per bin (sensory stimulation 50ms bins over 8 trials; NMDA application 1s bins over 2 trials); n/s – not significant. All PSTHs are constructed using responses from the same cell (CVB142c). Histogram data are expressed as mean ± SEM. * indicates $p<0.05$ when compared to control, unless otherwise indicated.

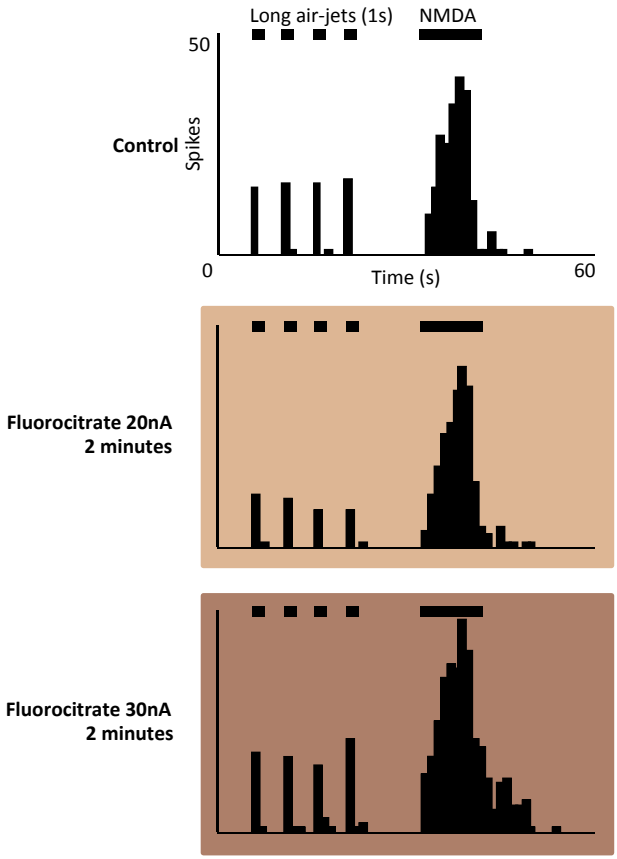

FIGURE 7.21 VB neurone responses to long-duration 10Hz train stimulation of the principal vibrissa and NMDA iontophoretic application before and during application of the selective glial inhibitor fluorocitrate. PSTHs of responses of a VB neurone to either long-duration (1000ms) 10Hz train stimulation of a single vibrissa or iontophoretic NMDA application under normal conditions and in the presence of increasing iontophoretic fluorocitrate application. Spikes - the total number of action potentials recorded per bin (sensory stimulation 50ms bins over 8 trials; NMDA application 1s bins over 2 trials); n/s – not significant. All PSTHs are constructed using responses from the same cell (CVB142e).

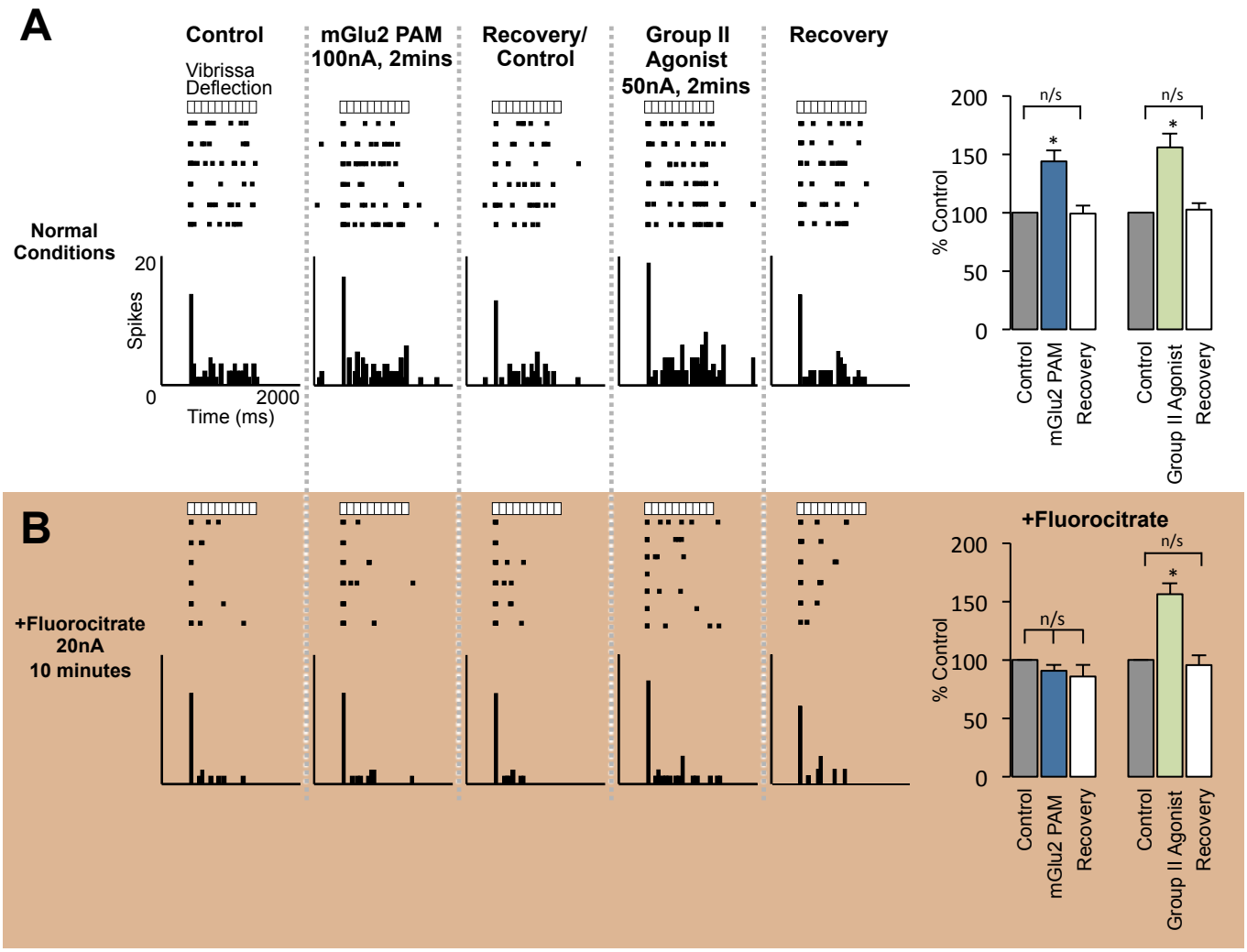

FIGURE 7.22 VB neurone responses before, during, and after iontophoretic application of the mGlu2 PAM LY487379 or Group II mGlu receptor agonist LY354740 either alone or co-applied with selective glial inhibitor fluorocitrate upon long-duration 10Hz stimulation of the principal vibrissa. A. On the left are raster displays and PSTHs representing responses from a single neurone to long-duration (1000ms) 10Hz stimulation of the principal vibrissa under control conditions, during application of the mGlu2 PAM, during a recovery/control period, during application of the Group II mGlu receptor agonist, and during recovery. On the right is a histogram representing the mean responses of a group of neurones (n=6) to long-duration stimulation of the principal vibrissa under the same conditions. **B.** On the left are raster displays PSTHs representing responses from a single neurone to long-duration 10Hz stimulation of the principal vibrissa in the presence of fluorocitrate under control conditions, during application of the mGlu2 PAM, during a recovery/control period, during application of the Group II mGlu receptor agonist, and during recovery. On the right is a histogram representing the mean responses of a group of neurones (n=6) to long-duration stimulation of the principal vibrissa under the same conditions. Spikes - the total number of action potentials recorded per 50ms bin over 6 trials; n/s – not significant. All PSTHs are constructed using responses from the same cell (CVB138a). Histogram data are expressed as mean ± SEM. * indicates $p<0.05$ when compared to control, unless otherwise indicated.

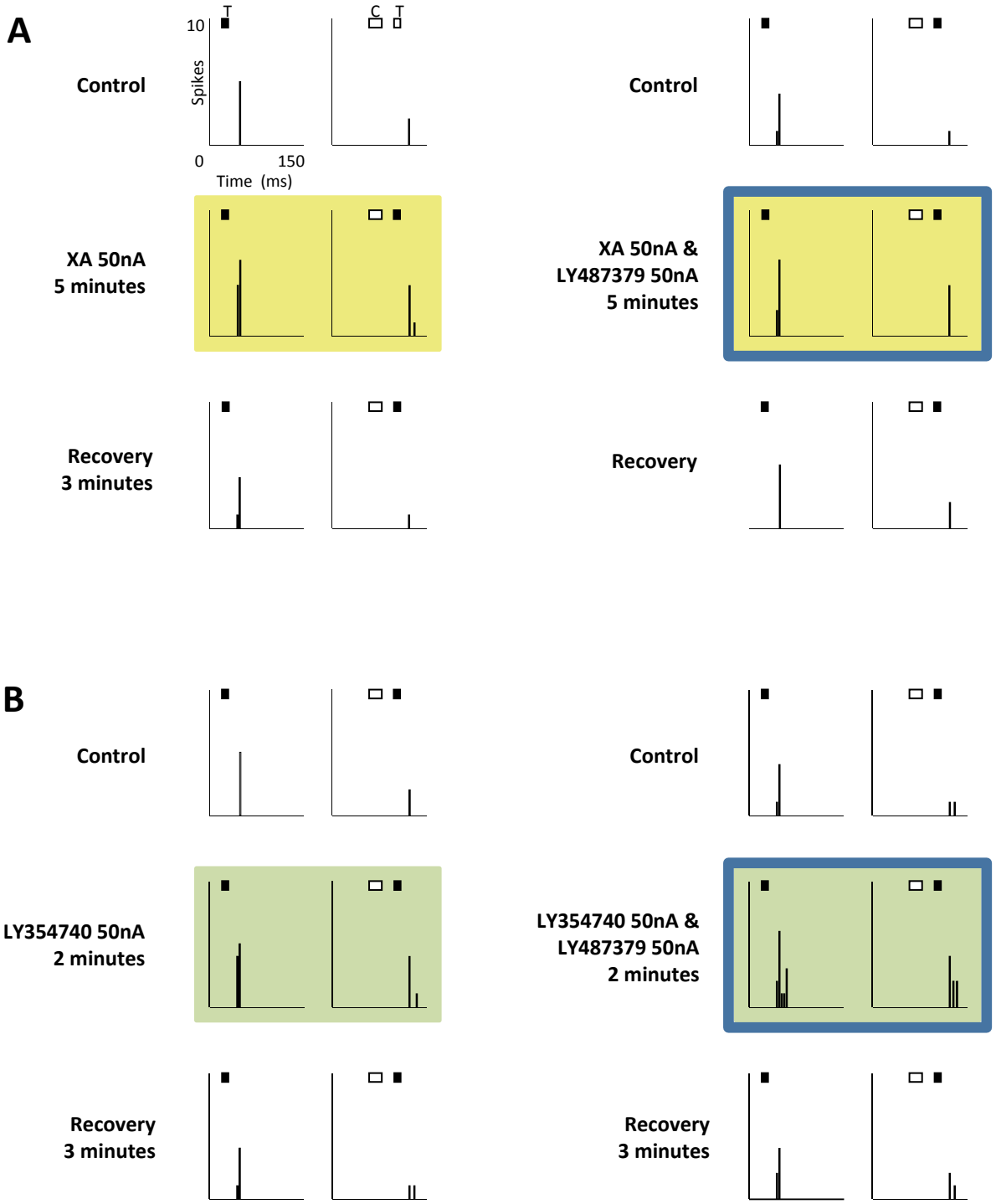

FIGURE 7.23. VB neurone responses before, during, and after iontophoretic application of either XA or the Group II mGlu receptor agonist LY354740 alone or co-applied with the mGlu2 PAM LY487379 upon execution of the condition-test paradigm. A. The PSTHs on the left represent responses from a single neurone upon execution of the condition-test paradigm under control conditions, during application of XA, and during recovery. The PSTHs on the right represent responses from the same neurone upon execution of the condition-test paradigm under control conditions, during co-application of XA and the mGlu2 PAM, and during recovery. **B.** The PSTHs on the left represent responses from the same neurone upon execution of the condition-test paradigm under control conditions, during application of the Group II mGlu receptor agonist, and during recovery. The PSTHs on the right represent responses from the same neurone upon execution of the condition-test paradigm under control conditions, during co-application of the Group II mGlu receptor agonist and the mGlu2 PAM, and during recovery. T – 10ms short-duration test stimulation to the principal vibrissa; C – 20ms conditioning stimulation to a secondary vibrissa; Spikes - the total number of action potentials recorded per 2ms bin over 6 trials. All PSTHs are constructed using responses from the same cell (CVB078e).

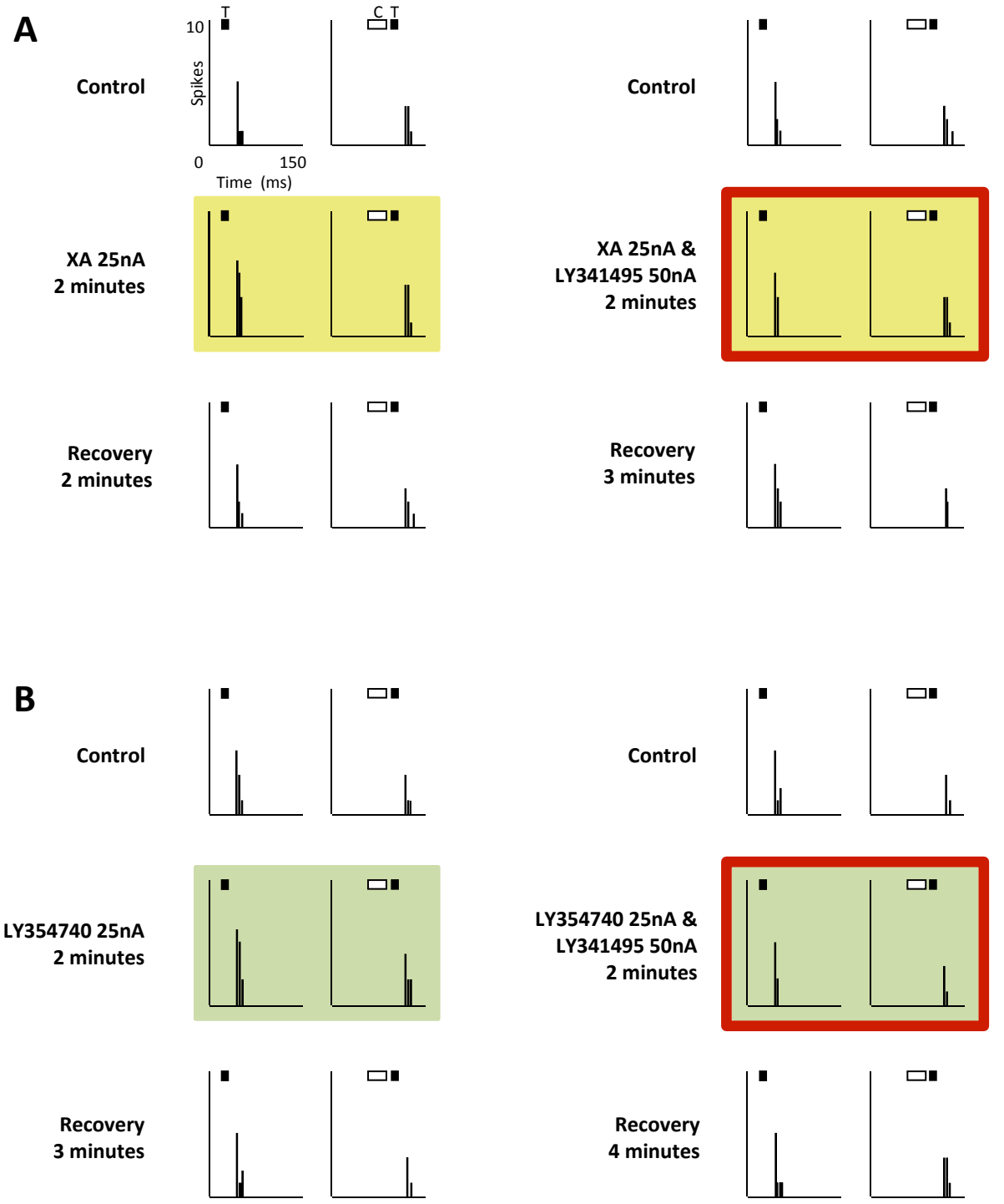

7.24. VB neurone responses before, during, and after iontophoretic application of either XA or the Group II mGlu receptor agonist LY354740 alone or co-applied with the Group II mGlu receptor antagonist LY341495 upon execution of the condition-test paradigm. A. The PSTHs on the left represent responses from a single neurone upon execution of the condition-test paradigm under control conditions, during application of XA, and during recovery. The PSTHs on the right represent responses from the same neurone upon execution of the condition-test paradigm under control conditions, during co-application of XA and the Group II mGlu receptor antagonist, and during recovery. **B.** The PSTHs on the left represent responses from the same neurone upon execution of the condition-test paradigm under control conditions, during application of the Group II mGlu receptor agonist, and during recovery. The PSTHs on the right represent responses from the same neurone upon execution of the condition-test paradigm under control conditions, during co-application of the Group II mGlu receptor agonist and the Group II mGlu receptor antagonist, and during recovery. T – 10ms short-duration test stimulation to the principal vibrissa; C – 30ms conditioning stimulation to a secondary vibrissa; Spikes - the total number of action potentials recorded per 2ms bin over 6 trials. All PSTHs are constructed using responses from the same cell (CVB075a).

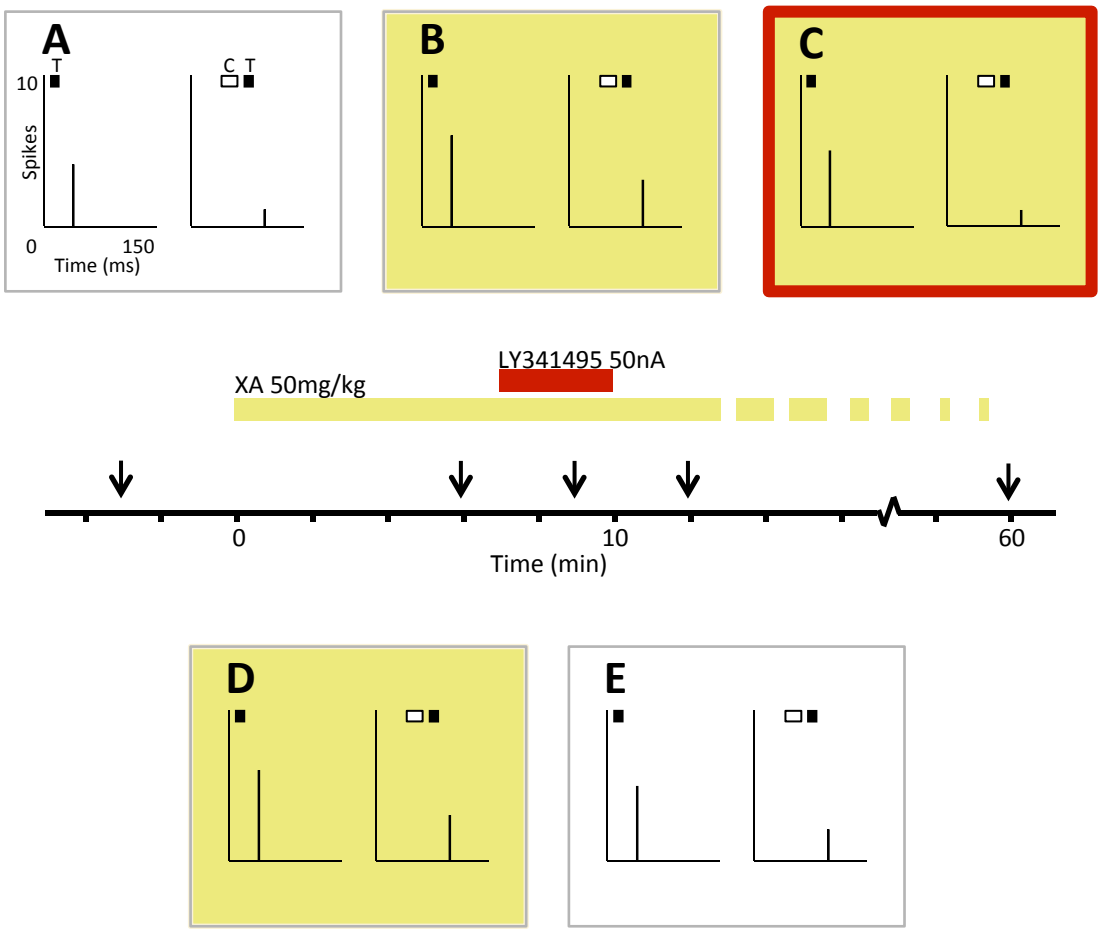

FIGURE 7.25. VB neurone responses before, during and following systemic XA administration upon execution of the condition-test paradigm. The Group II mGlu receptor antagonist LY341395 was iontophoretically co-applied for a short period when XA was affecting sensory inhibition. The PSTHs represent responses from a single neurone upon execution of the condition-test paradigm under control conditions (**A**), following systemic administration of XA (**B**), iontophoretic co-application of the Group II

C

antagonist application demonstrating systemic XA is still affecting sensory inhibition (**D**), and 60 minutes following systemic XA administration (**E**). T – 10ms short-duration test stimulation to the principal vibrissa; C – 20ms conditioning stimulation to a secondary vibrissa; Spikes - the total number of action potentials recorded per 2ms bin over 6 trials. All PSTHs are constructed using responses from the same cell (CVB096a).

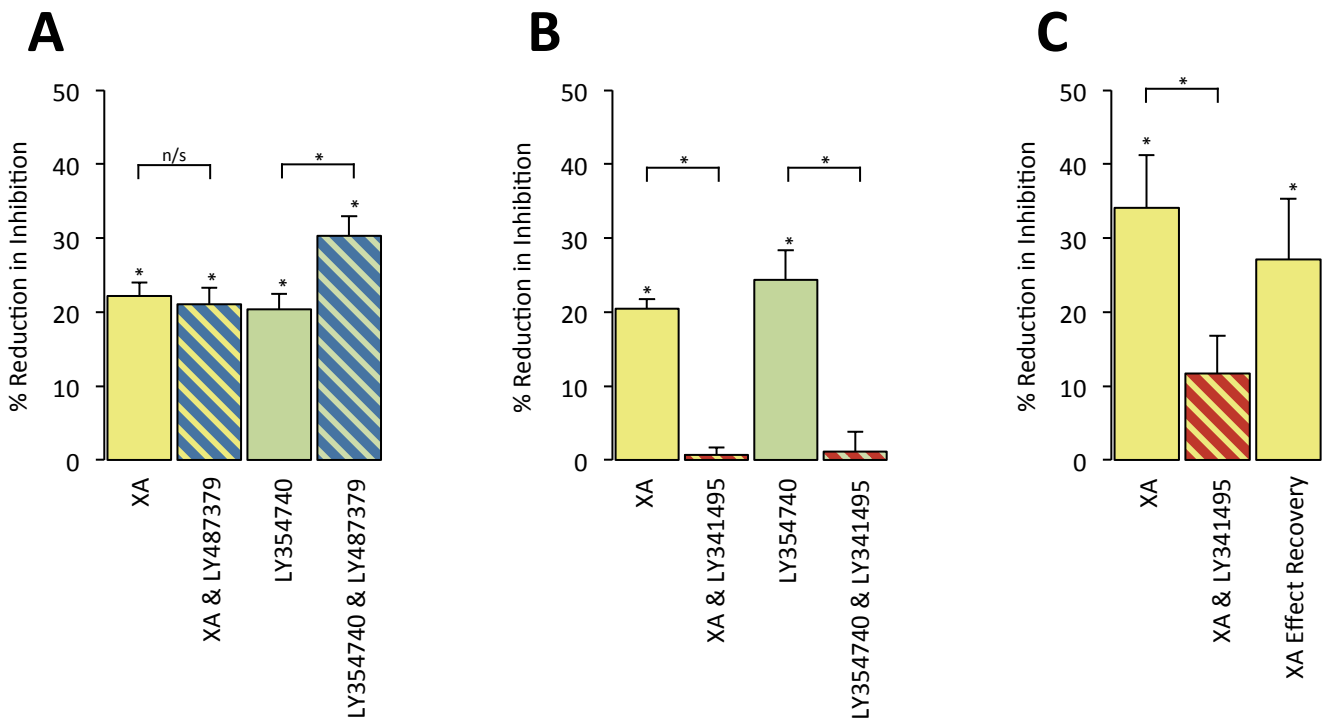

FIGURE 7.26. Summary of XA and Group II mGlu receptor agonist effects on sensory inhibition in the VB. A. The first two bars represent the mean reduction in sensory inhibition of a group of neurones compared to control upon application of XA either alone or in conjunction with the mGlu2 PAM (n=13) upon execution of the condition-test paradigm. The second two bars represent the mean reduction in sensory inhibition of a group of neurones compared to control upon application of the Group II mGlu receptor agonist either alone or in conjunction with the mGlu2 PAM (n=14) upon execution of the condition-test paradigm. **B.** The first two bars represents the mean reduction in sensory inhibition of a group of neurones compared to control upon application of XA either alone or in conjunction with the Group II mGlu receptor antagonist (n=11) upon execution of the condition-test paradigm. The second two bars represent the mean reduction in sensory inhibition of a group of neurones compared to control upon application of the Group II mGlu receptor agonist either alone or in conjunction with the Group II mGlu receptor antagonist (n=6) upon execution of the condition-test paradigm. **C.** This histogram represents the mean reduction in sensory inhibition of a group of neurones compared to control upon systemic application of XA alone, during iontophoretic co-application of the Group II mGlu receptor antagonist, and during recovery from the Group II mGlu receptor antagonist demonstrating systemic XA is still affecting sensory inhibition (n=6). n/s – not significant. Histogram data are expressed as mean ± SEM. * indicates $p<0.05$ when compared to control, unless otherwise indicated.

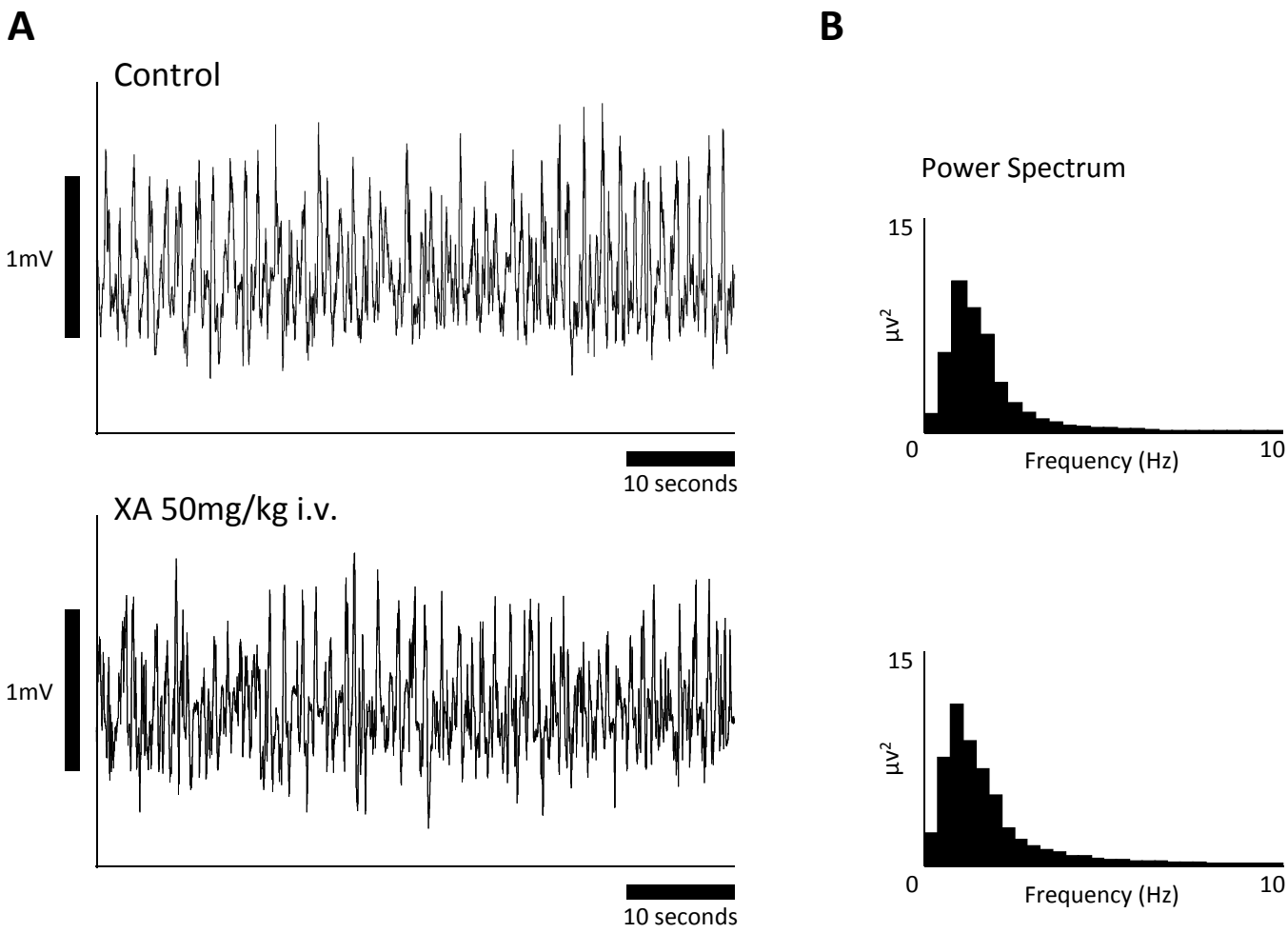

FIGURE 7.27. Effects of systemic XA on electro-cortical activity. A. Recordings of EEG waveforms before and after systemic XA administration. **B.** Power spectra of EEG data in **A.** Note that systemic XA administration does not affect EEG activity.

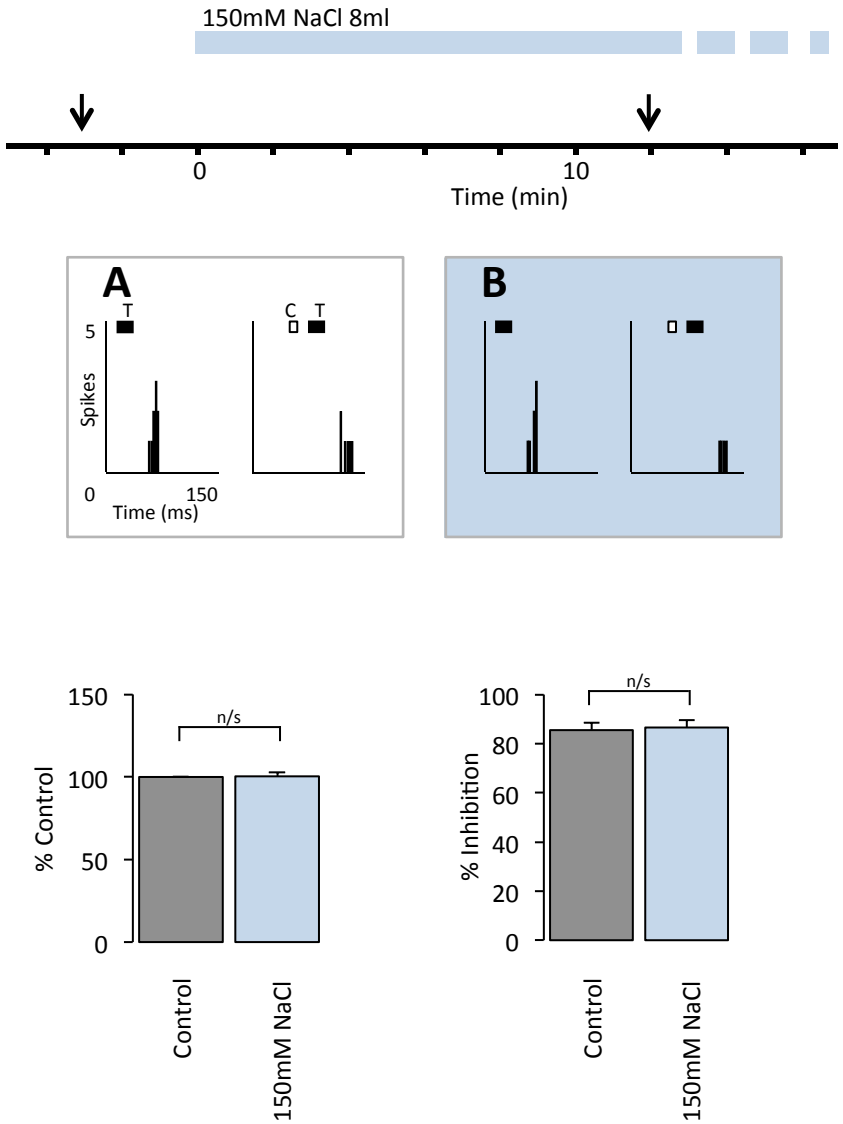

FIGURE 7.28. VB neurone responses before and during systemic saline (150mM NaCl) administration upon execution of the condition-test paradigm. The PSTHs represent responses from a single neurone upon execution of the condition-test paradigm under control conditions (**A**) and following systemic administration of saline (**B**). The bottom histograms represent the mean responses of a group of neurones (n=5) upon execution of the condition-test paradigm under the same conditions. T – 20ms short-duration test stimulation to the principal vibrissa; C – 10ms conditioning stimulation to a secondary vibrissa; Spikes - the total number of action potentials recorded per 2ms bin over 6 trials; n/s – not significant. All PSTHs are constructed using responses from the same cell (CVB101a). Histogram data are expressed as mean ± SEM.

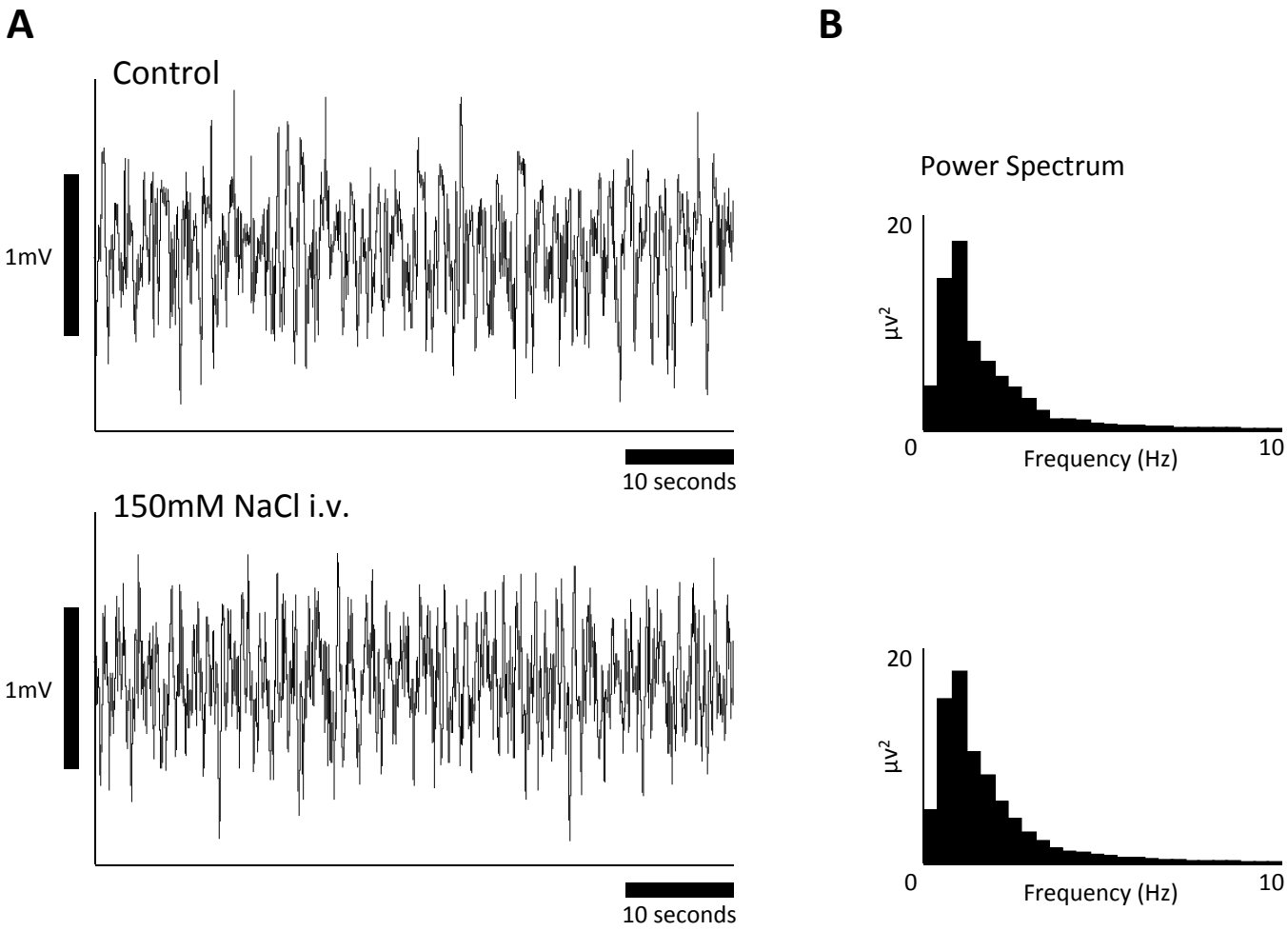

FIGURE 7.29. Effects of systemic saline on electro-cortical activity. A. Recordings of EEG waveforms before and after systemic saline administration. **B.** Power spectra of EEG data in **A.** Note that systemic saline administration does not affect EEG activity.

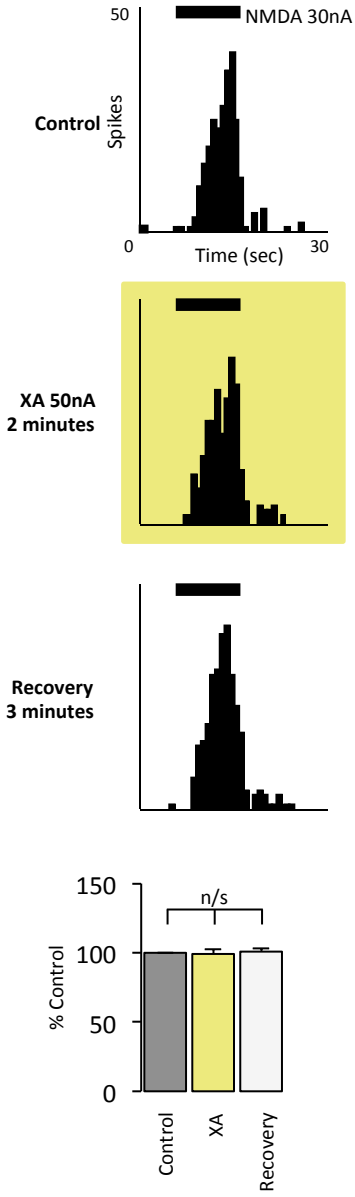

FIGURE 7.30. VB neurone responses to NMDA before, during, and after iontophoretic application of XA. The PSTHs represent responses from a single neurone to iontophoretic NMDA application during control conditions, during application of XA, and during recovery. The bottom histogram represents the mean response of a group of neurones to NMDA application during control conditions, during application of XA, and during recovery (n=8). Spikes - the total number of action potentials recorded per 1s bin over 2 trials; n/s – not significant. All PSTHs are constructed using responses from the same cell (CVB067a). Histogram data are expressed as mean ± SEM.

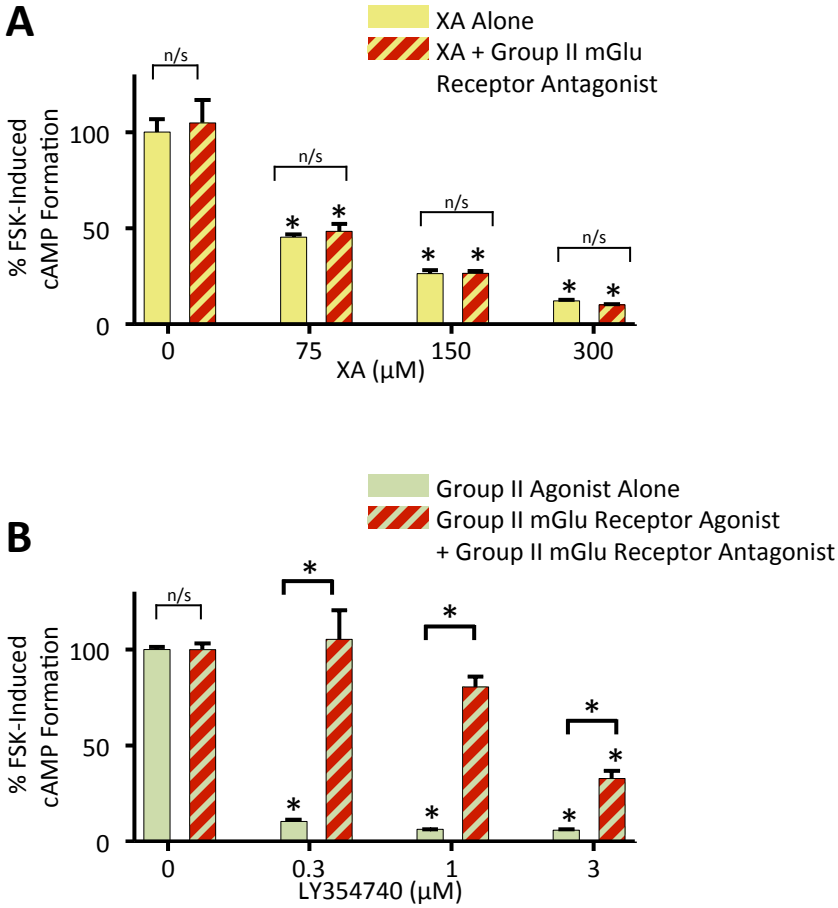

FIGURE 7.31. Effects of XA and the Group II mGlu receptor agonist LY354740 on FSK-induced cAMP formation. A. Action of XA to inhibit FSK-induced cAMP formation, as a percentage of the maximum stimulation achieved by FSK, in the presence or absence of the Group II mGlu receptor antagonist LY341495 (300nM). Note that XA reduces cAMP formation in a dose-dependent manner, but this is not blocked by the antagonist. **B.** Similar experiment to that shown in **A**, but using the Group II mGlu receptor agonist LY354740. Note that LY341495 antagonised the effect of LY354740 n/s – not significant. Histogram data are expressed as mean ± SEM. * indicates $p<0.05$ when compared to control, unless otherwise indicated.

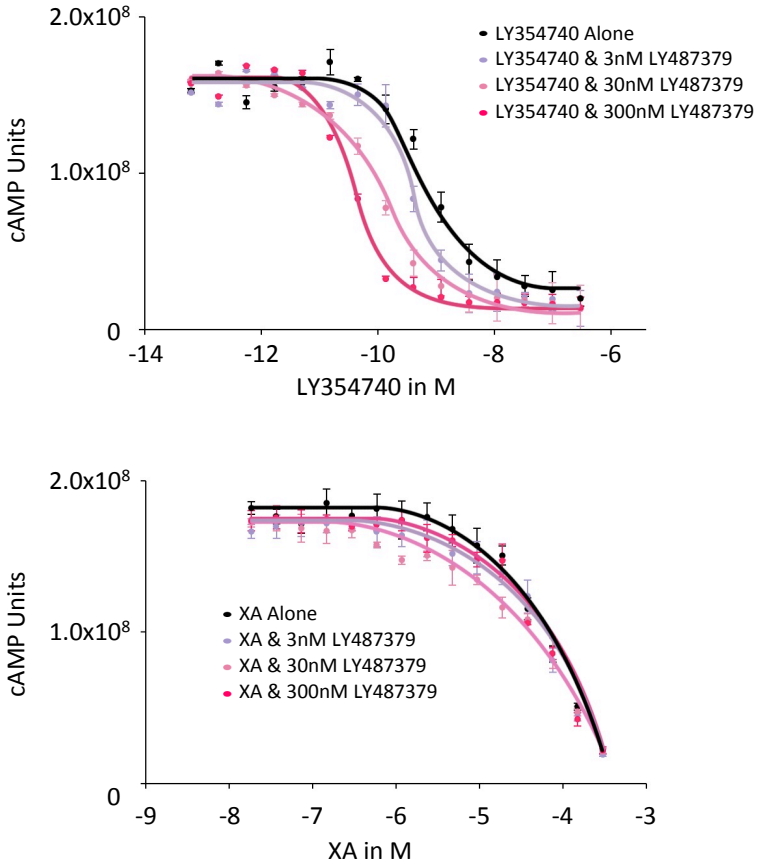

	LY354740 EC_{50} (nM)	XA EC_{50} (μM)
Control	1.9±0.3	66.7±3.6
3nM mGlu2 PAM	1.2±0.1	72.0±7.9
30nM mGlu2 PAM	0.8±0.9	78.3±9.8
300nM mGlu2 PAM	0.7±0.4*	70.6±4.7

FIGURE 7.32. Dose-response curves and computed EC_{50} values for the Group II mGu receptor agonist LY354740 and XA in the cAMP assay under control conditions and in the presence of increasing concentrations of the mGlu2 PAM LY487379. Note that the mGlu2 PAM had little effect on the EC_{50} for XA but did reduce the EC_{50} for the Group II mGlu receptor agonist. * indicates $p<0.05$ when compared to control, unless otherwise indicated.

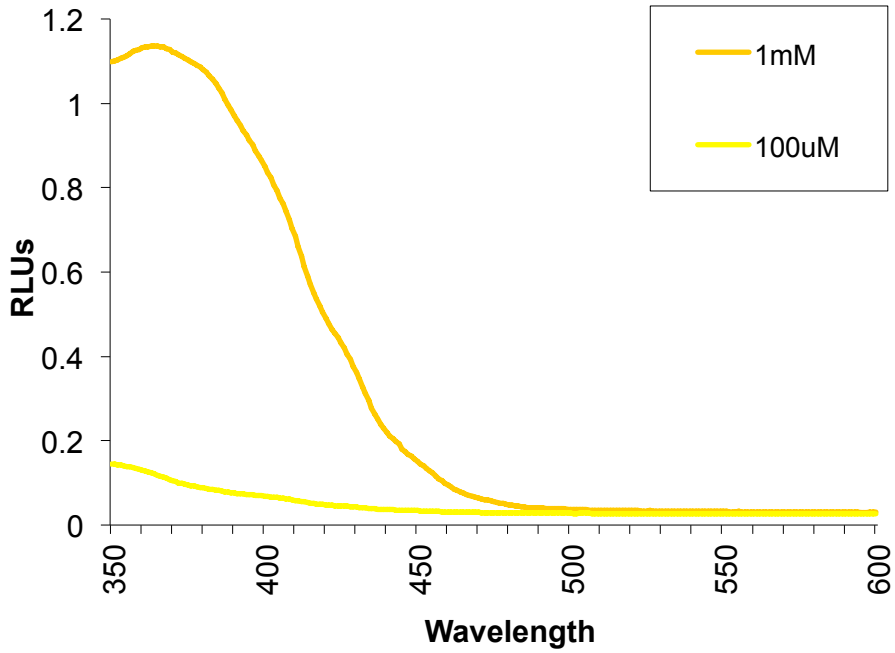

FIGURE 7.33. XA auto-fluoroscence upon exposure to light. XA was exposed to light wavelengths 320-600nM and autofluoroescence was measured in relative light units (RLUs).

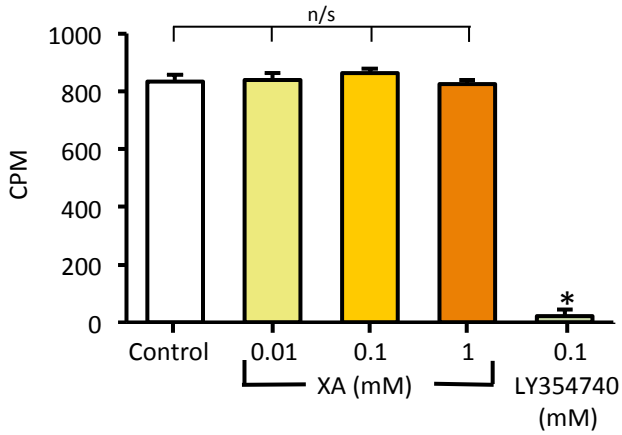

FIGURE 7.34. Effects of XA and the Group II mGlu receptor agonist LY354740 in the mGlu2 receptor radioligand binding assay. Results of binding experiments using [^{3}H]LY341495: XA (0.01-1mM) was not able to displace LY341495 binding whereas LY354740 (0.1mM) displaced binding completely. CPM - counts per minute; n/s – not significant. Histogram data are expressed as mean ± SEM. * indicates $p<0.05$ when compared to control, unless otherwise indicated.

Compound	Short-Duration Response	Long-Duration Response	Sensory Inhibition (Condition-Test Paradigm)	Recurrent Inhibition	Lateral Inhibition	Response to Ionotropic Glutamate Receptor Agonists (NMDA/AMPA)
LY354740	↑	↑	↓	↓	↓	-
LY487379	↑	↑	↓	↓	-	-
LY341495	↓	↓				
DMSO	-	-	-			
LY354740 & LY487379	↑	↑	↑			
LY354740 & DMSO	↑	↑	↑			
LY354740 & LY341495	-	-	-			
LY487379 & LY341495	-	-				
LY395756		↓				
LY395756 & LY487379		↑				
Fluorocitrate		↓				-
LY487379 in the presence of Fluorocitrate		-				
LY354740 in the presence of Fluorocitrate		↑				
Iontophoretic XA	↑		↑			-
Iontophoretic XA & LY341495	-		-			
i.v. XA	↑		↑			
i.v. XA & LY341495	-		-			
XA & PAM	↑		↑			

Table 7.1 Summary table of all the *in vivo* electrophysiological data obtained. Cells with either an ↑, ↓ or – represent the overall effect of a given compound on a given response profile generated from a specific experimental protocol. Cells left blank indicate that the combination of compound with experimental test was not carried out.

A

[XA] µM	% Control XA Alone	% Control XA plus Antagonist	CI XA Alone	CI XA plus Antagonist
0	100±7	104±12	89:110	80:118
75	45±1	48±4	44:48	44:49
150	26±2	27±1	24:30	24:29
300	12±1	10±1	11:13	10:11

B

[LY354740] µM	% Control LY354740 Alone	% Control LY354740 plus Antagonist	CI LY354740 Alone	CI LY354740 plus Antagonist
0	100±1	100±3	98:101	95:105
0.3	11±1	105±15	9:12	87:136
1	6±1	80±5	6:7	65:86
3	6±1	33±4	6:7	28:41

Table 7.2 The effects of XA and the Group II mGlu receptor agonist LY354740 on FSK-induced cAMP formation alone and in the presence of the Group II mGlu receptor antagonist LY341495. **A.** Summary of the XA effect on FSK-induced cAMP formation alone and in the presence of LY341495, along with confidence intervals (CI) for the effects of each concentration applied. **B.** Summary of the LY354740 effect on FSK-induced cAMP formation alone and in the presence of LY341495, along with confidence intervals (CI) for the effects of each concentration applied.

CHAPTER 8 DISCUSSION

It has been well established that GABAergic transmission from the TRN can be reduced through a specific activation of Group II mGlu receptors, resulting in a reduction in sensory-evoked lateral inhibition in the VB (Salt and Eaton, 1995a; b; Salt et al., 1996; Salt and Turner, 1998; Turner and Salt, 2003). The data presented in this thesis clearly support this previous work, whilst also furthering understanding of this mechanism by identifying that both Group II mGlu receptor subtypes contribute to the modulation of this inhibition, that both subtypes are likely activated by endogenously released glutamate upon physiological sensory stimulation, and by discerning the distinct cellular localisations of the two subtypes. Furthermore, I have investigated the action of the putative endogenous selective Group II mGlu receptor agonist XA in modulating this inhibition, and also how this compound interacts with the Group II mGlu receptors using *in vitro* pharmacological methods.

All experiments in this thesis were conducted *in vivo* in animals under general anaesthesia. It is well understood that sensory processing in the brain can be dramatically altered by anaesthesia, as indicated by considerable differences between brain activities in awake and anaesthetised states (Chapin et al., 1981; Shaw et al., 2001; Wang et al., 2010), and also by the depth of anaesthesia (Edeline et al., 1999; Freidburg et al., 1999). The levels of anaesthesia in the experiments conducted in this thesis were closely monitored, with experimental paradigms carried out only in conditions of light general anaesthesia (as indicated upon examination of the EEG), which have been previously demonstrated to elicit

neuronal responses close to those reported in awake animals (Edeline et al., 1999; Freidburg et al., 1999). However, it is important to acknowledge the advantages of using awake animals for recording neural activity when investigating sensory coding mechanisms in order to obtain data that precisely reflects the physiological state. Unfortunately, as the experimental paradigms executed in this thesis required the selective stimulation of individual vibrissae in order to reveal thalamic circuitry components, the same experiments would be difficult to conduct in head-restained awake, and therefore actively whisking, animals. Therefore, the data obtained in this thesis provides a basic understanding of thalamic circuitry function, which could be built upon in further complementary experiments to better understand the complex environment of physiological thalamic function in awake animals.

8.1 Group II mGlu receptor activation facilitates responses to sensory stimulation of the principal vibrissa

A potentiation of VB neurone responses to sensory stimulation of the principal vibrissa was observed upon application of the Group II mGlu receptor agonist LY354740. VB neurone responses to sensory stimulation are mediated by NMDA and AMPA receptors (Salt, 1986; 1987; Salt and Eaton, 1989), but excitatory responses to these ionotropic agonists were not perturbed upon Group II mGlu receptor agonist application. This indicates that non-specific effects are not being produced by application of the Group II mGlu receptor agonist. Furthermore, *in vitro* experiments show that the Group II mGlu receptor agonist can directly reduce TRN-evoked inhibitory postsynaptic potentials without affecting postsynaptic membrane properties of VB neurones (Turner and Salt, 2003). Thus the Group II mGlu

receptors are likely potentiating sensory responses by reducing recurrent inhibition, therefore enabling neurones to elicit enhanced responses. Indeed, use of the same sensory stimulation protocol revealed a similar effect on VB neurone responses when GABAergic transmission originating from the TRN was reduced by the GABA antagonist bicuculline (Salt, 1989). Co-application of the mGlu2 PAM further potentiated the Group II mGlu receptor agonist effect, indicating an mGlu2 component. As with the Group II mGlu receptor agonist, the mGlu2 PAM had no effect on responses evoked by NMDA or AMPA, indicating that this compound is not producing non-specific effects. Interestingly, the percentage-increase in VB neurone response to Group II mGlu receptor agonist application either alone or in conjunction with the mGlu2 PAM was significantly greater for the long-duration stimulus compared to the short-duration stimulus. The long-duration stimulus not only provides the VB neurone with a longer duration of excitatory input than the short-duration stimulus, but also evokes a longer recurrent inhibition. When this is reduced by Group II mGlu receptor agonist application, either alone or in conjunction with the mGlu2 PAM, the VB neurone is able to respond to a greater extent to the longer duration excitatory drive.

A particularly novel and important finding in this thesis is that the Group II mGlu receptor antagonist was able to reduce VB neurone responses to sensory stimulation when applied alone, especially when taken into account in conjunction with the effect of the mGlu2 PAM and the dual mGlu2 agonist/mGlu3 antagonist in the same experimental paradigm. The Group II mGlu receptor antagonist effect in reducing VB neuronal responses to sensory stimulation suggests that the Group II mGlu receptors are normally activated *in vivo* by endogenous ligand upon stimulation of principal vibrissae, with the Group II mGlu receptor

antagonist acting in competition with this endogenous ligand. The mGlu2 PAM effect supports this mechanism of endogenous activation, as the PAM must be acting to potentiate the effect of bound orthosteric agonist as it has no intrinsic agonist activity (Johnson et al., 2003), whilst also suggesting that there is an mGlu2 component to the overall Group II mGlu receptor effect on sensory inhibition. The dual mGlu2 agonist/mGlu3 antagonist effect also supports this mechanism of endogenous activation, as the overriding effect of this compound was that of antagonism, therefore likely acting in competition with this endogenous ligand at mGlu3 receptors, whilst also suggesting that there is an mGlu3 component. How endogenous Group II mGlu receptor activation may occur, and its physiological relevance, are considered in detail below.

8.2 Group II mGlu receptor activation reduces lateral inhibition in the VB evoked by sensory stimulation of the secondary vibrissa

A reduction in VB neurone lateral inhibition evoked by stimulation of a secondary vibrissa shortly before stimulation of the principal vibrissa was observed upon application of the Group II mGlu receptor agonist. This finding is consistent with previous *in vivo* studies that have used alternative Group II mGlu receptor agonists (e.g. (1S,3R)-ACPD, L-CCG-l, (2R,4R)-APDC) (Salt and Eaton, 1995a; b; Salt et al., 1996; Salt and Turner, 1998). In our present study, the mGlu2 PAM potentiated the agonist effect on sensory-evoked lateral inhibition, indicating an mGlu2 component.

8.3 The Group II mGlu receptors may be activated by 'glutamate spillover' from the sensory afferent synapse

As stated above in section 8.1, the effects of the Group II mGlu receptor antagonist, mGlu2 PAM and the dual mGlu2 agonist/mGlu3 antagonist are all indicative of endogenous activation of the Group II mGlu receptors upon sensory stimulation. By further examining the effects of the mGlu2 PAM in the condition-test protocol, it has been possible to delineate the potential source and identity of the endogenously released ligand.

When stimulation of the principal vibrissa was preceded by stimulation of a secondary vibrissa, application of the mGlu2 PAM alone did not alter the level of inhibition in VB. Although puzzling at first, this outcome provides a possible explanation as to how mGlu2 receptors are activated *in vivo*. As the PAM possesses no intrinsic agonist activity (Johnson et al., 2003), it is possible to speculate that it is potentiating the effects of endogenously released glutamate, which could lead to an increase in response to principal vibrissa stimulation. Indeed, it is the action of this endogenous glutamate that the Group II mGlu receptor antagonist and the dual mGlu2 receptor/mGlu3 antagonist may be acting to block, resulting in a reduction in the response of VB neurones. The source of this glutamate may be from excitatory afferent terminals, which could be sensory or cortical in origin. Ultrastructural studies indicate that there are no axo-axonic contacts onto GABAergic terminals, and cortical afferent terminals are not closely associated with TRN terminals in the rat VB (Ohara and Lieberman, 1993). Therefore, transmission from and receptors associated with corticothalamic afferent terminals are unlikely to be involved in this mechanism. However, ultrastructural studies do indicate that sensory afferent terminals are

located close to TRN afferent GABAergic terminals and glial processes on the soma or proximal dendrites of neurones in the rat VB (Ralston, 1983; Ohara and Lieberman, 1993). Glutamate may therefore be 'spilling over' from the sensory afferent synapse to activate Group II mGlu receptors localised on glial processes surrounding GABAergic terminals (Liu et al., 1998; Mineff and Valtschanoff, 1999), and/or mGlu3 receptors localized on TRN-originating GABAergic axons (Tamaru et al., 2001), leading to a reduction in recurrent inhibition with consequent facilitation of responses to sensory stimuli. Similar 'glutamate spillover' has been shown to activate Group II mGlu receptors *in vitro* (Alexander and Godwin, 2005; 2006; Chen and Bonham, 2005; Linden et al., 2005), making it appropriate to speculate that Group II mGlu receptors in the VB may be activated via this mechanism *in vivo*. In addition, Group II mGlu receptors have been demonstrated to regulate non-vesicular release of glutamate from glial cells via the cysteine-glutamate transporter in other brain regions (Xi et al., 2002; Moran et al., 2003; Baker et al., 2008). Such locations are therefore ideally suited for these receptors to modulate GABAergic transmission due to their close association with sensory afferent terminals on the soma and proximal dendrites of VB neurones (Ralston, 1983; Ohara and Lieberman, 1993).

However, in the condition-test stimulation protocol when principal vibrissa stimulation was preceded by stimulation of a secondary vibrissa, the above mechanism could not take place. In this scenario, inhibition in the VB via the TRN is provided laterally upon stimulation of the secondary vibrissa (Pinault and Deschênes, 1998; Crabtree, 1999) (**FIGURE 2.3).** This postsynaptic inhibition precedes the principal vibrissa excitation; therefore the subsequent release of glutamate from the sensory afferent terminal would be unable to reduce the

GABAergic transmission from the TRN by acting at Group II mGlu receptors, as inhibition of the VB neurone has already taken place. This was demonstrated with the mGlu2 PAM, as this compound was unable to alleviate lateral inhibition. Unfortunately a similar conclusion cannot be drawn for mGlu3 receptor activation, due to a lack of selective pharmacological tools for this receptor subtype.

An additional stimulation protocol was devised to further investigate the above hypothesis that mGlu2 receptors may be activated by 'glutamate spillover' from the sensory afferent synapse upon sensory stimulation. If such a mechanism does occur, then application of the mGlu2 PAM should only influence inhibition if there is direct driving of the VB neurone by its principal vibrissa (and therefore glutamate release from the sensory afferent synapse). In contrast, if inhibition is generated in the absence of excitatory activity by stimulation of a secondary vibrissa, then the mGlu2 PAM should be ineffective. There is normally little or no spontaneous activity of VB neurones under the recording conditions, and thus I applied NMDA to evoke neuronal activity, making it possible to observe inhibition on a background of NMDA-evoked excitation. Upon co-application of the mGlu2 PAM during this protocol, the level of recurrent inhibition upon stimulation of the principal vibrissa was reduced, whereas lateral inhibition remained unchanged upon stimulation of a secondary vibrissa. Therefore, principal vibrissa stimulation is required in order for mGlu2 receptors to reduce inhibition in the VB evoked by sensory stimulation, indicating that a local release of glutamate may be required for their activation. In order to demonstrate that lateral inhibition can indeed be reduced, the Group II mGlu receptor agonist was co-applied with NMDA and was shown to alleviate both recurrent and lateral inhibition.

8.4 Astrocytic mGlu2 receptors modulate synaptic transmission at the TRN-VB synapse via a presynaptic mechanism

Fluorocitrate has been established as a useful tool to examine specific properties of glial function due to its specific inhibition of this cell type (Fonnum et al., 1997) (see Results section 7.8). As the mGlu2 PAM effect on sensory-evoked recurrent inhibition in the VB was attenuated upon application of fluorocitrate, I have been able to infer that mGlu2 receptors are able to modulate the function of the TRN-VB synapse via a mechanism involving astrocytic activation. Indeed, ultrastructural studies have indicated that mGlu2 receptors are located on glial processes surrounding TRN terminals in the rodent VB (Liu et al., 1998; Mineff and Valtschanoff, 1999). In addition, I am also able to suggest that astrocytic activation leads to a mechanism that is likely facilitating disinhibition of the postsynaptic VB neurone via action at the presynaptic TRN bouton to increase the responsivity of the VB neurone to sensory stimulation, as opposed to providing a direct postsynaptic excitatory innervation. I have been able to delineate this by drawing together results from different experimental paradigms. Firstly, neither fluorocitrate nor the Group II mGlu receptor agonist and mGlu2 PAM perturb VB neuronal responses to NMDA when iontophoretically applied, indicating that neither normal astrocytic function nor Group II/mGlu2 receptor activation directly impinge upon the postsynaptic excitability of the VB neurone. The latter of these results also provides evidence against the involvement of somatodendritically expressed mGlu2 receptors; a population of receptors for which there is growing evidence that indicates they have profound effects upon neuronal function (Watanabe et al., 2003). Furthermore, it has been demonstrated that Group II mGlu receptor activation reduces inhibitory postsynaptic potentials evoked in VB neurones upon stimulation of the TRN in an

in vitro thalamic slice preparation (Turner and Salt, 2003). Taken together, these results indicate that astrocytic mGlu2 receptors act to modulate sensory-evoked recurrent inhibition in the VB via a mechanism independent of a direct effect on the postsynaptic neurone, and is therefore likely a presynaptic mechanism acting to reduce inhibitory synaptic transmission from the TRN to the VB. Such a mechanism could involve the release of gliotransmitters, which have been demonstrated to modulate synaptic transmission in other brain regions (Guthrie et al., 1999; Fellin et al., 2004; Panatier et al., 2006). Indeed, VB astrocytes have been demonstrated to acts as independent sources of glutamate (Parri et al., 2001; Parri and Crunelli, 2001), although it is important to note that a post-synaptic NMDA-mediated activation of VB neurones by VB astrocytes was observed, which suggests that astrocytic modulation of the TRN-VB synapse may be occurring at both the pre- and post-synaptic sites of the synapse.

Recent work conducted as part of a collarboration with Dr. Rheinallt Parri, Aston University, has provided data that further supports the hypothesis that mGlu2 receptors are able to affect synaptic transmission via astrocytic activation. In these experiments, calcium imaging was performed whereby actue thalamic slices were prepared from Wistar rats and loaded with the calcium indicator Fura-2AM and the specific astrocytic marker SR101. Fluorescence ratio images were acquired during application of the Group II mGlu receptor agonist LY354740 either alone or in conjunction with the application of the mGlu2 receptor PAM LY487379. Astrocytic intracellular calcium levels were monitored and the Group II mGlu receptor agonist was found to significantly elevate astrocytic intracellular calcium levels, which were further potentiated upon coapplication of the mGlu2 PAM. As an increase in

astrocytic intracellular calcium levels, which is indicative of astrocytic activation (Porter et al., 1996; Grosche et al., 1999; D'Ascenzo et al., 2007; Parri et al., 2010, can lead to the release of gliotransmitters (Guthrie et al., 1999; Fellin et al., 2004; Panatier et al., 2000), this data provides further evidence in addition to the work conducted in this thesis to support that astrocytic mGlu2 receptors may modulate the function of the TRN-VB synapse via induction of gliotransmitter release.

In addition, as the mGlu2 PAM possesses no intrinsic agonist activity, acting to potentiate activity of bound orthosteric agonist (Johnson et al., 2003), this mechanism likely occurs upon physiological sensory stimulation via endogenous activation of mGlu2 receptors. The source of this endogenous glutamate, as previously discussed, may be from ' glutamate spillover' from the sensory afferent terminals activating mGlu2 receptors localised on the glial processes (Liu et al., 1998; Minefff and Valtschanoff 1999), which are colocalised with TRN terminals on the soma and/or proximal dendrites of VB neurones (Ralston 1983; Ohara and Lieberman 1993). Indeed, it has been demonstrated that VB astrocytes respond to lemniscal afferent stimulation with an elevation in intracellular calcium (Parri et al., 2010), and this could be occurring via endogenous activation of astrocytic mGlu2 receptors. This mechanism may therefore represent a tripartite signalling pathway to modulate sensory processing in the rodent VB. A similar scheme exists in the hippocampus where astrocytes effectively modulate the strength of afferent fibres upon glutamate release (Jourdain et al., 2007).

It is of importance to note that it would not be possible to show that mGlu2 receptors are acting to reduce inhibitory synaptic transmission from the TRN using $GABA_A$ antagonists in the *in vivo* preparation used here. In this scenario, $GABA_A$ antagonists would block all inhibitory innervation to the VB from the TRN, and theoretically, if the proposed presynaptic mechanism of action were true, I would expect the mGlu2 PAM to have no effect under these conditions, as there would be no GABAergic innervation to alleviate. Alternatively, if a postsynaptic mechanism of action, whereby mGlu2 receptor activation would lead to an increase in postsynaptic VB neurone excitability were true, I would expect to see a further increase in VB neurone responses upon application of the mGlu2 PAM. This experimental paradigm was used by Binns et al., (2003), and application of the $GABA_A$ antagonist SR95531 induced an 184±16% increase in VB neurone responses to sensory stimulation. As there was such a huge increase in the responsiveness of the VB neurone, application of the mGlu2 PAM may not be able to further potentiate responses if it were acting via a postsynaptic mechanism. In this scenario, a 'false negative' result may occur, which would provide support for the presynaptic mechanism of action. As the results of this experimental paradigm would be inconclusive upon interpretation, it was therefore not performed.

8.5 Group II mGlu receptor physiology in the rat VB reflects the distinct cellular localisations of the two subtypes

Whilst the selective glial inhibitor fluorocitrate (Fonnum et al., 1997) was able to ameliorate the mGlu2 PAM effect on sensory-evoked recurrent inhibition in the VB, there was a surviving Group II mGlu receptor agonist effect. This provides support for an mGlu3 receptor component to the overall Group II mGlu receptor effect. Indeed, there is anatomical

evidence that mGlu3, but not mGlu2, receptors are located on TRN terminals within the VB (Tamaru et al., 2001), and that they are able to increase responses to sensory stimulation via a reduction in inhibition arising from the TRN (Turner et al., 2003). In addition, as discussed above, these mGlu3 receptors are also likely activated by endogenous 'glutamate spillover' from the sensory afferent-VB synapse, as the dual mGlu2 agonist/mGlu3 antagonist elicited a reduction in VB neuronal responses to vibrissal stimulations, therefore likely acting as an antagonist at mGlu3 receptors competing with orthosteric endogenous ligand.

It is of importance to note that there is also evidence from ultrastructural studies that indicate both mGlu2 and mGlu3 receptors are localised on glial processes surrounding the TRN-VB synapse (Liu et al., 1998; Mineff and Valtsachanoff, 1999), a Group II mGlu receptor distribution that is also reflected in the rodent LGN (Jeffrey et al., 1996). The data presented in this thesis supports these anatomical findings in the observation that mGlu2 receptors are able to modulate sensory-evoked inhibition in the VB via a mechanism involving astrocytic activation. However, due to a lack of commercially available mGlu3 selective ligands, I am currently unable to investigate whether there is an mGlu3 astrocytic component to the overall Group II mGlu receptor effect on sensory-evoked inhibition in the VB.

Whilst the rodent VB lacks inhibitory interneurones (Ralston, 1983; Barbaresi et al., 1986; Harris and Hendrickson, 1987; Ohara and Lieberman, 1993), their presence has been

anatomically confirmed in other rodent thalamic nuclei, such as the LGN, and in thalamic nuclei of higher-order species such as the cat and non-human primate (Sherman and Guillery 2001; Jones, 2008). It is therefore important to consider whether Group II mGlu receptors are localised on interneurones in these thalamic neuclei, and the resultant effects that their activation may have on thalamic circuitry function. Ultrastructural examination of Group II mGlu receptor distribution in the LGN has detected the presence of these receptors, and have localised them to astrocytic processes in this nucleus; however, there is little evidence to suggest that these receptors are also localised on intrinsic inhibitory interneurones (Jeffrey et al., 1996). Therefore, thalamic inhibitory interneurone function is unlikely to be directly affected by activation of the Group II mGlu receptors.

8.6 Xanthurenic Acid

8.6.1 *In vivo* electrophysiological investigations of XA

XA application was able to significantly reduce sensory-evoked lateral inhibition in the rat VB when applied either iontophoretically or systemically via i.v. injection, with systemic XA application able to alleviate lateral inhibition to a greater extent than iontophoretically applied XA. XA is likely able to penetrate the wider thalamic network that contributes to the function of the VB neurone from which we are recording from when applied systemically, and may therefore be able to modulate synaptic inhibition to a greater extent than can be achieved iontophoretically. The possibility that XA affected the overall function of the thalamocortical network seems less likely as XA did not alter the EEG when given systemically. Gobaille et al*.,* (2008) were able to find increased XA in a number of brain

regions following i.p. XA injection, leading them to postulate that XA is a potential signalling molecule in the rodent CNS. Furthermore, Fazio et al., (2012a) demonstrated that i.p. administration of XA can produce analgesia in the second phase of the formalin pain model, which is mediated by central CNS mechanisms. We have now demonstrated that peripheral i.v. injection of XA can indeed modulate VB neurone responses with physiological relevance.

Previous *in vivo* studies from this laboratory (Salt and Eaton, 1995a; b; Salt et al., 1996; Salt and Turner, 1998), and also the work conducted in this thesis, have shown that iontophoretic application of Group II mGlu receptor agonists (LY354740, [1S,3R]-ACPD, L-CCG-I, [2R,4R]-APDC) can reduce inhibition originating from the TRN. The action of XA in modulating lateral inhibition in the rat VB therefore concords with that of Group II mGlu receptor activation.

Application of XA, both iontophoretically and i.v., appears to produce specific agonism for the Group II mGlu receptors as co-application of the Group II mGlu receptor antagonist completely reversed the XA effect on lateral inhibition. Indeed, the iontophoretic ejection parameters used for the Group II mGlu receptor antagonist in this study have been previously demonstrated by ourselves to produce selective antagonism for the Group II mGlu receptors (Cirone and Salt, 2001). Furthermore, although VB neurone responses to sensory stimulation are mediated by ionotropic glutamate receptors (Salt, 1986; 1987; Salt and Eaton, 1989), excitatory responses to NMDA were not perturbed upon XA application, thus it is unlikely that XA is exerting its effects on sensory transmission via a postsynaptic

mechanism. The most likely interpretation of our *in vivo* data is that XA is reducing lateral inhibition in the VB via a specific activation of the Group II mGlu receptors. However, it is important to note that the Group II mGlu receptor antagonist when applied alone is able to reduce responses to sensory stimulation (Results section 7.5). This apparent reversal of the XA effect may therefore be due to the reduction of VB neurone responses to sensory stimulation via a mechanism independent of the XA mechanism of action, but appears as a reversal due to their two opposing modes of action (i.e. Group II mGlu receptor antagonism eliciting an increase in sensory inhibition, with XA acting to decrease sensory inhibition via a different mechanism of action).

8.6.2 Molecular pharmacological investigations of XA

To further test the possibility that XA modulates Group II mGlu receptor activity, I conducted a series of *in vitro* assays. Initially, I investigated performing functional assays with the FLIPR platform; however, fluorescence artefacts produced by XA hampered these efforts. I therefore utilised cAMP and radioligand binding assays. Although XA was found to not bind to the mGlu2 receptor orthosteric binding site, XA did significantly reduce FSK-induced cAMP formation, although the XA EC_{50} value was within the micromolar range (66µM), which is markedly different to that reported by Fazio et al., (2012a) (200nM). The mGlu2 receptor signal transduction pathway, coupled to $G_{i/o}$, ultimately results in a reduction in cAMP formation (Conn and Pin, 1997) so it is therefore logical to hypothesise that XA exerts its effects through mGlu2 receptor activation. However, co-application of the Group II mGlu receptor antagonist failed to ameliorate the XA effect on cAMP formation, nor was the mGlu2 PAM able to potentiate this XA effect. This indicates that the apparent

reversal of the XA effect *in vivo* by the Group II mGlu receptor antagonist may indeed be due to the activation of two distinct yet opposing mechanisms of action. Therefore, XA is not acting as a conventional mGlu2 receptor orthosteric agonist in these assays; however, given that XA was not potentiated by the mGlu2 PAM in the *in vivo* electrophysiology experiments, this raises the possibility that XA either has a modulatory effect on intracellular signal transduction mechanisms independent of the mGlu2 receptor, or that the pharmacology of XA at Group II mGlu receptors is context specific, as has been described for a negative allosteric modulator of the mGlu7 receptor (Niswender et al., 2010). Interestingly, another kynurenine metabolite, cinnabarinic acid, an analogue of XA and reportedly an mGlu4 receptor selective partial agonist, is also able to reduce cAMP formation independently of mGlu4 receptor activation (Fazio et al., 2012b).

At this point it is important to highlight that neither mGlu3-expressing DiscoveRx cells nor mGlu3-expressing membranes were available for the cAMP or radioligand binding assays during my placement at Merck Research Laboratories (PA, USA). Furthermore, there was not a cAMP assay-compatible blank cell line (i.e. void of mGlu receptor expression) available, so I could not assess whether XA was able to inhibit FSK-induced cAMP formation in the absence of mGlu2 receptor expression.

8.6.3 Potential mechanisms of action of XA

As the XA effect on lateral inhibition was not further potentiated upon co-application of the mGlu2 PAM, whereas the Group II mGlu receptor agonist effect was in the same population

of neurones in the *in vivo* electrophysiology experiments, this could be interpreted as XA acting as a selective mGlu3 ligand. However, XA was able to robustly reduce FSK-induced cAMP formation in cells selectively expressing mGlu2 receptors *in vitro,* as also demonstrated by (Fazio et al., 2012a). This highlights that any potential XA interaction with the Group II mGlu receptors is likely to be more complicated than initially perceived. Group II mGlu receptor orthosteric agonists bind to the receptors' large extracellular VTF domain, which is highly conserved across all the mGlu receptor subtypes (Conn and Pin, 1997) and has thus hindered the development of subtype selective orthosteric agonists. However, the recent identification of an allosteric binding site in the less highly conserved 7-TM region (TM4 and TM5) (Schaffhauser et al., 2003; Hemstapat et al., 2007; Hampson et al., 2008; Rowe et al., 2008) has enabled the development of subtype selective ligands. As XA did not displace [^{3}H]LY341495 binding at the mGlu2 receptor, it is unlikely that XA activates Group II mGlu receptors via interactions with the orthosteric site. Instead, XA could itself be binding to an allosteric site to activate the Group II mGlu receptors, blocking the action of the mGlu2 PAM at its allosteric site. In this situation, XA would need to be acting as an allosteric agonist, as opposed to a PAM, as it is able to reduce lateral inhibition evoked by stimulation of a secondary vibrissa. A PAM alone is unable to alleviate this type of sensory inhibition, as demonstrated *in vivo* in Part One (Results section 7.2). An allosteric agonist for the mGlu7 receptor has recently been characterised (Mitsukawa et al., 2005), demonstrating that compounds binding to the allosteric site can indeed activate mGlu receptors in the absence of orthosteric agonist. However, the Group II mGlu receptor antagonist was unable to block the action of XA *in vitro*. This suggests that this mechanism of action is unlikely; but, it is as of yet unknown whether an orthosteric antagonist can block the actions of allosteric agonists at the mGlu receptors (Doumazane et al., 2013). Alternatively, it is possible that XA

may be able to reduce FSK-induced cAMP formation via a mechanism independent of the Group II mGlu receptors, thus mimicking the action of Group II mGlu receptor activation. Finally, it is possible that XA may be activating the Group II mGlu receptors indirectly via increasing non-vesicular glutamate release by modulating the function of the cysteine-glutamate transporters located on glial cells (Xi et al., 2002; Moran et al., 2003; Baker et al., 2008). Ultra-structural studies indicate that glial processes surround TRN afferent GABAergic terminals in the rat VB (Ralston, 1983; Ohara and Lieberman, 1993), so it is possible that Group II mGlu receptors located on these TRN terminals (Tamaru et al., 2001), or on the glial cells themselves (Liu et al., 1998; Mineff and Valtschanoff, 1999), could be activated by this non-vesicular glutamate release to alleviate lateral inhibition. This could account for why the Group II mGlu receptor antagonist was able to block the effects of XA *in vivo,* as the antagonist would be blocking the action of endogenous glutamate, whereas the circuitry required for this mechanism of action is not maintained in the *in vitro* preparations, which may be why no antagonism of XA was observed in either the radioligand binding or the cAMP assays.

8.6.4 Modulation of hippocampal synaptic transmission by XA

In addition to the reports that XA may be an endogenous Group II mGlu receptor ligand (Fazio et al., 2012a), XA has also been reported to be a VGLUT inhibitor (Bartlett et al., 1998; Carrigan et al., 2002). In light of this, additional experiments using an *in vitro* hippocampal slice preparation were conducted (Neale et al., 2013). In summary, field excitatory postsynaptic potentials (fEPSPs) were recorded from the dentate gyrus (DG) and CA1 regions of mouse hippocampal slices *in vitro*. In the DG, addition of XA to the bathing

medium resulted in a dose-related reduction of fEPSP amplitudes, as did the VGLUT inhibitors Congo Red (Ahmed et al., 2011) and Rose Bengal (Pietrancosta et al., 2010) and the Group II mGlu receptor agonist LY354740. The Group II mGlu receptor antagonist LY341495 reversed the Group II mGlu receptor agonist effect, but not the XA effect. Furthermore, the Group II mGlu receptor agonist, but not XA, was able to reduce DG paired-pulse depression. Interestingly, in the CA1 region, in addition to the depression of synaptic transmission, alterations in the fEPSP waveform consistent with increases in excitability were observed. This effect concurs with previous reports that XA may be proconvulsant (Lapin, 1978a; b), and that XA was able to reduce lateral inhibition in the VB *in vivo*. These results provide further evidence that XA can modulate synaptic transmission, but with characteristics similar to that of VGLUT inhibition as opposed to Group II mGlu receptor activation.

8.7 Conclusions

It has been previously demonstrated that the Group II mGlu receptors (mGlu2/3) can modulate physiologically-evoked responses in the VB (Salt and Turner, 1998) by reducing inhibition from the TRN (Turner and Salt, 2003). Using single-neurone recording in the rat VB *in vivo* with local iontophoretic application of selective Group II mGlu receptor compounds, in this thesis I have provided evidence that supports this mechanism of action, whilst also providing evidence regarding the relative contributions of the two Group II mGlu receptor subtypes to this modulation, their distinct cellular localisations and potential endogenous mechanism of activation.

I have demonstrated that both mGlu2 and mGlu3 receptors contribute a component to the overall Group II mGlu receptor effect on sensory responses in the VB, and that they are both likely activated upon physiological sensory stimulation. This may be occurring upon endogenous 'glutamate spillover' from the synapses formed between excitatory sensory afferents and VB neurones following physiological sensory stimulation, and this can lead to a reduction in sensory-evoked inhibition arising from the TRN. I propose that this potential Group II mGlu receptor modulation of inhibition could play an important role in discerning relevant information from background activity upon physiological sensory stimulation: a novel mechanism that could be of importance in attention and cognitive processes, whose malfunction could result in maladaption of sensory perception, such as that which can occur in psychiatric disease. Indeed, upon the extension of this hyposthesis to consider widespread inhibitions that are thought to occur within the TRN upon intraneuronal TRN communication, enhancement of attentional mechanisms upon Group II mGlu receptor activation may become even more pertinent: upon activation of a TRN neurone, both its target VB neurone will undergo an inhibition, as will its surrounding TRN neurones. This would result in a reduction in responsivity of the target VB neurone to repeated stimulus presentation, with a concomitant increase in the responsivity of surrounding VB neurones. This later component would manifest, as any tonic inhibition of these suorrounding VB neurones by their own corresponding TRN neurones will have been alleviated, as the TRN neurones themselves will have undergone an inhibition as a result of intra-TRN communication. Therefore, when considering the involvement of the wider TRN network, Group II mGlu receptor modulction of inhibition may therefore become even more important in enabling relevant sensory information to be discerned from background activity.

I was also able to provide evidence that mGlu2 receptors are likely located on astrocytic processes surrounding the VB-TRN synapse, and are able to mediate an astrocytic mechanism of action that reduces inhibitory synaptic transmission from the TRN to the VB. To the best of my knowledge this provides the first evidence that mGlu2 receptors are able to activate astrocytes, and of the involvement of astrocytes in the modulation of heterosynaptic transmission. As VB astrocytes are able to respond to synaptic stimulation (Parri et al., 2010), maladaption of mGlu2 receptor-mediated endogenous astrocytic activation may therefore have functional implications for the processing of somatosensory information and for the preparation and execution of distinct motor and/or cognitive tasks.

Selective Group II mGlu receptor compounds that exploit this novel mechanism of endogenous activation may therefore be of importance in the modulation of sensory, attentional and cognitive processes for therapeutic strategies.

Finally, the data presented here and elsewhere (Neale et al., 2013) demonstrate that XA can modulate neuronal function in multiple brain regions. XA can therefore join the list of naturally occurring kynurenines, such as quinolinic acid and kynurenic acid (Stone, 1993), which are able modulate synaptic transmission. However, the precise mechanism(s) of action by which XA is able to exert these effects is unknown, but may occur via either modulation of cAMP formation or VGLUT inhibition. Further *in vitro* investigations are therefore required in order to ascertain the exact nature of the mechanism(s) by which XA is able to exert its effects on synaptic transmission in the mammalian brain.

8.8 Future Directions

The mediodorsal nucleus, a higher-order thalamic nucleus which relays information from the amygdala to the prefrontal cortex and limbic system, has been heavily implicated in the pathophysiology of schizophrenia (Alelu-Paz and Gimenez-Amaya, 2008). As the results presented in this thesis have thoroughly examined Group II mGlu receptor function in a sensory thalamic nucleus, I am now conducting experiments in the mediodorsal nucleus to discern any differences in Group II mGlu receptor function between sensory and limbic-related nuclei, which seems possible given the non-uniform distribution of these receptors (Gu et al., 2008). Indeed, mGlu2 receptor immunostaining is found heavily in fibres in the parts of the TRN which are associated with limbic circuits, rather than sensory circuits (Lourenço Neto et al., 2000; Gu et al., 2008), with mGlu3 receptor mRNA is heavily expressed in the TRN, but more so in sectors associated with sensory functions (Ohishi et al., 1998b). Such findings suggest that the roles of the Group II mGlu receptors may vary in the different sections of the thalamus. A consequence of this would be that pharmacological alteration of mGlu2 and mGlu3 receptor function with a subtype-selective agonist or antagonist may be able to selectively affect the function of restricted thalamo-cortico-thalamic circuits, thus giving a selective effect on either sensory or cognitive/limbic processes. As virtually nothing is currently known regarding Group II mGlu receptor function in thalamic areas outside of the sensory nuclei, this represents an exciting extension of the work conducted in this thesis.

CHAPTER 8 FIGURES

Page Number

FIGURE 8.1 Summary diagram of findings in this thesis regarding Group II mGlu receptors in the VB. 175

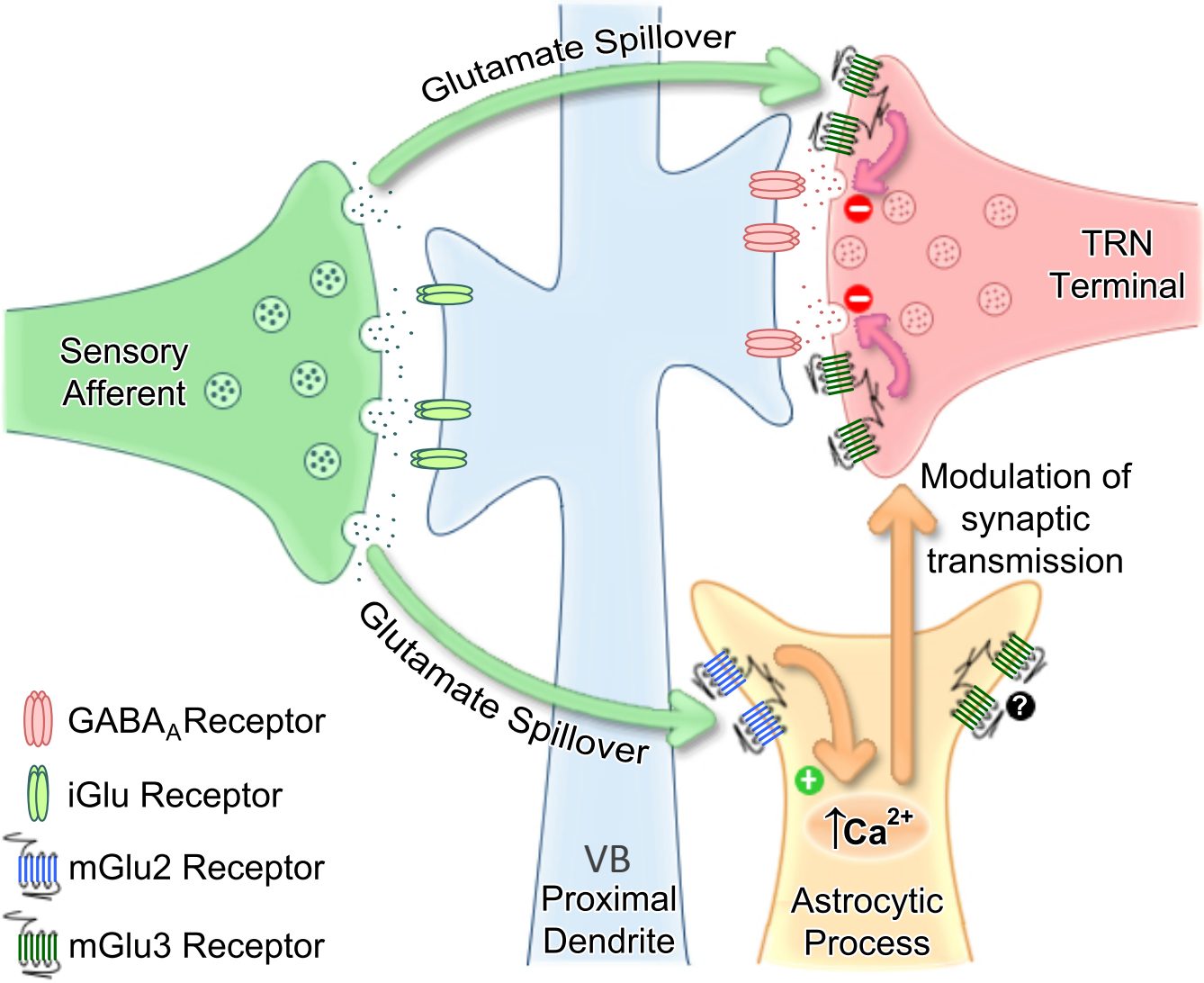

FIGURE 8.1. Summary diagram of findings in this thesis regarding Group II mGlu receptors in the VB. Using selective pharmacological compounds, I have been able to show that mGlu2 receptors are likely located on astrocytic processes surrounding the TRN-VB synapse, whilst mGlu3 receptors are likely located on the TRN terminals themselves in the VB. Ultrastructural studies indicate that mGlu3 receptors are also located on these astrocytic processes; however, due to lack of selective mGlu3 receptor compounds, I have been unable to investigate this purported mGlu3 receptor localisation. The location of mGlu3 receptors on the astrocytic process in this diagram is therefore accompanied by a question mark, indicating that further verification is required. Activation of astrocytic mGlu2 receptors likely facilitates elevations in intracellular calcium levels (indicated by a green plus), which may lead to gliotransmission and modulation of the function of the TRN-VB synapse, whilst neronal mGlu3 receptor activation is thought to decrease GABAergic transmission (indicated by the red minus signs). Both of the Group II mGlu receptor subtypes are likely activated via 'glutamate spillover' from the synapse formed between the sensory afferent and the VB proximal dendrite upon physiological sensory stimulation.

REFERENCES

Abe T, Sugihara H, Nawa H, Shigemoto R, Mizuno N, Nakanishi S (1992) Molecular characterization of a novel metabotropic glutamate receptor mGluR5 coupled to inositol phosphate/Ca2C signal transduction. J Biol Chem 267:13361-13368.

Aghajanian GK, Marek GJ (1999) Serotonin, via 5-HT2A receptors, increases EPSCs in layer V pyramidal cells of prefrontal cortex by an asynchronous mode of glutamate release. Brain Res 825:161-171.

Ahlsen G, Lindstrom S (1982) Mutual inhibition between perigeniculate neurones. Brain Res 236:482-486.

Ahmed SK, Etoga JL, Patel SA, Bridges RJ, Thompson CM (2011) Use of the hydantoin isostere to produce inhibitors showing selectivity toward the vesicular glutamate transporter versus the obligate exchange transporter system x(c)(-). Bioorg Med Chem Lett 21:4358-4362.

Ahnaou A, Dautzenberg FM, Geys H, Imogai H, Gibelin A, Moechars D, Steckler T, Drinkenburg WH (2009) Modulation of group II metabotropic glutamate receptor (mGlu2) elicits common changes in rat and mice sleep-wake architecture. Eur J Pharmacol 603:62-72.

Alexander GM, Godwin DW (2005) Presynaptic inhibition of corticothalamic feedback by metabotropic glutamate receptors. J Neurophysiol 94:163-175.

Alexander GM, Godwin DW (2006) Unique presynaptic and postsynaptic roles of Group II metabotropic glutamate receptors in the modulation of thalamic network activity. Neuroscience 141:501-513.

Alloway KD (2008) Information processing streams in rodent barrel cortex: the differential functions of barrel and septal circuits. Cereb Cortex 18:979-989.

Alloway KD, Mutic JJ, Hoffer ZS, Hoover JE (2000) Overlapping corticostriatal projections from the rodent vibrissal representations in primary and secondary somatosensory cortex. J Comp Neurol 428:51-67.

Anwyl R (1999) Metabotropic glutamate receptors: electrophysiological properties and role in plasticity. Brain Res Brain Res Rev 29:83-120.

Aoyama N, Takahashi N, Saito S, Maeno N, Ishihara R, Ji X, Miura H, Ikeda M, Suzuki T, Kitajima T, Yamanouchi Y, Kinoshita Y, Yoshida K, Iwata N, Inada T, Ozaki N (2006) Association study between kynurenine 3-monooxygenase gene and schizophrenia in the Japanese population. Genes Brain Behav 5:364-368.

Armstrong-James M, Callahan CA (1991) Thalamo-cortical processing of vibrissal information in the rat. II spatiotemporal convergence in the thalamic ventroposterior medial nucleus (VPm) and its relevance to generation of receptive fields of S1 cortical 'barrel' neurones. J Comp Neurol 303:211-224.

Arnth-Jensen N, Jabaudon D, Scanziani M (2002) Cooperation between independent hippocampal synapses is controlled by glutamate uptake. Nat Neurosci 5:325-331.

Aronica E, van Vliet EA, Mayboroda OA, Troost D, da Silva FH, Gorter JA (2000) Upregulation of metabotropic glutamate receptor subtype mGluR3 and mGluR5 in reactive astrocytes in a rat model of mesial temporal lobe epilepsy. Eur J Neurosci 12:2333-2344.

Asanuma C (1992) Noradrenergic innervation of the thalamic reticular nucleus: a light and electron microscopic immunohistochemical study in rats. J Comp Neurol 319:299-311.

Asanuma C (1994) GABAergic and pallidal terminals in the thalamic reticular nucleus of squirrel monkeys. Exp Brain Res 101:439-451.

Baba A, Saga H, Hashimoto H (1993) Inhibitory glutamate response on cyclic AMP formation in cultured astrocytes. Neurosci Lett 149:182-184.

Baker DA, Madayag A, Kristiansen LV, Meador-Woodruff JH, Haroutunian V, Raju I (2008) Contribution of cystine-glutamate antiporters to the psychotomimetic effects of phencyclidine. Neuropsychopharmacology 33:1760-1772.

Balázs R, Patel AY, Richter D (1973) Metabolic compartments in the brain. Their properties and relation to morphological sructures, In: Metabolic Compartmentation in the brain. R Balázs and YE Cremer (Eds). MacMillan London pp 167-189.

Barbaresi P, Spreafico R, Frassoni C, Rustioni A (1986) GABAergic neurons are present in the dorsal column nuclei but not in the ventroposterior complex of rats. Brain Res 382:305-326.

Barbas H, Zikopoulos B (2007) The prefrontal cortex and flexible behavior. Neuroscientist 13:532-545.

Bartlett RD, Esslinger CS, Thompson CM, Bridges RJ (1998) Substituted quinolines as inhibitors of L-glutamate transport into synaptic vesicles. Neuropharmacology 37:839-846.

Battaglia G, Monn JA, Schoepp DD (1997) In vivo inhibition of veratridine-evoked release of striatal excitatory amino acids by the group II metabotropic glutamate receptor agonist LY354740 in rats. Neurosci Lett 229:161-164.

Beinert H, Kennedy, MC (1993) Aconitase, a two-faced protein: Enzyme and iron regulatory factor. The FASEB Journal 7: 1442–9.

Beinert H, Kennedy MC, Stout CD (1996) Aconitase as iron−sulfur protein, enzyme, and iron-regulatory protein. Chemical Reviews 96: 2335–74.

Belford GR, Killackey HP (1979a) The development of vibrissae representation in subcortical trigeminal centers of the neonatal rat. J Comp Neurol 188:63-74.

Belford GR, Killackey HP (1979b) Vibrissae representation in subcortical trigeminal centers of the neonatal rat. J Comp Neurol 183:305-321.

Benneyworth MA, Xiang Z, Smith RL, Garcia EE, Conn PJ, Sanders-Bush E (2007) A selective positive allosteric modulator of metabotropic glutamate receptor subtype 2 blocks a hallucinogenic drug model of psychosis. Mol Pharmacol 72:477-484.

Berl S, Clarke DD (1969) Comparmentation of amino acid metabolism. Handbook of Neurochemistry. Vol 2. Plenum Press, New York. Pages 447-472.

Bessis AS, Rondard P, Gaven F, Brabet I, Triballeau N, Prezeau L, Acher F, Pin JP (2002) Closure of the Venus flytrap module of mGlu8 receptor and the activation process: Insights from mutations converting antagonists into agonists. Proc Natl Acad Sci U S A 99:11097-11102.

Binet V, Duthey B, Lecaillon J, Vol C, Quoyer J, Labesse G, Pin JP, Prezeau L (2007) Common structural requirements for heptahelical domain function in class A and class C G protein-coupled receptors. J Biol Chem 282:12154-12163.Bonde MM, Sheikh SP, Hansen JL (2006) Family C 7TM receptor dimerization and activation. Endocr Metab Immune Disord Drug Targets 6:7-16.

Binns KE, Turner JP, Salt TE (2003) Kainate receptor (GluR5)-mediated disinhibition of responses in rat ventrobasal thalamus allows a novel sensory processing mechanism. J Physiol 551:525-537.

Bishop PO, Burke W, Davis R (1962a) Single-unit recording from antidromically activated optic radiation neurones. J Physiol 162:432-450.

Bishop PO, Burke W, Davis R (1962b) The identification of single units in central visual pathways. J Physiol 162:409-431.

Bourassa J, Pinault D, Deschénes M (1995) Corticothalamic projections from the cortical barrel field to the somatosensory thalamus in rats: a single-fibre study using biocytin as an anterograde tracer. Eur J Neurosci 7:19-30.

Brabet I, Parmentier ML, De Colle C, Bockaert J, Acher F, Pin JP (1998) Comparative effect of L-CCG-I, DCG-IV and gamma-carboxy-L-glutamate on all cloned metabotropic glutamate receptor subtypes. Neuropharmacology 37:1043-1051.

Bradley PB, Dray A (1973) Modification of the responses of brain stem neurones to transmitter substances by anaesthetic agents. Br J Pharmacol 48:212-224.

Bradshaw CM, Szabadi E (1974) The measurement of dose in microelectrophoresis experiments. Neuropharmacology 13:407-415.

Brecht M, Sakmann B (2002) Whisker maps of neuronal subclasses of the rat ventral posterior medial thalamus, identified by whole-cell voltage recording and morphological reconstruction. J Physiol 538:495-515.

Brnardic EJ, Fraley ME, Garbaccio RM, Layton ME, Sanders JM, Culberson C, Jacobson MA, Magliaro BC, Hutson PH, O'Brien JA, Huszar SL, Uslaner JM, Fillgrove KL, Tang C, Kuo Y, Sur SM, Hartman GD (2010) 3-Aryl-5-phenoxymethyl-1,3-oxazolidin-2-ones as positive allosteric modulators of mGluR2 for the treatment of schizophrenia: Hit-to-lead efforts. Bioorg Med Chem Lett 20:3129-3133.

Bureau I, von Saint Paul F, Svoboda K (2006) Interdigitated paralemniscal and lemniscal pathways in th mouse barrel cortex. PLoS Biol 4:e382.

Bushell TJ, Jane DE, Tse HW, Watkins JC, Garthwaite J, Collingridge GL (1996) Pharmacological antagonism of the actions of group II and III mGluR agonists in the lateral perforant path of rat hippocampal slices. Br J Pharmacol 117:1457-1462.

Carai MA, Colombo G, Froestl W, Gessa GL (2004) In vivo effectiveness of CGP7930, a positive allosteric modulator of the GABAB receptor. Eur J Pharmacol 504:213-216.

Carrigan CN, Bartlett RD, Esslinger CS, Cybulski KA, Tongcharoensirikul P, Bridges RJ, Thompson CM (2002) Synthesis and in vitro pharmacology of substituted quinoline-2,4-dicarboxylic acids as inhibitors of vesicular glutamate transport. J Med Chem 45:2260-2276.

Cartmell J, Curtis AR, Kemp JA, Kendall DA, Alexander SP (1993) Subtypes of metabotropic excitatory amino acid receptor distinguished by stereoisomers of the rigid glutamate analogue, 1-aminocyclopentane-1,3-dicarboxylate. Neurosci Lett 153:107-110.

Cartmell J, Monn JA, Schoepp DD (1999) The metabotropic glutamate 2/3 receptor agonists LY354740 and LY379268 selectively attenuate phencyclidine versus d-amphetamine motor behaviors in rats. J Pharmacol Exp Ther 291:161-170.

Cartmell J, Schoepp DD (2000) Regulation of neurotransmitter release by metabotropic glutamate receptors. J Neurochem 75:889-907.

Cartmell J, Monn JA, Schoepp DD (2000a) Attenuation of specific PCP-evoked behaviors by the potent mGlu2/3 receptor agonist, LY379268 and comparison with the atypical antipsychotic, clozapine. Psychopharmacology (Berl) 148:423-429.

Cartmell J, Monn JA, Schoepp DD (2000b) The mGlu(2/3) receptor agonist LY379268 selectively blocks amphetamine ambulations and rearing. Eur J Pharmacol 400:221-224.

Carvell GE, Simons DJ (1987) Thalamic and corticocortical connections of the second somatic sensory area of the mouse. J Comp Neurol 265:409-427.

Casabona G, Knopfel T, Kuhn R, Gasparini F, Baumann P, Sortino MA, Copani A, Nicoletti F (1997) Expression and coupling to polyphosphoinositide hydrolysis of group I metabotropic glutamate receptors in early postnatal and adult rat brain. Eur J Neurosci 9:12-17.

Castro-Alamancos MA, Connors BW (1997) Thalamocortical synapses. Prog Neurobiol 51:581-606.

Ceresoli G, Guidetti P, Schwarcz R (1997) Metabolism of [5-(3)H]kynurenine in the developing rat brain in vivo: effect of intrastriatal ibotenate injections. Brain Res Dev Brain Res 100:73-81.

Chapin JK, Waterhouse BD, Woodward DJ (1981) Differences in cutaneous sensory response properties of single somatosensory cortical neuorns in awake and haliothane anesthetized rats. Brain Res Bull 6:63-70.

Chen CY, Bonham AC (2005) Glutamate suppresses GABA release via presynaptic metabotropic glutamate receptors at baroreceptor neurones in rats. J Physiol 562:535-551.

Cheng SC, Kumar S, Casella GA (1972) Effects of fluoroacetate and fluorocitrate on the metabolic compartmentation of tricarboxylic acid cycle in rat brain slices. Brain Res. 42:117-128.

Cherlyn SY, Woon PS, Liu JJ, Ong WY, Tsai GC, Sim K (2010) Genetic association studies of glutamate, GABA and related genes in schizophrenia and bipolar disorder: a decade of advance. Neurosci Biobehav Rev 34:958-977.

Chiaia NL, Rhoades RW, Bennett-Clarke CA, Fish SE, Killackey HP (1991) Thalamic processing of vibrissal information in the rat. I. Afferent input to the medial ventral posterior and posterior nuclei. J Comp Neurol 314:201-216.

Chopra M, Yao Y, Blake TJ, Hampson DR, Johnson EC (2009) The neuroactive peptide N-acetylaspartylglutamate is not an agonist at the metabotropic glutamate receptor subtype 3 of metabotropic glutamate receptor. J Pharmacol Exp Ther 330:212-219.

Ciccarelli R, Sureda FX, Casabona G, Di Iorio P, Caruso A, Spinella F, Condorelli DF, Nicoletti F, Caciagli F (1997) Opposite influence of the metabotropic glutamate receptor subtypes mGlu3 and -5 on astrocyte proliferation in culture. Glia 21:390-398.

Cirone J, Salt TE (2001) Group II and III metabotropic glutamate receptors contribute to different aspects of visual response processing in the rat superior colliculus. J Physiol 534:169-178.

Cirone J, Pothecary CA, Turner JP, Salt TE (2002) Group I metabotropic glutamate receptors (mGluRs) modulate visual responses in the superficial superior colliculus of the rat. J Physiol 541:895-903.

Clarke DD (1991) Fluoroacetate and fluorocitrate: Mechanism of action. Neurochem Res. 16:1055-1058.

Clarke WB, Bowsher D (1962) Terminal distribution of primary afferent trigeminal fibers in the rat. Exp Neurol 6:372-383.

Coleman KA, Mitrofanis J (1996) Organization of the visual reticular thalamic nucleus of the rat. Eur J Neurosci 8:388-404.

Conn PJ, Pin JP (1997) Pharmacology and functions of metabotropic glutamate receptors. Annu Rev Pharmacol Toxicol 37:205-237.

Cornwall J, Cooper JD, Phillipson OT (1990) Projections to the rostral reticular thalamic nucleus in the rat. Exp Brain Res 80:157-171.

Corti C, Restituito S, Rimland JM, Brabet I, Corsi M, Pin JP, Ferraguti F (1998) Cloning and characterization of alternative mRNA forms for the rat metabotropic glutamate receptors mGluR7 and mGluR8. Eur J Neurosci 10:3629-3641.

Corti C, Crepaldi L, Mion S, Roth AL, Xuereb JH, Ferraguti F (2007) Altered dimerization of metabotropic glutamate receptor 3 in schizophrenia. Biol Psychiatry 62:747-755.

Cox CL, Sherman SM (1999) Glutamate inhibits thalamic reticular neurons. J Neurosci 19:6694-6699.

Cox CL, Huguenard JR, Prince DA (1995) Cholecystokinin depolarizes rat thalamic reticular neurons by suppressing a K+ conductance. J Neurophysiol 74:990-1000.

Cox CL, Zhou Q, Sherman SM (1998) Glutamate locally activates dendritic outputs of thalamic interneurons. Nature 394:478-482.

Crabtree JW (1999) Intrathalamic sensory connections mediated by the thalamic reticular nucleus. Cell Mol Life Sci 56:683-700.

Crick F (1984) Function of the thalamic reticular complex: the searchlight hypothesis. Proc Natl Acad Sci U S A 81:4586-4590.

Cropper EC, Eisenman JS, Azmitia EC (1984) An immunocytochemical study of the serotonergic innervation of the thalamus of the rat. J Comp Neurol 224:38-50.

Cross BA, Dyer RG (1971) Unit activity in rat diencephalic islands--the effect of anaesthetics. J Physiol 212:467-481.

Cruikshank SJ, Urabe H, Nurmikko AV, Connors BW (2010) Pathway-specific feedforward circuits between thalamus and neocortex revealed by selective optical stimulation of axons. Neuron 65:230-245.

Cryan JF, Kelly PH, Chaperon F, Gentsch C, Mombereau C, Lingenhoel K, Froestl W, Bettler B, Kaupmann K, Spooren WP (2004) Behavioral characterization of the novel GABAB receptor-positive modulator GS39783 (N,N'-dicyclopentyl-2-methylsulfanyl-5-nitro-pyrimidine-4,6-diamine): anxiolytic-like activity without side effects associated with baclofen or benzodiazepines. J Pharmacol Exp Ther 310:952-963.

Cucchiaro JB, Uhlrich DJ, Sherman SM (1993) Ultrastructure of synapses from the pretectum in the A-laminae of the cat's lateral geniculate nucleus. J Comp Neurol 334:618-630.

Curtis DR, Eccles RM (1958) The excitation of Renshaw cells by pharmacological agents applied electrophoretically. J Physiol 141:435-445.

D'Ascenzo M, Fellin T, Terunuma M, Revilla-Sanchez R, Meaney DF, Auberson YP, Moss SJ, Haydon PG (2007) mGluR5 stimulates gliotransmission in the nucleus accumbens. Proc Natl Acad Sci U S A 104:1995-2000.

Debarbieux F, Brunton J, Charpak S (1998) Effect of bicuculline on thalamic activity: a direct blockade of IAHP in reticularis neurons. J Neurophysiol 79:2911-2918.

Del Castillo J, Katz B (1955) On the localization of acetylcholine receptors. J Physiol 128:157-181.

Desai MA, Conn PJ (1991) Excitatory effects of ACPD receptor activation in the hippocampus are mediated by direct effects on pyramidal cells and blockade of synaptic inhibition. J Neurophysiol 66:40-52.

Deschénes M, Madariaga-Domich A, Steriade M (1985). Dendrodendritic synapses in the cat reticularis thalami nucleus: a structural basis for thalamic spindle synchronization. Brain Res 334:165-168.

Deschénes M, Veinante P, Zhang ZW (1998) The organization of corticothalamic projections: reciprocity versus parity. Brain Res Brain Res Rev 28:286-308.

Deschénes M, Timofeeva E, Lavallee P, Dufresne C (2005) The vibrissal system as a model of thalamic operations. Prog Brain Res 149:31-40.

Desîlets-Roy B, Varga C, Lavallee P, Deschénes M (2002) Substrate for cross-talk inhibition between thalamic barreloids. J Neurosci 22:RC218.

Devonshire IM, Grandy TH, Dommett EJ, Greenfield SA (2010) Effects of urethane anaesthesia on sensory processing in the rat barrel cortex revealed by combined optical imaging and electrophysiology. Eur J Neurosci. 32:786-797.

Diamond ME, Armstrong-James M, Ebner FF (1992) Somatic sensory responses in the rostral sector of the posterior group (POm) and in the ventral posterior medial nucleus (VPM) of the rat thalamus. J Comp Neurol 318:462-476.

Diamond ME, von Heimendahl M, Knutsen PM, Kleinfeld D, Ahissar E (2008) 'Where' and 'what' in the whisker sensorimotor system. Nat Rev Neurosci 9:601-612.

Dominguez C, Prieto L, Valli MJ, Massey SM, Bures M, Wright RA, Johnson BG, Andis SL, Kingston A, Schoepp DD, Monn JA (2005) Methyl substitution of 2-aminobicyclo[3.1.0]hexane 2,6-dicarboxylate (LY354740) determines functional activity at metabotropic glutamate receptors: identification of a subtype selective mGlu2 receptor agonist. J Med Chem 48:3605-3612.

Dorfl J (1985) The innervation of the mystacial region of the white mouse: A topographical study. J Anat 142:173-184.

Doumazane E, Scholler P, Fabre L, Zwier JM, Trinquet E, Pin JP, Rondard P (2013) Illuminating the activation mechanisms and allosteric properties of metabotropic glutamate receptors. Proc Natl Acad Sci U S A 110:E1416-1425.

Duvoisin RM, Zhang C, Ramonell K (1995) A novel metabotropic glutamate receptor expressed in the retina and olfactory bulb. J Neurosci 15:3075-3083.

Eaton SA, Jane DE, Jones PL, Porter RH, Pook PC, Sunter DC, Udvarhelyi PM, Roberts PJ, Salt TE, Watkins JC (1993) Competitive antagonism at metabotropic glutamate receptors by (S)-4-carboxyphenylglycine and (RS)-alpha-methyl-4-carboxyphenylglycine. Eur J Pharmacol 244:195-197.

Edeline JM, Manunta Y, Nodal FR, Bajo VM (1999) Do auditory responses recorded from awake animals reflect the anatomical parcellation of the auditory thalamus? Hear Res 131:135-152.

Erhardt S, Blennow K, Nordin C, Skogh E, Lindstrom LH, Engberg G (2001) Kynurenic acid levels are elevated in the cerebrospinal fluid of patients with schizophrenia. Neurosci Lett 313:96-98.

Erzurumlu RS, Jhaveri S (1992) Trigeminal ganglion cell processes are spatially ordered prior to the differentiation of the vibrissa pad. J Neurosci 12:3946-3955.

Evans RH, Smith DA (1982) Effect of urethane on synaptic and amino acid-induced excitation in isolated spinal cord preparations. Neuropharmacology 21:857-860.

Fazio F, Molinaro G, Iacovelli L, Bernabucci M, Mauro G, Di Menna L, Notartomaso S, Zappulla C, Battaglia G, Nicoletti F, Bruno V, Di Marco R (2012a) Xanthurenic Acid as a novel putative agonist of Group II metabotropic glutamate receptors. Curr Neuropharmacol 9:19.

Fazio F, Lionetto L, Molinaro G, Bertrand HO, Acher F, Ngomba RT, Notartomaso S, Curini M, Rosati O, Scarselli P, Di Marco R, Battaglia G, Bruno V, Simmaco M, Pin JP, Nicoletti F, Goudet C (2012b) Cinnabarinic acid, an endogenous metabolite of the kynurenine pathway, activates type 4 metabotropic glutamate receptors. Mol Pharmacol 81:643-656.

Fellin T, Pascual O, Gobbo S, Pozzan T, Haydon PG, Carmignoto G (2004) Neuronal synchrony mediated by astrocytic glutamate through activation of extrasynaptic NMDA receptors. Neuron 43:729-743.

Fitzsimonds RM, Dichter MA (1996) Heterologous modulation of inhibitory synaptic transmission by metabotropic glutamate receptors in cultured hippocampal neurons. J Neurophysiol 75:885-893.

Flint DH, Allen, RM (1996) Iron−sulfur proteins with nonredox functions. Chemical Reviews 96 (7): 2315–34.

Flor PJ, Van Der Putten H, Ruegg D, Lukic S, Leonhardt T, Bence M, Sansig G, Knopfel T, Kuhn R (1997) A novel splice variant of a metabotropic glutamate receptor, human mGluR7b. Neuropharmacology 36:153-159.

Fonnum F (1984) Glutamate: a neurotransmitter in mammalian brain. J Neurochem 42:1-11.

Fonnum F, Johnsen A, Hassel B (1997) Use of fluorocitrate and fluoroacetate in the study of brain metabolism. Glia 21:106-113.

Friedberg MH, Lee SM, Ebner FF (1999) Modulation of receptive field properties of thalamic somatosensory neurons by the depth of anesthesia. J Neurophysiol 81:2243-2252.

Furuta T, Nakamura K, Deschénes M (2006) Angular tuning bias of vibrissa-responsive cells in the paralemniscal pathway. J Neurosci 26:10548-10557.

Galici R, Echemendia NG, Rodriguez AL, Conn PJ (2005) A selective allosteric potentiator of metabotropic glutamate (mGlu) 2 receptors has effects similar to an orthosteric mGlu2/3 receptor agonist in mouse models predictive of antipsychotic activity. J Pharmacol Exp Ther 315:1181-1187.

Galici R, Jones CK, Hemstapat K, Nong Y, Echemendia NG, Williams LC, de Paulis T, Conn PJ (2006) Biphenyl-indanone A, a positive allosteric modulator of the metabotropic glutamate receptor subtype 2, has antipsychotic- and anxiolytic-like effects in mice. J Pharmacol Exp Ther 318:173-185.

Galvez T, Urwyler S, Prezeau L, Mosbacher J, Joly C, Malitschek B, Heid J, Brabet I, Froestl W, Bettler B, Kaupmann K, Pin JP (2000) Ca(2+) requirement for high-affinity gamma-aminobutyric acid

(GABA) binding at GABA(B) receptors: involvement of serine 269 of the GABA(B)R1 subunit. Mol Pharmacol 57:419-426.

Gama L, Wilt SG, Breitwieser GE (2001) Heterodimerization of calcium sensing receptors with metabotropic glutamate receptors in neurons. J Biol Chem 276:39053-39059.

Gandia JA, De Las Heras S, Garcia M, Gimenez-Amaya JM (1993) Afferent projections to the reticular thalamic nucleus from the globus pallidus and the substantia nigra in the rat. Brain Res Bull 32:351-358.

Gentet LJ, Ulrich D (2003) Strong, reliable and precise synaptic connections between thalamic relay cells and neurones of the nucleus reticularis in juvenile rats. J Physiol 546:801-811.

Ghose S, Gleason KA, Potts BW, Lewis-Amezcua K, Tamminga CA (2009) Differential expression of metabotropic glutamate receptors 2 and 3 in schizophrenia: a mechanism for antipsychotic drug action? Am J Psychiatry 166:812-820.

Gilman AG (1989) The Albert Lasker Medical Awards. G proteins and regulation of adenylyl cyclase. JAMA 262:1819-1825.

Gjoni T, Urwyler S (2008) Receptor activation involving positive allosteric modulation, unlike full agonism, does not result in GABAB receptor desensitization. Neuropharmacology 55:1293-1299

Gobaille S, Kemmel V, Brumaru D, Dugave C, Aunis D, Maitre M (2008) Xanthurenic acid distribution, transport, accumulation and release in the rat brain. J Neurochem 105:982-993.

Golshani P, Liu XB, Jones EG (2001) Differences in quantal amplitude reflect GluR4- subunit number at corticothalamic synapses on two populations of thalamic neurons. Proc Natl Acad Sci U S A 98:4172-4177.

Gomeza J, Mary S, Brabet I, Parmentier ML, Restituito S, Bockaert J, Pin JP (1996) Coupling of metabotropic glutamate receptors 2 and 4 to G alpha 15, G alpha 16, and chimeric G alpha q/i proteins: characterization of new antagonists. Mol Pharmacol 50:923-930.

Gonzalez-Maeso J, Ang RL, Yuen T, Chan P, Weisstaub NV, Lopez-Gimenez JF, Zhou M, Okawa Y, Callado LF, Milligan G, Gingrich JA, Filizola M, Meana JJ, Sealfon SC (2008) Identification of a serotonin/glutamate receptor complex implicated in psychosis. Nature 452:93-97.

Gonzalo-Ruiz A, Lieberman AR (1995a) Topographic organization of projections from the thalamic reticular nucleus to the anterior thalamic nuclei in the rat. Brain Res Bull 37:17-35.

Gonzalo-Ruiz A, Lieberman AR (1995b) GABAergic projections from the thalamic reticular nucleus to the anteroventral and anterodorsal thalamic nuclei of the rat. J Chem Neuroanat 9:165-174.

Goudet C, Gaven F, Kniazeff J, Vol C, Liu J, Cohen-Gonsaud M, Acher F, Prezeau L, Pin JP (2004) Heptahelical domain of metabotropic glutamate receptor 5 behaves like rhodopsin-like receptors. Proc Natl Acad Sci U S A 101:378-383.

Granseth B, Ahlstrand E, Lindstrom S (2002) Paired pulse facilitation of corticogeniculate EPSCs in the dorsal lateral geniculate nucleus of the rat investigated in vitro. J Physiol 544:477-486.

Grilli M, Raiteri L, Patti L, Parodi M, Robino F, Raiteri M, Marchi M (2006) Modulation of the function of presynaptic alpha7 and non-alpha7 nicotinic receptors by the tryptophan metabolites, 5-hydroxyindole and kynurenate in mouse brain. Br J Pharmacol 149:724-732.

Groenewegen HJ (1988) Organization of the afferent connections of the mediodorsal thalamic nucleus in the rat, related to the mediodorsal-prefrontal topography. Neuroscience 24:379-431.

Grosche J, Matyash V, Möller T, Verkhratsky A, Reichenbacj A, Kettenmann H (1999) Microdomains for neuron-glia interaction: parallel fiber signaling to Bergmann glial cells. Nat Neurosci 2:139-143.

Gu G, Lorrain DS, Wei H, Cole RL, Zhang X, Daggett LP, Schaffhauser HJ, Bristow LJ, Lechner SM (2008) Distribution of metabotropic glutamate 2 and 3 receptors in the rat forebrain: Implication in emotional responses and central disinhibition. Brain Res 1197:47-62.

Guidetti P, Eastman CL, Schwarcz R (1995) Metabolism of [5-3H]kynurenine in the rat brain in vivo: evidence for the existence of a functional kynurenine pathway. J Neurochem 65:2621-2632.

Guidetti P, Hoffman GE, Melendez-Ferro M, Albuquerque EX, Schwarcz R (2007) Astrocytic localization of kynurenine aminotransferase II in the rat brain visualized by immunocytochemistry. Glia 55:78-92.

Guillery RW (1967) Patterns of fiber degeneration in the dorsal lateral geniculate nucleus of the cat following lesions in the visual cortex. J Comp Neurol 130:197-221.

Guillery RW (1995) Anatomical evidence concerning the role of the thalamus in corticocortical communication: a brief review. J Anat 187 (Pt 3):583-592.

Guillery RW, Harting JK (2003) Structure and connections of the thalamic reticular nucleus: Advancing views over half a century. J Comp Neurol 463:360-371.

Guthrie PB, Knappenberger J, Segal M, Bennett MV, Charles AC, Kater SB (1999) ATP released from astrocytes mediates glial calcium waves. J Neurosci 19:520-528.

Hackler EA, Byun NE, Jones CK, Williams JM, Baheza R, Sengupta S, Grier MD, Avison M, Conn PJ, Gore JC (2010) Selective potentiation of the metabotropic glutamate receptor subtype 2 blocks phencyclidine-induced hyperlocomotion and brain activation. Neuroscience 168:209-218.

Haidarliu S, Ahissar E (2001) Size gradients of barreloids in the rat thalamus. J Comp Neurol 429:372-387.

Hale PT, Sefton AJ, Baur LA, Cottee LJ (1982) Interrelations of the rat's thalamic reticular and dorsal lateral geniculate nuclei. Exp Brain Res 45:217-229.

Hallanger AE, Levey AI, Lee HJ, Rye DB, Wainer BH (1987) The origins of cholinergic and other subcortical afferents to the thalamus in the rat. J Comp Neurol 262:105-124.

Hampson DR, Rose EM, Antflick JE (2008) The structure of metabotropic glutamate receptors. In: The Glutamate Receptors (Gereau RWt, Swanson GT, eds), pp 363-386. Totowa, NJ: Human Press.

Harich S, Gross G, Bespalov A (2007) Stimulation of the metabotropic glutamate 2/3 receptor attenuates social novelty discrimination deficits induced by neonatal phencyclidine treatment. Psychopharmacology (Berl) 192:511-519.

Harris RM (1986) Morphology of physiologically identified thalamocortical relay neurons in the rat ventrobasal thalamus. J Comp Neurol 251:491-505.

Harris RM, Hendrickson AE (1987) Local circuit neurons in the rat ventrobasal thalamus--a GABA immunocytochemical study. Neuroscience 21:229-236.

Hartings JA, Simons DJ (2000) Inhibition suppresses transmission of tonic vibrissa-evoked activity in the rat ventrobasal thalamus. J Neurosci 20:RC100.

Hassel B, Paulsen RE, Johson A, Fonnum F (1992) Selective inhibition of glial cell metabolism in vivo by fluorocitrate. Brain Res 576:120-124.

Hassel B, Westergaard N, Schousboe A, Fonnum F (1995) Metabolic differences between primary cultures of astrocytes and neurons from cerebellum and cerebral cortex: Effects of fluorocitrate. Neurochem Res 20:413-420.

Hayama T, Hashimoto K, Ogawa H (1994) Anatomical location of a taste-related region in the thalamic reticular nucleus in rats. Neurosci Res 18:291-299.

Hayashi Y, Tanabe Y, Aramori I, Masu M, Shimamoto K, Ohfune Y, Nakanishi S (1992) Agonist analysis of 2-(carboxycyclopropyl)glycine isomers for cloned metabotropic glutamate receptor subtypes expressed in Chinese hamster ovary cells. Br J Pharmacol 107:539-543.

Hemstapat K, Da Costa H, Nong Y, Brady AE, Luo Q, Niswender CM, Tamagnan GD, Conn PJ (2007) A novel family of potent negative allosteric modulators of group II metabotropic glutamate receptors. J Pharmacol Exp Ther 322:254-264.

Henderson TA, Jacquin MF (1995) What makes subcortical barrels? Requisite trigeminal circuitry and developmental mechanisms. Barrel Cortex Cerebral Cortex 11:123-187.

Hermans E, Challiss RA (2001) Structural, signalling and regulatory properties of the group I metabotropic glutamate receptors: prototypic family C G-protein-coupled receptors. Biochem J 359:465-484.

Hermes ML, Renaud LP (2010) Post- and presynpatic group II metabotropic glutamate receptors reduce neuronal excitability in rat midline paraventricular thalamic nucleus. J Pharmacol Exp Ther 336:840-849.

Heyliger SO, Goodman CB, Ngong JM, Soliman KF (1998) The analgesic effects of tryptophan and its metabolites in the rat. Pharmacol Res 38:243-250.

Hilmas C, Pereira EF, Alkondon M, Rassoulpour A, Schwarcz R, Albuquerque EX (2001) The brain metabolite kynurenic acid inhibits alpha7 nicotinic receptor activity and increases non-

alpha7 nicotinic receptor expression: physiopathological implications. J Neurosci 21:7463-7473.

Hollmann M, Heinemann S (1994) Cloned glutamate receptors. Annu Rev Neurosci 17:31-108.

Holmes O, Houchin J (1966) Units in the cerebral cortex of the anaesthetized rat and the correlations between their discharges. J Physiol 187:651-671.

Hoogland PV, Welker E, Van der Loos H (1987) Organization of the projections from barrel cortex to thalamus in mice studied with Phaseolus vulgaris-leucoagglutinin and HRP. Exp Brain Res 68:73-87.

Hou L, Klann E (2004) Activation of the phosphoinositide 3-kinase-Akt-mammalian target of rapamycin signaling pathway is required for metabotropic glutamate receptor-dependent long-term depression. J Neurosci 24:6352-6361.

Houamed KM, Kuijper JL, Gilbert TL, Haldeman BA, O'Hara PJ, Mulvihill ER, Almers W, Hagen FS (1991) Cloning, expression, and gene structure of a G protein-coupled glutamate receptor from rat brain. Science 252:1318-1321.

Houser CR, Vaughn JE, Barber RP, Roberts E (1980) GABA neurons are the major cell type of the nucleus reticularis thalami. Brain Res 200:341-354.

Hu G, Duffy P, Swanson C, Ghasemzadeh MB, Kalivas PW (1999) The regulation of dopamine transmission by metabotropic glutamate receptors. J Pharmacol Exp Ther 289:412-416.

Huang Q, Zhou D, Chase K, Gusella JF, Aronin N, DiFiglia M (1992) Immunohistochemical localization of the D1 dopamine receptor in rat brain reveals its axonal transport, pre- and postsynaptic localization, and prevalence in the basal ganglia, limbic system, and thalamic reticular nucleus. Proc Natl Acad Sci U S A 89:11988-11992.

Huguenard JR (1999) Neuronal circuitry of thalamocortical epilepsy and mechanisms of antiabsence drug action. Adv Neurol 79:991-999.

Iacovelli L, Bruno V, Salvatore L, Melchiorri D, Gradini R, Caricasole A, Barletta E, De Blasi A, Nicoletti F (2002) Native group-III metabotropic glutamate receptors are coupled to the mitogen-activated protein kinase/phosphatidylinositol-3-kinase pathways. J Neurochem 82:216-223.

Irving AJ, Schofield JG, Watkins JC, Sunter DC, Collingridge GL (1990) 1S,3R-ACPD stimulates and L-AP3 blocks Ca2+ mobilization in rat cerebellar neurons. Eur J Pharmacol 186:363-365.

Ito M (1988) Response properties and topography of vibrissa-sensitive VPM neurons in the rat. J Neurophysiol 60:1181-1197.

Iversen L, Mulvihill E, Haldeman B, Diemer NH, Kaiser F, Sheardown M, Kristensen P (1994) Changes in metabotropic glutamate receptor mRNA levels following global ischemia: increase of a putative presynaptic subtype (mGluR4) in highly vulnerable rat brain areas. J Neurochem 63:625-633.

Jacquin MF, Chiaia NL, Klein BG, Rhoades RW (1989) Structure-function relationships in the rat brainstem subnucleus interpolaris: VI. Cervical convergence in cells deafferented at birth and a potential primary afferent substrate. J Comp Neurol 283:513-525.

Jacquin MF, Chiaia NL, Haring JH, Rhoades RW (1990) Intersubnuclear connections within the rat trigeminal brainstem complex. Somatosens Mot Res 7:399-420.

Jane DE, Pittaway K, Sunter DC, Thomas NK, Watkins JC (1995) New phenylglycine derivatives with potent and selective antagonist activity at presynaptic glutamate receptors in neonatal rat spinal cord. Neuropharmacology 34:851-856.

Jane DE, Jones PL, Pook PC, Salt TE, Sunter DC, Watkins JC (1993) Stereospecific antagonism by (+)-alpha-methyl-4-carboxyphenylglycine (MCPG) of (1S,3R)-ACPD-induced effects in neonatal rat motoneurones and rat thalamic neurones. Neuropharmacology 32:725-727.

Javitt DC (2009) Sensory processing in schizophrenia: neither simple nor intact. Schizophr Bull 35:1059-1064.

Jeffery G, Sharp C, Malitschek B, Salt TE, Kuhn R, Knöpfel T (1996) Cellular localisation of metabotropic glutamate receptors in the amammalian optic nerve: a mechanism for axon-glia communication. Brain Res 741:75-81.

Jingami H, Nakanishi S, Morikawa K (2003) Structure of the metabotropic glutamate receptor. Curr Opin Neurobiol 13:271-278.

Johnson BG, Wright RA, Arnold MB, Wheeler WJ, Ornstein PL, Schoepp DD (1999) [3H]-LY341495 as a novel antagonist radioligand for group II metabotropic glutamate (mGlu) receptors: characterization of binding to membranes of mGlu receptor subtype expressing cells. Neuropharmacology 38:1519-1529.

Johnson MP, Baez M, Jagdmann GE, Jr., Britton TC, Large TH, Callagaro DO, Tizzano JP, Monn JA, Schoepp DD (2003) Discovery of allosteric potentiators for the metabotropic glutamate 2 receptor: synthesis and subtype selectivity of N-(4-(2-methoxyphenoxy)phenyl)-N-(2,2,2-trifluoroethylsulfonyl)pyrid-3-ylmethylamine. J Med Chem 46:3189-3192.

Joly C, Gomeza J, Brabet I, Curry K, Bockaert J, Pin JP (1995) Molecular, functional, and pharmacological characterization of the metabotropic glutamate receptor type 5 splice variants: comparison with mGluR1. J Neurosci 15:3970-3981.

Jones EG (1975) Some aspects of the organization of the thalamic reticular complex. J Comp Neurol 162:285-308.

Jones EG (1985) The Thalamus. New York: Raven.

Jones EG (2007) The Thalamus, 2nd Edition. New York: Cambridge University Press.

Jourdain P, Bergersen LH, Bhaukaurally K, Bezzi P, Santello M, Domercq M, Matute C, Tonello F, Gundersen V, Volterra A (2007) Glutamate exocytosis from astrocytes controls synaptic strength. Nat Neurosci 10:331-339.

Kalivas PW (2009) The glutamate homeostasis hypothesis of addiction. Nat Rev Neurosci 10:561-572.

Kammermeier PJ, Yun J (2005) Activation of metabotropic glutamate receptor 1 dimers requires glutamate binding in both subunits. J Pharmacol Exp Ther 312:502-508.

Kemp M, Roberts P, Pook P, Jane D, Jones A, Jones P, Sunter D, Udvarhelyi P, Watkins J (1994) Antagonism of presynaptically mediated depressant responses and cyclic AMP-coupled metabotropic glutamate receptors. Eur J Pharmacol 266:187-192.

Kemp MC, Jane DE, Tse HW, Roberts PJ (1996) Agonists of cyclic AMP-coupled metabotropic glutamate receptors in adult rat cortical slices. Eur J Pharmacol 309:79-85.

Killackey HP (1973) Anatomical evidence for cortical subdivisions based on vertically discrete thalamic projections from the ventral posterior nucleus to cortical barrels in the rat. Brain Res 51:326-331.

Killackey HP, Belford GR (1979) The formation of afferent patterns in the somatosensory cortex of the neonatal rat. J Comp Neurol 183:285-303.

Kingston AE, Ornstein PL, Wright RA, Johnson BG, Mayne NG, Burnett JP, Belagaje R, Wu S, Schoepp DD (1998) LY341495 is a nanomolar potent and selective antagonist of group II metabotropic glutamate receptors. Neuropharmacology 37:1-12.

Kniazeff J, Bessis AS, Maurel D, Ansanay H, Prezeau L, Pin JP (2004) Closed state of both binding domains of homodimeric mGlu receptors is required for full activity. Nat Struct Mol Biol 11:706-713.

Kolmac CI, Mitrofanis J (1997) Organisation of the reticular thalamic projection to the intralaminar and midline nuclei in rats. J Comp Neurol 377:165-178.

Koralek KA, Jensen KF, Killackey HP (1988) Evidence for two complementary patterns of thalamic input to the rat somatosensory cortex. Brain Res 463:346-351.

Krenz WD, Nguyen D, Perez-Acevedo NL, Selverston AI (2000) Group I, II, and III mGluR compounds affect rhythm generation in the gastric circuit of the crustacean stomatogastric ganglion. J Neurophysiol 83:1188-1201.

Kristensen P, Suzdak PD, Thomsen C (1993) Expression pattern and pharmacology of the rat type IV metabotropic glutamate receptor. Neurosci Lett 155:159-162.

Kultas-Ilinsky K, Yi H, Ilinsky IA (1995) Nucleus reticularis thalami input to the anterior thalamic nuclei in the monkey: a light and electron microscopic study. Neurosci Lett 186:25-28.

Kunishima N, Shimada Y, Tsuji Y, Sato T, Yamamoto M, Kumasaka T, Nakanishi S, Jingami H, Morikawa K (2000) Structural basis of glutamate recognition by a dimeric metabotropic glutamate receptor. Nature 407:971-977.

Lahiri S, Quastel JH (1963) Fluoroacetate and the metabolism of ammonia in the brain. Biochem J 89:157-163.

Land PW, Buffer SA, Jr., Yaskosky JD (1995) Barreloids in adult rat thalamus: three-dimensional architecture and relationship to somatosensory cortical barrels. J Comp Neurol 355:573-588.

Landisman CE, Long MA, Beierlein M, Deans MR, Paul DL, Connors BW (2002) Electrical synapses in the thalamic reticular nucleus. J Neurosci 22:1002-1009.

Landisman CE, Connors BW (2007) VPM and PoM nuclei of the rat somatosensory thalamus: intrinsic neuronal properties and corticothalamic feedback. Cereb Cortex 17:2853-2865.

Lapin IP (1978a) Stimulant and convulsive effects of kynurenines injected into brain ventricles in mice. J Neural Transm 42:37-43.

Lapin IP (1978b) Convulsions and tremor in immature rats after intraperitoneal injection of kynurenine and its metabolites. Pharmacol Res Commun 10:81-84.

Laurie DJ, Boddeke HW, Hiltscher R, Sommer B (1996) HmGlu1d, a novel splice variant of the human type I metabotropic glutamate receptor. Eur J Pharmacol 296:R1-R3.

Lavallee P, Deschénes M (2004) Dendroarchitecture and lateral inhibition in thalamic barreloids. J Neurosci 24:6098-6105.

Lee HB, Blaufox MD (1985) Blood volume in the rat. J Nucl Med 26:72-76.

Lee SM, Friedberg MH, Ebner FF (1994) The role of GABA-mediated inhibition in the rat ventral posterior medial thalamus. II. Differential effects of GABAA and GABAB receptor antagonists on responses of VPM neurons. J Neurophysiol 71:1716-1726.

Lee JJ, Croucher MJ (2003) Actions of Group I and Group II metabotropic glutamate receptor ligands on 5-hydroxytryptamine release in the rat cerebral cortex in vivo: differential roles in the regulation of central serotonergic neurotransmission. Neuroscience 117:671-679.

Leklem JE (1971) Quantitative aspects of tryptophan metabolism in humans and other species: a review. Am J Clin Nutr 24:659-672.

Levey AI, Hallanger AE, Wainer BH (1987) Cholinergic nucleus basalis neurons may influence the cortex via the thalamus. Neurosci Lett 74:7-13.

Li XM, Li CC, Yu SS, Chen JT, Sabapathy K, Ruan DY (2007) JNK1 contributes to metabotropic glutamate receptor-dependent long-term depression and short-term synaptic plasticity in the mice area hippocampal CA1. Eur J Neurosci 25:391-396.

Linden AM, Bergeron M, Schoepp DD (2005) Comparison of c-Fos induction in the brain by the mGlu2/3 receptor antagonist LY341495 and agonist LY354740: evidence for widespread endogenous tone at brain mGlu2/3 receptors in vivo. Neuropharmacology 49 Suppl 1:120-134.

Liu XB, Jones EG (1999) Predominance of corticothalamic synaptic inputs to thalamic reticular nucleus neurons in the rat. J Comp Neurol 414:67-79.

Liu XB, Warren RA, Jones EG (1995) Synaptic distribution of afferents from reticular nucleus in ventroposterior nucleus of cat thalamus. J Comp Neurol 352:187-202.

Liu XB, Munoz A, Jones EG (1998) Changes in subcellular localization of metabotropic glutamate receptor subtypes during postnatal development of mouse thalamus. J Comp Neurol 395:450-465.

Liu XB, Jones EG (2003) Fine structural localization of the connexin-36 immunoreactivity in mouse cerebral cortex and thalamus. J Comp Neurol 466:457-467.

Llinas R, Pare D (1997) Coherent oscillations in specific and nonspecific thalamocortical networks and their role in cognition. Oxford: Elsevier.

Lombardi G, Alesiani M, Leonardi P, Cherici G, Pellicciari R, Moroni F (1993) Pharmacological characterization of the metabotropic glutamate receptor inhibiting D-[3H]-aspartate output in rat striatum. Br J Pharmacol 110:1407-1412.

Lorrain DS, Baccei CS, Bristow LJ, Anderson JJ, Varney MA (2003a) Effects of ketamine and N-methyl-D-aspartate on glutamate and dopamine release in the rat prefrontal cortex: modulation by a group II selective metabotropic glutamate receptor agonist LY379268. Neuroscience 117:697-706.

Lorrain DS, Schaffhauser H, Campbell UC, Baccei CS, Correa LD, Rowe B, Rodriguez DE, Anderson JJ, Varney MA, Pinkerton AB, Vernier JM, Bristow LJ (2003b) Group II mGlu receptor activation suppresses norepinephrine release in the ventral hippocampus and locomotor responses to acute ketamine challenge. Neuropsychopharmacology 28:1622-1632.

Lourenço Neto F, Schadrack J, Berthele A, Zieglgansberger W, Tolle TR, Castro-Lopes JM (2000) Differential distribution of metabotropic glutamate receptor subtype mRNAs in the thalamus of the rat. Brain Res 854:93-105.

Lozsadi DA (1994) Organization of cortical afferents to the rostral, limbic sector of the rat thalamic reticular nucleus. J Comp Neurol 341:520-533.

Lu SM, Lin RC (1993) Thalamic afferents of the rat barrel cortex: a light- and electron-microscopic study using Phaseolus vulgaris leucoagglutinin as an anterograde tracer. Somatosens Mot Res 10:1-16.

Lujan R, Roberts JD, Shigemoto R, Ohishi H, Somogyi P (1997) Differential plasma membrane distribution of metabotropic glutamate receptors mGluR1 alpha, mGluR2 and mGluR5, relative to neurotransmitter release sites. J Chem Neuroanat 13:219-241.

Ma PM (1991) The barrelettes--architectonic vibrissal representations in the brainstem trigeminal complex of the mouse. I. Normal structural organization. J Comp Neurol 309:161-199.

Ma PM (1993) Barrelettes--architectonic vibrissal representations in the brainstem trigeminal complex of the mouse. II. Normal post-natal development. J Comp Neurol 327:376-397.

Ma PM, Woolsey TA (1984) Cytoarchitectonic correlates of the vibrissae in the medullary trigeminal complex of the mouse. Brain Res 306:374-379.

Maione S, Palazzo E, de Novellis V, Stella L, Leyva J, Rossi F (1998) Metabotropic glutamate receptors modulate serotonin release in the rat periaqueductal gray matter. Naunyn Schmiedebergs Arch Pharmacol 358:411-417.

Makoff A, Volpe F, Lelchuk R, Harrington K, Emson P (1996) Molecular characterization and localization of human metabotropic glutamate receptor type 3. Brain Res Mol Brain Res 40:55-63.

Malherbe P, Kratzeisen C, Lundstrom K, Richards JG, Faull RL, Mutel V (1999) Cloning and functional expression of alternative spliced variants of the human metabotropic glutamate receptor 8. Brain Res Mol Brain Res 67:201-210.

Marek GJ, Wright RA, Schoepp DD, Monn JA, Aghajanian GK (2000) Physiological antagonism between 5-hydroxytryptamine(2A) and group II metabotropic glutamate receptors in prefrontal cortex. J Pharmacol Exp Ther 292:76-87.

Marti M, Paganini F, Stocchi S, Bianchi C, Beani L, Morari M (2001) Presynaptic group I and II metabotropic glutamate receptors oppositely modulate striatal acetylcholine release. Eur J Neurosci 14:1181-1184.

Martinez-Hernandez A, Bell KP, Norenberg MD (1977) Glutamine synthetase localisation in brain. Science 195:1356-1358.

Masu M, Tanabe Y, Tsuchida K, Shigemoto R, Nakanishi S (1991) Sequence and expression of a metabotropic glutamate receptor. Nature 349:760-765.

Miller CL, Llenos IC, Dulay JR, Weis S (2006) Upregulation of the initiating step of the kynurenine pathway in postmortem anterior cingulate cortex from individuals with schizophrenia and bipolar disorder. Brain Res 1073-1074:25-37.

Miller CL, Llenos IC, Cwik M, Walkup J, Weis S (2008) Alterations in kynurenine precursor and product levels in schizophrenia and bipolar disorder. Neurochem Int 52:1297-1303.

Miller CL, Llenos IC, Dulay JR, Barillo MM, Yolken RH, Weis S (2004) Expression of the kynurenine pathway enzyme tryptophan 2,3-dioxygenase is increased in the frontal cortex of individuals with schizophrenia. Neurobiol Dis 15:618-629.

Milligan G (2008) A day in the life of a G protein-coupled receptor: the contribution to function of G protein-coupled receptor dimerization. Br J Pharmacol 153 Suppl 1:S216-229.

Minakami R, Katsuki F, Yamamoto T, Nakamura K, Sugiyama H (1994) Molecular cloning and the functional expression of two isoforms of human metabotropic glutamate receptor subtype 5. Biochem Biophys Res Commun 199:1136-1143.

Minchin MCW, Beart PM (1975) Compartmentation of amino acid metabolism in the rat dorsal root ganglion: a metabolic and autoradiographic study. Brain Res 83:437-449.

Minderhoud JM (1971) An anatomical study of the efferent connections of the thalamic reticular nucleus. Exp Brain Res 112:435-446.

Mineff E, Valtschanoff J (1999) Metabotropic glutamate receptors 2 and 3 expressed by astrocytes in rat ventrobasal thalamus. Neurosci Lett 270:95-98.

Mineff EM, Weinberg RJ (2000) Differential synaptic distribution of AMPA receptor subunits in the ventral posterior and reticular thalamic nuclei of the rat. Neuroscience 101:969-982.

Minnery BS, Simons DJ (2003) Response properties of whisker-associated trigeminothalamic neurons in rat nucleus principalis. J Neurophysiol 89:40-56.

Mitchell SJ, Silver RA (2000) Glutamate spillover suppresses inhibition by activating presynaptic mGluRs. Nature 404:498-502.

Mitsukawa K, Yamamoto R, Ofner S, Nozulak J, Pescott O, Lukic S, Stoehr N, Mombereau C, Kuhn R, McAllister KH, van der Putten H, Cryan JF, Flor PJ (2005) A selective metabotropic glutamate receptor 7 agonist: activation of receptor signaling via an allosteric site modulates stress parameters in vivo. Proc Natl Acad Sci U S A 102:18712-18717.

Moghaddam B, Adams BW (1998) Reversal of phencyclidine effects by a group II metabotropic glutamate receptor agonist in rats. Science 281:1349-1352.

Moldrich RX, Chapman AG, De Sarro G, Meldrum BS (2003) Glutamate metabotropic receptors as targets for drug therapy in epilepsy. Eur J Pharmacol 476:3-16.

Monn JA, Valli MJ, Johnson BG, Salhoff CR, Wright RA, Howe T, Bond A, Lodge D, Spangle LA, Paschal JW, Campbell JB, Griffey K, Tizzano JP, Schoepp DD (1996) Synthesis of the four isomers of 4-aminopyrrolidine-2,4-dicarboxylate: identification of a potent, highly selective, and systemically-active agonist for metabotropic glutamate receptors negatively coupled to adenylate cyclase. J Med Chem 39:2990-3000.

Monn JA, Valli MJ, Massey SM, Wright RA, Salhoff CR, Johnson BG, Howe T, Alt CA, Rhodes GA, Robey RL, Griffey KR, Tizzano JP, Kallman MJ, Helton DR, Schoepp DD (1997) Design, synthesis, and pharmacological characterization of (+)-2-aminobicyclo[3.1.0]hexane-2,6-dicarboxylic acid (LY354740): a potent, selective, and orally active group 2 metabotropic glutamate receptor agonist possessing anticonvulsant and anxiolytic properties. J Med Chem 40:528-537.

Monn JA, Valli MJ, Massey SM, Hansen MM, Kress TJ, Wepsiec JP, Harkness AR, Grutsch JL, Jr., Wright RA, Johnson BG, Andis SL, Kingston A, Tomlinson R, Lewis R, Griffey KR, Tizzano JP, Schoepp DD (1999) Synthesis, pharmacological characterization, and molecular modeling of heterobicyclic amino acids related to (+)-2-aminobicyclo[3.1.0] hexane-2,6-dicarboxylic acid (LY354740): identification of two new potent, selective, and systemically active agonists for group II metabotropic glutamate receptors. J Med Chem 42:1027-1040.

Moran MM, Melendez R, Baker D, Kalivas PW, Seamans JK (2003) Cystine/glutamate antiporter regulation of vesicular glutamate release. Ann N Y Acad Sci 1003:445-447.

Mutel V, Trube G, Klingelschmidt A, Messer J, Bleuel Z, Humbel U, Clifford MM, Ellis GJ, Richards JG (1998) Binding characteristics of a potent AMPA receptor antagonist [3H]Ro 48-8587 in rat brain. J Neurochem 71:418-426.

Muto T, Tsuchiya D, Morikawa K, Jingami H (2007) Structures of the extracellular regions of the group II/III metabotropic glutamate receptors. Proc Natl Acad Sci U S A 104:3759-3764.

Nakajima Y, Iwakabe H, Akazawa C, Nawa H, Shigemoto R, Mizuno N, Nakanishi S (1993) Molecular characterization of a novel retinal metabotropic glutamate receptor mGluR6 with a high agonist selectivity for L-2-amino-4-phosphonobutyrate. J Biol Chem 268:11868-11873.

Nakanishi S (1992) Molecular diversity of glutamate receptors and implications for brain function. Science 258:597-603.

Nakanishi S, Nakajima Y, Masu M, Ueda Y, Nakahara K, Watanabe D, Yamaguchi S, Kawabata S, Okada M (1998) Glutamate receptors: brain function and signal transduction. Brain Res Brain Res Rev 26:230-235.

Neale SA, Salt TE (2006) Modulation of GABAergic inhibition in the rat superior colliculus by a presynaptic group II metabotropic glutamate receptor. J Physiol 577:659-669.

Neale SA, Copeland CS, Uebele VN, Thomson FJ, Salt TE (2013) Modulation of Hippocampal Synaptic Transmission by the Kynurenine Pathway Member Xanthurenic Acid and Other VGLUT Inhibitors. Neuropsychopharmacology 38:1060-1067.

Neki A, Ohishi H, Kaneko T, Shigemoto R, Nakanishi S, Mizuno N (1996) Metabotropic glutamate receptors mGluR2 and mGluR5 are expressed in two non-overlapping populations of Golgi cells in the rat cerebellum. Neuroscience 75:815-826.

Nicoletti F, Bockaert J, Collingridge GL, Conn PJ, Ferraguti F, Schoepp DD, Wroblewski JT, Pin JP (2011) Metabotropic glutamate receptors: from the workbench to the bedside. Neuropharmacology 60:1017-1041.

Nikiforuk A, Popik P, Drescher KU, van Gaalen MM, Relo AL, Mezler M, Marek G, Schoemaker H, Gross G, Bespalov A (2010) Effects of a positive allosteric modulator of mGlu2 receptors LY487379 on cognitive flexibility and impulsive-like responding in rats. J Pharmacol Exp Ther 335:665-673.

Nilsson LK, Linderholm KR, Engberg G, Paulson L, Blennow K, Lindstrom LH, Nordin C, Karanti A, Persson P, Erhardt S (2005) Elevated levels of kynurenic acid in the cerebrospinal fluid of male patients with schizophrenia. Schizophr Res 80:315-322.

Niswender CM, Conn PJ (2010) Metabotropic glutamate receptors: physiology, pharmacology, and disease. Annu Rev Pharmacol Toxicol 50:295-322.

Niswender CM, Johnson KA, Miller NR, Ayala JE, Luo Q, Williams R, Saleh S, Orton D, Weaver CD, Conn PJ (2010) Context-dependent pharmacology exhibited by negative allosteric modulators of metabotropic glutamate receptor 7. Mol Pharmacol 77:459-468.

Nordquist RE, Steckler T, Wettstein JG, Mackie C, Spooren W (2008) Metabotropic glutamate receptor modulation, translational methods, and biomarkers: relationships with anxiety. Psychopharmacology (Berl) 199:389-402.

O'Hara PJ, Sheppard PO, Thogersen H, Venezia D, Haldeman BA, McGrane V, Houamed KM, Thomsen C, Gilbert TL, Mulvihill ER (1993) The ligand-binding domain in metabotropic glutamate receptors is related to bacterial periplasmic binding proteins. Neuron 11:41-52.

Ohara PT (1988) Synaptic organization of the thalamic reticular nucelaus. J Electron Microsc Tech 10:283-292.

Ohara PT, Lieberman AR (1985) The thalamic reticular nucleus of the adult rat: experimental anatomical studies. J Neurocytol 14:365-411.

Ohara PT, Lieberman AR (1993) Some aspects of the synaptic circuitry underlying inhibition in the ventrobasal thalamus. J Neurocytol 22:815-825.

Ohara PT, Havton LA (1994) Preserved features of thalamocortical projection neuron dendritic architecture in the somatosensory thalamus of the rat, cat and macaque. Brain Res 648:259-264.

Ohishi H, Shigemoto R, Nakanishi S, Mizuno N (1993a) Distribution of the messenger RNA for a metabotropic glutamate receptor, mGluR2, in the central nervous system of the rat. Neuroscience 53:1009-1018.

Ohishi H, Shigemoto R, Nakanishi S, Mizuno N (1993b) Distribution of the mRNA for a metabotropic glutamate receptor (mGluR3) in the rat brain: an in situ hybridization study. J Comp Neurol 335:252-266.

Ohishi H, Ogawa-Meguro R, Shigemoto R, Kaneko T, Nakanishi S, Mizuno N (1994) Immunohistochemical localization of metabotropic glutamate receptors, mGluR2 and mGluR3, in rat cerebellar cortex. Neuron 13:55-66.

Okamoto N, Hori S, Akazawa C, Hayashi Y, Shigemoto R, Mizuno N, Nakanishi S (1994) Molecular characterization of a new metabotropic glutamate receptor mGluR7 coupled to inhibitory cyclic AMP signal transduction. J Biol Chem 269:1231-1236.

Okamoto T, Sekiyama N, Otsu M, Shimada Y, Sato A, Nakanishi S, Jingami H (1998) Expression and purification of the extracellular ligand binding region of metabotropic glutamate receptor subtype 1. J Biol Chem 273:13089-13096.

Okuda S, Nishiyama N, Saito H, Katsuki H (1996) Hydrogen peroxide-mediated neuronal cell death induced by an endogenous neurotoxin, 3-hydroxykynurenine. Proc Natl Acad Sci U S A 93:12553-12558.

Ornstein PL, Arnold MB, Bleisch TJ, Wright RA, Wheeler WJ, Schoepp DD (1998) [3H]LY341495, a highly potent, selective and novel radioligand for labeling Group II metabotropic glutamate receptors. Bioorg Med Chem Lett 8:1919-1922.

Page G, Khidir FA, Pain S, Barrier L, Fauconneau B, Guillard O, Piriou A, Hugon J (2006) Group I metabotropic glutamate receptors activate the p70S6 kinase via both mammalian target of rapamycin (mTOR) and extracellular signal-regulated kinase (ERK 1/2) signaling pathways in rat striatal and hippocampal synaptoneurosomes. Neurochem Int 49:413-421.

Panatier A, Theodosis DT, Mothet JP, Touquet B, Pollegioni L, Poulain DA, Oliet SH (2006) Glia-derived D-serine controls NMDA receptor activity and synaptic memory. Cell 125:775-784.

Pare D, Steriade M, Deschénes M, Oakson G (1987) Physiological characteristics of anterior thalamic nuclei, a group devoid of inputs from reticular thalamic nucleus. J Neurophysiol 57:1669-1685.

Parmentier M-L, Pin JP, Bockaert J, Grau Y (1996) Cloning and functional expression of a Drosophila metabotropic glutamate receptor expressed in the embryonic central nervous system. J Neurosci 1:6687-6694.

Parri HR, Crunelli V (2001) Pacemaker calcium oscillations in thalamic astrocytes in situ. Neuroreport 12:3897-3900.

Parri HR, Gould TM, Crunelli V (2001) Spontaneous astrocytic Ca^{2+} oscillations in situ drive NMDAR-mediated neuronal excitation. Nat Neurosci 4:803-812.

Parri HR, Gould TM, Crunelli V (2010) Sensory and cortical activation of distinct glial cell subtypes in the somatosensory thalamus of young rats. Eur J Neurosci 32:29-40.

Parsons CG, Danysz W, Quack G, Hartmann S, Lorenz B, Wollenburg C, Baran L, Przegalinski E, Kostowski W, Krzascik P, Chizh B, Headley PM (1997) Novel systemically active antagonists of the glycine site of the N-methyl-D-aspartate receptor: electrophysiological, biochemical and behavioral characterization. J Pharmacol Exp Ther 283:1264-1275.

Patil ST, Zhang L, Martenyi F, Lowe SL, Jackson KA, Andreev BV, Avedisova AS, Bardenstein LM, Gurovich IY, Morozova MA, Mosolov SN, Neznanov NG, Reznik AM, Smulevich AB, Tochilov VA, Johnson BG, Monn JA, Schoepp DD (2007) Activation of mGlu2/3 receptors as a new approach to treat schizophrenia: a randomized Phase 2 clinical trial. Nat Med 13:1102-1107.

Paulsen RE, Contestabile A, Villant L, Fonnum F (1987) An in vivo model for studying function of brain tissue temporarily devoid of glial cell metabolism: The use of fluorocitrate. J Neurochem 48:1377-1385.

Paxinos G, Watson C (1986) The Rat Brain in the Stereotaxic Co-ordinates, 2nd Edition Edition. San Diego, CA: Academic Pres.

Perkins MN, Stone TW (1982) An iontophoretic investigation of the actions of convulsant kynurenines and their interaction with the endogenous excitant quinolinic acid. Brain Res 247:184-187.

Peschanski M, Lee CL. Ralston HJ (2984) The structural organization of the ventrobasal complex of the rat as revealed by the analysis of physiologically characterized neurons injected intracellularly with horseradish peroxidase. Brain Res 297:63-74.

Peters RA (1963) Biochemical lesions and lethal synthesis. Pergammon Press, London.

Petersen CC (2007) The functional organization of the barrel cortex. Neuron 56:339-355.

Petralia RS, Wang YX, Niedzielski AS, Wenthold RJ (1996a) The metabotropic glutamate receptors, mGluR2 and mGluR3, show unique postsynaptic, presynaptic and glial localizations. Neuroscience 71:949-976.

Petralia RS, Wang YX, Niedzielski AS, Wenthold RJ (1996b) The metabotropic glutamate receptors, mGluR2 and mGluR3, show unique postsynaptic, presynaptic and glial localizations. Neuroscience:949-976.

Pierret T, Lavallee P, Deschénes M (2000) Parallel streams for the relay of vibrissal information through thalamic barreloids. J Neurosci 20:7455-7462.

Piet R, Bonhomme R, Theodosis DT, Poulain DA, Oliet SH (2003) Modulation of GABAergic transmission by endogenous glutamate in the rat supraoptic nucleus. Eur J Neurosci 17:1777-1785.

Piet R, Vargova L, Sykova E, Poulain DA, Oliet SH (2004) Physiological contribution of the astrocytic environment of neurons to intersynaptic crosstalk. Proc Natl Acad Sci U S A 101:2151-2155.

Pietrancosta N, Kessler A, Favre-Besse FC, Triballeau N, Quentin T, Giros B, El Mestikawy S, Acher FC (2010) Rose Bengal analogs and vesicular glutamate transporters (VGLUTs). Bioorg Med Chem 18:6922-6933.

Pin JP, Waeber C, Prezeau L, Bockaert J, Heinemann SF (1992) Alternative splicing generates metabotropic glutamate receptors inducing different patterns of calcium release in Xenopus oocytes. Proc Natl Acad Sci U S A 89:10331-10335.

Pin JP, Bockaert J (1995) Get receptive to metabotropic glutamate receptors. Curr Opin Neurobiol 5:342-349.

Pin JP, Duvoisin R (1995) The metabotropic glutamate receptors: structure and functions. Neuropharmacology 34:1-26.

Pin JP, Galvez T, Prezeau L (2003) Evolution, structure, and activation mechanism of family 3/C G-protein-coupled receptors. Pharmacol Ther 98:325-354.

Pin JP, Joly C, Heinemann SF, Bockaert J (1994) Domains involved in the specificity of G protein activation in phospholipase C-coupled metabotropic glutamate receptors. EMBO J 13:342-348.

Pinault D (1994) Golgi-like labeling of a single neuron recorded extracellularly. Neurosci Lett 170:255-260.

Pinault D (1996) A novel single-cell staining procedure performed in vivo under electrophysiological control: morpho-functional features of juxtacellularly labeled thalamic cells and other central neurons with biocytin or Neurobiotin. J Neurosci Methods 65:113-136.

Pinault D (2004) The thalamic reticular nucleus: structure, function and concept. Brain Res Brain Res Rev 46:1-31.

Pinault D (2011) Dysfunctional thalamus-related networks in schizophrenia. Schizophr Bull 37:238-243.

Pinault D, Deschénes M (1998a) Projection and innervation patterns of individual thalamic reticular axons in the thalamus of the adult rat: a three-dimensional, graphic, and morphometric analysis. J Comp Neurol 391:180-203.

Pinault D, Deschénes M (1998b) Anatomical evidence for a mechanism of lateral inhibition in the rat thalamus. Eur J Neurosci 10:3462-3469.

Pinault D, Smith Y, Deschénes M (1997) Dendrodendritic and axoaxonic synapses in the thalamic reticular nucleus of the adult rat. J Neurosci 17:3215-3233.

Pisani A, Bonsi P, Catania MV, Giuffrida R, Morari M, Marti M, Centonze D, Bernardi G, Kingston AE, Calabresi P (2002) Metabotropic glutamate 2 receptors modulate synaptic inputs and calcium signals in striatal cholinergic interneurons. J Neurosci 22:6176-6185.

Poisik O, Raju DV, Verreault M, Rodriguez A, Abeniyi OA, Conn PJ, Smith Y (2005) Metabotropic glutamate receptor 2 modulates excitatory synaptic transmission in the rat globus pallidus. Neuropharmacology 49 Suppl 1:57-69.

Poncer JC, Shinozaki H, Miles R (1995) Dual modulation of synaptic inhibition by distinct metabotropic glutamate receptors in the rat hippocampus. J Physiol 485 (Pt 1):121-134.

Porter JT, McCarthy KD (1999) Hippocampal astrocytes in situ respond to glutamate released from synaptic terminals. J Neurosci 16:5073-5081.

Prezeau L, Manzoni O, Homburger V, Sladeczek F, Curry K, Bockaert J (1992) Characterization of a metabotropic glutamate receptor: direct negative coupling to adenylyl cyclase and involvement of a pertussis toxin-sensitive G protein. Proc Natl Acad Sci U S A 89:8040-8044.

Prezeau L, Carrette J, Helpap B, Curry K, Pin JP, Bockaert J (1994a) Pharmacological characterization of metabotropic glutamate receptors in several types of brain cells in primary cultures. Mol Pharmacol 45:570-577.

Prezeau L, Carrette J, Helpap B, Curry K, Pin JP, Bockaert J (1994b) Pharmacological characterization of metabotropic glutamate receptors in several types of brain cells in primary cultures. Mol Pharmacol 45:570-577.

Price JL, Slotnick BM (1983) Dual olfactory representation in the rat thalamus: an anatomical and electrophysiological study. J Comp Neurol 215:63-77.

Ralston HHI (1983) The synaptic organization of the ventrobasal thalamus in the rat, cat and monkey. In *Somatosensory Integration in the Thalamus*. Amsterdam: Elsevier Science.

Ray JP, Russchen FT, Fueller TA, Price JL (1992) Sources of presumptive glutamatergic/aspartergic afferets to the mediodorsal nucleus of the thalamus in the rat. J Comp Neurol 320:435-456.

Ray JP, Price JL (1992) The organization of the thalamocortical connections of the mediodorsal thalamic nucleus in the rat, related to the ventral forebrain-prefrontal cortex topography. J Comp Neurol 323:167-197.

Romano C, Yang WL, O'Malley KL (1996) Metabotropic glutamate receptor 5 is a disulfide-linked dimer. J Biol Chem 271:28612-28616.

Rondard P, Liu J, Huang S, Malhaire F, Vol C, Pinault A, Labesse G, Pin JP (2006) Coupling of agonist binding to effector domain activation in metabotropic glutamate-like receptors. J Biol Chem 281:24653-24661.

Rorick-Kehn LM, Johnson BG, Knitowski KM, Salhoff CR, Witkin JM, Perry KW, Griffey KI, Tizzano JP, Monn JA, McKinzie DL, Schoepp DD (2007) In vivo pharmacological characterization of the structurally novel, potent, selective mGlu2/3 receptor agonist LY404039 in animal models of psychiatric disorders. Psychopharmacology (Berl) 193:121-136.

Rowe BA, Schaffhauser H, Morales S, Lubbers LS, Bonnefous C, Kamenecka TM, McQuiston J, Daggett LP (2008) Transposition of three amino acids transforms the human metabotropic glutamate receptor (mGluR)-3-positive allosteric modulation site to mGluR2, and additional characterization of the mGluR2-positive allosteric modulation site. J Pharmacol Exp Ther 326:240-251.

Rub U, Del Turco D, Del Tredici K, de Vos RA, Brunt ER, Reifenberger G, Seifried C, Schultz C, Auburger G, Braak H (2003) Thalamic involvement in a spinocerebellar ataxia type 2 (SCA2) and a spinocerebellar ataxia type 3 (SCA3) patient, and its clinical relevance. Brain 126:2257-2272.

Salt TE (1986) Mediation of thalamic sensory input by both NMDA receptors and non-NMDA receptors. Nature 322:263-265.

Salt TE (1987) Excitatory amino acid receptors and synaptic transmission in the rat ventrobasal thalamus. J Physiol 391:499-510.

Salt TE (1989) Gamma-aminobutyric acid and afferent inhibition in the cat and rat ventrobasal thalamus. Neuroscience 28:17-26.

Salt TE, Eaton SA (1989) Function of non-NMDA receptors and NMDA receptors in synaptic responses to natural somatosensory stimulation in the ventrobasal thalamus. Exp Brain Res 77:646-652.

Salt TE, Eaton SA (1995a) Distinct presynaptic metabotropic receptors for L-AP4 and CCG1 on GABAergic terminals: pharmacological evidence using novel alpha-methyl derivative mGluR antagonists, MAP4 and MCCG, in the rat thalamus in vivo. Neuroscience 65:5-13.

Salt TE, Eaton SA (1995b) Modulation of sensory neurone excitatory and inhibitory responses in the ventrobasal thalamus by activation of metabotropic excitatory amino acid receptors. Neuropharmacology 34:1043-1051.

Salt TE, Eaton SA (1996) Functions of ionotropic and metabotropic glutamate receptors in sensory transmission in the mammalian thalamus. Prog Neurobiol 48:55-72.

Salt TE, Eaton SA, Turner JP (1996) Characterization of the metabotropic glutamate receptors (mGluRs) which modulate GABA-mediated inhibition in the ventrobasal thalamus. Neurochem Int 29:317-322.

Salt TE, Turner JP (1998) Modulation of sensory inhibition in the ventrobasal thalamus via activation of group II metabotropic glutamate receptors by 2R,4R-aminopyrrolidine-2,4-dicarboxylate. Exp Brain Res 121:181-185.

Sanchez-Vives MV, Bal T, McCormick DA (1997) Inhibitory interactions between perigeniculate GABAergic neurons. J Neurosci 17:8894-8908.

Santello M, Cali C, Bezzi P (2012) Gliotransmission and the tripartite synapse. Adv Exp Med Biol 970:307-331.

Sartorius LJ, Nagappan G, Lipska BK, Lu B, Sei Y, Ren-Patterson R, Li Z, Weinberger DR, Harrison PJ (2006) Alternative splicing of human metabotropic glutamate receptor 3. J Neurochem 96:1139-1148.

Sathyasaikumar KV, Stachowski EK, Wonodi I, Roberts RC, Thaker GK, Schwarcz R (2009) Impairment of kynurenine 3-monooxygenase in the frontal cortex of individuals with schizophrenia: association with the eye tracking endophenotype. In: Society for Neuroscience Annual Meeting. Chicago, IL: Society for Neuroscience.

Saugstad JA, Kinzie JM, Shinohara MM, Segerson TP, Westbrook GL (1997) Cloning and expression of rat metabotropic glutamate receptor 8 reveals a distinct pharmacological profile. Mol Pharmacol 51:119-125.

Schaffhauser H, Rowe BA, Morales S, Chavez-Noriega LE, Yin R, Jachec C, Rao SP, Bain G, Pinkerton AB, Vernier JM, Bristow LJ, Varney MA, Daggett LP (2003) Pharmacological characterization and identification of amino acids involved in the positive modulation of metabotropic glutamate receptor subtype 2. Mol Pharmacol 64:798-810.

Schaffhauser H, Cartmell J, Jakob-Rotne R, Mutel V (1997) Pharmacological characterization of metabotropic glutamate receptors linked to the inhibition of adenylate cyclase activity in rat striatal slices. Neuropharmacology 36:933-940.

Scheibel ME, Scheibel AB (1966) The organization of the nucleus reticularis thalami: a Golgi study. Brain Res 1:43-62.

Schoepp DD, Johnson BG, True RA, Monn JA (1991) Comparison of (1S,3R)-1-aminocyclopentane-1,3-dicarboxylic acid (1S,3R-ACPD)- and 1R,3S-ACPD-stimulated brain phosphoinositide hydrolysis. Eur J Pharmacol 207:351-353.

Schoepp DD, Johnson BG, Monn JA (1992a) Inhibition of cyclic AMP formation by a selective metabotropic glutamate receptor agonist. J Neurochem 58:1184-1186.

Schoepp DD, Johnson BG, Sacaan AI, True RA, Monn JA (1992b) In vitro and in vivo pharmacology of 1S,3R- and 1E,3S-ACPD: evidence for a role of metabotropic glutamate receptors in striatal motor function. Mol Pharmacol 2:33-37.

Schoepp DD, Johnson BG, Salhoff CR, Valli MJ, Desai MA, Burnett JP, Mayne NG, Monn JA (1995) Selective inhibition of forskolin-stimulated cyclic AMP formation in rat hippocampus by a novel mGluR agonist, 2R, 4R-4-aminopyrolidine-2, 4-dicarboxylate. Neuropharmacology 34:843-850.

Schoepp DD, Salhoff CR, Wright RA, Johnson BG, Burnett JP, Mayne NG, Belagaje R, Wu S, Monn JA (1996) The novel metabotropic glutamate receptor agonist 2R,4R-APDC potentiates stimulation of phosphoinositide hydrolysis in the rat hippocampus by 3,5-dihydroxyphenylglycine: evidence for a synergistic interaction between group 1 and group 2 receptors. Neuropharmacology 35:1661-1672.

Schoepp DD, Johnson BG, Wright RA, Salhoff CR, Mayne NG, Wu S, Cockerman SL, Burnett JP, Belegaje R, Bleakman D, Monn JA (1997) LY354740 is a potent and highly selective group II metabotropic glutamate receptor agonist in cells expressing human glutamate receptors. Neuropharmacology 36:1-11.

Schoepp DD, Johnson BG, Wright RA, Salhoff CR, Monn JA (1998) Potent, stereoselective, and brain region selective modulation of second messengers in the rat brain by (+)LY354740, a novel group II metabotropic glutamate receptor agonist. Naunyn Schmiedebergs Arch Pharmacol 358:175-180.

Schoepp DD, Jane DE, Monn JA (1999) Pharmacological agents acting at subtypes of metabotropic glutamate receptors. Neuropharmacology 38:1431-1476.

Schoepp DD, Marek GJ (2002) Preclinical pharmacology of mGluR2/3 receptor agonists: novel agents for schizophrenia? CNS Neurol Disord Drug Targets 1:215-225.

Schoepp DD, Wright RA, Levine LR, Gaydos B, Potter WZ (2003) LY354740, an mGlu2/3 receptor agonist as a novel approach to treat anxiety/stress. Stress 6:189-197.

Schulz HL, Stohr H, Weber BH (2002) Characterization of three novel isoforms of the metabotrobic glutamate receptor 7 (GRM7). Neurosci Lett 326:37-40.

Schwarcz R, Rassoulpour A, Wu HQ, Medoff D, Tamminga CA, Roberts RC (2001) Increased cortical kynurenate content in schizophrenia. Biol Psychiatry 50:521-530.

Schwarcz R, Sathyasaikumar KV, Stachowski EK, Wonodi I, Roberts RC, Thaker GK (2009) Impaired cortical kynurenine pathway metabolism in schizophrenia: focus on kynurenine 3-monooxygenase. In: The 12th International Congress on Schizophrenia Research. San Diego, CA.

Sefton AJ (1969) The electrical activity of the anterior colliculus in the rat. Vision Res 9:207-222.

Semyanov A, Kullmann DM (2000) Modulation of GABAergic signaling among interneurons by metabotropic glutamate receptors. Neuron 25:663-672.

Shaw FZ, Chen RF, Yen CT (2001) Dynamic changes of touch- and laser heat-evoked field properties of primary somatosensory cortex in awake and pentobarbital-anesthetized rats. Brain Red 911:105-115.

Sherman SM (2007) The thalamus is more than just a relay. Curr Opin Neurobiol 17:417-422.

Sherman SM, Koch C (1986) The control of retinogeniculate transmission in the mammalian lateral geniculate nucleus. Exp Brain Res 63:1-20.

Sherman SM, Guillery RW (2001) Exploring the Thalamus. New York: Academic Press.

Sherman SM, Guillery RW (2002) The role of the thalamus in the flow of information to the cortex. Philos Trans R Soc Lond B Biol Sci 357:1695-1708.

Shigemoto R, Kinoshita A, Wada E, Nomura S, Ohishi H, Takada M, Flor PJ, Neki A, Abe T, Nakanishi S, Mizuno N (1997) Differential presynaptic localization of metabotropic glutamate receptor subtypes in the rat hippocampus. J Neurosci 17:7503-7522.

Shosaku A (1986) Cross-correlation analysis of a recurrent inhibitory circuit in the rat thalamus. J Neurophysiol 55:1030-1043.

Shosaku A, Sumitomo I (1983) Auditory neurons in the rat thalamic reticular nucleus. Exp Brain Res 49:432-442.

Shosaku A, Kayama Y, Sumitomo I (1984) Somatotopic organization in the rat thalamic reticular nucleus. Brain Res 311:57-63.

Shosaku A, Kayama Y, Sumitomo I, Sugitani M, Iwama K (1989) Analysis of recurrent inhibitory circuit in rat thalamus: neurophysiology of the thalamic reticular nucleus. Prog Neurobiol 32:77-102.

Sigel E, Buhr A (1997) The benzodiazepine binding site of GABAA receptors. Trends Pharmacol Sci 18:425-429.

Sillito AM, Jones HE (2002) Corticothalamic interactions in the transfer of visual information. Philos Trans R Soc Lond B Biol Sci 357:1739-1752.

Simon AP, Poindessous-Jazat F, Dutar P, Epelbaum J, Bassant MH (2006) Firing properties of anatomically identified neurons in the medial septum of anesthetized and unanesthetized restrained rats. J Neurosci 26:9038-9046.

Simons DJ (1978) Response properties of vibrissa units in rat SI somatosensory neocortex. J Neurophysiol 41:798-820.

Simons DJ, Carvell GE (1989) Thalamocortical response transformation in the rat vibrissa/barrel system. J Neurophysiol 61:311-330.

Sohal VS, Huguenard JR (2003) Inhibitory interconnections control burst pattern and emergent network synchrony in reticular thalamus. J Neurosci 23:8978-8988.

Sonnewald U, Westergaard N, Schousboe A, Svendsen JS, Unsgård G, Petersen SB (1993) Direct demonstration by ^{13}C NMR spectroscopy that glutamine from astrocytes is a precursor for GABA synthesis in neurons. Neurochem Int 22:19-29.

Spacek J, Lieberman AR (1974) Ultrastructure and three-dimensional organization of synaptic glomeruli in rat somatosensory thalamus. J Anat 117:487-516.

Stefani A, Pisani A, Mercuri NB, Bernardi G, Calabresi P (1994) Activation of metabotropic glutamate receptors inhibits calcium currents and GABA-mediated synaptic potentials in striatal neurons. J Neurosci 14:6734-6743.

Stehberg J, Acuna-Goycolea C, Ceric F, Torrealba F (2001) The visceral sector of the thalamic reticular nucleus in the rat. Neuroscience 106:745-755.

Steriade M (1993) Modulation of information processing in thalamocortical systems: chairman's introductory remarks. Prog Brain Res 98:341-343.

Steriade M, Parent A, Hada J (1984) Thalamic projections of nucleus reticularis thalami of cat: a study using retrograde transport of horseradish peroxidase and fluorescent tracers. J Comp Neurol 229:531-547.

Stone TW (1984) Microiontophoresis and pressure ejection. Chichester: John Wily & Sons.

Stone TW (1993) Neuropharmacology of quinolinic and kynurenic acids. Pharmacol Rev 45:309-379.

Stone TW (2007) Kynurenic acid blocks nicotinic synaptic transmission to hippocampal interneurons in young rats. Eur J Neurosci 25:2656-2665.

Stone TW, Perkins MN (1981) Quinolinic Acid: a potent endogenous excitant at amino acid receptors in the CNS. Eur J Pharmacol 72:411-412.

Suzuki Y, Moriyoshi E, Tsuchiya D, Jingami H (2004) Negative cooperativity of glutamate binding in the dimeric metabotropic glutamate receptor subtype 1. J Biol Chem 279:35526-35534.

Tai Y, Yi H, Ilinsky IA, Kultas-Ilinsky K (1995) Nucleus reticularis thalami connections with the mediodorsal thalamic nucleus: a light and electron microscopic study in the monkey. Brain Res Bull 38:475-488.

Tamaru Y, Nomura S, Mizuno N, Shigemoto R (2001) Distribution of metabotropic glutamate receptor mGluR3 in the mouse CNS: differential location relative to pre- and postsynaptic sites. Neuroscience 106:481-503.

Tamas G, Buhl EH, Lorinez A, Somogyi P (2000) Proximally targeted GABAergic synapses and gap junctions synchronize cortical interneurons. Nat Neurosci 3:366-371.

Tanabe Y, Masu M, Ishii T, Shigemoto R, Nakanishi S (1992) A family of metabotropic glutamate receptors. Neuron 8:169-179.

Tanabe Y, Nomura A, Masu M, Shigemoto R, Mizuno N, Nakanishi S (1993) Signal transduction, pharmacological properties, and expression patterns of two rat metabotropic glutamate receptors, mGluR3 and mGluR4. J Neurosci 13:1372-1378.

Taylor DL, Jones F, Kubota ES, Pocock JM (2005) Stimulation of microglial metabotropic glutamate receptor mGlu2 triggers tumor necrosis factor alpha-induced neurotoxicity in concert with microglial-derived Fas ligand. J Neurosci 25:2952-2964.

Testa CM, Standaert DG, Young AB, Penney JB, Jr. (1994) Metabotropic glutamate receptor mRNA expression in the basal ganglia of the rat. J Neurosci 14:3005-3018.

Timofeeva E, Lavallee P, Arsenault D, Deschénes M (2004) Synthesis of multiwhisker-receptive fields in subcortical stations of the vibrissa system. J Neurophysiol 91:1510-1515.

Tempia F, Miniaci MC, Anchisi D, Strata P (1998) Postsynaptic current mediated by metabotropic glutamate receptors in cerebellar Purkinje cells. J Neurophysiol 80:520-528.

Thomsen C, Bruno V, Nicoletti F, Marinozzi M, Pellicciari R (1996) (2S,1'S,2'S,3'R)-2-(2'-carboxy-3'-phenylcyclopropyl)glycine, a potent and selective antagonist of type 2 metabotropic glutamate receptors. Mol Pharmacol 50:6-9.

Torvik A (1956) Afferent connections to the sensory trigeminal nuclei, the nucleus of the solitary tract and adjacent structures; an experimental study in the rat. J Comp Neurol 106:51-141.

Tsuchiya D, Kunishima N, Kamiya N, Jingami H, Morikawa K (2002) Structural views of the ligand-binding cores of a metabotropic glutamate receptor complexed with an antagonist and both glutamate and Gd3+. Proc Natl Acad Sci U S A 99:2660-2665.

Turner JP, Salt TE (2003) Group II and III metabotropic glutamate receptors and the control of the nucleus reticularis thalami input to rat thalamocortical neurones in vitro. Neuroscience 122:459-469.

Ulrich D, Huguenard JR (1996) GABAB receptor-mediated responses in GABAergic projection neurones of rat nucleus reticularis thalami in vitro. J Physiol 493 (Pt 3):845-854.

Urbain N, Deschénes M (2007) A new thalamic pathway of vibrissal information modulated by the motor cortex. J Neurosci 27:12407-12412.

Urenjak J, Obrenovitch TP (2000) Neuroprotective potency of kynurenic acid against excitotoxicity. Neuroreport 11:1341-1344.

Urwyler S, Mosbacher J, Lingenhoehl K, Heid J, Hofstetter K, Froestl W, Bettler B, Kaupmann K (2001). Positive allosteric modulation of native and recombinant gamma-aminobutyric acid(B) recpetors by 2,6-Di-tert-butyl-4-(3-hydroxy-2,2-dimethyl-propyl)-phenol (CGP7930) and its aldehyde analog CGP13501. Mol Pharmacol 60:963-971.

Urwyler S, Pozza MF, Lingenhoehl K, Mosbacher J, Lampert C, Froesti W, Koller M, Kaupmann K (2003) N,N'Dicyclopentyl-2-methylsulfanyl-5-nitro-pyrimidine-4,6-diamine (GS39783) and structurally related compounds: novel allosteric enhancers of gamma-aminobutyric acidB receptor function. J Pharmacol Exp Ther 307:322-330.

Valerio A, Ferraboli S, Paterlini M, Spano P, Barlati S (2001) Identification of novel alternatively-spliced mRNA isoforms of metabotropic glutamate receptor 6 gene in rat and human retina. Gene 262:99-106.

Varga C, Sik A, Lavallee P, Deschénes M (2002) Dendroarchitecture of relay cells in thalamic barreloids: a substrate for cross-whisker modulation. J Neurosci 22:6186-6194.

Veinante P, Deschénes M (1999) Single- and multi-whisker channels in the ascending projections from the principal trigeminal nucleus in the rat. J Neurosci 19:5085-5095.

Veinante P, Jacquin MF, Deschénes M (2000a) Thalamic projections from the whisker-sensitive regions of the spinal trigeminal complex in the rat. J Comp Neurol 420:233-243.

Veinante P, Lavallee P, Deschénes M (2000b) Corticothalamic projections from layer 5 of the vibrissal barrel cortex in the rat. J Comp Neurol 424:197-204.

Velayos JL, Jimenez-Castellanos J, Jr., Reinoso-Suarez F (1989) Topographical organization of the projections from the reticular thalamic nucleus to the intralaminar and medial thalamic nuclei in the cat. J Comp Neurol 279:457-469.

Vignes M, Clarke VR, Davies CH, Chambers A, Jane DE, Watkins JC, Collingridge GL (1995) Pharmacological evidence for an involvement of group II and group III mGluRs in the presynaptic regulation of excitatory synaptic responses in the CA1 region of rat hippocampal slices. Neuropharmacology 34:973-982.

Villa AE (1990) Physiological differentiation within the auditory part of the thalamic reticular nucleus of the cat. Brain Res Brain Res Rev 15:25-40.

Virgili M, Paulsen RE, Villani L, Contestabile A, Fonnum F (1991) Temporary impairment of Müller cell metabolism in the rat retina by intravitreal injections of fluorocitrate. Exp Eye Res 53:115-122.

Vogt KE, Nicoll RA (1999) Glutamate and gamma-aminobutyric acid mediate a heterosynaptic depression at mossy fiber synapses in the hippocampus. Proc Natl Acad Sci U S A 96:1118-1122.

Wada E, Shigemoto R, Kinoshia A, Ohishi H, Mizuno N (1998) Metabotropic glutmate receptor subtypes in axon terminals of projection fibres from the main and accessory olfactory bulbs: a light and electron microscopy immunohistochemical study in the rat. J Comp Neurol 393:493-504.

Waite PM, Tracey DJ (1985) The Rat Nervous System, 2nd Edition. New York: Academic Press.

Waite PM, Ho SM, Henderson TA (2000) Afferent ingrowth and onset of activity in the rat trigeminal nucleus. Eur J Neurosci 12:2781-2792.

Wang N, Zhang Y, Wang JY, Gao G, Luo F (2010) Effects of pentobarbital anesthesia on nociceptive processing in the medial and lateral pain pathways in rats. Neurosci Bull 26:188-196.

Wang S, Bickford ME, Van Horn SC, Erisir A, Godwin DW, Sherman SM (2001) Synaptic targets of thalamic reticular nucleus terminals in the visual thalamus of the cat. J Comp Neurol 440:321-341.

Wang X, Sommer FT, Hirsch JA (2011) Inhibitory circuits for visual processing in thalamus. Curr Opin Neurobiol 21:726-733.

Watanabe D, Nakanishi S (2003) mGluR2 postsynaptically senses granule cell inputs at Golgi cell synapses. Neuron 39: 821-829.

Watkins JC, Evans RH (1981) Excitatory amino acid transmitters. Annu Rev Pharmacol Toxicol 21:165-204.

Wei H, Leeds P, Chen RW, Wei W, Leng Y, Bredesen DE, Chuang DM (2000) Neuronal apoptosis induced by pharmacological concentrations of 3-hydroxykynurenine: characterization and protection by dantrolene and Bcl-2 overexpression. J Neurochem 75:81-90.

Weinberger NM, Bakin JS (1998) Learning-induced physiological memory in adult primary auditory cortex: receptive fields plasticity, model, and mechanisms. Audio Neurotol 3:145-167.

Welker C (1971) Microelectrode delineation of fine grain somatotopic organization of (SmI) cerebral neocortex in albino rat. Brain Res 26:259-275.

Welker C (1976) Receptive fields of barrels in the somatosensory neocortex of the rat. J Comp Neurol 166:173-189.

Williams MN, Zahm DS, Jacquin MF (1994) Differential foci and synaptic organization of the principal and spinal trigeminal projections to the thalamus in the rat. Eur J Neurosci 6:429-453.

Woltering TJ, Adam G, Wichmann J, Goetschi E, Kew JN, Knoflach F, Mutel V, Gatti S (2008a) Synthesis and characterization of 8-ethynyl-1,3-dihydro-benzo[b][1,4]diazepin-2-one derivatives: part 2. New potent non-competitive metabotropic glutamate receptor 2/3 antagonists. Bioorg Med Chem Lett 18:1091-1095.

Woltering TJ, Wichmann J, Goetschi E, Adam G, Kew JN, Knoflach F, Ballard TM, Huwyler J, Mutel V, Gatti S (2008b) Synthesis and characterization of 1,3-dihydro-benzo[b][1,4]diazepin-2-one derivatives: Part 3. New potent non-competitive metabotropic glutamate receptor 2/3 antagonists. Bioorg Med Chem Lett 18:2725-2729.

Woolf NJ, Butcher LL (1986) Cholinergic systems in the rat brain: III. Projections from the pontomesencephalic tegmentum to the thalamus, tectum, basal ganglia, and basal forebrain. Brain Res Bull 16:603-637.

Woolsey TA, Van der Loos H (1970) The structural organization of layer IV in the somatosensory region (SI) of mouse cerebral cortex. The description of a cortical field composed of discrete cytoarchitectonic units. Brain Res 17:205-242.

Wright RA, Arnold MB, Wheeler WJ, Ornstein PL, Schoepp DD (2001) [3H]LY341495 binding to group II metabotropic glutamate receptors in rat brain. J Pharmacol Exp Ther 298:453-460.

Wroblewska B, Wroblewski JT, Pshenichkin S, Surin A, Sullivan SE, Neale JH (1997) N-acetylaspartylglutamate selectively activates mGluR3 receptors in transfected cells. J Neurochem 69:174-181.

Wu S, Wright RA, Rockey PK, Burgett SG, Arnold JS, Rosteck PR, Jr., Johnson BG, Schoepp DD, Belagaje RM (1998) Group III human metabotropic glutamate receptors 4, 7 and 8: molecular cloning, functional expression, and comparison of pharmacological properties in RGT cells. Brain Res Mol Brain Res 53:88-97.

Wu HQ, Pereira EF, Bruno JP, Pellicciari R, Albuquerque EX, Schwarcz R (2010) The astrocyte-derived alpha7 nicotinic receptor antagonist kynurenic acid controls extracellular glutamate levels in the prefrontal cortex. J Mol Neurosci 40:204-210.

Xi ZX, Baker DA, Shen H, Carson DS, Kalivas PW (2002) Group II metabotropic glutamate receptors modulate extracellular glutamate in the nucleus accumbens. J Pharmacol Exp Ther 300:162-171.

Yen CT, Jones EG (1983) Intracellular staining of physiolocically identified neurons and axons in the somatosensory thalamus of the cat. Brain Res 280:148-154.

Yokoi M, Kobayashi K, Manabe T, Takahashi T, Sakaguchi I, Katsuura G, Shigemoto R, Ohishi H, Nomura S, Nakamura K, Nakao K, Katsuki M, Nakanishi S (1996) Impairment of hippocampal mossy fiber LTD in mice lacking mGluR2. Science 273:645-647.

Zhang L, Jones EG (2004) Corticothalamic inhibition in the thalamic reticular nucleus. J Neurophysiol 91:759-766.

Zhu H, Ryan K, Chen S (1999) Cloning of novel splice variants of mouse mGluR1. Brain Res Mol Brain Res 73:93-103.

Zucker RS, Regehr WG (2002) Short-term synaptic plasticity. Anny Rev Physiol 64:355-405.

APPENDIX

Original research articles published in peer-reviewed journals as a result of research conducted during this thesis can be found inserted into the back cover.